Investigating small extracellular vesicle miRNA as biomarkers for Alzheimer's disease

Toby Aarons

A thesis submitted in fulfilment of the requirements of the University of Salford for the degree of Doctor of Philosophy

Translational Medicine Unit

Biomedical Research and Innovation Centre

School of Science, Engineering and Environment

University of Salford

2023

Supervisory Team

Dr Gemma Lace

Dr Arijit Mukhopdhyay

Table of contents

List of figures

List of tables

List of abbreviations

AD – Alzheimer's disease

Aβ – Amyloid beta (β)

APP/AβPP – Amyloid beta precursor protein

APS – Ammonium persulfate

ALS – Amyotrophic lateral sclerosis

ApoE – Apolipoprotein E

ApoE4 – Apolipoprotein E4 genotype

AT270+ tau – Phosphorylated tau isoform

ATG – Autophagy related

ATP – Adenosine triphosphate

BACE1 - Beta-secretase 1

BBB – Blood-brain barrier

BCA – Bicinchoninic acid

BCSFB – Blood- Cerebrospinal fluid barrier

BDEV – Brain derived extracellular vesicle

BDNF –Brain-derived neurotrophic factor

BSA – Bovine serum albumin

C14 cluster – Chromosome 14 microRNA cluster

Ca^{2+} -- Calcium Ion

CAA – Cerebral amyloid angiopathy

CADRO – Common Alzheimer's Disease and Related Disorders Research Ontology

CD – Cluster of differentiation

cDNA – Complementary deoxyribonucleic acid

CMO – Cell Mask Orange

CNS – Central nervous system

CREB – cAMP response binding protein

CSF – Cerebrospinal fluid

DLB – Dementia with Lewy bodies

DMT – Disease modifying therapies

DMEM – Dulbecco's Modified Eagle Medium

dNTP – (Deoxyribose) Nucleoside triphosphates

DTT – Dithiothreitol

ECL – Electrochemiluminescence

ECM – Extracellular matrix

ELISA – Enzyme-linked immunosorbent assay

EPA – Eicosapentaenoic acid

ESCRT – Endosomal sorting complex required for transport

EV – Extracellular vesicles

FACS – Fluorescence-activated cell sorting

FAD – Familial Alzheimer's disease

FBS – Fetal bovine serum

FDG – Fluorodeoxyglucose

F-NTA – Fluorescence nanoparticle tracking analysis

FTLD – Frontotemporal lobar dementia

GLP-1 – Glucagon-like peptide-1

GO – Gene ontology

GSL – Glycosphingolipid

H_2O_2 – Hydrogen peroxide

HRP – Horseradish peroxidase

i.c.v – Intracerebroventricular

IL – Interleukin

ILV – Intraluminal vesicles

IPSC – Induced pluripotent stem cell

KEGG – Kyoto Encyclopaedia of Genes and Genomes

LOAD – Late-ons*et* Alzheimer's disease

LPS – Lipopolysaccharide

LTP – Long term potentiation

MAP – Microtubule associated protein

MAPK – Mitogen activated protein kinase

MCI – Mild cognitive impairment

MHC – Major histocompatibility complex

miRNA/miR – Micro Ribonucleic acid

MISEV – Minimal information for studies of extracellular vesicles

$MnCl_2$ – Magnesium Chloride

mRNA – Messenger Ribonucleic acid

MV – Microvesicles

MVB – Multi-vesicular bodies

NMDA – N-methyl-D-aspartate

MMSE – Mini-Mental State Examination

NF – Neurofilament

NFT – Neurofibrillary tangles

NFκB – Nuclear Factor Kappa B

NGS – Next generation sequencing

Nlg1 – Neuroligin 1

NPC – Neural progenitor cell

NSE – Neuron specific enolase

NTC – No-template control

Oligo dT – Deoxythymine sequence

PBS – Phosphate buffer solution

PCA – Principal component analysis

PCR – Polymerase chain reaction

PE – Phycoerythrin

PET – Positron emission tomography

PolyA – Poly-Adenine

PrP – Prion protein

PSEN1 – Presenilin 1

qRT-PCR – Quantitative reverse-transcription Polymerase chain reaction

Rab35 – Rab GTPase 35

RA – Retinoic acid

RISC – RNA-induced silencing complex

RNA – Ribonucleic acid

RNPs – Ribonucleoprotein

ROS – Reactive oxygen species

sAPPβ – Soluble Amyloid beta precursor protein

SD – Standard deviation

SDS – Sodium dodecyl sulphate

SEC – Size exclusion chromatography

SEM – Standard error of the mean

sEV – Small extracellular vesicle

SH-SY5Y – Neuroblastoma cell line

siRNA – short interfering Ribonucleic acid

SIRT1 – Silent information regulator 1

SNCA – Alpha synuclein

SNP – single nucleotide polymorphism

SOD – Superoxide dismutase

SV2A – Synaptic vesicle protein 2A

Syt1 – Synaptotagmin 1

TDP-43 - TAR DNA-binding protein-43

TEM – Transmission electron microscopy

TEMED – Tetramethyl ethylenediamine

TNF-α – Tumour necrosis factor alpha

TSG101 – Tumour susceptibility gene 101

UBS – Ubiquitin-proteasome system

UTR – Untranslated region

YOAD – Young-onset Alzheimer's disease

Acknowledgments

First of all, I want to thank my supervisors, Gemma and Arijit, for giving me the opportunity to be at this point now. I will always appreciate their constant guidance, support, and wisdom at all times, and am grateful that they always went beyond being a supervisor of a PhD project, and put so much effort into supporting my growth as an individual. I am thankful to have been taken under the wing of great supervisors and great people!

To the Lace and Mukhopadhyay groups, who I've had the privilege of sharing many great times together, thank you for your support and friendship throughout. Particularly to Sowmya, who went through all the PhD checkpoints with me and who trailblazed the lab, without her I would have been lost! Thanks to those that led the way and looked after me in my early years, Neha and Richard, and Oyindamola, Joe, and Nishtha, who have been fantastic company and great friends! Thanks to everyone who has given me advice as well!

Thanks to everyone who has suffered along the way with me in Salford: Sonia, Fanni, John, Chiara, Zahra, Toni, Adesuwa, Grace, Muna, who are all going to go and do great things. Special mention goes out to Rumana, who was my rock in TM and Salford from the beginning, thanks for always going above and beyond!

To my friends, Silver Susan, Pie Friends, Alysha and everyone at home, thanks for the morale support and being there through it all! Thanks to everyone at football and MMU for providing a good way to end the week and an opportunity for a drink.

Finally, thanks to my family, there aren't probably enough words for the amount I need to say thanks for, but thanks for letting me stay at home when I ran out of money for starters!

I can't finish without acknowledging everyone who has provided me food on many (many!) occasions, my knees hurt a lot more than they used to, but my heart is better for it! I will also thank the fridge magnet with the inspirational quote in my kitchen, I read that a lot when I was writing…

I dedicate this to my aunt, who will always inspire me to be adventurous and to go and see the world.

Abstract

Alzheimer's disease (AD) is the leading cause of dementia, a syndrome impacting over 900,000 people in the UK alone. There are currently no disease modifying treatments for AD, which is largely attributable to the heterogenous basis of the disease which is known to have multiple genetic and environmental contributors. Early identification of the pathogenic drivers of disease could help with both the diagnosis of specific dementia subtypes and the development of more targeted, personalised, therapeutic interventions.

Extracellular vesicles (EVs) can cross the blood-brain-barrier and have been shown to carry AD associated cargoes, including amyloid-β and tau. EV miRNA presents a promising avenue for biomarkers for AD. Within this project, EVs were isolated from fibroblasts, hydrogen peroxide treated SH-SY5Y cells and human brain tissue, by sequential centrifugation and separation by size exclusion chromatography. Isolated EVs were characterised using western blotting, fluorescence nanoparticle tracking analysis, and transmission electron microscopy. MiRNA analysis was performed using qPCR and small RNA sequencing.

Isolated EVs displayed size ranges in line with small EVs (< 150 nm) and expressed EV associated proteins, including tetraspanins CD9, CD63 and CD81, while not expressing cellular associated markers. Small RNA sequencing identified a panel of upregulated (miR-203a, miR-141, miR-361, miR-30a, and miR-125b-1) and downregulated (miR-582 and miR-1248) miRNAs in brain derived EVs (BDEVs) in AD. In fibroblast derived EVs, miR-146, miR-92a and miR-134 were upregulated in both qPCR and RNA sequencing, while miR-134 was downregulated in SH-SY5Y EVs. When stratified for females, miR-27a and miR-668 displayed increased dysregulation in BDEVs in AD. miR-185, miR-132 and miR-660 showed converse patterns of dysregulation in AD, between fibroblast derived and brain derived EVs. In both, fibroblast derived and brain derived EVs, miR-660 was inversely dysregulated in AD between males and females.

Combined we highlight a panel of EV miRNAs that show promise as biomarkers for AD that express centrally and peripherally, that can support early intervention of disease.

Key words: Alzheimer's disease, extracellular vesicles, miRNA, fibroblast, brain tissue, SH-SY5Y, biomarkers

1 Chapter 1: Introduction

1.1 Alzheimer's disease

1.1.1 Alzheimer's disease and dementia

Dementia is a term used to describe a set of impaired cognitive symptoms that gradually inhibit normal daily functioning. The diseases which cause dementia are predominantly perceived as disorders of memory impairment, but a multitude of behavioural and functional changes can occur during the different disease progressions based on the underlying brain abnormalities. The current ageing population has introduced dementia as a global health challenge. Worldwide prevalence levels are projected to triple by 2050, presenting a major burden to health services, economies and the estimated 150 million people and their families who will be affected by some form of dementia (Prince *et al*, 2015). In the UK alone, there are currently 900,000 people living with dementia, which is also predicted to rise sharply (Wittenberg et al, 2019). It is apparent that the lack of disease modifying treatments in AD is a major challenge for health organisations, as without new interventions, the numbers predicted in these reports will be more likely to be reached. Even a treatment to slow the development of symptoms in AD would have a significant impact on lowering the burdens, both personally and financially, on individuals and health organisations alike (Wittenberg et al, 2019).

The causes of dementia are widely heterogeneous, accommodated by the vast complexity of the neuronal networks that make up the brain, and their molecular underpinning. Therefore, while there are numerous safeguards and neuroprotective mechanisms in place, the accumulation of factors gradually exert pressure onto the brain, as well as the rest of the body (De Strooper and Karran, 2016). AD is the most common disease underlying the dementia spectrum, this is followed by vascular dementia, however more recently a mixed pathology dementia has been categorised, as Alzheimer's and neurovascular pathology are commonly found in parallel to each other (Wittenberg et al, 2019). Dementia with Lewy bodies (DLB), when combined with cases of Parkinson's disease

dementia (PDD) as the collective Lewy body dementia (LBD), accounts for approximately 20% of all late-life dementia. Therefore, it is second only to Alzheimer's pathology as a distinct cause of dementia (Heidebrink, 2002). Fronto-temporal lobar dementia (FTLD) consists of multiple dementias, such as behavioural-variant FTLD, primary progressive aphasia and Pick's disease (Rohrer *et al*, 2011). FTLD prevalence is relatively low compared to other causes of dementia, at approximately 10%, which significantly increases in dementia cases under the age of 65 years, where it is the second most common cause of young-onset dementia (Wittenberg et al, 2019). FTLD and motor neuron disease/ amyotrophic lateral sclerosis (MND/ALS) are linked on the same spectrum (ALS-FTD), with similar genetic underpinning (Strong *et al*, 2017). Other rarer causes of dementia can include Creutzfeldt-Jakob disease and normal pressure hydrocephalus (Stoeck *et al*, 2012; Jaraj *et al*, 2017).

AD accounts for approximately 2/3 of dementia cases. As well as the memory deficits, AD patients can display impaired problem solving, spatial perception, reading and ability to interact socially, amongst numerous other characterised deficits that can contribute to an impaired quality of life (Alzheimer's Association, 2018). AD involves the aggregation of the pathological neurofibrillary tangles and extracellular plaques associated with hyperphosphorylated tau and amyloid-β (Aβ) proteins (Hardy *et al*, 1992; De Strooper and Karran, 2016). The accumulation of neuropathology is associated with progressive neuronal damage, which is the driving force behind the subsequent cognitive impairment (Palop and Mucke, 2010).

Aβ is one of the longest associated mechanisms for AD, originally being identified in extracellular plaques which were commonly observed in the AD brain (Glenner and Wong, 1984), and the basis of the frequently used Thal neuropathological staging of AD (Thal et al, 2002). The amyloid cascade was developed based on weight of evidence linking Aβ to disease progression (Selkoe and Hardy, 2016), including the role of the amyloid precursor protein (APP) gene in familial AD (FAD) (Chartier-Harlin et al, 1991). Further evidence also observed that processing of APP by beta- and gamma-secretases also triggered the accumulation of Aβ protein in FAD (Citron et al, 1992; Rogaev et al, 1995). The proteolysis of Aβ can form different sized Aβ species, the two most prominent being $A\beta_{1\text{-}42}$ and $A\beta_{1\text{-}40}$ (Gravina et al, 1995), with the longer $A\beta_{1\text{-}42}$ species being observed as more neurotoxic and

associated with AD plaques (Scheuner et al, 1996). The $A\beta_{1-40}$ species has been observed more so in cerebral amyloid angiopathy (CAA), where there is an accumulation of Aβ in the vasculature of the brain (Rovelet-Lecrux et al, 2006). Aβ leads to neuronal damage through multiple dysregulated pathways, including in a forward feedback loop of induction of reactive oxygen species (ROS), which in turn can interact with Aβ and other molecules, including lipids, that can be subsequently neurotoxic (Subramaniam et al, 2002; Cheignon et al, 2018). The interactions that Aβ have in the brain depend on the form and solubility of the molecule, with $A\beta_{1-42}$ more likely to aggregate as it is less soluble than $A\beta_{1-40}$ (Scheuner et al, 1996). In fact, it is important to note that Aβ is highly conserved and important for normal function in mammals (Tharp and Sarkar, 2013), with broad roles in synaptic signalling (Rice et al, 2019) and plasticity (Hick et al, 2015). Aβ has been observed to promote brain-derived neurotrophic factor (BDNF) expression, which is an important protein for neurogenesis (Zimbone et al, 2018).

The Aβ cascade hypothesis details the central role of Aβ aggregation in the development of AD, through intermediary neurotoxicity (Selkoe and Hardy, 2016). Changes in function of the proteolytic cleavage of APP, result in larger, less soluble proteins which have increased tendency to misfold, such as the $A\beta_{1-42}$ monomer. Interactions between monomers result in the aggregation of neurotoxic $A\beta_{1-42}$ oligomers, which can subsequently aggregate into larger fibrils of $A\beta_{1-42}$ at a faster rate than smaller Aβ species, including $A\beta_{1-40}$ (Cohen et al, 2015). The larger fibrils accumulate extracellularly to form dense Aβ plaques (Selkoe and Hardy, 2016).

Therefore, the Aβ species is important when discussing AD, and soluble Aβ oligomers can inhibit long term potentiation (LTP) and the formation of synapses (Shankar et al, 2008), reducing postsynaptic densities (Koffie et al, 2009). As Aβ aggregates into large plaques consisting of β-sheets of insoluble fibrils, they can also form an intermediate soluble protofibril form. These formations have also been observed to exact multiple neurotoxic effects on neuronal cells, including the inhibition of LTP (O'Nuallain et al, 2010). The end stage amyloid plaques have been found to interfere with synaptic neurons, triggering a hyperactivity response (Zott et al, 2019). Aβ plaques also display multiple other routes of neurotoxicity, triggering neuroimmune responses and altering the neuronal structure (Meyer-Luehmann et al, 2008), as well as accumulating deposits of Aβ oligomers which

cause damage to synapses beyond the immediate range of the plaque (Koffie et al, 2009). Aβ does not just exert a direct influence on neuronal stability, but can also interact and interfere with cerebral vasculature. $A\beta_{1-42}$ oligomers triggers pericytes to constrict capillaries that are feeding the brain by 30%, a mechanism that is mediated by the production of ROS and the expression of endothelin-1 (Nortley et al, 2019). Combined, there is a depth of literature that observes Aβ as a central mediator of neurodegeneration in AD.

The other major neuropathological player in AD is the neurofibrillary tangles of hyperphosphorylated tau (Wood et al, 1986), the basis of the fundamental Braak neuropathological staging of AD (Braak and Braak, 1995). Tau is important in neuronal stability through its binding microtubules, which is partly mediated by its state of phosphorylation (Cleveland et al, 1977). Tau's significance to normal physiological function is emphasized by the high levels of conservation of the microtubule-associated protein tau (MAPT) gene across species (Neve et al, 1986; Sündermann et al, 2016). The large variation in proteoforms of tau may give some reason to the heterogeneity in AD, as there is wide variation in the toxicity of the different tau isoforms. Tau is found in 6 isoforms in the human brain (0N3R, 0N4R, 1N3R, 1N4R, 2N3R and 2N4R, Lace et al, 2007), having either 3 or 4 microtubule binding domains (3R and 4R, respectively) and 1 of 3 variably sized N-terminal regions (0N, 1N or 2N). Phosphorylation of tau has been proposed to trigger aggregation of tau into a neurotoxic form, as phosphorylation regulates the micro-tubule binding function of tau (Hoover et al, 2010). Post-translational modifications of tau, such as phosphorylation (Long and Holtzman, 2019), as well as interactions with Aβ (Vergara et al, 2019) can trigger tau to aggregate into insoluble oligomers, which subsequently aggregate into neurofibrillary tangles (NFTs).

Over 90 posttranslational modifications have been observed on tau in the AD brain, with modifications such as phosphorylation to the 0N and 4R isoforms of tau causing higher levels of aggregation as AD progresses (Wesseling et al, 2020). However, phosphorylation of tau happens during different non-pathogenic physiological processes, such as during sleep (Guisle et al, 2020) and brain development (Yu et al, 2009), highlighting that relationships between phosphorylation and neuropathology are not clear cut, and more likely depend on specific groups of phosphorylated isoforms interacting with other factors

to drive AD. For example, the presence of Aβ can exacerbate the accumulation of tau pathology (Bennett et al, 2017) as well as influence the phosphorylation of isoforms (Horie et al, 2020), suggesting there is synergy between the neuropathology in progressing AD. As with Aβ, it is unclear which formulation of tau species or stage of aggregation is the most damaging to neurons, though further mapping of tau posttranslational modifications to the downstream function, ability to aggregate, and neurotoxicity will be important in separating the heterogeneity of AD (Arakhamia et al, 2020). Pathogenic tau has been associated with many challenges to neurons, including binding to synaptic vesicles and subsequently interfering with mobility and release from presynaptic terminals (Zhou et al, 2017). The interaction of tau oligomers at the synapse also triggers the dysfunction of the physiological ubiquitin-proteasome system (UPS), which can lead to further unregulated modification of tau and other proteins, misbalancing the molecular mechanisms that are important for neuronal function (Tai et al, 2012). There is a wealth of information linking tau to neurodegeneration in AD and other tauopathies. Studies show that pathological tau can also dysregulate activity and signalling of pyramidal neurons in the neocortex (Crimmins et al, 2012; Menkes-Caspi et al, 2015), reduce action potential firing in hippocampal neurons (Hatch et al, 2017), and disrupt synaptic plasticity and LTP (Tracy et al, 2016; Sohn et al, 2019). Tau can also trigger neuroinflammatory responses (Maphis et al, 2015), and induce neuronal death through epigenetic dysregulation and subsequent transposable elements, which can become damaging with neuronal aging (Frost et al, 2014; Wood et al, 2016; Sun et al, 2018). In fact, general reduction in tau species may be beneficial in countering multiple of the neuropathological observations in the AD brain, including neuronal loss (DeVos et al, 2017). However, given that tau is also an essential physiological protein, such global targeting methods could be deleterious (Kent et al, 2020), and more targeted approaches to anti-tau and anti-Aβ (discussed below) therapies would improve benefit to detriment ratio. Therefore, further ways to expand diagnosis of subpopulations of AD with differential neuropathology would greatly support this approach.

More studies are noting that the accumulation of either Aβ or tau neuropathology alone are not as well correlated with downstream pathological responses and neuronal damage, as when both types of neuropathology are observed in unison (Pascoal et al, 2017; Prokop

et al, 2019; Busche and Hyman, 2020). This highlights that while the comprehension of AD associated neuropathology has been present for over a century (Alzheimer, 1907; Hippius and Neundörfer, 2003), the pathways by which they contribute to pathogenesis are still not completely defined. While research up to now has provided promising targets for treatment, focusing on the hallmarks and some genetic risk factors of AD, it remains without any treatments that have successfully slowed or stopped the progression of neurodegeneration (Karran and De Strooper, 2016). This may be down to the difficulty in diagnosing neurodegenerative diseases before the symptoms appear, at which point, according to the gathering consensus, the pathology may have spread beyond a stage at which current treatments are effective. In fact, current evidence indicates that neuropathology accumulation in the brain can take place between 10-20 years prior to the onset of symptoms (Brookmeyer and Abdalla, 2018; Dang et al, 2018; Roberts et al, 2018).

Most pharmaceutical interventions in the pipeline for AD are targeting disease modification (68% in phase 3 clinical trials), the highest proportion of which is targeting amyloid (Cummings et al, 2022). A list of current of phase 3 clinical trials for disease modifying therapies (DMT) is displayed below (Table 1.1, taken and adapted from Cummings et al, 2022).

Table 1.1. Phase 3 clinical trials of disease modifying therapies for Alzheimer's disease.

Candidates listed are part of ongoing phase 3 trials that are targeting common Alzheimer's disease and related disorders research ontology (CADRO) pathways. The mechanism of actions highlights how the candidate is proposed to reduce the pathways contribution to AD (Cummings et al, 2022).

Agent	CADRO mechanism class	Mechanism of action	Stage of AD targeted	Estimated end date
Aducanumab	Amyloid	Monoclonal antibody directed at Aβ plaques and oligomers	Prodromal AD	Oct-23
AGB101 (low-dose levetiracetam)	Synaptic Plasticity/ Neuroprotection	SV2A modulator; to reduce Aβ-induced neuronal hyperactivity	MCI Prodromal AD	Dec-22
Atuzaginstat (COR388)	Synaptic Plasticity/ Neuroprotection	Bacterial protease inhibitor targeting gingipain produced by *P. gingivalis* to reduce neuroinflammation and hippocampal degeneration	Mild to moderate AD	Dec-22
Blarcamesine (ANAVEX2-73)	Synaptic plasticity/ Neuroprotection	Sigma-1 receptor agonist, M2 autoreceptor antagonist; to ameliorate oxidative stress, protein misfolding, mitochondrial dysfunction, and inflammation	MCI Early AD	Jun-22
Donanemab	Amyloid	Monoclonal antibody specific for pyroglutamate form of Aβ	Prodromal AD	Aug-25
Donanemab & Aducanumab	Amyloid	Monoclonal antibody specific for pyroglutamate form of Aβ (donanemab); monoclonal antibody directed at plaques and oligomers (aducanumab); given in separate arms of the trial	Early symptomatic AD	Jun-23
Gantenerumab	Amyloid	Monoclonal antibody directed at Aβ plaques and oligomers	Prodromal to mild AD	Oct-26
Gantenerumab & Solanezumab	Amyloid	Monoclonal antibody directed at Aβ plaques and oligomers (gantenerumab); Monoclonal antibody directed at Aβ monomers (solanezumab); given in separate arms of the trial	Prevention Pre-symptomatic FAD	Jul-22
GV-971	Gut-brain axis	Algae-derived acidic oligosaccharides; changes microbiome to reduce peripheral and central inflammation	Mild to moderate AD	Oct-26
Hydralazine	Oxidative stress	Free radical scavenger	Mild to moderate AD	Dec-23
Icosapent ethyl (IPE)	Oxidative stress	Purified form of the omega-3 fatty acid EPA; to improve synaptic function and reduce inflammation	Prevention High risk AD	Jan-23

Lecanemab (BAN2401)	Amyloid	Monoclonal antibody directed at Aβ protofibrils	Early AD Preclinical AD	Aug-24
Losartan & Amlodipine & Atorvastatin + exercise	Vasculature	Angiotensin II receptor blocker (losartan), calcium channel blocker (amlodipine), cholesterol agent (atorvastatin)	Risk reduction High risk AD	Jan-22
Metformin	Metabolism and bioenergetics	Insulin sensitizer to improve CNS glucose metabolism	MCI	Apr-25
NE3107	Inflammation	MAPK-1/3 inhibitor; reduces proinflammatory NFκB activation	Mild to moderate AD	Jan-23
Nilotinib BE	Proteostasis/ Proteinopathies	Tyrosine kinase inhibitor; autophagy enhancer; promotes clearance of Aβ and tau	Early AD	Jun-26
Omega-3 (DHA+EPA)	Oxidative stress	Antioxidant	Prodromal AD High risk AD	Dec-23
Semaglutide	Metabolism and bioenergetics	GLP-1 agonist; reduces neuroinflammation and improves insulin signaling in the brain	Early AD	Apr-26
Simufilam (PTI-125)	Synaptic Plasticity/ Neuroprotection	Filamin A protein inhibitor; stabilizes amyloid-alpha-7 nicotinic receptor interaction	Mild to moderate AD	Oct-23
Solanezumab	Amyloid	Monoclonal antibody directed at Aβ monomers	High risk AD	Jun-23
Tricaprilin	Metabolism and bioenergetics	Caprylic triglyceride; induces ketosis and improves mitochondrial and neuronal function	Mild to severe AD	Feb-24
TRx0237	Tau	Tau protein aggregation inhibitor	MCI AD	Mar-23
Valiltramiprosate (ALZ-801)	Amyloid	Prodrug of tramiprosate; inhibits Aβ aggregation into toxic oligomers	Early AD	May-24

Abbreviations: Aβ, amyloid beta; BE, bioequivalent; CADRO, Common Alzheimer's disease and Related Disorders Research Ontology; EPA, eicosapentaenoic acid; GLP-1, glucagon-like peptide-1; MAPK, mitogen activated protein kinase; NFκB, Nuclear Factor Kappa B; SV2A, synaptic vesicle protein 2A; MCI, mild cognitive impairment. clinicaltrials.gov.

While as of 2022, there are no disease modifying treatments for AD, that robustly halt or even slow down the progression of symptoms, the field may be on the brink of change. In one of the most promising clinical trials for targeting cognitive decline in AD, it has been

observed that the human IgG1 monoclonal antibody, Lecanemab, against Aβ soluble protofibrils, reduced the fibrils and participants displayed slowed decline in cognitive impairment, over an 18-month time course (van Dyck et al, 2022). Notably, this trial was targeted towards early AD (McKhann et al, 2011), which highlights that the interventions are most effective when targeting AD at the earliest stage possible, which is why it is essential that more comprehensive biomarkers are discovered to support this (Veitch et al, 2018; Reiss et al, 2021). Furthermore, the efficacy of anti-amyloid therapies remains debated in AD. The recent approval of aducanumab, another anti-amyloid therapy, remains controversial, given the cognitive benefit outcome was disagreed upon (Walsh et al, 2021). While other concurrent anti-amyloid trials are not showing consistent cognitive end points (Salloway et al, 2021; Mintun et al, 2021), which could highlight that anti-amyloid therapies may not be consistently effective across the entire AD population. This also points out the need for more biomarkers for AD, not just to detect AD as early as possible, but also to determine whether different subpopulations of a largely heterogenous AD population can be distinguished, which can then stratify future trials and improve clinical outcomes.

Recent attention has been directed to the risk factors for AD and dementia, with modifiable environmental factors accounting for approximately 40% of all dementia cases that have been identified (Figure 1.1, Livingston *et al*, 2020). These factors include socio-economic factors such as less education and increased alcohol intake, as well as smoking and obesity. Other factors include depression, physical inactivity, diabetes, hypertension, hearing loss, traumatic brain injury (TBI), air pollution and social isolation (Livingston *et al*, 2020).

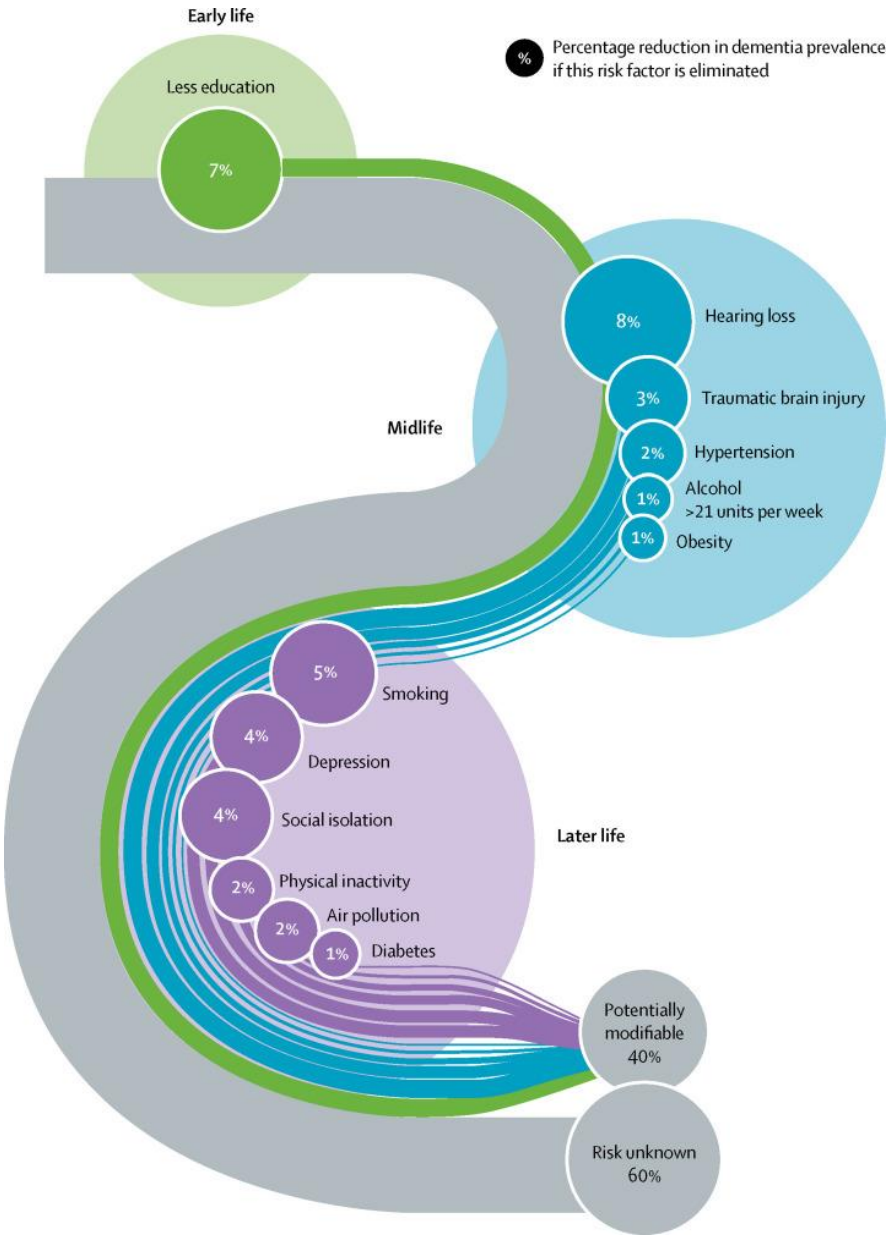

Figure 1.1. Modifiable risk factors for Alzheimer's disease.

Current estimation of the proportion of risk of AD that is potentially modifiable at various stages of life, including early life (green), midlife (blue) and later life (purple). A larger bubble next to the corresponding environmental risk factor indicates a higher estimated risk to contribute to AD onset. Taken from Livingston et al (2020).

There is a developing consensus that targeting these modifiable risk factors could proportionately reduce, or at least delay the onset of symptomatic AD in large populations, based on correct stratification (Livingston *et al*, 2020). Trials that have attempted to target multiple of the measurable risk factors for AD in one study, including cardiovascular risk factors, have shown that adjusting diet, exercise and other general health management

can be beneficial in slowing cognitive decline (Rosenburg et al, 2017). Importantly, when the study population was stratified based on preliminary cortical thickness in AD, in brain regions such as entorhinal, inferior and middle temporal regions, a potential measure to determine staging of AD based on structural changes, it found that participants that had less observed brain changes, were more susceptible to cognitive benefits from the intervention (Stephen et al, 2019). Similar observations were seen in other studies that provided self-managed intervention for participants with cardiovascular risk factors for AD, with the greatest effect seen in the younger subpopulation (65-70 years), where AD pathogenesis has not progressed as much (Richard et al, 2019). Again, this emphasises the need for early diagnostic criteria for AD, given that both pharmaceutical and multimodal risk factor interventions both have shown more promising results when targeting participants with less advanced AD associated changes. On top of that, biomarkers that can differentiate subpopulations based on different presentation of MCI or varying risk factors, will lead towards personalised treatments for AD (Kivipelto et al, 2020).

There are also various contributary genetic risk factors, alongside the predominant risk factor of age (Hébert *et al*, 2010). Of the genetic risk factors for sporadic AD, the *APOE* (apolipoprotein) gene is the most prevalent, with approximately 60% of people diagnosed with AD having at least one *APOE-e4* copy (Ward *et al*, 2012). The *APOE* gene has three alleles (*ApoE-e2, ApoE-e3 and ApoE-e4),* based on single nucleotide polymorphisms near the gene (rs429358 (C > T) and rs7412 (C > T)) which code for different APOE protein isoforms (Zannis et al, 1982). Between the isoforms, *ApoE-e4* is structurally distinct, with increased interaction between the N- and C-terminal domains (Belloy et al, 2019). Apolipoprotein E has been shown to play a fundamental role in brain metabolic homeostasis, including lipid transport and neuronal signalling, as well as the transport, aggregation, and clearance of Aβ (Liu *et al*, 2013). Therefore, changes in the function of this protein can significantly alter the risk of developing AD (Liu *et al*, 2013). Interestingly, the *APOE-e2* allele is associated with reduced risk of AD, highlighting the need for further research into this protein and its variants, and how these variants may influence disease processes both antagonistically (*APOE-e4)* and protectively (*APOE-e2*; Reiman *et al*, 2020). There are certain genetic mutations that can significantly increase the risk of developing AD, namely FAD, which is associated with an earlier onset of symptom development. This

type of AD is associated with mutations in the amyloid precursor protein (*APP*) gene, as well as for the presenilin 1 and presenilin 2 genes (*PSEN1 and PSEN1*) (Ryman *et al*, 2014). Presenilin mutations influence the gamma and beta secretase processing of APP, which causes variations in the production of $A\beta_{1\text{-}40}$ / $A\beta_{1\text{-}42}$ protein (Sun et al, 2017), and disrupting normal neuronal functioning as discussed above. Mutations to the presenilin genes can also result in loss of function detrimental effects in AD, independent of the amyloid cascade (Shen and Kelleher, 2007). Presenilin 2, for example, has important roles in calcium (Ca^{2+}) signalling, and mutations in AD can result in inefficient handling of Ca^{2+}, hereby limiting efficient autophagic function (Fedeli et al, 2019). Presenilin 1 loss of function has been linked to impaired synaptic plasticity and hippocampal memory function (Xia et al, 2015). FAD accounts for approximately 1% of all AD cases (Alzheimer's Association, 2018), even then there is variation between age and symptoms at onset, which highlights the multifactorial influence of other risk factors that also accompany a variation of mutations to these highly penetrant risk genes (Ryman *et al*, 2014). Genetic variations in miRNAs, such as the miR-1229 rs2291418 allele, have also been attributed to increased risk of AD (Ghanbari et al, 2016), highlighting the need to further understand the genetic contributions to disease, including the complex genetic-epigenetic interactions, if we are to develop new diagnostic tools and treatments.

Earlier diagnosis will fundamentally improve treatment options, both allowing for intervention at earlier stages as well as potentially defining subpopulations in which a personalised therapy can be administered. This will also improve as a more comprehensive understanding of the contribution of neuropathology and the damage it causes, particularly at the early stages of AD, to neuronal integrity, and how this impacts disease progression.

Current hallmark proteins associated with neurodegenerative disease are the first logical target for biomarker selection (Figure 1.2). Combined PET (Positron emission tomography) imaging and cerebrospinal fluid (CSF) strategies have been recommended, including scanning for tau, Aβ and neuronal injury, while analysing the same neuropathology in the CSF (Jack *et al*, 2016), however, there is still an ongoing discussion as to what stage distinct neuropathology contributes to neurodegenerative disease. Moreover, with the vastly multifactorial nature of AD, understanding the early disease contributors and pathway

disruptions that precedes neuropathology development and neuronal damage, would provide novel early therapeutic targets and the potential for personalised treatment approaches. For example, the impact of neuroinflammation is established to be a major factor in the progression of numerous neurodegenerative diseases and can exacerbate the spread of neuropathology (Hickman *et al*, 2018; Henstridge *et al*, 2019). Neuroinflammation is a largely multifactorial response that can be driven by tau (Wang et al, 2018; Stancu et al, 2019) and Aβ pathology (Heneka et al, 2013; Terrill-Usery et al, 2014; Zhao et al, 2018), however it can also work to counter AD (Keran-Shaul et al, 2017; Lee et al, 2018), showing that even the molecular mechanisms underlying AD are largely complex and heterogenous. AD can be driven by conditions such as obesity (Puig et al, 2012), sleep disturbance (Irwin and Vitiello, 2019), head trauma (de Rivero Vaccari et al, 2018; Winston et al, 2019; Li et al, 2020) and oxidative stress (Miller and Sadeh, 2014, Venegas et al, 2017). One clinical trial investigated statins, which may limit neuroinflammation particularly related to head trauma (Peng et al, 2014; Xu et al, 2017), in patients with concussion and found that use of statins reduced the risk of dementia by 13% in 5 years following concussion (Redelmeier, Manzoor and Thiruchelvam, 2019).

There is consistent evidence that AD is heterogenous, with individuals presenting with complex set of risk factors prior to disease onset. Therefore, being able to identify early drivers of disease, such as neuroinflammation or oxidative stress, along with early pathological changes, will provide a novel perspective for the development of preventative and early diagnostic strategies.

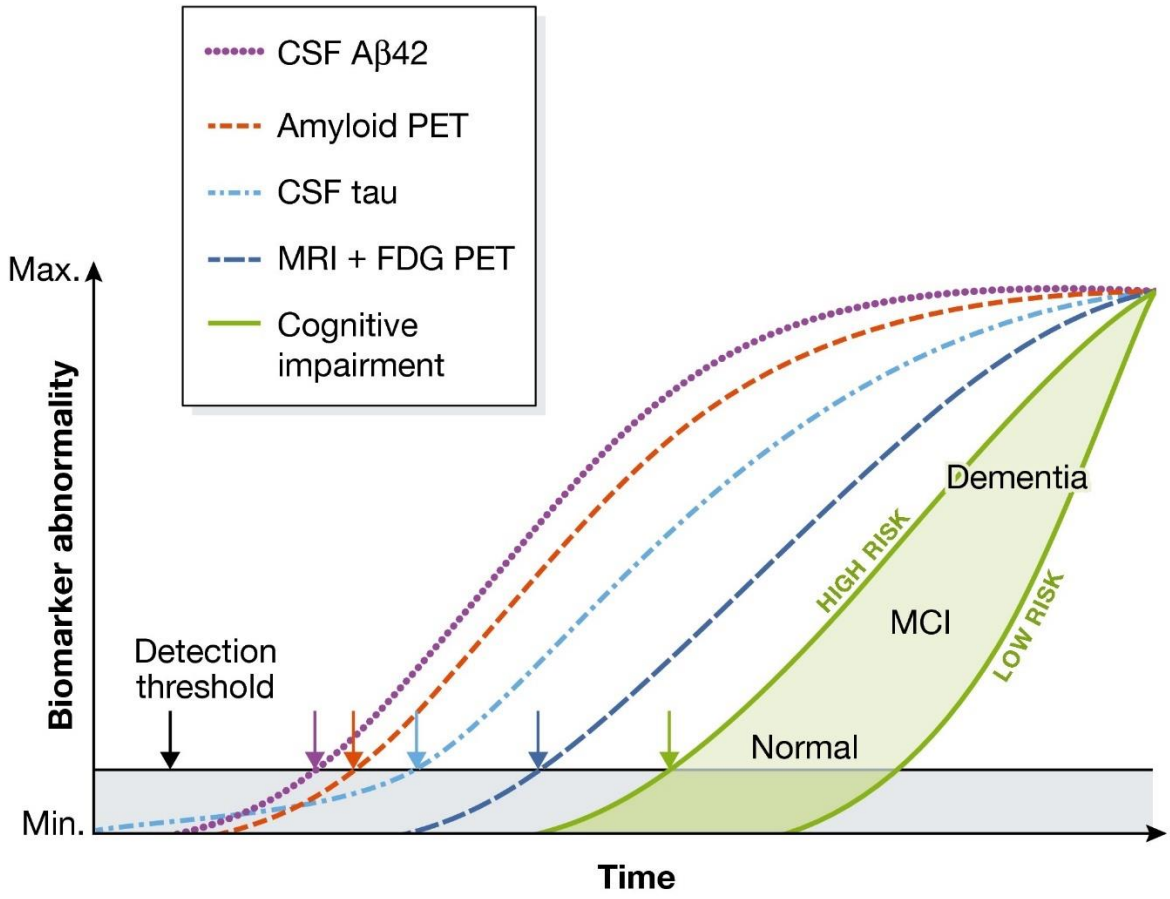

Figure 1.2 Current biomarker candidates for Alzheimer's disease.

Focus for current biomarkers for AD have been on the hallmark neuropathology, tau and Aβ. Tests have been developed to detect these proteins in the CSF (displayed) and blood of patients, and compare them to neuropathological imaging in the brain (PET). Fluid biomarkers are more accessible and so can potentially identify AD changes at an earlier pre-symptomatic stage. Graph shows theoretical time points at which these tests could detect abnormal AD associated changes, in relation to each other and the onset of symptoms, highlighted in green (cognitive impairment). PET – positron emission tomography; Aβ42 – Amyloid beta 1-42; FDG – fluorodeoxyglucose; MCI – mild cognitive impairment; Detection threshold = stage of disease at which the provisional biomarker can be detected as differential expressed to normal. Taken from Selkoe and Hardy (2016).

1.1.2 Oxidative stress and Alzheimer's disease

Along with the accumulation of neuropathology, one of the most well characterised molecular changes that occurs in AD is increased oxidative stress, which has been established in AD for 30 years (Markesbery, 1997). Oxidative stress is defined as 'An

imbalance between oxidants and antioxidants in favour of the oxidants, leading to a disruption of redox signalling and control and/or molecular damage', and therefore can encompass numerous molecular changes (Sies and Jones, 2007). Some of the subclassifications of oxidative stress associated with AD encompass mitochondrial dysfunction and increased levels of reactive oxygen species (ROS), including hydrogen peroxide (H_2O_2) (Huang *et al*, 1999; Cosín-Tomàs et al, 2019). Notably, signs of impaired mitochondrial activity, including impaired glucose and lipid metabolism (Valla *et al*, 2010; Doll et al, 2017) and changes to mitochondrial trafficking, morphology and function (Trushina *et al*, 2012; Wang et al, 2014; Misrani et al, 2021), have been observed within the early stages of AD development, and have been hypothesised to precede the accumulation of neuropathology. High levels of ROS and damaged mitochondria can both trigger neuroinflammation driven neurodegeneration (Joshi et al, 2019), highlighting the complex interplay between factors that precede AD. Others have observed that oxidative stress occurs in brain regions that are less susceptible to AD associated damage, therefore, investigating these areas may provide further insight into the changes that occur in the brain at the earlier stages (Youssef et al, 2018). Oxidative stress has also been identified as a potential therapeutic target for AD, with improvements in downstream mitochondrial function apoptosis and functional memory (Chen et al, 2018; Ali et al, 2018; Zhang et al, 2019; Martini et al, 2019). Currently, there are multiple phase 3 clinical trials that are pharmaceutically targeting oxidate stress pathways (Table 1.1, Cummings et al, 2022), both at preclinical and early stages of AD to investigate the efficacy of reducing the risk of development and progression of cognitive decline. Hydralazine is one such repurposed anti-hypertensive drug on trial, which is proposed to be neuroprotective through targeting nuclear factor E2-related factor 2 (Nrf2), which subsequently activates downstream antioxidative pathways (Dehghan et al, 2017). It has also previously been observed to protect against lipid oxidation and Aβ fibril formation (Maheshwari et al, 2010), as well as protecting against H_2O_2 induced neurotoxicity in the SH-SY5Y human neuroblastoma cell line (Guo et al, 2019). Trials are also targeting Icosapent Ethyl (a purified omega-3 ester) due to its broad spectrum of influence, including reducing triglycerides, cholesterol, and inflammation (Bays et al, 2013), as well as reduced risk of cardiovascular insults (Bhatt et al, 2019). Notably, one of the main outcomes of the trial is the oxidative responses, given

that Icosapent Ethyl is also an anti-oxidant, particularly inhibiting lipid peroxidation (Bhatt et al, 2020).

Markers of metabolic changes can also be observed in peripheral biofluids in early-stage AD and mild cognitive impairment (MCI), including disturbed energy metabolism and mitochondrial function pathways in the CSF (Trushina *et al*, 2013). This suggests that oxidative stress related impairment is both underlying AD pathogenesis and potentially capable of being used in biomarker analysis of AD changes. However, as with other current AD diagnostic methods, measuring oxidative stress in the brain is not viable and work still needs to be performed to determine whether these factors can be measured peripherally.

Oxidative stress has been implicated in mediating the dysfunction of synapses caused by Aβ (Calkins *et al,* 2011) and the downstream effects of neuropathological accumulation, including lipid peroxidation (Rosales-Corral *et al,* 2012) and excitotoxicity from N-methyl-D-aspartate (NMDA) receptor mediated Ca^{2+} influx (Snyder *et al*, 2005). Interestingly, oxidative stress can also impact the formation of neuropathology, for example, lipid peroxidation can modify tau epitopes which promote the formation of phosphorylated neurofibrillary tangles (Liu *et al*, 2005). Furthermore, ROS such as H_2O_2 can interact with Aβ, altering its metal binding affinity and causing the production of more ROS, creating a positive feedback loop which could intensify AD progression (Cheignon *et al*, 2016; 2017).

With oxidative stress having such an apparent role in early AD (Butterfield et al, 2010; Arimon et al, 2015; Cheignon *et al*, 2016; 2017), it is important that studies investigate the underlying oxidate stress in models of AD, as it drives neuropathological accumulation and progression (Calkins *et al,* 2011; Arimon et al, 2015) which in turn triggers further lipid peroxidation (Di Domenico et al, 2017; Martins et al, 2018), contributing to synaptic damage and neurodegeneration (Scheff et al, 2016; Martins et al, 2018). When considering models that can target the early changes in AD, it is interesting to note that fibroblasts derived from AD patients display an oxidative phenotype (Ramamoorthy *et al*, 2012), and therefore warrant further investigation. Also, as factors such as oxidative stress drive neuropathological changes in AD, they could also contribute to the spread of neuropathology seen in multiple neurodegenerative disease, as factors such as lipid metabolism and peroxidation have been observed to influence tau deposition (van der

Kant et al, 2020), highlighting that the underlying mechanisms in early AD contribute to subsequent disease progression.

1.1.3 Pathological spread hypothesis

Evidence is gathering that neurodegenerative diseases may anatomically progress with the 'spread' of neuropathology being demonstrated across cell synapses (Lace *et al*, 2009; Pickett *et al*, 2016). Most notably this has been demonstrated in the infectious prion diseases such as Creutzfeldt-Jakob disease, in which the prion protein (PrP) isoforms (PrP^{SC}) transfers transcellularly both in an intra- and inter-organismal manner (Prusiner, 1982; Mays and Soto, 2016). Moreover, the prion-like spread hypothesis has been applied to the transfer of other misfolded proteins complicit in neurodegeneration within the brain, including tau and α-synuclein (Kane *et al*, 2000; Frost and Diamond, 2010; Polymenidou and Cleveland, 2011, 2012; Dunning *et al*, 2013; Walsh and Selkoe, 2016; Yamada *et al*, 2017). The neuropathology has been shown to spread from one brain region to another, preceding the symptomatologic changes that occur as damage to the different functional regions occurs (Figure *1.3*; Lace *et al*, 2009; Masters *et al*, 2015; Schmidt *et al*, 2016).

A recent highlight also brings to light the potential ability of Aβ and tau proteins to be transmitted via an iatrogenic route, where seeding has been observed both after neurosurgical procedures and intramuscular injection (Li *et al*, 2008; Jaunmuktane *et al*, 2015; Purro *et al*, 2018). While it is emphasised that current results do not suggest that Aβ is contagious, it does imply that neuropathology can spread from cell to cell, in ways that are not fully categorised.

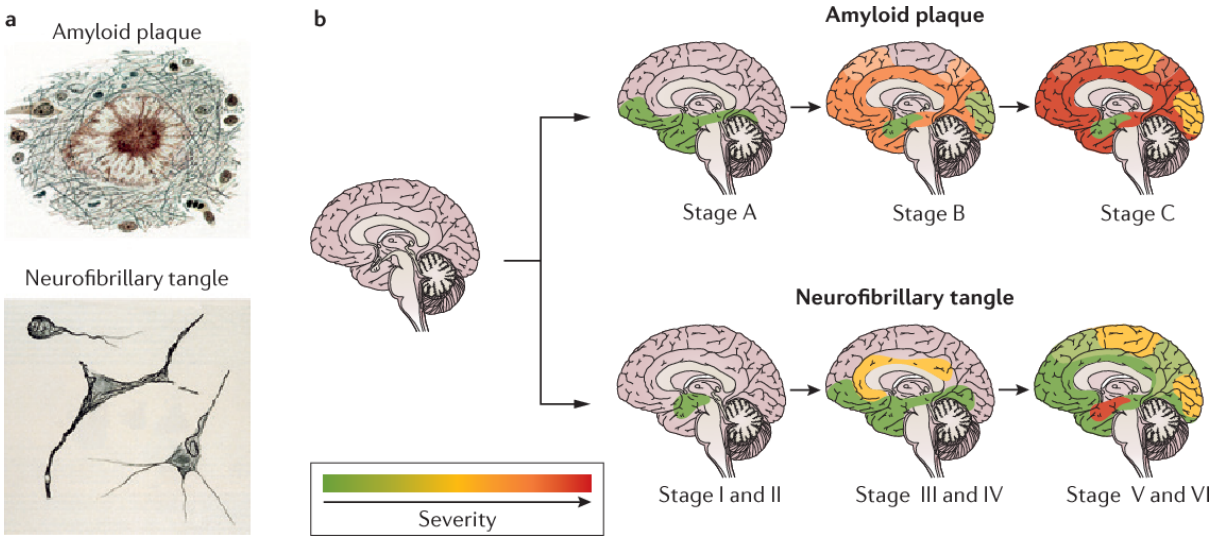

Figure 1.3. The pathological spread of Alzheimer's disease.

AD neuropathology accumulates and spreads in the brain in a hierarchical manner, with both amyloid plaques (A, top) and neurofibrillary tangles (A, bottom) depositing progressively in correspondence to staging of disease. B) Both plaques and tangles typically are observed initially in the temporal and frontal lobes, with amyloid preceding the accumulation of tau. As the disease progressed, neuropathology spreads to other areas of the brain, including the temporal and occipital lobes. Severity indicates the level of neuropathology that accumulates within the brain region at specific time points. Taken from Masters et al (2015).

The question remains, how would the neuropathology spread between cells? Considering the gathering consensus that neuropathology spreads in pre-symptomatic AD, then to elucidate these mechanisms would provide a series of molecular targets that we could utilise to intervene therapeutically, and importantly at potentially reversible stages.

Answers have been sought based on misfolded proteins incorporating into specific cell secretory pathways, but the means to which they would be able to do this remain unclear. Though one mechanism that appears plausible is the intracellular uptake of neuropathological cargo, which can be then released into the brain extracellular space, as well as the CSF and blood, in extracellular vesicles.

1.2 Extracellular vesicles

1.2.1 Extracellular vesicles – History and definitions

Extracellular vesicles (EVs) are nanosized biological particles that are secreted out of the cellular membrane into the extracellular space. The concept of EVs has been known to scientists for almost half a century, when technology reached the capabilities to measures objects on such a scale, with initial reports describing their role in platelet coagulation (Bastida *et al*, 1984). From then, it has been shown that EVs are shed from virtually all cell types, including those of a neuronal lineage (Faure *et al*, 2006). Even then, the field of EV research has only recently taken hold with the development of more sophisticated techniques which could categorise and observe the roles which EVs played within different cells and systems, as well as their cargo (Gould and Raposo, 2013).

The understanding of EV function has progressed since the initial observations of EVs, where, based on their expression of membrane proteins, it was hypothesised that they were used to recycle old membranes from the cell surface (Colombo *et al*, 2014). However, with discoveries that EVs were enriched in various cargo, from the first observed proteins, major histocompatibility (MHC) class II molecules (Raposo *et al*, 1996), up to the more recent discoveries of RNA, including small RNAs such as miRNAs, (Ratajczak *et al*, 2006; Valadi *et al*, 2007; Skog *et al*, 2008), it has become clear that EVs are involved in a more comprehensive set of processes than previously considered.

The discovery that EVs contained such a broad cargo sparked the interest into their functions, not least their role in intercellular signalling. In addition, EVs have been observed to display CD47 which inhibit their uptake by phagocytes (Kamerkar *et al*, 2017), a protein previously observed to be utilised by tumours (Liu *et al*, 2017). These so called ‘do not eat me’ signals support the EV’s ability to travel stably within the circulation (Kamerkar *et al*, 2017), supporting their potential use as biomarkers.

One of the other key roles of EVs is to facilitate the release of waste products from the cell via exocytosis and reduce stress resulting from cytotoxicity. EV biogenesis is closely linked to macro autophagy by the endolysosomal pathway, as well as via complexes fundamental to autophagy (e.g. ATG5-ATG16 complex) that have been observed to also contribute to

EV biogenesis (reviewed by Xu *et al*, 2018). Since defects in autophagy are well characterised in AD (Nixon, 2013), further research into the autophagy-EV cross-talk could develop a greater understanding of how EVs can contribute to cellular homeostasis, and alternatively, how they may propagate cellular waste. Once within the extracellular space, the EVs and their cargo can be taken up by a recipient cell via multiple pathways, potentially leading to the transfer of molecules that are neurotoxic and this could have implications in the spread of neuropathology in neurodegenerative disease (Maas *et al*, 2017; Abdulrahman *et al*, 2018).

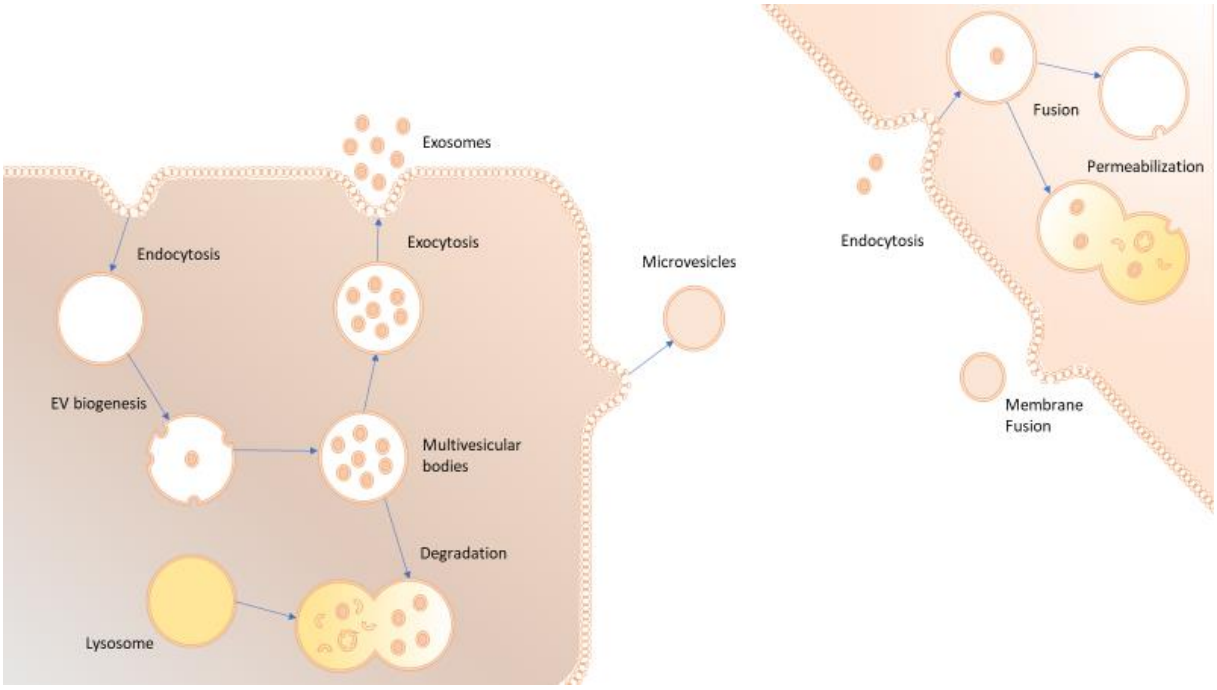

Figure 1.4. Extracellular vesicle biogenesis and transfer.

Exosomes are formed through the endosomal pathway. The endosomal sorting complex required for transport (ESCRT) machinery promotes the invagination of early endosomes to form multivesicular bodies (MVBs), containing intraluminal vesicles (ILVs). MVBs can fuse with lysosomes, promoting the degradation of any internal biomolecules, or with the cellular membrane, where the ILVs are secreted into the extracellular space as exosomes. Microvesicles are formed independently of the endosomal pathway, with outward budding of the cellular membrane partially promoted by the ESCRT machinery. Extracellular vesicles can interact with cell surface receptors, which either initiate intake of the vesicles via endocytosis or fusion of the vesicles to the cellular membrane. Extracellular vesicles taken in via endocytosis can subsequently fuse with the endosomal membrane. Both pathways result in the release of the cargo into the cell. Created in Microsoft PowerPoint.

EVs are generally classified into microvesicles (MVs) and exosomes, where they are primarily differentiated by their mode of release from the cell membrane (Figure *1.4*). Exosome secretion is one of the end stages of the endosomal pathway, a process by which a cell membrane invaginates, taking up fluid and membrane receptors, forming an intracellular vesicle called an early endosome (Booth *et al*, 2006). During endocytosis, the early endosomes undergo a maturation process where they develop into late endosomes, which can then fuse with lysosomes or are engulfed and degraded by autophagosomes. However, while the early endosome is undergoing maturation, further membrane invagination can occur within the endosomal bodies, resulting in the formation of multiple intraluminal vesicles (ILVs) within the endosomal membrane. Notably, ILV formation is predominantly regulated by a series of proteins, including tetraspanins, that are a part of the endosomal sorting complex required for transport (ESCRT) machinery (Colombo *et al*, 2014; Christ *et al*, 2017), some of which are used as markers to categorise EVs (Table 1.2). This is because the ESCRT proteins are taken up in membrane of the ILVs as they mediate the invagination of endosomes. ILV containing multi-vesicular bodies (MVBs) can then bind to the cell membrane, which releases the cargo from the cell (Colombo *et al*, 2014). The ILVs secreted into the extracellular space are termed exosomes, which have a typical diameter of 40 to 150 nm.

MVs are formed independently of the endosomal pathway (Figure *1.4*), via the outward budding of the cellular membrane, although this process is also partially regulated by the ESCRT machinery. While the method of secretion from the cell body differs, there is a lot of similarity between MVs and exosomes that causes difficulty in distinguishing between the EV subtypes, from the display of ESCRT markers on the vesicles to a cross-over in smaller vesicle diameter. MVs encompass much larger vesicles as well, with a currently defined range from 50 to 2000 nm (Maas *et al*, 2017).

It is current difficult to accurately determine the origin and biogenesis of an EV, and so, be able to categorise an EV sample as exosomes vs MVs, for example. Therefore, the international consensus recommends the use of terms such as small extracellular vesicle (sEV) for particles that have been measured within a definitive range (i.e.: < 200nm) (Théry *et al*, 2018). Any further descriptive information about the composition of the EV will add further support to the study, including origin of EV – including cell (if from cell culture) or

biofluid (blood, tissue, CSF, saliva, etc), cell culture details– including passage number, seeding densities, treatments, cell conditions, media composition, EV harvesting protocols, biochemical composition (markers associated with the isolated EV sample, Table 1.2) and storage conditions of the isolated EV samples.

EVs have been observed to play a significant role in the progression of tumours in multiple cancers, including in different models of cancers derived from the lung, breast, and prostate (Maacha et al, 2019). Different mechanisms whereby EVs progress cancers have been investigated, including the activation of other non-cancerous cells within the microenvironment (Giusti et al, 2018), promotion of angiogenesis (Kucharzewska et al, 2013), suppression of immune responses (Yamada et al, 2016), and progressing cancers through the various stages of metastasis (Peinado et al, 2012). The reason that EVs appear to be involved in such a broad range of cancer associated pathways, is because they have been observed to contain a diverse range of molecular cargo (Gould and Raposo, 2013), which is modulated based on their cell of origin and the underlying conditions and stress that the cell is undergoing (Maacha et al, 2019; Tian et al, 2021). However, this is also the same reason they have shown promise as biomarkers for multiple cancers, displaying distinct proteomes (Crescitelli et al, 2020; Cordonnier et al, 2020; Hoshino et al, 2020) and transcriptomes (Thind and Wilson, 2016; Min et al, 2018). Where there are now rich datasets of EV profiling for multiple cancers, there is not as much information available for EVs derived from the brain. This presents an interesting avenue for research, given how EVs are being displayed as future biomarkers for cancer, the is also potential for secreted EVs to provide a window into the changes that occur in the brain.

Table 1.2. Protein markers used for EV characterisation.

Table is adapted from the Minimal information for studies of extracellular vesicles (MISEV) 2018 guidelines (Table 3 in Théry et al, 2018). The guidelines recommend that a protein marker from sections 1a or 1b, 2a (optionally 2b), 3a or 3b should be measured in an isolated EV fraction to determine the purity of the sample. Furthermore, markers from section 4 should be used with section 3 markers for further analysis of the purity of the sample, particularly if the study is measuring small extracellular vesicles (< 200 nm). Antibodies against markers highlighted in ***bold*** *have been acquired for this study. * = protein families.*

1- **Markers associated to EV plasma membrane.**	**2-** **Markers found within EVs.**	**3-** **Markers on non-EV particles used for negative control.**	**4-** **Markers associated with apoptotic bodies and organelles.**
1a: non-tissue specific. • Tetraspanins (***CD63, CD81***, *CD82*) • Multi-pass membrane proteins (*CD47*; heterotrimeric G proteins *GNA**) • MHC class I (*HLA-A/B/C, H2-K/D/Q*), • Integrins (*ITGA*/ITGB**) • Transferrin receptor (*TFR2)* • Other markers include: *LAMP1/2, SDC,* EMMPRIN *(BSG); ADAM10;* CD73 *(NT5E*), *CD55, CD59*, *SHH* 1b: cell/tissue specific (denotes cell presenting the marker). • Some tetraspanins: *TSPAN8* (epithelial cell), *CD37* and CD53 (leukocytes), ***CD9*** (absent from NK, B and some MSC) • *Other cell specific markers include: ERBB2* (breast cancer), *EPCAM* (epithelial), CD90 (*THY1*; MSCs); CD45 (*PTPRC*; immune cells), CD41 (*ITGA2B*) or CD42a (*GP9)* (platelets); Acetylcholinesterase/*AChE-S* (neurons), amyloid beta A4/*APP* (neurons); multidrug resistance-associated protein (*ABCC1*)	2a: Ability to bind to lipids or membranes. • ESCRT-I/II/III (***TSG101****, CHMP**) • ESCRT accessory proteins: ALIX (*PDCD6IP), VPS4A/B* • Other markers include: *ARRDC1*, Flotillins-1 and 2 (***FLOT1****/2*), annexins (*ANXA**), Heat shock proteins HSC70 (*HSPA8*), and HSP84 (*HSP90AB1*) microtubule-associated Tau *(MAPT*, neurons) 2b: Associated with EVs in a non-specific manner. • Heat shock protein HSP70 (*HSPA1A*) • Cytoskeleton: actin (*ACT**) • tubulin (*TUB**) • Enzymes (*GAPDH*)	3a: Lipoproteins • Apolipoproteins A1/2 and B *APOA1/2, APOB, APOB100*, • Albumin (*ALB*) 3b: Protein and protein/nucleic acid aggregates. • Tamm-Horsfall protein (Uromodulin/*UMOD*) (urine) • Ribosomal proteins	4a: Nucleus. • Histones (*HIST1H**) • Lamin A/C (*LMNA*) 4b: Mitochondria. • *IMMT* • cytochrome C *(CYC1)* • *TOMM20* 4c: Endoplasmic reticulum and Golgi apparatus. • **Calnexin (CANX)** • Grp94 (HSP90B1) • BIP (HSPA5) • **GM130 (GOLGA2)** 4d: Other potential contaminating sources include autophagosomes and cytoskeleton. • ATG9A • Actinin1/4 (ACTN1/4) • Cytokeratin 18 (KRT18)

1.2.2 Extracellular vesicles in the brain

With the observations of the cellular 'spread' hypothesis within multiple neurodegenerative diseases, and of EVs facilitating the transport of proteins and nucleic acids between cells (Skog et al, 2008; Prada et al, 2018; Pluta et al, 2018), particularly when promoting the spread of tumours (Maacha et al, 2019; Hoshino et al, 2020), EVs present a candidate from which more may be learned about neuronal communication and neuropathogenesis progression.

Some of the first observations of EV function within the central nervous system (CNS) were described within the current century, including in Wnt signalling and neurogenesis (Greco *et al*, 2001; Marzesco *et al*, 2005), with subsequent analysis into the secretion of EVs from all distinct brain cells (Faure *et al*, 2006; Fitzner *et al*, 2011; Hooper *et al*, 2012; Prada *et al*, 2013; Dickens *et al*, 2017). Recently, EVs have begun to be described in multiple roles of maintaining homeostasis within the CNS, including neuroprotection (Fruhbeis *et al*, 2013), synaptic pruning (Bahrini *et al*, 2015), neurotrophic release (Goetzl *et al*, 2018), neural regeneration (Court *et al*, 2011; Lopez-Verrilli *et al*, 2013; Goncalves *et al*, 2015) and differentiation (Takeda and Xu, 2015). In fact, the numerous contributions to neuronal health mediated by EVs have implicated them as a promising route to target future therapy after neuronal damage or degeneration (Ma *et al*, 2018; Zhang *et al*, 2019).

EVs support neuronal health through the facilitation of heterogenous cellular communication, such as the cross-talk of neuron and glial cells (Paolicelli *et al*, 2018; Szepesi *et al*, 2018). Microglia are extensively involved in maintaining the health and function of neighbouring neurons, doing so by multiple means not limited to providing neurotrophic support (Parkhurst *et al*, 2013) as well as synaptic pruning and neural network modelling (Paolicelli *et al*, 2011; Zhan *et al*, 2014). The similarities in EV and microglial function in the CNS suggests that EVs facilitate some of the extensive control that microglia maintain over neuronal cells.

Notably, EVs are utilised in the communication from neuronal cell to microglia as well, and are involved in the feedback loops that these neuronal support cells monitor to maintain the health of the brain. EVs secreted from oligodendrocytes are selectively taken up by

microglia, where they degrade the EV and the contained membranes from the parent cell (Fitzner *et al*, 2011). This presents a functional mechanism for disposal of waste products that is separate from the typical microglial inflammatory response, and whether a similar function can be applied to other brain cells for the disposal of cytosolic and membranous waste will need to be assessed with further research. The ability of EVs to influence glial cell physiology is also demonstrated by a study which showed the role of EVs in the regulation of microglial phenotypes. The investigation showed EV transfer of miR-124 from a cellular model for motor neuron disease (using superoxide dismutase 1 (SOD1) (G93A) transfected NSC-34 motor neuron like cells), triggered an increased production of Interleukin 1β (IL-1β), tumour necrosis factor α (TNF-α) and MHC-II in N9 microglial cells (Pinto *et al*, 2017). Another recent study has shown that reactive glial cells, exposed to inflammatory or degenerative stimuli, secreted EVs that were enriched in miR-146a-5p. These secreted EVs were recorded to transfer their miRNA cargo to neurons, with visualisation of a transient fusion to the plasma membrane. This is particularly significant as MiR-146a-5p selectively represses the translation of Synaptotagmin 1 and Neuroligin 1, essential in dendritic spine formation and synapse stability, respectively, which was shown in morphological loss of neuronal dendritic spine density and reduction in the strength of synaptic currents (Prada *et al*, 2018).

The implications of EVs communicative function may be expanded with the observations that EVs cross the blood-brain barrier (BBB) (Chen *et al*, 2016; García-Romero *et al*, 2017), which with regards to their potential ability to remain stable within circulation (Kamerkar *et al*, 2017), could allude to other transcellular crosstalk between the brain and the rest of the body. Indeed, recent investigation has found that intravenous administration of purified EVs, derived from the serum of lipopolysaccharide (LPS) treated mice, into wild-type mice provokes the activation of microglia in the CNS (Li *et al*, 2018). Although it was unclear to what extent the infused EVs were responsible for the subsequent neuroinflammation (as they also induced systemic inflammation in the mice), there was a small uptake of fluorescently labelled EVs into the brain. More so, to bypass the systemic immune activation, the EVs were then administered via Intracerebroventricular (i.c.v) infusion, which induced significant microglial activation (Li *et al*, 2018). Overall, EVs have displayed a strong potential as a communicative vector, with the ability to pass on both

functional and damaging biomolecules, which are a direct reflection of the conditions of the cell of origin. This insight into the cell highlights the potential for EVs to 'betray' a particular disease state, by analysing its cargo for biomarkers. Yet this has not been investigated extensively in AD, particularly investigating EVs peripherally and in oxidative stress conditions, where there is the most potential for development of biomarkers.

1.2.3 Extracellular vesicles and Alzheimer's disease

With the establishment of a prominent role for EVs in neuronal homeostasis, conversely, research is also beginning to attribute them to the contribution of neurodegenerative disease, both as a medium for pathogenic spread, and across a broader scope of dysregulated communication within the brain. Whilst there is emerging evidence that EVs play a role in the 'spread' of AD neuropathological species, it is unclear how EV cargoes vary in distinct types of neurodegenerative disease, particularly in relation to the miRNA fingerprint.

In AD, it is well known that there is a stereotypical accumulation of Aβ and tau protein aggregates, but how this neuropathology spreads across the brain are unclear (Walsh and Selkoe, 2016). Almost as long as EVs have been known to be secreted from brain cells, EVs have been observed to carry Aβ40 and Aβ42 peptides which can be secreted from neurons into the extracellular space (Rajendran *et al*, 2006). This was also one of the first results showing that Aβ can utilise the endocytic pathway (Cataldo *et al*, 2004), with APP processing occurring in the early endosome, resulting in the subsequent observation of Aβ presence within MVBs. While the eventual Aβ contents of the EV was minute in comparison to within the MVBs, the cumulative effect could still be significant. A follow up study expanded on the findings, showing expression of flotillin-1 (found on the EV membrane) on intracellular vesicles containing Aβ, as well as within extracellular Aβ plaques (Rajendran *et al*, 2007). The concept that hallmark neurodegenerative proteins such as Aβ and PrP^{Sc} can be processed through the endocytic pathway, provided a novel route of investigation into their spread into the extracellular environment, where subsequent transfer to neural cells in the vicinity is not beyond possibility (Vella *et al*, 2007). EVs have been described to exacerbate neurodegeneration in AD. Myeloid MVs were significantly upregulated in the CSF of AD patients, as well as within MCI converting to AD patients, but not in the MCI non-

AD-converters, in comparison to matched healthy controls (Agosta, 2014). The same group had observed that when reactive microglia derived MVs were introduced to hippocampal neuron cultures, incubated with AD associated Aβ42 peptides, they enhanced the formation of soluble neurotoxic Aβ forms in the extracellular space (Joshi *et al*, 2013). Agosta suggested that microglia derived MVs ability to process the neurotoxic Aβ forms could be accounting for their findings of their 2014 study, in which the myeloid MVs (isolated from the CSF) were also associated with atrophy of the hippocampus, and in MCI patents, an increased damage to the white matter regions of the brain (Agosta *et al*, 2014). EVs associated with Aβ could be detrimental to neuronal homeostasis, by other means than direct neurotoxicity. Reports have found that EVs isolated from the CSF of AD patients and culture medium from neuronal cells harbouring presenilin 1 mutations, associated with FAD/ early-onset AD, can inhibit neuronal Ca^{2+} handling and mitochondrial function (Eitan *et al*, 2016).

It is not just Aβ aggregation that has been promoted by EVs, but also the spread of tau pathology. Some of the earlier work detected tau isoforms within EVs isolated from a M1C neuroblastoma tauopathy cell model, it was observed that there was a notable enrichment of tau species that were phosphorylated in a comparable manner to disease associated tau (Saman *et al*, 2012). Moreover, they reported the presence of AT270+ tau within EVs isolated from the CSF, which was enriched in early AD patients compared to the rest of the sampled cohort, suggesting an active role in pathogenesis (Saman *et al*, 2012). The researchers followed to show that EVs, isolated from neuroblastoma cell lines overexpressing the tau isoform 4R0N, are also enriched in a range of proteins not associated with EVs. Interestingly, a selection of the enriched proteins showed links to AD pathogenesis, such as Presenilin 1 (PSEN1), which is linked to abnormal Aβ processing, and alpha synuclein (SNCA) (Saman *et al*, 2014). Similar enrichment of AD associated proteins was seen in neuronal EVs isolated from patients with Down syndrome, further implying the early active role EVs may play in neuropathology progression (Hamlett *et al*, 2017). This is because there are AD associated genes (including *APP)* on chromosome 21, which is found in triplicate in Down syndrome (Coyle et al, 1988). This increase in *APP* expression drives an increased risk of developing AD in Down syndrome individuals (Hartley et al, 2015). Astrocyte derived EVs isolated from the plasma of AD patients also presented with

significantly higher levels of the AD associated proteins, beta-secretase 1 (BACE1) and soluble Aβ precursor protein (sAPPβ), as well as lower glial-derived growth factor, in comparison to matched cognitively healthy controls (Goetzl *et al*, 2016). Whether these changes precede or follow other AD pathogenesis is currently uncertain, though the group also found reductions in septin-8, the transcript variants of which regulate BACE-1 (Kurkinen *et al*, 2016), in AD derived EVs, which may suggest dysfunction in the astrocytic maintenance of APP processing.

A key recent finding on the function of tau associated EVs in AD neurodegenerative pathology, was observed using an adeno-associated virus transfected mouse model of AD, in which depletion of microglia inhibited the ability of the mutant tau to spread. They showed that microglia enabled the spread of tau through the brain by phagocytosing the tau and secreting tau associated EVs (Asai *et al*, 2015). Other investigation has alluded to EVs not just having a role in the spread of neuropathology but also in enabling misfolded tau to seed the aggregation of further tau pathology. As well as noting the presence of differentially phosphorylated tau species in EVs from cultured neurons, it was observed that tau associated EVs from transgenic mouse models could trigger the aggregation of endogenous tau and intracellular tau inclusions in wild type mice. Notably, EV membrane components were measured in the tau inclusions, suggesting that they aid the nucleation of tau (Polanco *et al*, 2016). While the provisional results require further analysis before a functional association between EVs and seeding is established, it does provide further routes in which EVs may play an active role in early neuropathological development (Holmes *et al*, 2014; Holmes and Diamond, 2014). Conversely, subsequent analysis did not provide evidence that tau-associated EVs could mediate the seeding of neurofibrillary tangles. Although as mentioned by the researcher, the experiment may not have used the required amount of tau associated EVs to reach their hypothesised concentration threshold for induction of intracellular tau aggregation (Baker *et al*, 2016). An alternative pathway in which EVs may contribute to pathological tau progression is via a trans-synaptic route (Lachenal *et al*, 2011), a theory proposed based on previous observations that tau can spread into the extracellular space in response to neuronal activity (Pooler *et al*, 2013). Supporting this is the observation that depolarisation of cortical neurons can induce the secretion of EVs, which were detected to incorporate tau, and that that EV mediated

transfer of tau was performed across a microfluidics device (Wang *et al*, 2017). The group recorded that tau contained within EVs was hypo-phosphorylated in comparison to cytosolic tau, although the functional implication of this remains unclear. Recently, work has found that EVs are associated with the permeabilization of lysosomes upon fusion with endosomes, as they fuse with the endolysosome, which allows EV associated tau seeds to escape into the cytosol. The acidic endolyosomal environment promotes aggregation of tau seeds, but the lipid membrane of EVs protected them from degradation and EVs fused with the endolysosome membrane, releasing its cargo into the cytosol (Polanco et al, 2021). Together, this evidence suggests that EVs play a significant role in AD pathogenesis, through the assisted seeding and spread of neuropathology, however, this change in biomolecular cargo will provide an important insight into AD, which this study aims to investigate to understand whether it could be utilised as a biomarker.

Not all observed relationships between EVs and neuropathology have been linked to detrimental effects in the brain. Studies have shown that EVs can provide a platform for monomeric Aβ interaction to enhance Aβ amyloidogenesis and fibrillogenesis (Yuyama *et al*, 2012). Notably, the EV associated acceleration of fibrillogenesis can provide a glycosphingolipid (GSL) target, which enables a more efficient uptake of Aβ by microglia and reduced the overall level of extracellular Aβ. Therefore, while evidence has described an association with EV biogenesis and Aβ production, the relationship remains unclear as to what extent this is neuropathological or neuroprotective, which is likely to be influenced by specific cargo changes. Within the rat hippocampus, i.c.v infusion of CSF derived EVs appears to inhibit the toxic effect of Aβ oligomers on LTP, potentially by sequestering the oligomers and enabling more efficient uptake by microglia (An *et al*, 2013), although whether specific cellular derived EVs work in a comparable manner remains to be seen. This process was more efficient with PrP^C expressing EVs, which support evidence that PrP^C binds to Aβ (Lauren *et al*, 2009; Freir *et al*, 2011). Again, chronic i.c.v infusion of EVs into APP transgenic mice, this time from a neuroblastoma cell line, caused a significant inhibition in synaptotoxicity due to GSL mediated EV sequestering of Aβ plaques and improved Aβ clearance by microglia (Yuyama *et al*, 2014). This was expanded upon to show that neuronal-derived EVs, infused into the brains of APP transgenic mice reduced Aβ deposition. The neuronal derived EVs expressed the GSL previously reported to enable

binding to Aβ, however this was not the case in glial-derived EVs (Yuyama *et al*, 2015). Another line of research that adds weight to the potential neuroprotective effects of EVs in AD is that they contain neuroprotective molecules, which could be spread by neurons in response to build up of pathology. One such example is the observed secretion of cystatin C from mouse primary neurons via EVs (Ghidoni *et al*, 2011), cystatin C being previously reported to exert neurotrophic conditions in the brain (Taupin *et al*, 2000; Palmer *et al*, 2001). At least 9 different cystatin C glycoforms were reported to be secreted with EVs, suggesting they play a role in neurotrophic responses, although study into the destination of cystatin C containing EVs would further allude the functional consequences of this relationship. The study did also record, however, that in the presence of primary neurons over expressing presenilin mutations, all the recorded cystatin C glycoforms were downregulated in EVs, suggesting that there is a functional link in neurodegenerative disease. A proposed mechanism is that cystatin C binds soluble Aβ and inhibits oligomerisation (Mi *et al*, 2007), therefore, cystatin C EVs could target intra- and extra-cellular Aβ and present it for degradation by glial cells.

Non-pathology associated EV relationships with AD have also been described. Expression of neurotrophic factors have been observed to be reduced in EVs derived from CSPG4 oligodendrocyte neural precursor cells, extracted from the plasma of AD compared to age-matched control patients. All of hepatocyte growth factors, type 1 insulin-like growth factor and fibroblast growth factors -2 and -13, important in neuronal health, were lower in mild AD patients in comparison to healthy controls (Goetzl *et al*, 2018). The result was repeated longitudinally, again showing a reduction in all the measured growth factors within EVs in comparison to matched controls, at the preclinical stages of AD and on follow up (between 3-8 years after) where the levels had remained consistent (Goetzl *et al*, 2018). This shows the pleotropic effect that AD has on EV function within neuronal cells, and although no progression in the reduction in neurotrophic levels in EVs with disease progression was observed, it still indicates another means by which EVs may be mediating the impact of AD on brain homeostasis.

Other means by which EVs are associated with neurodegenerative disease beyond the spread of neuropathology, are for example, with the potential effect of the apolipoprotein E4 (ApoE4) genotype on EV biogenesis. ApoE4 has long been known as a risk factor for AD

(Corder *et al*, 1993; Ward *et al*,2012) and for age-associated cognitive decline separate from the Aβ and tau neuropathology (Liu *et al*, 2013). ApoE4 has been shown to play a fundamental role in brain homeostasis, including lipid transport and neuronal signalling. So, the pathways through which ApoE4 may contribute to neuronal instability are numerous, but one that may be more notable is its consequential dysregulation of the endosomal-lysosomal pathway, potentially through the dysregulation of endosomal–lysosomal related genes, including Rab GTPases (Nuriel *et al*, 2017). Therefore, by process of association, the ApoE4 mutation could influence EV biogenesis, which is functionally linked to the endosomal pathway. Recently, it has been observed in humans and mice models that having a *e4* allele (homo- or heterozygous) results in significantly lower EVs isolated from frozen brain tissue, compared to homozygous *e3* allele holders, in an age dependant manner. Moreover, the ESCRT component Tumour susceptibility gene 101 (TSG101) was downregulated both at the transcriptional and protein levels, as well as Rab35, a RAB GTPase that facilitates MVB attachment to the plasma membrane (Peng *et al*, 2018). Taken together, these findings show an inhibition of ApoE4 on EV biogenesis and secretion, which is mediated through altered lipid metabolism, a function of ApoE. This is supported by the studies finding increased cholesterol levels within the EVs of the ApoE4 mice (Peng *et al*, 2018), mirroring lipid accumulation observed in AD. Previous descriptions of cholesterol-based regulation of intracellular membrane trafficking, notably MVBs, through the upregulation of Rab7, shows a functional pathway in which lipid metabolism could influence EV secretion (Chen *et al*, 2008). Interestingly, mice carrying the Apo *e4* allele showed increases in the number and size of early endosomes at 18 but not at 12 months old, as well as an increase in the number of lysosomes, which suggests that the influence was only showing relatively late in the lifespan of the mice (Nuriel *et al*, 2017). It is possible that the lipid accumulation-associated inhibition of EV secretion, shown to occur at 12 months in *e4* mice, produces a block in the endosomal pathway that causes subsequent endosomal disruptions, with the trigger of dysregulated pathways such as V-type ATPases and Rab GTPases (Nuriel *et al*, 2017). These disruptions could in turn promote neuronal dysregulation association with AD and neuropathology independent cognitive decline (Peng *et al*, 2018).

While the evidence suggests a significant role for EVs in AD, there is still a lack of understanding about the complete nature of their impact on disease progression. In particular, there is a gap in understanding the turnover of molecules such as RNA in EVs, and how these variations in cargo packaging and delivery influence physiological and disease associated conditions (Dellar et al, 2022). Therefore, further investigation into variation in EV cargoes and the conditions that influence EV biogenesis, cargo uptake and secretion is essential to determine how, when and where they progress AD, and whether these changes can be identified at an early enough stage to promote the development of disease modifying therapies.

1.3 MicroRNA – Small non-coding RNA

1.3.1 Extracellular vesicle microRNA in Alzheimer's disease

One set of cargoes in EVs that has vast potential in elucidating the intricate regulatory network within the CNS are mRNAs and microRNAs (Valadi *et al*, 2007). MicroRNAs (miRNAs) are small non-coding RNA molecules that post-transcriptionally regulate the expression of numerous proteins (Figure *1.5*). Their primary mode of action is through their reverse complementarity to sequence fragments, presented in the 3' untranslated regions of many mRNAs, enabling them to bind a range of specific targets, inhibiting subsequent protein translation (Lewis *et al*, 2005).

It was recently shown that the expression of miRNAs can be enriched in neuronal derived EVs, where the relative expression in comparison to total RNA was greater than what was observed within the cell body (Goldie *et al*, 2014), highlighting that the contribution of EV transfer of miRNA is an active process, and not necessarily a passive response to changes within the cell. Similar findings have been reported regarding the enrichment of messenger (m)RNAs (Huang *et al*, 2013). Additionally, mice with a conditional knockdown of Dicer, a part of the miRNA biogenesis machinery, in neural progenitor cells (NPCs), displays impaired neurogenesis and cognitive function. Subsequent investigation has shown that administration of cerebral endothelial derived EVs to the Dicer knockout mice, rescued the reduction in neurogenesis associated miRNAs in NPCs and cognitive function in the mice, suggesting a key role of EV miRNAs in the brain (Zhang *et al*, 2017).

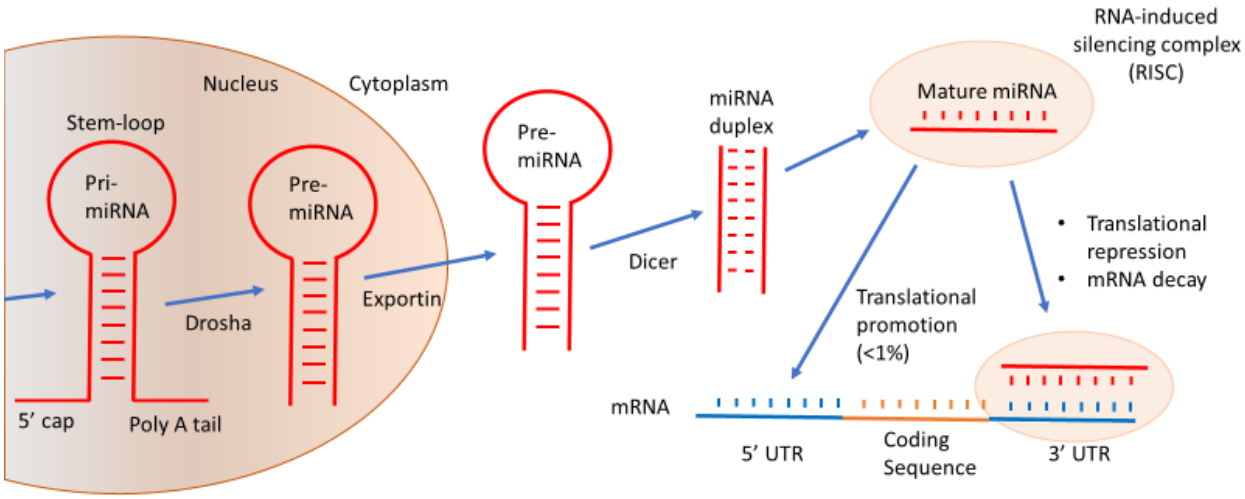

Figure 1.5. The biogenesis of miRNAs.

MiRNA genes are transcribed by DNA polymerase III into the primary (pri-)miRNA stem-loop structure, with a 5 prime cap and a poly adenine tail, similar to mRNA constructs. Drosha, a ribonuclease III enzyme, cleaves the pri-miRNA into the stem-loop pre-miRNA, which is subsequently transported into the cytoplasm by exportin 5. Another ribonuclease III enzyme, Dicer, cleaves the stem-loop from the pre-miRNA, leaving the miRNA duplex with the 3 and 5 prime strands. Either the 3' or 5' strand are preferentially loaded into an argonaut protein that is part of the RNA-induced silencing complex (RISC). The miRNA guides the RISC complex to the mRNA through complementary sequences.

In terms of neurodegenerative diseases, there has been an accumulation of evidence to indicated that miRNAs from the plasma and CSF can be used as potential biomarkers for AD (Schipper *et al*, 2007; Cogswell *et al*, 2008; Kiko *et al*, 2014), although further study is required to determine the functional mechanisms by which they may exacerbate the disease. In some cases, TAR DNA-binding protein-43 (TDP-43), mutations of which have been strongly associated with FTLD and ALS, has been observed to promote the biogenesis of specific miRNAs (miR-132-3p, miR-132-5p, and miR-143-3p) that regulate neuronal outgrowth during differentiation (Kawahara and Mieda-Sato, 2012). Other investigations have found the downregulation of miR-219 in brain tissue from AD and severe primary age-related tauopathy. Subsequent analysis observed that downregulation of miR-219 in a *Drosophila* tau model exacerbated the neurotoxicity of mutant tau accumulation, whereas upregulation of miR-219 ameliorated neuronal homeostasis. This appeared to be due to the direct regulation of MAPT by miR-219, giving one such functional route miRNAs may mediate neurodegeneration, admittedly one part of a much larger network, although the

cumulative contribution to understanding of its regulation will no doubt be beneficial to future analysis (Santa-Maria *et al*, 2015).

The investigation of miRNA cargo in EVs is a young field of study and so studies are few, and fewer still when looking solely within the brain, but even then, there appears to be great promise to progress understanding of neuronal regulation. Initial sequencing studies of EV miRNA changes in neurodegenerative disease, observed that prion infected neuronal cells released EVs containing a series of enriched miRNAs. Interestingly, some of the miRNAs have previously been shown to be alternately regulated in other neurodegenerative diseases, such as let-7i, miR-29b, miR-424, miR-128 and miR-146 in AD (Li *et al*, 2011; Wang *et al*, 2011; Hébert *et al*, 2008), as well as prion diseases, highlighting some of the first results to show the diagnostic capability of EV miRNAs (Bellingham *et al*, 2012). One of the first studies to identify EV miRNA changes associated with AD, showed that expression of miR-193b was downregulated in EVs isolated from the blood of MCI, in comparison to matched controls. In addition, EV miR-193b was further reduced in the blood of AD patients, compared to MCI patients as well as controls, suggesting a progressive change that was not mirrored by total miR-193b changes in the blood, indicating an EV specific change that may transfer from the brain (Liu *et al*, 2014). Subsequent testing observed diminished EV miR-193b taken from the CSF of AD patients in comparison to controls, supporting the results. Although the functional relevance of miR-193b remains uncertain, the report did show a negative correlation between miR-193b and APP (mRNA and protein) expression in cellular models, suggesting a regulatory function for miR-193b linked to AD (Liu *et al*, 2014).

Overall, while research into EV miRNAs has the potential to elucidate the molecular mechanisms behind the 'spread' of neuropathology, there are still gaps in the literature as to what miRNA cargo is varied in neurodegenerative conditions, as well as functional relevance of these variations. This highlights the potential of this project to investigate specific neurodegenerative stress conditions, how it is impacting the secretion of miRNAs in EVs, and how this is contributing to the 'spread' of neuropathology. MiRNAs could potentially play a significant role in the propagation of pathogenesis in AD, and therefore could also be utilised as a biomarker in pre-symptomatic stages of the disease.

1.3.2 Extracellular vesicles as biomarkers for Alzheimer's disease

miRNAs contained within EVs can maintain stability in the circulation by being protected within the vesicle's membrane (Zandberga *et al*, 2012), therefore, if EV associated miRNAs can be found in the periphery that mirror functionally relevant changes in the brain, this would highlight their potential as a biomarker in all stages of neurodegenerative disease progression. However, circulating miRNAs are present in human serum without the need for EV transport, and may also provide a functional role in intercellular signalling that needs to be further classified on top of EV miRNA (Turchinovich *et al*, 2013). Even so, EV miRNAs may provide a more specific biomarker that more accurately mirrors change in the brain, in comparison to other circulating miRNA of which the levels could be influenced by sources from the peripheral systems. It has already been shown that small RNAs can bypass the BBB in an EV mediated manner (Haqqani *et al*, 2013), supported by studies observing EVs crossing the BBB (Chen *et al*, 2016; García-Romero *et al*, 2017). Although the mechanism by which EVs can bypass the brain endothelial cells of the BBB is still uncertain, they could display receptors required for transcytosis, including transferrin, insulin, and low-density lipoprotein receptors (Haqqani *et al*, 2013). EVs containing short interfering (si)RNA, validated to target BACE1, successfully crossed from the peripheral system into the brain, as shown by the 60% and 62% knock down in mRNA and protein BACE1, respectively (Alvarez-Erviti *et al*, 2011). More recently, observation of the effect of peripheral inflammatory response on the blood-CSF barrier (BCSFB) indicated that choroid plexus epithelium, situated within the BCSFB, releases EVs enriched with pro-inflammatory miRNAs in response to inflammation. Thus, indicating that there are still unestablished means by which EVs mediate communication between the brain and the periphery (Balusu *et al*, 2016).

More recent sequencing analysis has added to the consensus that EV miRNA can work as a prognostic biomarker for AD. Through next-generation sequencing and quantitative reverse-transcription polymerase chain reaction (qRT-PCR) validation, EV miRNA was analysed in human serum samples, by which a cohort of 16 miRNAs were detected that were differentially expressed in AD. This miRNA signature, when added to the known risk factors of age, sex and ApoE4 allele presentation, could predict AD with a high accuracy, including 87% sensitivity and 77% specificity, in a separate validation cohort (Cheng *et al*,

2015). The chosen biomarker cohort may well be more accurate than the study presented, as it was noted that healthy participants that were incorrectly diagnosed as AD by the model, had progressed Aβ burden based on neuroimaging. This could suggest the model may have some capability to predict MCI to AD conversion, although to support this, it will require further study following the progression of the participants predicted to progress, as well as subsequent validation with a larger sample size. It is noted that the validated model includes miRNAs that have previously been implicated in AD pathogenesis (Cogswell *et al*, 2008; Hébert *et al*, 2010; Vilardo *et al*, 2010; Kumar *et al*, 2011; Frigerio *et al*, 2013). Though notably, there have not been as many studies that have analysed miRNAs from EVs taken directly from the brain, which would give unparalleled insight into understanding their changes in association with disease conditions. Moreover, considering the advantages of peripheral biomarkers for AD, no current study has observed EV miRNA derived from peripheral cells in AD, and considering that there is interest in biofluid based EV biomarkers, more knowledge needs to be gathered on the relative cellular source of EVs in serum, for example (Vandendriesscheab et al, 2022). This would greatly improve the specificity of these studies, as determining whether certain tissues, alongside the brain, display specific EV miRNA changes, could improve targeting of EV biomarkers both from tissue and biofluids.

One pathway to address validating a miRNA cohort as of diagnostic value to AD is to establish the miRNAs in separate studies. Another high throughput study of EV miRNAs in AD was performed, in which a panel of 7 EV miRNAs were able to inform a machine learning algorithm which participants had AD with an accuracy of 83-89%, without any other data input (Lugli *et al*, 2015). Notably, only one of the miRNAs found in this study was also part of the miRNA signature used in the previous study, miR-342-3p (Cheng *et al*, 2015). This could be due to factors outside of participant variability, for example different techniques were used to isolate EV fractions (Cheng and colleagues used an EV RNA isolation kit, whereas Lugli and colleagues used differential centrifugation), which makes it difficult to directly compare the results with certainty that the studies are comparing the same EV fragments. This highlights the importance of developing a consensus on the best definitions of EVs and determining the best techniques for isolation and categorisation, to enable further confidence in the results being published (Gould and Raposo, 2013; Théry *et al*,

2018). While it is reiterated that the extent to which individual miRNAs may contribute to the neuropathology of AD remains controversial, the separate observations of miR-342-3p warrant further analysis of its potential functional implication in AD and its role as a biomarker. MiR-34a is another such miRNA that has been implicated in AD, due to observations of its overexpression in the temporal cortex and hippocampus in the 3xTg-AD mouse model, as well as in the temporal cortex in human AD patients. It was found that miR-34a could be secreted from the host cell and transferred to adjacent neurons, via EVs (Sarkar *et al*, 2016). Subsequent analysis by the group identified that miR-34a regulated the expression of proteins involved in synaptic plasticity, which corroborates previous findings (Agostini *et al*, 2011; Wibrand *et al*, 2012).

It remains to be questioned whether changes in EV miRNA are separate from the changes in circulating miRNA, therefore it is interesting to note that recent studies have compared the two in relation to AD. Whereas the free miRNAs were found to be downregulated completely in the CSF from AD patients compared to matched controls, expression was observed in the EV-enriched fraction (Riancho *et al*, 2017). Notably, miR-9-5p and miR-598 were observed to be differentially regulated between the raw CSF and EV enriched fraction of CSF taken from patients with AD. Specifically, miR-9-5p and miR-598 showed no expression in AD CSF samples, but were expressed in the EV enriched samples. Conversely, the miRNAs expressed in the control CSF samples were not expressed in the EV enriched samples. In addition, the EV miRNAs were, albeit non-significantly, over expressed in the AD patient samples compared to controls, displaying the opposite relationship to the raw CSF samples (Riancho *et al*, 2017). Further study needs to be carried out to show the differential trafficking of miRNAs during AD, from which increased understanding of the specific role of EVs may be elucidated. A crucial step towards this is the determination of whether miRNA is specifically or randomly packaged into EVs, as well as mechanisms by which this process takes place. While some pathways have been proposed, a consensus remains to be established on the exact mechanisms for packaging miRNAs, and on any cell-specific differences, that could shed light on novel targets to understanding AD progression (Kim *et al*, 2017). A recent study found that miR-125b-5p, miR-451a and miR-605-5p, taken from the purified EV fragment derived from the CSF, were differentially regulated in both Young-onset and Late-onset AD (YOAD and LOAD), highlighting the diagnostic potential of

EV miRNAs to identify specific AD subtypes. Notably, miR-16-5p was downregulated in YOAD but not LOAD, suggesting a novel target in distinguishing the pathophysiology between the diseases (McKeever *et al*, 2018).

Little is currently known about how neurodegenerative associated conditions (oxidative stress, inflammations, etc) in AD influence EV secretion, and less still about the impact on EV cargoes such as miRNAs. Some observations of oxidative stress conditions in cancer have been noted, for example, the receptor protein NK cell receptor Natural Killer Group 2, member D (NKG2D) ligand is upregulated in EVs derived from H_2O_2 treated lymphoma cells, which subsequently dampened natural killer cell responses (Hedlund et al, 2011). In Ewing's sarcoma (a cancer primarily occurring in bone) transposable RNA elements with extended open reading frames were reduced in EVs derived from cells treated with sodium arsenate, which triggers tumour associated oxidative stress responses (Evdokimova et al, 2022), therefore suggesting that in some disease conditions, oxidative stress does dysregulate miRNA expression in EVs. Oxidative stress may impact EV miRNA loading by inducing O-GlcNAcylation of hnRNPA2B1 in EVs (Lee et al, 2019), since hnRNPA2B1 has been shown to promote miRNA loading into EVs (Villarroya-Beltri et al, 2013), this is a plausible mechanism that may contribute to observations by Evdokimova et al (2022), as well as in other conditions, including in the brain where O-GlcNAcylation is very abundant (Wulff-Fuentes et al, 2021). Oxidative stress has been found to impact the uptake of lipoproteins in EVs, as apoD levels were reduced in circulating EVs in AD, a relationship that was more apparent in APOE ε4 carriers (Ben Khedher et al, 2021). This relationship has been observed in the brain, where astrocytes transfer apoD to neurons, potentially as a protective response to oxidative stress conditions (Pascua-Maestro et al, 2019). Beyond this, there is a gap in knowledge about the changes in EV cargo, particularly miRNA, in AD oxidative stress conditions, and exploration of this gap shows promise to identify novel biomarkers.

Given the diagnostic capabilities of EVs, particularly in biofluids for AD, further investigation needs to be carried out in models that relate to AD with an exploration of less-invasive options for future testing of EV cargoes. Currently, while the bulk of peripheral research into AD has been in biofluids, there is limited study into other peripheral cells. Notably, peripheral fibroblasts from AD patients display numerous AD phenotypic changes,

including an oxidative stress phenotype (Ramamoorthy *et al*, 2012), lysosomal dysfunction (Coffey *et al*, 2014), autophagy dysfunction (Martín-Maestro, 2017), alterations to circadian rhythm and DNA methylation (Cronin *et al*, 2017) and mitochondrial dysfunction (Pérez *et al*, 2017). Therefore, further investigation into these cells could uncover accessible biomarkers before AD symptoms have progressed irreversibly. So far, this is the first study that is investigating EV miRNA in AD fibroblasts, as well as progressing the currently limited research into EV miRNA in response to oxidative stress, related to AD.

1.4 Chromosome 14 miRNA cluster – Alzheimer's disease biomarkers

While evidence for the role of miRNAs in AD is growing, the effect of individual miRNAs on physiological outcomes has been observed to be limited. Primarily, they are considered to be fine tuners of gene expression that maintain homeostasis at the protein level (Bartel, 2009). Nonetheless, miRNAs have been observed to impact cellular physiology, and one means by which miRNAs have displayed a more decisive regulatory role is via their synergistic effects with other miRNAs derived from the same polycistronic cluster (Ventura *et al*, 2008; Kim *et al*, 2009). miRNA clusters are defined as sets of miRNAs that are co-transcribed together through the action of a shared promoter sequence, and are not sandwiching other independently transcribed sequences, either sense or antisense, between one another (Chiang *et al*, 2010). Clusters of co-regulated miRNAs have been observed to cooperatively target the same gene (Ventura *et al*, 2008) or even multiple genes in a physiological pathway or network (Kim *et al*, 2009), which highlights their importance to physiological outcomes.

One of the largest miRNA clusters discovered in the human genome is the chromosome 14 cluster (C14MC), located in the chromosome 14q32.31, which encompasses over 50 miRNA genes (Seitz *et al*, 2004). Table 1.3 displays the miRNAs within C4MC, with their 3p and 5p mature sequences. The cluster has been characterised in multiple brain cancers, including neuroblastoma, medulloblastoma and oligodendrogliomas (Gattolliat *et al*, 2011; Lucon *et al*, 2013; Kumar *et al*, 2018), however its regulation in neurodegenerative diseases remains less characterised.

Interestingly, individual expression of numerous miRNAs from the cluster have been identified to alter in AD and related disease models. miR-377, miR-412, miR-485-3p, miR-382, miR-487a, miR-487b, miR-381, miR-376, miR-495, miR-329, miR-299-5p, miR-411 and miR-379 were all downregulated in AD human brain tissue, with miR-300 upregulated in the same study (Wang *et al*, 2011). Other miRNAs within the cluster have been observed to influence upstream pathways in AD, including miR-369, loss of which was shown to promote tau phosphorylation (Yao *et al*, 2020). miR-409-5p is downregulated in an APP/PS1 double transgenic mice model of AD, as well as with $A\beta_{1–42}$ exposure, although miR-409-5p overexpression generated neurotoxicity, indicating further research is required into this relationship (Guo *et al*, 2019). miR-323-3p has been observed to regulate APP, although it was not influenced by variations in the *APP 3'UTR,* there are numerous other variations not tested in the study that could influence its function (Delay *et al*, 2011). As well as immediate AD implications, the cluster has numerous roles in neuronal function and homeostasis where dysregulation, either as a direct or indirect consequence of neurodegeneration, could exacerbate the disease progression. One example showed mir-134 upregulation led to translational repression of essential neuronal plasticity proteins, including cAMP response binding protein (CREB) and brain-derived neurotrophic factor (BDNF). This corresponded with impaired LTP function in mice, which was rescued with mir-134 knockdown (Gao *et al*, 2010). This highlights the fact that there are numerous routes by which analysis of the cluster could elucidate a clearer role in its potential as a biomarker of AD.

Table 1.3. List of C14MC miRNAs.

List of miRNAs that are part of the chromosome 14 cluster, with the corresponding identification (accession) code in the miRBase repository. Sequences of both the 5 prime and 3 prime mature forms of each miRNA are displayed.

MiRNA name	miRBase accession code	5p mature miRNA sequence	3p mature miRNA sequence
hsa-mir-656	MI0003678	AGGUUGCCUGUGAGGUGUUCA	AAUAUUAUACAGUCAACCUCU
hsa-mir-410	MI0002465	AGGUUGUCUGUGAUGAGUUCG	AAUAUAACACAGAUGGCCUGU
hsa-mir-369	MI0000777	AGAUCGACCGUGUUAUAUUCGC	AAUAAUACAUGGUUGAUCUUU
hsa-mir-412	MI0002464	UGGUCGACCAGUUGGAAAGUAAU	ACUUCACCUGGUCCACUAGCCGU
hsa-mir-409	MI0001735	AGGUUACCCGAGCAACUUUGCAU	GAAUGUUGCUCGGUGAACCCCU
hsa-mir-541	MI0005539	AAAGGAUUCUGCUGUCGGUCCCACU	UGGUGGGCACAGAAUCUGGACU
hsa-mir-377	MI0000785	AGAGGUUGCCCUUGGUGAAUUC	AUCACACAAAGGCAACUUUUGU
hsa-mir-496	MI0003136		UGAGUAUUACAUGGCCAAUCUC
hsa-mir-154	MI0000480	UAGGUUAUCCGUGUUGCCUUCG	AAUCAUACACGGUUGACCUAUU
hsa-mir-323b	MI0014206	AGGUUGUCCGUGGUGAGUUCGCA	CCCAAUACACGGUCGACCUCUU
hsa-mir-485	MI0002469	AGAGGCUGGCCGUGAUGAAUUC	GUCAUACACGGCUCUCCUCUCU
hsa-mir-668	MI0003761	UGCGCCUCGGGUGAGCAUG	UGUCACUCGGCUCGGCCCACUAC
hsa-mir-134	MI0000474	UGUGACUGGUUGACCAGAGGGG	CCUGUGGGCCACCUAGUCACCAA
hsa-mir-382	MI0000790	GAAGUUGUUCGUGGUGGAUUCG	AAUCAUUCACGGACAACACUU
hsa-mir-487a	MI0002471	GUGGUUAUCCCUGCUGUGUUCG	AAUCAUACAGGGACAUCCAGUU
hsa-mir-655	MI0003677	AGAGGUUAUCCGUGUUAUGUUC	AUAAUACAUGGUUAACCUCUUU
hsa-mir-544a	MI0003515		AUUCUGCAUUUUUAGCAAGUUC
hsa-mir-889	MI0005540	AAUGGCUGUCCGUAGUAUGGUC	UUAAUAUCGGACAACCAUUGU
hsa-mir-539	MI0003514	GGAGAAAUUAUCCUUGGUGUGU	AUCAUACAAGGACAAUUUCUUU
hsa-mir-487b	MI0003530	GUGGUUAUCCCUGUCCUGUUCG	AAUCGUACAGGGUCAUCCACUU
hsa-mir-381	MI0000789	AGCGAGGUUGCCCUUUGUAUAU	UAUACAAGGGCAAGCUCUCUGU
hsa-mir-1185-2	MI0003821	AGAGGAUACCCUUUGUAUGUU	AUAUACAGGGGGAGACUCUCAU
hsa-mir-1185-1	MI0003844	AGAGGAUACCCUUUGUAUGUU	AUAUACAGGGGGAGACUCUUAU
hsa-mir-300	MI0005525		UAUACAAGGGCAGACUCUCUCU
hsa-mir-376a-1	MI0000784	GUAGAUUCUCCUUCUAUGAGUA	AUCAUAGAGGAAAAUCCACGU
hsa-mir-376b	MI0002466	CGUGGAUAUUCCUUCUAUGUUU	AUCAUAGAGGAAAAUCCAUGUU
hsa-mir-654	MI0003676	UGGUGGGCCGCAGAACAUGUGC	UAUGUCUGCUGACCAUCACCUU
hsa-mir-376a-2	MI0003529	GGUAGAUUUUCCUUCUAUGGU	AUCAUAGAGGAAAAUCCACGU
hsa-mir-376c	MI0000776	GGUGGAUAUUCCUUCUAUGUU	AACAUAGAGGAAAUUCCACGU
hsa-mir-495	MI0003135	GAAGUUGCCCAUGUUAUUUUCG	AAACAAACAUGGUGCACUUCUU
hsa-mir-543	MI0005565		AAACAUUCGCGGUGCACUUCUU
hsa-mir-1193	MI0014205	GGGAUGGUAGACCGGUGACGUGC	
hsa-mir-494	MI0003134	AGGUUGUCCGUGUUGUCUUCUCU	UGAAACAUACACGGGAAACCUC
hsa-mir-329-2	MI0001726	GAGGUUUUCUGGGUUUCUGUUUC	AACACACCUGGUUAACCUCUUU
hsa-mir-329-1	MI0001725	GAGGUUUUCUGGGUUUCUGUUUC	AACACACCUGGUUAACCUCUUU
hsa-mir-758	MI0003757	GAUGGUUGACCAGAGAGCACAC	UUUGUGACCUGGUCCACUAACC
hsa-mir-323a	MI0000807	AGGUGGUCCGUGGCGCGUUCGC	CACAUUACACGGUCGACCUCU
hsa-mir-1197	MI0006656		UAGGACACAUGGUCUACUUCU
hsa-mir-380	MI0000788	UGGUUGACCAUAGAACAUGCGC	UAUGUAAUAUGGUCCACAUCUU
hsa-mir-299	MI0000744	UGGUUUACCGUCCCACAUACAU	UAUGUGGGAUGGUAAACCGCUU
hsa-mir-411	MI0003675	UAGUAGACCGUAUAGCGUACG	UAUGUAACACGGUCCACUAACC
hsa-mir-379	MI0000787	UGGUAGACUAUGGAACGUAGG	UAUGUAACAUGGUCCACUAACU

1.5 Summary

With the recent development of techniques to isolate, categorise and analyse EVs, the role of EVs in neurodegenerative diseases is quickly being established. It is also evident that miRNA regulatory pathways are significantly altered in AD, and that some of their influence can be spread via their secretion in EVs. Therefore, the next step is to understand how the function of EVs, and their miRNA cargo are changed under neurodegenerative conditions in both neuronal and peripheral models of AD. This will support their potential use as biomarkers, which could help overcome the challenges of predicting the early changes in AD. Thus, they have the potential to be incorporated into a biomarker framework that could support diagnoses, understanding of neuropathological progression and the development of therapeutics to halt or prevent AD.

1.6 Aims

The aims of the research (Figure 1.6) are:

- Develop an EV isolation methodology that could isolate and separate EVs from both cell culture medium and human brain tissue
- Characterise EVs isolated from fibroblast cell culture medium and brain tissue
- Investigate the RNA cargo of SEC isolated sEVs, in order to determine whether they were localised within the sEVs or as part of co-isolated non-EV molecules
- Interrogate miRNA cargo of sEVs from fibroblast and SH-SY5Y cell culture and human brain tissue
- Analyse biological pathways associated with candidate dysregulated miRNAs, to determine their functional relevance in AD

The hypothesis of the research is that the expression of EV miRNA will change with progression of AD associated conditions, in brain tissue and peripheral fibroblast cells.

The long-term goal of the research is to investigate whether miRNA cargo of sEVs derived from AD specific models could be used as a biomarker for AD.

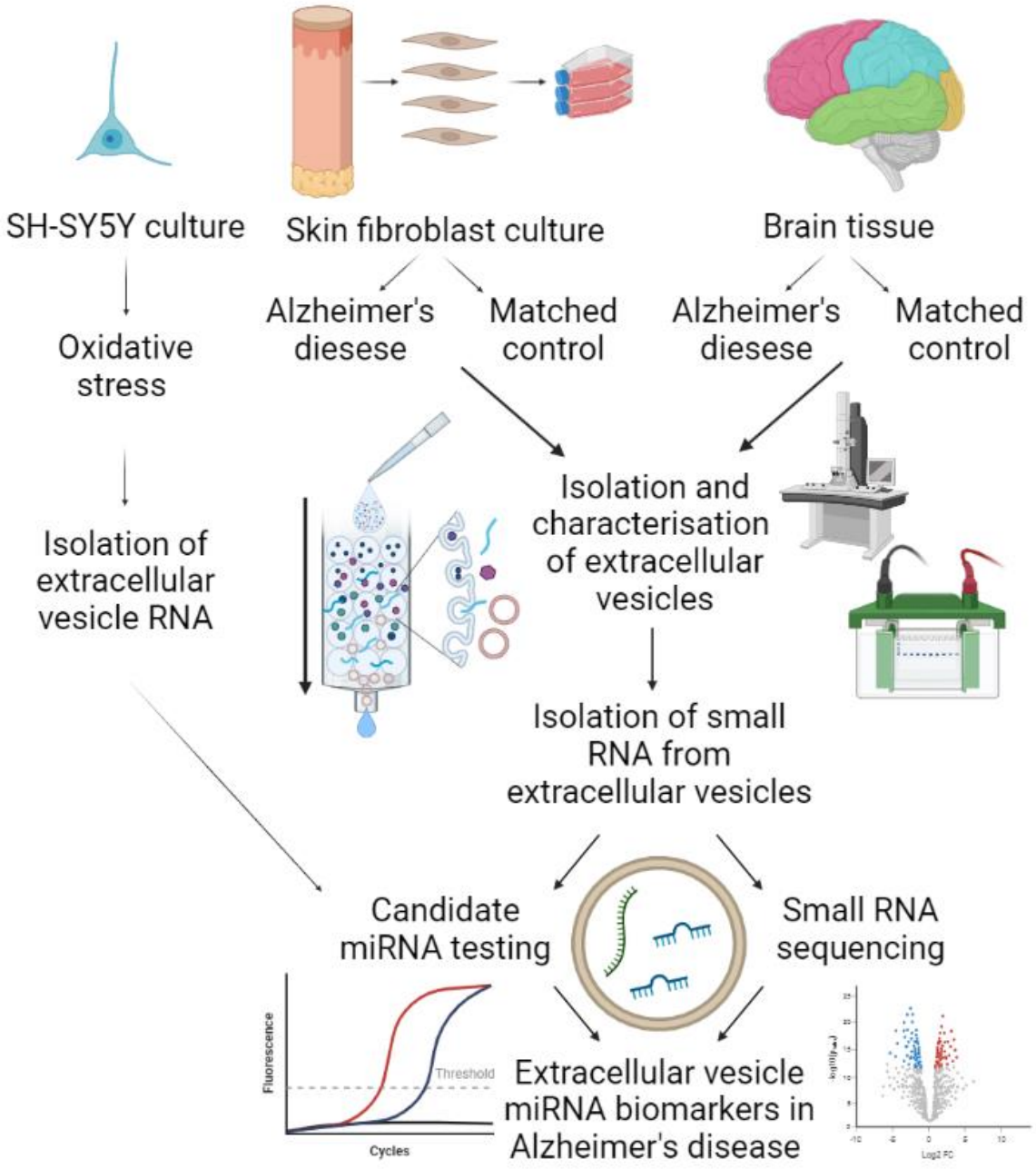

Figure 1.6. Study workflow

Graphical summary of project workflow. Two cohorts were investigated, looking at brain tissue and fibroblast cultures, with AD and matched controls in each cohort. Initial steps involved isolating EVs from both biological samples using size exclusion chromatography. Characterisation of isolated EVs was performed using TEM, western blotting and NTA. Extracellular vesicle RNA was isolated from SH-SY5Y cells that underwent oxidative stress, while RNA was isolated from characterised EVs in the two cohorts, and investigation of miRNA biomarker candidates was performed using qPCR and small RNA sequencing.

2 Chapter 2: Methodology

2.1 Ethics

Ethics was obtained locally, and the use of the human brain tissue had been approved by the Manchester brain bank.

Local ethical approval for this project was granted by the University of Salford and since the tissue used in this project was collected by the Manchester Brain Bank the ethical approval for the tissue collection has been granted to them (REC 09/H0906/52).

2.2 Cell culture

2.2.1 Cell lines

Skin fibroblasts were purchased from the Coriell cell repository (USA). Fibroblast characteristics are presented in Table 2.1. Patients were clinically diagnosed with AD of a sporadic onset, with no AD genetic risk factors reported, including characterised *PSEN1, PSEN2* and *APP* mutations. Average ages of the donors were 58.7 years old for the AD group and 63.3 years old for the neuronally healthy group. SH-SY5Y neuroblastoma cells were purchased from Sigma Aldrich (UK).

Table 2.1. Characteristics of fibroblasts

Core characteristics of the fibroblasts from the Coriell cell repository, including the reference code for each cell line on www.coriell.org, sex and age at donation of the tissue.

Disease status	Cell line	Sex	Age (Years, At Sampling)
Alzheimer's disease	AG05809	Female	63
	AG07872	Male	53
	AG06869	Female	60
Healthy brain ageing	AG08379	Female	60
	AG08125	Male	64
	AG08517	Female	66

2.2.2 Maintenance

Patient derived fibroblasts (Coriell) were cultured in Minimum Essential Medium Eagle (MEM) with 15% fetal bovine serum, 2 mM L-glutamine and penicillin-streptomycin (10 000 U/ml penicillin - 10,000 µg/mL streptomycin), 1% non-essential amino acids (NEAAs), and were maintained at 37°C and 5% CO_2 in a humidified atmosphere. Cells were sub-cultured at 80% confluency.

SH-SY5Y cells were cultured in Dulbecco's Modified Eagle Medium (DMEM) with 10% fetal bovine serum (FBS), 2 mM L-glutamine and penicillin-streptomycin (10 000 U/ml penicillin - 10,000 µg/mL streptomycin) and were maintained at 37°C and 5% CO_2 in a humidified atmosphere. Cells were sub-cultured at between 70-80% confluency up to passage 15, at which point cells display selective population phenotypes.

Mycoplasma testing was performed on cell lines using PCR detection (Applied biological materials).

2.2.3 SH-SY5Y differentiation

SH-SY5Y cells were cultured for differentiation into mature neurons (Agholme et al, 2010). Initial differentiation involved replacing the DMEM medium with DMEM F:12, including L-glutamine and penicillin-streptomycin. Retinoic acid (All-trans retinoic acid, RA), as well as serum free medium, was used to drive differentiation, with final concentrations of 10 µM and 1 µM in media used for 10- and 21-day protocols, respectively (Agholme et al, 2010; Shipley et al, 2016). N2 supplement was used to support the survival and differentiation of the neuroblastoma cells in place of FBS. Both protocols involved prior incubation of 6-well plates with laminin for 1 hour at 37°C, which was subsequently washed with phosphate buffer solution (PBS). Cells were counted and seeded at a starting density of 6 x 10^4 cells per well (9.6 cm^2), in normal DMEM medium, which was replaced with the differentiation medium after 24 hours, with subsequent half medium changes every 48 hours. Half media changes were used to limit stress to the cells during progressive serum starvation.

Differentiation of the SH-SY5Y cells was primarily categorised by morphology, involving the extension of neurites and the halt to proliferation, as determined by observation of cell cultures (appendix Figure).

2.2.4 Oxidative stress induction of SH-SY5Y cells with hydrogen peroxide

Cells were treated with H_2O_2 to induce an oxidative stress response based on established literature (Zhang et al, 2007). Upon day 10 of differentiation, cells were washed and incubated with fresh differentiation media containing 150 µM H_2O_2 for 24 hours, after which media was harvested.

2.2.5 Pre-processing extracellular vesicles from fibroblast culture medium

EVs were extracted from cell culture medium using previously published protocols and based on the MISEV guidelines (Witwer *et al*, 2013; Théry *et al*, 2018). Fibroblasts were seeded in T-175 cell culture flasks at a density of 2 x 10^4 cells/cm to achieve 10 million cells per cell line, approximately 80% confluence (Figure 2.1), at which the medium was replaced with medium utilising EV-depleted FBS (Lonza), and the cells were incubated for 72 hours. Fibroblasts were passaged and cell counts were taken upon harvesting of the media, to normalise EV numbers. Cells were counted with a 1:1 dilution in 0.5% trypan blue stain (Biosera).

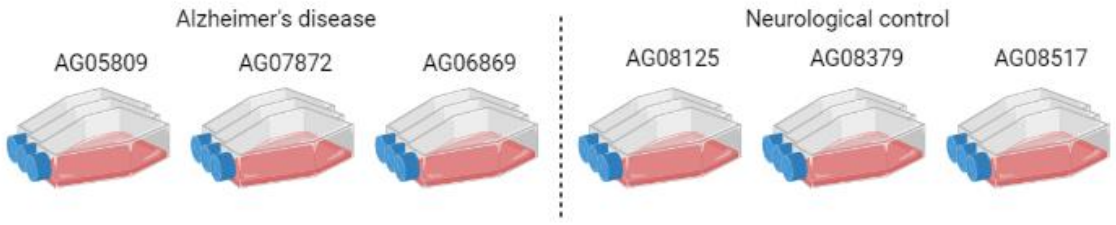

Figure 2.1. Fibroblast culture plan

Fibroblasts were cultured in triplicate in T-175s, detailed above, to get the maximum number of cells to collect EVs. Biological triplicates of AD and neurological healthy control cell lines were used to incorporate variation between individuals. Image created with BioRender.com.

Isolated cell culture medium (~60 ml) was immediately spun at 300*g* for 10 minutes to pellet cells and larger cellular material, after which the supernatant was transferred to a new tube and the process was repeated at 1000*g* for 10 minutes and 10,000*g* for 48 minutes to pellet the remaining cellular debris and apoptotic bodies. The supernatant was then pressed through a 0.22 µm filter (Millipore) to ensure vesicle fractions were purified of any material over the size cut-off, the filter was pre-blocked with a 0.1% BSA (bovine serum albumin, ThermoFisher) solution to maximise retention of EVs through the filter. The supernatant was immediately processed as described in 2.4. Harvesting extracellular vesicles from medium and tissue.

2.2.6 MTT Assay

To determine whether the use of exo-depleted FBS affected cell viability in the fibroblasts, the MTT (3-(4,5-dimethylthiazol-2-yl)-2,5-diphenyltetrazolium bromide) assay was performed. Fibroblasts were seeded in triplicate in a 96-well plate at 10,000 cells per well. Following the protocol for EV isolation, cells were incubated for 24 hours to allow cells to acclimatise, after which the medium was replaced with medium utilising different concentrations of EV-depleted FBS (Lonza; 5%, 7.5%, 10%, 12.5% and 15%), alongside the control of 10% normal FBS, and the cells were incubated for 72 hours. MTT was added to the medium at a final concentration of 5 mg/ml, and the plate was incubated for 3 hours.

2.3 Brain tissue

2.3.1 Brain tissue collection

Frozen post-mortem brain tissues (frontal cortex) were obtained from the Manchester Brain Bank.

Patient demographics for the AD (*n* = 3) and cognitively normal (*n* = 3) individuals used in this study are shown in Table 2.2. AD patients were clinically diagnosed with AD with subsequent pathological confirmation, while disease associated brain weight loss is observed in the AD groups . Samples were matched as closely as possible for age, sex, and post-mortem delay (PMD).

Table 2.2. Patient demographics of post-mortem brain tissue

Core characteristics of AD and healthy ageing groups. Both groups matched for sex and post-mortem delay, and showed differences in age, Braak stage, ApoE 4 allele carriers and total brain weight at collection.

Disease status	Alzheimer's disease (*n* = 3)	Healthy brain ageing (*n* = 3)	*P* value
Sex (% female)	66%	66%	>0.9999
Age (Years)	70.33 ± 9.02	87.33 ± 4.62	0.0439
Braak stage (0-VI)	VI	0-II	
ApoE 4 allele (%)	67%	0%	0.0161
Brain weight (g)	986 ± 161	1302 ± 101	0.0452
Post-mortem delay (hours)	98.17 ± 2.93	113.70 ± 38.14	0.5214

2.3.2 Processing brain tissue to isolate extracellular vesicles

To separate the EVs in the extracellular space from the other cellular material in the frozen brain tissue, samples underwent a gentle dissociation and digestion with collagenase type 3 (Abnova) in hibernate-E medium (ThermoFisher), as described in previous studies (Vella *et al*, 2017; Huang *et al,* 2020).

Tissue was sliced on dry ice with sterile scalpels (Swann-Morton), to ensure minimal degradation and contamination of samples. Two isolations were collected, two smaller 25 mg sections for direct homogenisation (for protein and RNA isolation, labelled as brain homogenate or BH) and a larger 250 mg section for EV isolation, which was sliced and immediately incubated in the collagenase type 3/ hibernate-E medium (75 U/ml and 800 µl per 100 mg tissue, respectively) at 37°C for 20 minutes. During the incubation, the solution was gently inverted after 5 minutes, gently pipetted with a 25 ml stripette (Sarstedt) after 15 minutes, and immediately returned to ice at 20 minutes, where 100x protease and phosphatase inhibitor (PI/PS) was added (ThermoFisher) to 1x.

After the dissociation step, tissue was spun at 300*g* at 4°C for 10 mins. The supernatant was transferred to a fresh tube while the pellet containing the cellular material was washed

with PBS + PI/PS, separated into two fractions, and homogenised (for protein and RNA isolation, labelled as brain homogenate plus collagenase or BH+C). The transferred supernatant was processed by centrifugation at 2000*g* at 4°C for 15 mins, then the subsequent supernatant was pressed through a 0.22 µm filter at a slow rate of 5ml per minute, and then centrifuged at 10,000*g* at 4°C for 30 mins. These steps were performed to minimise the contamination of cellular material into the EV fractions. The processed samples were incubated with a high-salt precipitation buffer (Cell Guidance Systems) in a 2:1 (sample: buffer) ratio overnight, as described below (2.4 Harvesting extracellular vesicles from medium and tissue).

2.3.3 Brain tissue homogenisation

Both brain tissue sectioned directly for homogenisation (brain homogenate/BH) and brain tissue that underwent collagenase treatment (brain homogenate plus collagenase/BH+C) were homogenised as follows.

For protein isolation, tissue was suspended in either 700 µl or 1 ml (for BH and BH+C, respectively; volume based on guidelines for different sized sections: BH – 25 mg, BH+C – 250 mg) ice cold RIPA buffer with PI/PS (ThermoFisher) where it was sequentially broken down by pipetting with 1 ml, 200 µl, 20 µl pipettes, followed by passing the mixture through 18-, 21- and 23-gauge needles (Terumo) until the tissue was completely lysed. Lysates were incubated on ice for 15 minutes with regular vortexing, followed by being centrifuged at 14000*g* at 4°C for 15 min, after which the clarified supernatant was transferred and stored at -20°C.

For RNA isolation, tissue was suspended in either 700 µl or 1 ml (for BH and BH+C, respectively) Qiazol (Qiagen) where it was sequentially broken down by pipetting with 1 ml, 200 µl, 20 µl pipettes, followed by passing the mixture through 18-, 21- and 23-gauge needles until the tissue was completely lysed. RNA was isolated from the lysate using the same protocol as described below in section 2.6 Isolating RNA from extracellular vesicles, and subsequently stored at -80°C for future use.

2.4 Harvesting extracellular vesicles from medium and tissue

After separate pre-processing steps, isolation of EVs from medium and tissue was performed using size elution chromatography (SEC, Figure *2.2*) with a precipitation step (Exo-spin, Cell guidance systems), based on recommendations from the MISEV guidelines (Théry *et al*, 2018). The exo-spin method was performed as per the company guidelines, briefly, pre-processed supernatant was mixed with exo-spin buffer in a 2:1 ratio and incubated overnight to precipitate EVs. The solution was spun at 10,000*g* for 96 minutes to pellet the precipitated EVs. EV pellets were resuspended in fresh PBS and applied above the membrane of a pre-prepared exo-spin column. The columns were spun at 50*g* until all the supernatant had passed through the column, followed by the application of PBS to the membrane with another spin at 50*g* for 1 minute to elute the EVs in a new tube (approximate 200 µl yield).

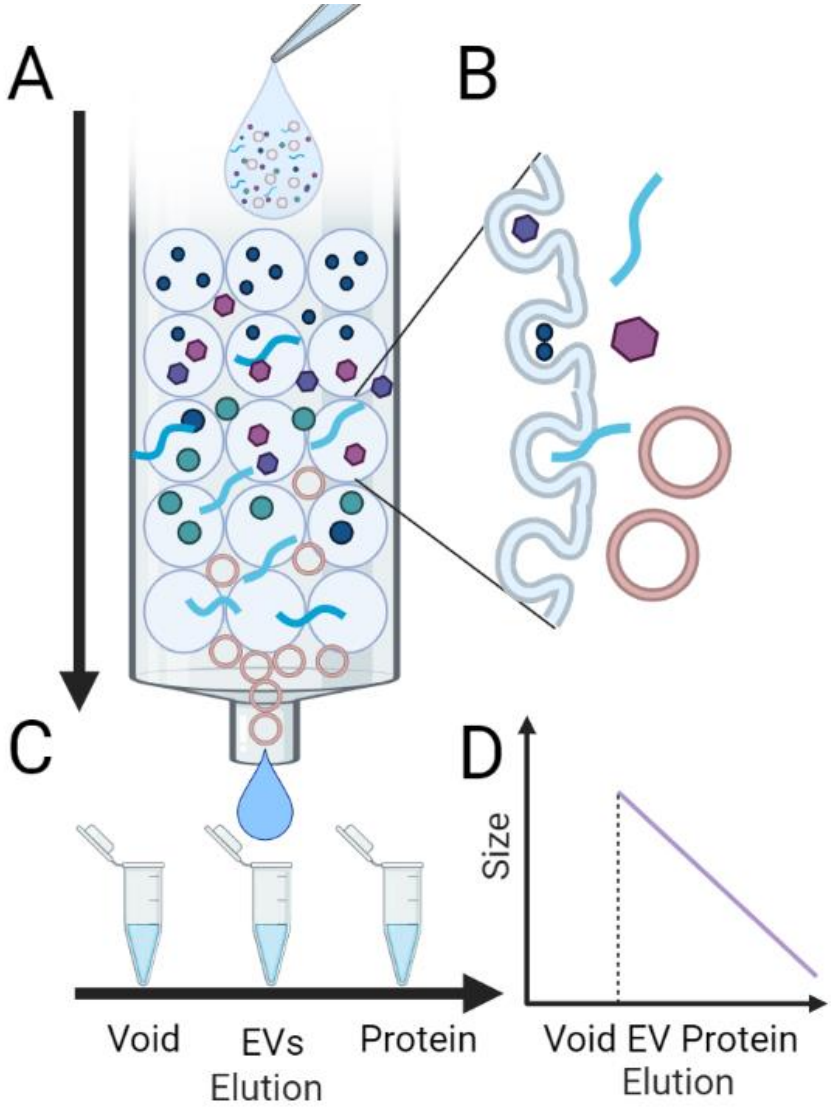

Figure 2.2. Process of size exclusion chromatography

A) A mixed population, including EVs, proteins and lipids, is pipetted onto the column bed, where the mixture flows through the Sepharose resin either by gravity or centrifugation. The resin is made of porous beads, which trap smaller particles while larger particles flow through the column. B) A magnification of a bead, highlighting how particles small enough to fit into the pores get trapped, whereas larger particles (including EVs) interact minimally with the resin. As the column is washed, the smaller particles are flushed from the pores and continue through the column. C) The mixture is washed through the column and elutions of a set volume are collected.. D) The first fractions are the 'void' volume, where the solution does not contain detectable particles as the molecules have not passed through the column yet. The first detectable particles will the larger molecules, such as EVs, which passed through the column relatively uninterrupted, followed by molecules of decreasing size, including free proteins, corresponding to their interaction with the resin. Image created with BioRender.com.

2.5 Protease and RNase treatment of extracellular vesicles

To determine the topology of RNA in association to EVs, the EV samples were treated with Proteinase K and RNase A. Publications in the field have shown that RNA enclosed in EVs is protected from RNase treatment (Driedonks *et al*, 2020), therefore, this treatment can distinguish between EV RNA and free RNA. Samples were divided, with 50 µl undergoing treatment enzymatic treatment and 50 µl incubated with equal volumes of PBS, all other steps remained the same. First, Proteinase K (ThermoFisher), to a final concentration of 20 ug/mL, was added to the EV samples, which was incubated at 37°C for 30 mins. Halt™ Protease Inhibitor Cocktail (100X) (ThermoFisher) was added to stop the Proteinase K reaction and were incubated on ice for 10 minutes. Finally, samples were treated with RNase A, to a final concentration of 10 ug/mL, and incubated at 37°C for 30 mins. QIAzol (Qiagen) was immediately added to the EV samples to inhibit the RNase reaction and to proceed to RNA isolation.

2.6 Isolating RNA from extracellular vesicles

RNA was isolated from EVs using the miRNeasy Micro Kit (Qiagen), following the incubation with QIAzol. At this stage, the exogenous spike-in *C. elegans miR-39 (cel-mir-39*, Qiagen*)* was added to the lysate, according to the manufacturers protocol (3.5 µl of 1.6 x 10^8 copies/µl). The lysate was vortexed and then incubated at room temperature for 30 min. 90 µl chloroform was added and the mixture was shaken vigorously, and then incubated at room temperature for 5 min. The mixture was centrifuged at 12,000*g* for 15 min at 4°C. Once the phases had clearly separated, the upper aqueous phase was pipetted, without disturbing the interphase, to a new tube and two volumes of 100% ethanol was added to precipitate the sample. The samples were centrifuged through the RNeasy MinElute spin column at ≥8000*g* for 15 s at room temperature. Clean up of the sample took place via centrifugation of 700 µl and then 500 µl of RWT and RPE buffer, respectively, through the spin column at ≥8000*g* for 15 s at room temperature. A second RPE buffer wash was performed at ≥8000*g* for 2 min at room temperature. The membrane was dried by centrifuging the spin column in a new tube at 15000*g* for 5 min. The spin column was transferred to a new tube and 14 µl RNase-free H_2O (ThermoFisher) was pipetted onto the

membrane, which was then centrifuged for 1 min at 15000*g*. The eluate containing the isolated RNA was stored at -80°C, ready for downstream qPCR and small RNA sequencing.

2.7 Harvesting extracellular vesicle RNA from SH-SY5Y culture medium

Total EV RNA was isolated from cell culture medium using the exoRNeasy Serum/Plasma kit (Qiagen). Briefly, equal volumes of XBB buffer were added to medium and mixed. The mixture was pipetted into the spin columns and centrifuged at 500*g* for 1 min, then the flow through was discarded. 10 ml XWB buffer was pipetted into the spin columns and centrifuged for 5000*g* for 5 min, then the spin column was transferred to a new collection tube. 700 µl QIAzol (Qiagen) was pipetted directly onto the spin column membrane, and centrifuged for 5000*g* for 5 min, from which the lysate was collected in a new tube. Following this, RNA was collected using the same protocol as above (2.6 Isolating RNA from extracellular vesicles).

2.8 Quantifying RNA from samples

Isolated RNA was quantified using the fluorometric dye incorporated in the Qubit RNA HS Assay Kit on the Qubit 3 Fluorometer (ThermoFisher), selecting the RNA protocol. miRNA quantitation was performed using the Qubit miRNA Assay Kit (ThermoFisher), selecting the miRNA protocol. The Qubit assays were performed as per the manufacturers protocol, briefly RNA samples were diluted 200-fold with the prepared Qubit working solution and ran against the standards provided.

2.9 Harvesting protein from fibroblasts and extracellular vesicles

Cell lines were harvested post EV isolation, with 1 million cells used for cell lysates. Briefly, cells were trypsinised, spun down and counted using trypan blue (Biosera). 1 million cells were pelleted and washed with ice-cold PBS, followed by the addition of 1 ml of RIPA buffer (ThermoFisher). EVs were mixed 1:1 with RIPA buffer. The sample was mixed and incubated for 15 minutes on ice, then centrifuged at 14000*g* for 15 minutes to pellet the debris, with the supernatant containing the protein. Samples were used for protein analysis and western blotting.

2.10 Extracellular vesicle characterisation

2.10.1 Total protein quantification

Total protein analysis of extracellular vesicles was performed using the BCA (Bicinchoninic acid) assay (ThermoFisher), with sample readings being corroborated with the Qubit Protein Assay Kit (ThermoFisher). The BCA assay was performed as per manufacturer guidelines, briefly EV samples were diluted 80-fold in PBS and plotted against a standard curve of pre-prepared BSA dilutions (25-2000 µg/ml). The standards or the diluted EV samples was pipetted into the respective wells of a microplate, followed by the BCA working reagent. The plate was shaken to mix and incubated at 37°C for 30 mins. Samples were read on the plate reader (Scanit) at 562 nm.

The Qubit assay was performed as per the manufacturers protocol, briefly EV samples were diluted 200-fold with the prepared Qubit working solution and ran against the standards provided. Samples were read on the Qubit 3.0 Fluorometer (ThermoFisher).

2.10.2 Western Blotting

Characterisation of EV associated proteins and intercellular associated negative controls was performed using Western blotting. Gels were cast using 1.5 mm glass separators (Bio-rad), with the resolving gel at 10/12% acrylamide constitution, depending on the size of the protein of interest. SDS gels were cast as per the Bio-rad recommendations. Resolving gels were made using 10/12% acrylamide depending on the desired final constitution, with 1.5M of Tris-HCL (pH 8.8), 10% SDS, 10% APS (Ammonium persulfate) and 0.002 % TEMED (Tetramethyl ethylenediamine). Gels were left to set for 45-60 minutes with a fine layer of water-saturated butanol on top to ensure even layers, after which the butanol was aspirated, and the glass was rinsed thoroughly with dH_2O and dried with lint-free tissue. Stacking gels were poured on top and made using 5% acrylamide, 0.5M of Tris-HCL (pH 6.8), 10% SDS, 10% APS and 0.002 % TEMED. A 10 well comb with a 50 µl capacity was inserted and the gel was left 30 minutes to set.

An equal amount of protein (quantified by BCA) from EV samples and cell lysates/brain homogenates was loaded per well into the gel, with most experiments set at 20 µg, though

in some experiments where markers displayed low expression, the EV protein loaded increased up to 30 µg. Samples were prepared with 4x Laemmli sample buffer (Bio-Rad) in non-reducing conditions and boiled at 70°C for 10 minutes. Denatured samples were then loaded into the wells of the gel alongside 10 µl PageRuler^{TM} Plus pre-stained protein ladder (ThermoFisher, 10 to 250 kDa). Running buffer was made up of tris base (25nM), glycine (192 mM) and 1% SDS.

Electrophoresis was performed at 80V (10V per cm gel) while the samples concentrated in the stacking gel, after which the running conditions were maintained at constant 100V (0.02A per gel) for approximately 90 minutes or until the dye front reached the bottom of the gel. After electrophoresis, gels were washed in transfer buffer (tris base (25nM), glycine (192 mM), 20% methanol) and sandwiched against a 0.2 µm nitrocellulose membrane, where the separated protein was blotted in standard transfer conditions (100V for 60 minutes, temperature regulated with ice and cooling unit).

Membranes were briefly washed in wash buffer/PBST (0.1% Tween 20) to remove any electrolyte solution, after which some where incubated with Ponceau Red (Sigma-Aldrich) for 5-10 minutes to determine the transfer efficacy. Blocking of the membrane was performed with 5% BSA in Phosphate buffered saline and 0.1% Tween 20 (PBST) with gentle agitation for 2 hours.

Membranes were incubated with the primary antibodies (mouse anti-human) in 2.5% BSA PBST solution: anti-CD9 (1:2000 – 0.25 µg/ml), anti-CD63 (1:5000 – 0.1 µg/ml), anti-CD81 (1:2000 – 0.25 µg/ml) (ThermoFisher, Invitrogen 10626D, 10628D, 10630D, respectively), TSG-101 (1:2000, 0.5 µg/ml, Abcam, Ab83), and flotillin-1 (1:2000 - 0.5 µg/ml), calnexin (1:10,000 – 0.05 µg/ml) and GM130 (1:10,000 – 0.05 µg/ml) (Proteintech, 67968-1-Ig, 66903-1-Ig, 66662-1-Ig, respectively), overnight at 4°C with gentle agitation.

Membranes were washed in PBST for 3 x 10 minutes at room temperature, with vigorous agitation, after which they were incubated with HRP (horseradish peroxidase) conjugated goat anti-mouse secondary antibody (1:5000, Cell signalling, # 7076), for 1 hour at room temperature. Membranes were washed again in PBST for 3 x 10 minutes to remove any unbound antibody.

Proteins were detected using ECL (Electrochemiluminescence), with West Femto Maximum Sensitivity Substrate ECL (Thermo Scientific™ SuperSignal™). Signal was visualised using the Gbox (Syngene) and the Odyssey XF (Li-Cor).

Semi-quantification of Western blot band intensities was performed using ImageJ software (https://imagej.net/ij/index.html). A standardised selection area was determined for individual images, with size of the area maintained for all bands in the blot. Quantification was carried out by inverting the mean grey area of the bands and normalising to the background. Ratios were performed on AD cases against healthy neurological controls.

2.10.3 Nanoparticle tracking analysis

EVs were characterised and visualised by nanoparticle tracking analysis (NTA) using the ZetaView (Particle Metrix, Germany) to interpret the total number, concentration, and polydispersity. The protocol was performed based on company guidelines. Samples were diluted in PBS starting at 1:1000 and adjusted until the EV concentrations were in the desired concentration range of the ZetaView, between 50-200 particles per frame. The machine was flushed with sterile PBS, to clear impurities which would interfere with the measurements. The sample was subsequently injected into the machine, which was scanning in scatter mode at a wavelength of 520 nm. ZetaView settings were calibrated according to the manufacturers protocol, including measurements at 25°C and at 11 camera positions to determine an average of the EV sample composition. Polystyrene beads (100nm, Analytik, P/N 700093) were used to calibrate the system prior to analysis.

2.10.4 Fluorescence nanoparticle tracking analysis

Isolated EVs underwent fluorescence nanoparticle tracking analysis (f-NTA) using the ZetaView (Particle Metrix, Germany), the protocol was performed based on company guidelines. As the machine's wavelength is 520 nm the long wave pass cut off filter is slightly higher at 550 nm, meaning that all fluorescent conjugates need to emit at a higher wavelength than 550 nm to be distinguished from the scatter. ZetaView settings were calibrated according to the manufacturers protocol, as with the NTA scatter detection, but a low bleach mode was used to optimise measurement of fluorescence. Further, 100 nm

fluorescent polystyrene beads (Analytik) were used to calibrate and optimise the system prior to fluorescent analysis. Optimisation included a dye-only control

EV samples were labelled with CD9, CD63 and CD81 (Biolegend, 312118, 353022, 349520, respectively), all conjugated with the PE/Dazzle^{TM} 594 fluorochrome. The final PE/Dazzle dilution was determined by running a serial dilution and measuring the background, with 1:100,000 (0.005 µg/ml) the highest concentration that does not produce background signal. Samples were incubated at room temperature with either an individual antibody or the mix of antibodies for 2, 6 and 24 hours, to determine the optimal antibody incubation times. Signal did not increase significantly beyond 2 hours. Therefore, all experiments were incubated for 2 hours at room temperature, prior to measurement. EV samples were injected and measured in both scatter and fluorescence mode.

EVs were also labelled with Cell Mask Orange (CMO, Invitrogen, C10045) solution according to company guidelines. The final CMO dilution was determined by running a serial dilution and measuring the background, with 1:10,000,000 the highest concentration that does not produce background signal. Briefly, EVs were mixed 9 parts to 1 with pre-diluted CMDR (1:1000), after which the solution was incubated for 1 hour at room temperature in the dark to allow the dye to bind to the membranes. The mixture was then diluted 1:1000 and measured on the ZetaView in both scatter and fluorescent modes.

Fluorescent ratios (%F) were measured by determining the number of fluorescent particles (c_F = Fluorescent count) compared to the number of particles from the same sample detected in scatter (c_S = Scatter count), as follows:

$$\%F = \frac{c_F}{c_S} \cdot 100\% \qquad [1]$$

2.10.5 Transmission electron microscopy

EVs were directly visualised with transmission electron microscopy (TEM) to confirm the presence of particles with the size and structure characteristic of EVs. This work was performed at the University of Liverpool. Briefly, a 10 µl EV sample was used for the imaging which was suspended on a carbon coated grid, and subsequently processed as follows: washing with PBS, fixation with 1% glutaraldehyde, washing with ddH_2O, staining

with the electron dense uranyl acetate (1%), and further staining and preservation with 4% uranyl acetate/2% methyl cellulose (in a 1:9 ratio). After the sample was processed, it was drained and dried. Imaging was performed at 120KV on a FEI Tecnai G2 Spirit with Gatan RIO16 digital camera.

2.11 Targeting candidate miRNA in extracellular vesicles

2.11.1 Reverse transcription

RNA was taken from the fibroblast-derived EVs and brain-derived EVs (6 ng and 10 ng, respectively) and converted to cDNA using the QuantiMir Kit (System Biosciences). Everything was performed on ice where possible unless they were being incubated in the Alpha Cycler 1 (PCRmax). Briefly, 5 µl of total RNA was mixed with the polyA tail mastermix, consisting of 5X Poly-Adenine (PolyA) buffer, 25 mM $MnCl_2$, 5 mM ATP and PolyA polymerase. After a 30 min incubation at 37°C, to allow the PolyA tail to synthesise, oligo dT adaptors were added to the samples, which were subsequently incubated at 60°C for 5 min. The samples were cooled to room temperature, after which the cDNA synthesis mixture was added, consisting of 5X reverse transcription buffer, dNTP mix, 0.1 M Dithiothreitol (DTT), RNase-free H_2O and reverse transcriptase. Samples were incubated at 42°C for 1 hour, after which they were heated to 95°C for 10 min to stop the reaction. cDNA samples were stored at -20°C.

2.11.2 PCR amplification

PCR reaction mixes were prepared according to the manufacturer's protocol and consisted of SensiFAST SYBR® No-ROX Kit (Meridian Bioscience), the miRNA specific forward primer (Eurofins), universal reverse primer (System Biosciences) and RNase-free H_2O (ThermoFisher). The miRNA specific forward primer was the same sequence as the mature miRNA, which were confirmed on miRbase (https://mirbase.org/, release 22.1, accessed 2022). The universal reverse primer is complementary to the QuantiMir oligo-dT adapter that was used to create the first strand cDNA in 2.11.1 Reverse transcription. A list of the non-chromosome 14 candidate miRNAs is displayed in Table 2.3.

Table 2.3. List of sequences for candidate microRNAs

MicroRNA	microRNA sequence
Mir-16-5p	UAGCAGCACGUAAAUAUUGGCG
MiR-17-5p	CAAAGUGCUUACAGUGCAGGUAG
Mir-19a-5p	AGUUUUGCAUAGUUGCACUACA
Mir-19b-5p	AGUUUUGCAGGUUUGCAUCCAGC
Mir-20a-5p	AGAGGUUGCCCUUGGUGAAUUC
Mir-21-5p	UAGCUUAUCAGACUGAUGUUGA
Mir-92a-5p	UGUGACUGGUUGACCAGAGGGG
Mir-106a-5p	UAAAGUGCUUACAGUGCAGGUAG
Mir-106b-5p	UAAAGUGCUGACAGUGCAGUA
Mir-146a-5p	UGAGAACUGAAUUCCAUGGGUU
miR-155-5p	UUAAUGCUAAUCGUGAUAGGGGUU

The mastermix was combined with the cDNA template or RNase-free H_2O for the no-template control (NTC). All samples were analysed in duplicate. PCR amplification was performed on the Rotor-Gene Q (Qiagen) with PCR cycling conditions shown in Table *2.4*.

Table 2.4. Cycling conditions for RT-PCR

Step	Description	Temperature (°C)	Time	Cycles per step
1	Initial incubation	50	2 min	1
2	Initial denaturation	95	10 min	1
3	Denaturation Annealing/ Elongation	95 60	15 s 1 min	40
4	Melt-profile analysis	Ramp 50-95	~5 min	1

Cycle thresholds (Ct) values were determined in the exponential phase of amplification plots after the reaction had completed. Relative expression of miRNAs was determined using the $2^{\wedge-\Delta\Delta Ct}$ method (Livak and Schmittgen, 2001), where differences in Ct values between the miRNA of interest and U6 (endogenous) or *cel-39* spike-in (EV) controls (ΔCt) were compared between disease and control samples (ΔΔCt). Specifically, ΔCt values of the control biological replicates were averaged to create an internal control, which all

samples were compared against to form the ΔΔCt. The fold gene expression is determined by log transforming the ΔΔCt values by $2^{\wedge\Delta\Delta Ct}$, as the Ct values are log2 scale. Melt curves were monitored to determine the PCR product was the correct size, the presence of primer dimers and amplification in the NTCs.

2.12 Small RNA sequencing of extracellular vesicle cargo

2.12.1 Library preparation

For library preparation, 6 ng and 10 ng RNA were taken from the fibroblast-derived EVs and brain-derived EVs, respectively. RNA was processed using the Small RNA-Seq Library Prep Kit for Illumina (Lexogen), according to the manufacturer's protocol. Adapters and primers used in the kit were diluted to 0.3x, as RNA input was lower than 100 ng. All steps that required conditions other than room temperature were performed in a pre-heated thermocycler. The RNA/cDNA library was generated as displayed in Figure 2.3.

To ligate the 3' adapter to the RNA, both the RNA and the 3' adapter were incubated together at 70˚C for 2 mins, denaturing any secondary structures and leaving single stranded (ss)RNA, which increases the efficiency of the downstream reactions. The denatured mixture was incubated with a ligation and enzyme mastermix for 1 hour at 28˚C. Once the 3' ligation had finished, the rection mixture was passed through a purification column to remove any unbound 3' adapter. The 5' adapter was denatured as the RNA and 3' adapter were, after which it was mixed with a ligation and enzyme mastermix. The RNA was incubated with the pre-prepared mastermix for 1 hour at 28˚C to ligate the 5' adapter. The 3' and 5' adapter-ligated RNA was mixed with the reverse transcription primer and denatured at 70˚C for 2 mins. The denatured sample was mixed with a mastermix of first strand cDNA synthesis mix and enzyme mix, and incubated for 1 hour at 50˚C.

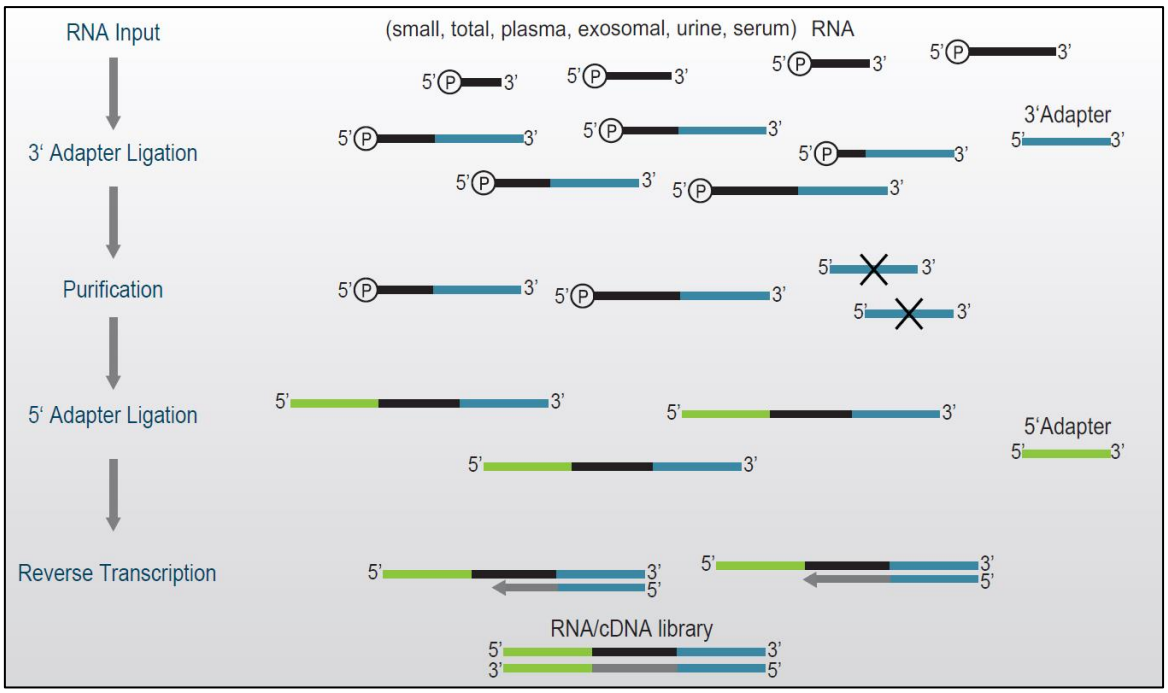

Figure 2.3. RNA/cDNA Library Generation

Schematic adapted from Lexogen (https://www.lexogen.com/small-rna-seq-library-prep-kit/, accessed 2022). Details the steps involved in library generation, including 3' adapter ligation, 5' adapter ligation and reverse transcription of RNA to RNA/cDNA library. Black – RNA, blue – 3' adapter, green – 5' adapter.

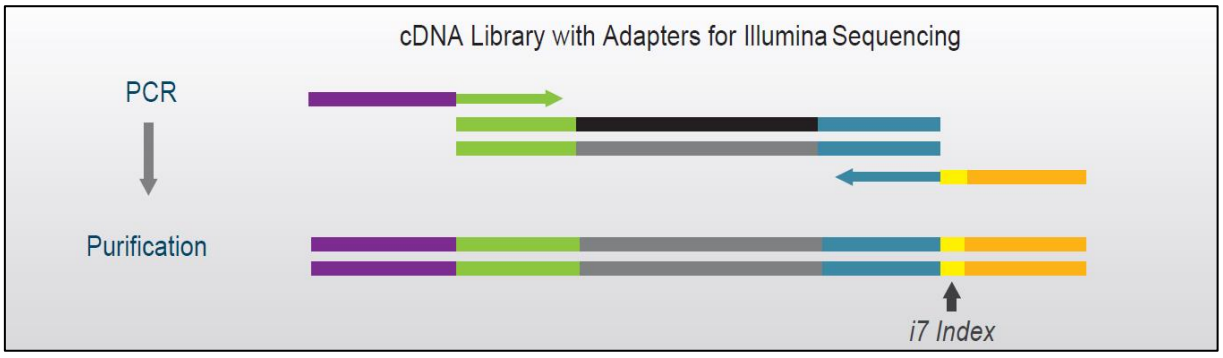

Figure 2.4. Library amplification

Schematic adapted from Lexogen (https://www.lexogen.com/small-rna-seq-library-prep-kit/, accessed 2022). Details the steps involved in library amplification, including PCR amplification of cDNA libraries, at which stage, i7 Illumina indexes (yellow), and p5/p7 Illumina adapters (purple/orange) were incorporated for downstream sequencing of the libraries.

Library amplification (Figure 2.4) was performed as follows. To amplify the RNA/cDNA amplified by endpoint PCR, the samples were combined with a mastermix consisting of PCR mix, P5 adapter primer, and H_2O, followed by the specific Small RNA i7 Index Primer required for multiplexing. The libraries underwent PCR thermocycling, including 98 °C for 30 seconds to denature all the product, then 22 cycles of 98 °C for 10 seconds, 60 °C for 30 seconds, and 72 °C for 15 seconds to amplify the product, and a final extension at 72 °C for 10 minutes. During this amplification, the P5 and P7 Illumina adapters were incorporated for the downstream sequencing. Each sequencing run incorporated four samples (multiplexed), therefore, each sample was incubated with a specific i7 adapter, which is read during sequencing to track the read back to the correct sample and demultiplex the run. PCR products were purified of any PCR reagents left in the mixture by being passed through a purification column, where they were washed with column wash buffer and then eluted with 20 µl of Elution Buffer, thereby also concentrating the libraries, which were ready for quality control and Illumina sequencing (Figure 2.5). As the RNA used for the libraries was small RNA enriched, no further purification was required for small RNA sequencing.

Figure 2.5. Illumina sequencing using Lexogen libraries

Schematic adapted from Lexogen (https://www.lexogen.com/small-rna-seq-library-prep-kit/, accessed 2022). Details the read orientation of the Lexogen libraries on the Illumina system. Small RNA sequencing required only single read sequencing (5' to 3') due to the 50-cycle read (described below) covering the miRNA span (~21 bp). As samples were multiplexed (multiple samples on the same sequencing run), a subsequent i7 index primer binds to the 3' adapter (blue) to read the i7 index of the sample, which allows the sequencing run to determine which reads were from which sample during the run.

2.12.2 Library quality control and quantification

Libraries prepared with the Small RNA-Seq Library Prep Kit (Lexogen) were quality checked to ensure that the small RNA fragment had been amplified for sequencing with minimum contamination. They were also quantified to make sure the correct amount of library was loaded in the MiSeq (Illumina), reducing the chance of under- or over-clustering.

Library quality checks were performed with high sensitivity capillary electrophoresis, using the TapeStation system (Agilent), which can visualise the fragment size (bp) of the library and any potential contaminants, such as linker-linker artifacts. Libraries were run with the High Sensitivity D1000 ScreenTape Assay (TapesStation), briefly, samples or the High Sensitivity D1000 Ladder were mixed with the High Sensitivity D1000 Sample Buffer, vortexed and spun down to load into the TapeStation 2200 system. The D100 ladder has a size range of 35 – 1000 bp with a sizing range of ±10%, granting high resolution visualisation of fragment sizes (bp). The average fragment sizes (bp) for each sample were determined by selecting the enriched region on the Tapestation plot, which corresponded with the small RNA fraction.

Quantification was performed by qPCR and fluorescent detection (Qubit). qPCR based detection used the NGSBIO Library Quant Kit for Illumina (PCR Biosystems), which specifically amplifies the adapter ligated library. Libraries were diluted by 10^6x in dilution buffer and combined with a mastermix of 2x qPCRBIO SyGreen Mix, 10x Illumina Primers and PCR grade dH_2O. A set of DNA standards that range from 0.2 fM to 2 pM were also combined with the PCR mastermix in a set of separate PCR tubes. The qPCR thermocycling was ran with 1 cycle of polymerase activation at 95˚C for 1 min, followed by 40 cycles of denaturation (95˚C for 15 seconds) and annealing/extension (63˚C for 45 seconds), with a melt analysis. A standard curve was plotted using the DNA standards, which was used to calculate the concentration of the diluted libraries. The original library concentration (nM) was worked out by:

$$Library\ Conc\ (nM) = reaction\ Conc\ (nM) \times dilution\ factor\ (10\text{^}6\ ) \times \frac{452}{average\ fragment\ length}$$

[2]

Average fragment length was determined by TapeStation (Agilent) capillary electrophoresis, above.

Libraries were also quantified using the fluorometric dye incorporated in the Qubit dsDNA HS Assay Kit on the Qubit 3 Fluorometer (ThermoFisher), selecting the dsDNA protocol. The Qubit assay was performed as per the manufacturers protocol, briefly libraries were diluted 200-fold with the prepared Qubit working solution and ran against the standards provided.

2.12.3 Illumina MiSeq small RNA sequencing

Sequencing was performed according to the Illumina guidelines, with the Illumina standard normalisation method used to denature and dilute libraries. The sequencing chemistry used was the MiSeq Reagent Kit v2, therefore, libraries were pre-diluted to 4 nM with PCR grade dH_2O, based on the quantified values with the Qubit (ThermoFisher). The 4 nM libraries were denatured with freshly prepared 0.2 N NaOH at room temperature for 5 minutes. Denatured libraries were then diluted to 20 pM with pre-chilled hybridisation buffer (HT1), which also ensured that the NaOH was diluted to below 1 mM, a low enough concentration that it would not interfere with downstream library hybridisation to the flow cell. Libraries were further diluted to 8 pM with HT1, the recommended input for Illumina v2 chemistry. A 12.5 pM PhiX library (~45% GC and ~55% AT) was spiked-in to the 8 pM libraries to ensure there was enough nucleotide diversity for optimal sequencing performance, as the Illumina system can have difficulty correctly attributing signal to the correct cluster in low diversity libraries, which can affect base calling and quality score calculations. PhiX libraries were pre-diluted to 4 nM with Tris-Cl (pH 8.5 with 0.1% Tween

20), and then denatured and diluted to 20 pM as described above. A final dilution of the PhiX library to 12.5 pM was made with HT1, which was then spiked-in to the libraries at a 1% concentration, and the combined library was loaded into the reagent cartridge.

The reagent cartridge, pre-cleaned flow cell, incorporation buffer (PR2) and empty waste bottle were loaded into the MiSeq according to the system guide. Sequencing was performed on the MiSeq (Illumina) using v2 chemistry and a 50-cycle read, with analysis, filtering and base calling directly ran on BaseSpace. All runs were multiplexed with 4 libraries, with the corresponding i7 index sequence loaded on the sample sheet, with the Illumina adapter sequence and generate fastQ analysis workflow. Runs were monitored for quality scores, cluster density, clusters passing filter and yield of bases called during the run.

2.13 Small RNA sequencing data analysis

2.13.1 Quality control of RNA sequencing data

For each sequencing run, four fastQ files were produced, corresponding to the four libraries that were multiplexed. All fastQ files were uploaded to Galaxy (The Galaxy Community, 2022) for processing and analysis. Initial quality checks of the RNA sequencing data were performed using fastQC (Version 0.73; Andrew, S., accessed 2022), which checks the data for basic statistics, including total reads and average sequence length and GC%, per base sequencing quality (Q-score), per base sequence, N and GC content, sequence length distribution and duplication levels, overrepresented sequences and identified adapter content.

Q-scores are a prediction that a base called during sequencing is incorrect, with a Q40 indicating that the probability of a wrong base call is 1 in 10,000, reducing by a factor of 10 for Q30, Q20 and then Q10, which indicates that the probability of a wrong base call is 1 in 10. Q-scores over 30 were considered to have passed the sequencing quality check. Per base sequences, N and GC content checked that there was an even distribution of nucleotides and GC vs AT across the whole read and no individual was overrepresented, and that there was no unidentifiable nucleotide content (N). Sequence length distribution

checked the length of individual reads, with reads lower than 16 bp omitted from the analysis. Sequence duplication levels were checked to observe whether there had been any enrichment bias during library preparation or sequencing, which was also confirmed by analysing overrepresented sequences (>0.1% of reads), that also can identify any contaminating factors or adapter sequences that need to be filtered. Identified adapter content compares read sequences to the Illumina adapter sequences. With small RNA sequencing there is a high proportion of adapter content that needed to be trimmed and filtered as the read length is longer than the RNA of interest (such as ~22bp miRNA vs the 50 bp Illumina read depth).

2.13.2 Trimming and adapter clipping of sequencing reads

After the preliminary quality of raw reads was analysed, the data in fastQ format was processed using Cutadapt (Version 4.0; Martin, M., 2011), which removed adapter and other contaminant sequences. The 3' adapter sequence incorporated in the Small RNA-Seq Library Prep Kit (Lexogen), 5'- TGGAATTCTCGGGTGCCAAGGAACTCCAGTCAC – 3', which was responsible for most overrepresented sequences in the fastQ report, was trimmed from all reads. After trimming, all reads that were shorter than 16 bp and higher than 31 bp were filtered. Trimmed files were checked by fastQC to determine whether the remaining reads passed the quality checks.

2.13.3 Sequencing read alignment

Trimmed reads were aligned to the reference Human (Homo sapiens) genome (Hg38) using Bowtie2 (Version 2.4.5; Langmead and Salzberg, 2012). The aligned format output is as a BAM file, along with an analysis of the alignment percentage, including whether the data was a unique alignment or had aligned multiple times in the reference genome. SAMtools (Version 2.0.4) packages: stats flagstat and idxstats (Li et al, 2009) were used to assess the output of the alignment, including observing the total reads, uniquely mapped reads, duplicates, reads mapping per chromosome. Alignment statistics were visualised using MultiQC (Version 1.11; Ewels et al, 2016).

2.13.4 Generation of miRNA read counts

Reads that were aligned to the reference (Hg38) genome in BAM format were counted using htseq-count (Version 0.9.1; Anders, S., 2014), while mapping to the miRbase mature miRNA annotation (miRbase (https://mirbase.org/, release 22.1, accessed 2022) inputted in GFF format. Alignment of features was determined by union mode, where any individual (including partial alignment) overlap was mapped to the determined miRNA, while reads that mapped at least partially to multiple miRNAs were classified as ambiguous and filtered. A minimum alignment quality of 20 (Phred scale) was used as cut off to be included in the feature count. Counts were recorded into counts tables/files.

2.13.5 Differential expression analysis of miRNAs

Counts files were compared between AD and control samples in DESeq2 (Version 2.11.40.7; Love et al, 2016), a Bioconductor package that tests for differential expression using a negative binomial distribution model. Factors levels were labelled as 'Alzheimer' and 'Control', with the replicate count files inputted into the corresponding factor level. Normalisation of counts was performed using the median of ratios method, which creates a reference sample/ geometric mean of all analysed samples and refers all samples against the reference, while accounting for sequencing depth and RNA composition. Internal QC of miRNA counts is performed in DESeq2 to filter out low count reads and increase the power to detect differentially expressed miRNA. DESeq2 outputs results in a table including mapped miRNA, the log fold change, standard error, P-value, and adjusted P-value/ false discovery rate based on Benjamini-Hochberg. The second result is the graphical output, including principal component analysis (PCA), sample-sample ratios, and dispersion estimates.

2.13.6 Visualisation of differentially expressed miRNAs

Differentially expressed miRNAs were visualised by the Volcano Plot in the ggplot2 package (Version 0.0.5), using the DESeq2 tabular output. Adjusted P value was plotted against log fold change, with a significance threshold of $p < 0.05$ and a fold change threshold of >1.

2.14 Statistical analysis

Statistical analysis was performed using Graphpad Prism packages (GraphPad Software, San Diego). Statistical differences were analysed using unpaired two-tailed T-tests or one-way ANOVAs with Dunnett's multiple comparisons. Correlations were performed using Pearson correlation tests. All values were displayed as mean ± SD, unless otherwise stated. P-values of >0.05 were displayed as statistically significant.

3 Chapter 3: Isolation and characterisation of small extracellular vesicles

3.1 Introduction

Studies involving EVs require a comprehensive workflow, starting from the biological source material, with a clear methodology on how to isolate EVs from the distinct material, cell culture medium, tissue or otherwise, and concluding with a robust characterisation that provides confidence that relevant downstream analysis is of EV associated changes and not due to other contaminants. Optimisation of these workflows was primarily performed in human fibroblasts from AD patients and neurological healthy controls, as well as SH-SY5Y neuroblastoma cells (Supporting documents: Appendix), while full characterisation was performed in fibroblast derived EVs and brain tissue derived EVs.

3.1.1 Aims

The aims of this chapter were to develop an EV isolation methodology that could separate EVs from both cell culture medium and human brain tissue, maintaining a pure population that was depleted in other cellular material, while having a good yield of EVs to be able to perform proteomic and transcriptomic analysis. Within this chapter, the study also aims to comprehensively characterise EVs isolated from fibroblast cell culture medium and brain tissue, according to the MISEV guidelines (Théry *et al*, 2018). This involves characterising EV morphology, size, and protein profiles, in order to determine that they express EV associate proteins and are in a size range expected of an EV subtype (small EVs: 50-200 nm, medium/large EVs: >200 nm).

3.2 Optimising cell culture conditions for isolation of small extracellular vesicles

3.2.1 Extracellular vesicle free media did not affect cell viability

With all cell culture models, it is important to clearly state the conditions used for culture, including medium compositions and seeding protocols. This is also important for EV studies (Théry *et al*, 2018), as medium supplements, in particular FBS, contain EVs that can be co-isolated with EVs released from cell culture. The FBS derived EVs contain RNA, which could impact downstream investigations of miRNA in this study (Shelke et al, 2014). Therefore, commercially available EV depleted medium (Gibco) was used, in order to ensure that isolated EVs are derived directly from the fibroblasts in cell culture, and not FBS.

While the use of commercially available EV depleted FBS reduces batch variability, the proprietary nature of such products warrants caution and investigation into the effect on recipient cell cultures. The two main EV depletion methods are by ultracentrifugation and chemical precipitation, with varying results on the degree of EV depletion (Kornilov et al, 2018; Lehrich et al, 2018). While the commercial data states '≥ 90% of exosomes depleted' and unimpeded cell viability, with supplementary data, as well as sample publications showing efficient removal of EVs from FBS and stable cell proliferation with addition of this FBS (Takov et al, 2017; Guerreiro et al, 2018), there are publications showing that EV depleted FBS has a reduced ability to support cell growth depending on the cell type being cultured (Shelke et al, 2014; Eitan et al, 2015; Aswad et al, 2016). In account of this, this study evaluated the viability of the fibroblasts, through MTT, after 72 hours in EV-depleted medium (Figure 3.1). It was observed that reduced concentrations of EV-depleted FBS resulted in a drop in cell viability compared to 10% normal FBS (5% = 54.3% viability, p = 0.0002; 7.5% = 59.8% viability, p= 0.0006). The same percentage of EV depleted FBS (10%) resulted in a decrease in cell viability (10% = 81.9% viability, p= 0.1376), while increasing the percentage to 12.5% EV depleted FBS against 10% normal FBS resulted in an increase in viability (12.5% = % viability, p= 0.7051). The 10% and 12.5% EV depleted conditions were comparable to normal FBS conditions, therefore the study continued with 10% EV-depleted FBS.

Regarding SH-SY5Y culture, as the differentiation technique required serum starvation, there was no need to supplement the medium with EV depleted FBS. Differentiation was observed through morphology during a 21-day protocol (Appendix Figure), while qPCR was used to identify a set of candidate miRNA that were differentially expressed in SH-SY5Y derived sEVs during differentiation (Appendix Table 6.1).

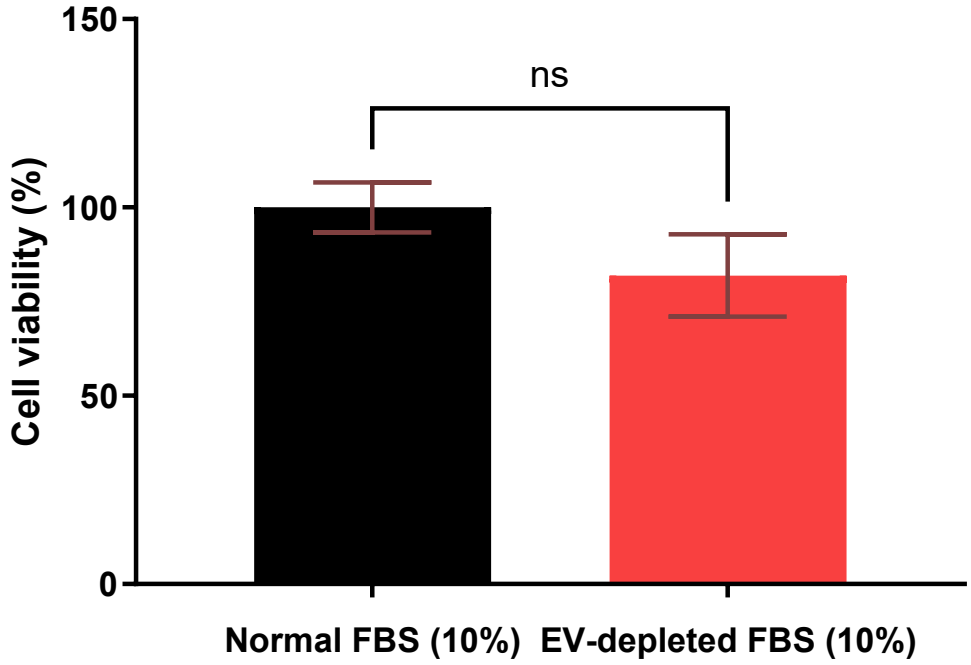

Figure 3.1. EV-depleted fetal bovine serum did not affect fibroblast cell viability

*Cells were incubated with either normal FBS (10%) or EV depleted FBS (10%) for 72 hours. FBS percentage based on proportion of total medium. Cell viability was determined with MTT (absorbance = 540 nm. Error bars ±SD. N = 3 (technical repeats). T-tests: *** P < 0.001, * P <0.05. ns = not significant.*

3.2.2 Size exclusion chromatography isolates a purer extracellular vesicle RNA population than membrane affinity isolation

Once cell cultures were determined to be stable with EV depleted FBS, work began with determining the optimum isolation method for small extracellular vesicles from cell culture. Two methods were assessed based on recommendation from the UKEV guidelines and after sourcing literature within the field (MISEV guidelines, Théry *et al*, 2018), which

were the use of direct EV RNA isolation using membrane affinity columns and isolating sEVs with SEC.

Optimisation of EV RNA isolation using membrane affinity and SEC was performed using the SH-SY5Y neuroblastoma cell line and commercially acquired fibroblasts derived from AD patients and neurologically healthy controls. Both models were routinely checked for morphology, mycoplasma infection and other factors that could influence cellular mechanisms.

Quantification of RNA isolated from fibroblasts based on both methods showed that membrane affinity columns produced almost 10-fold higher RNA levels than RNA isolated from SEC purified sEVs (Figure 3.2). No difference was observed between AD and neurological healthy control samples (Figure 4.2).

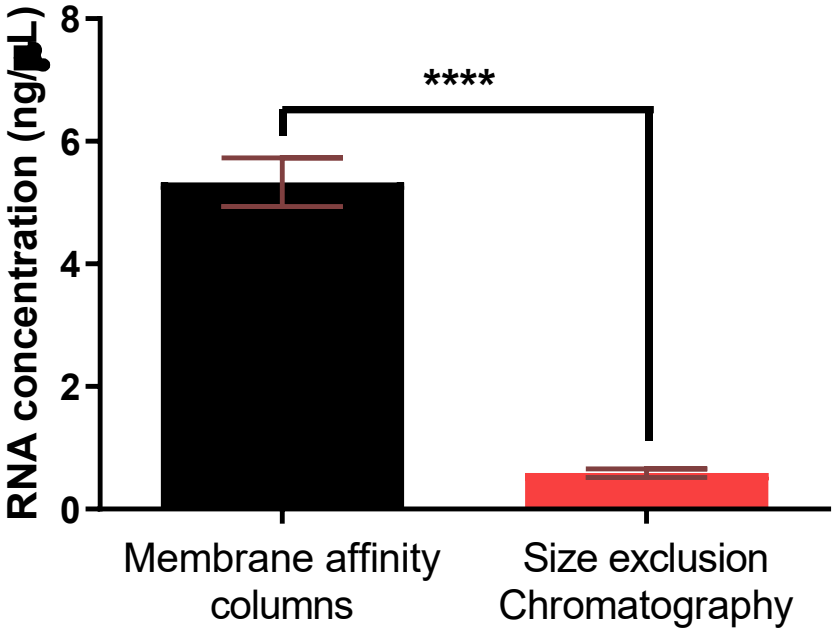

Figure 3.2. RNA concentration from fibroblast derived small extracellular vesicles was significantly higher when isolated with membrane affinity columns than with size exclusion chromatography

*RNA was quantified by Qubit after being isolated from fibroblast derived EVs by Membrane affinity columns and SEC. Membrane affinity columns display a ten-fold increase in RNA concentration compared to SEC (SEC = 0.59 ng/µl, membrane affinity = 5.20 ng/µl), indicating much higher levels of co-purified non-vesicular extracellular RNA, such as associated with ribonucleoproteins. T-test: **** P < 0.0001, N = 3 (technical repeats), Error bars = ±SD. SEC – size exclusion chromatography.*

Direct EV RNA isolation from cell culture medium using affinity columns is limited by an inability to confirm the source material from which the RNA is derived, in that the isolated EVs are immediately lysed and homogenised for RNA isolation. There are various membrane targets used for EV capture, including heat-shock proteins, heparin and tetraspanins (Ghosh et al, 2014; Balaj et al, 2015; Sharma et al, 2017), which means the isolated population of EVs will differ between methods, based on what they present on their membranes. Furthermore, the higher yield compared to the more defined 'purer' method of SEC (Théry *et al*, 2018) suggests that it could include non-EV sources such as ribonucleoprotein proteins (RNPs). This corresponds with other publications that have shown affinity columns, such as the one this study used, to be suboptimal in the isolation of pure EVs, with a high degree of co-isolated lipoprotein and other non-EV associated proteins (Stranska et al, 2018). Based on these findings, the study proceeded with SEC based EV isolations.

3.3 Visualisation of small extracellular vesicles by transmission electron microscopy

3.3.1 Visualising small extracellular vesicles isolated from fibroblasts

Transmission electron micrographs (Figure 3.3) showed that SEC isolations from fibroblast culture medium contains particles with the EV associated lipid bilayer membrane, which were consistent with small EVs (50-200 nm). Representative images from AD and neurological healthy control fibroblasts are displayed. There were no discernible differences between AD and control sEVs, including size or morphology.

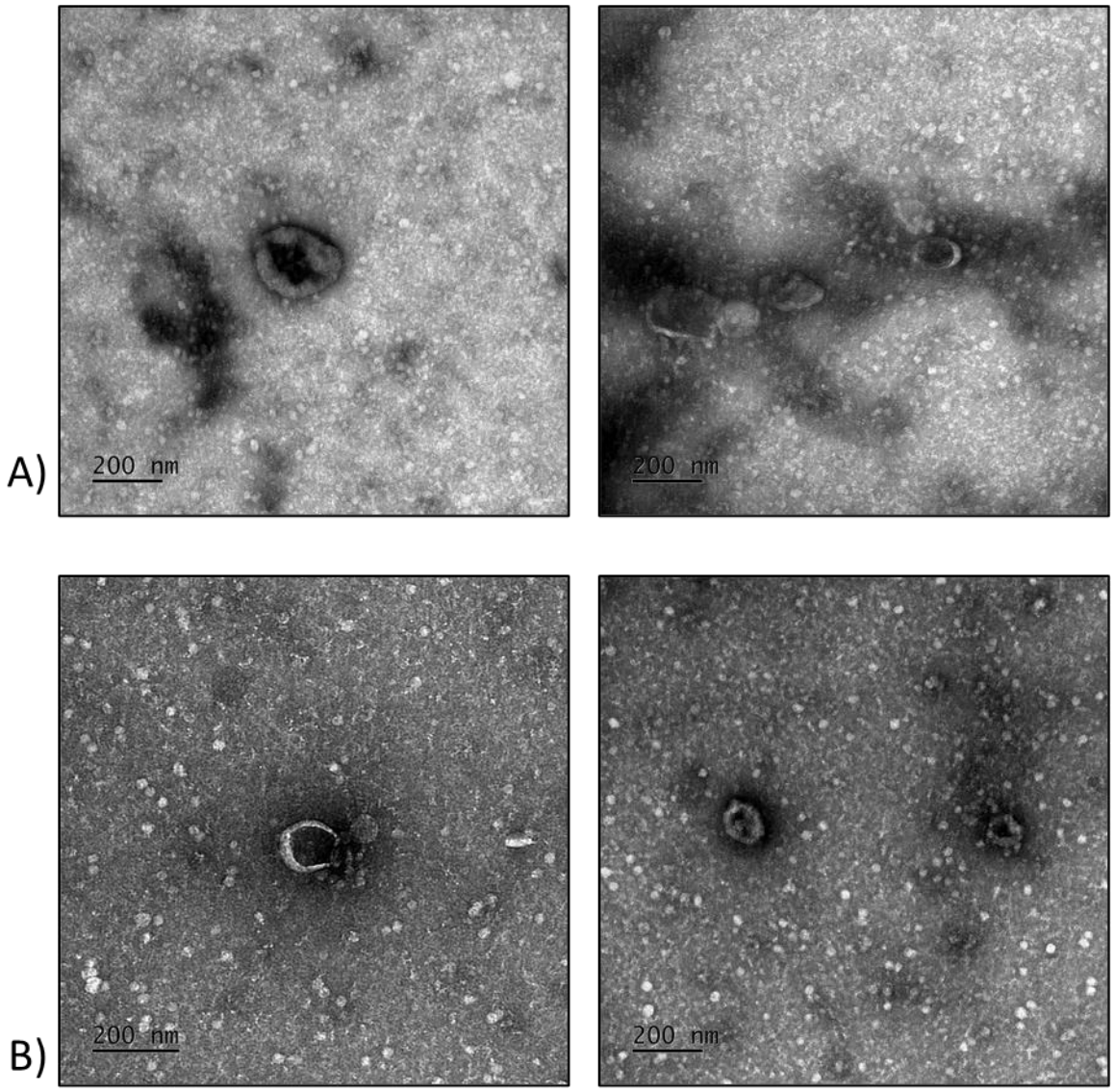

Figure 3.3. Fibroblast derived samples display particles with the size and morphology of small extracellular vesicles

Images of isolated EVs taken by transmission electron microscopy. A) Representative images from neurological healthy control fibroblasts. B) Representative images from AD fibroblasts. Particles display lipid bilayer membranes and are 200 nm or below in diameter. Scale bar = 200 nm

3.3.2 Visualisation of small extracellular vesicles isolated from brain tissue

Transmission electron micrographs (Figure 3.4) showed that SEC isolations from brain tissue contain particles with the EV associated lipid bilayer membrane, which were consistent with small EVs (50-200 nm). Representative images from AD and neurological

healthy control samples are displayed. There were no discernible differences between AD and control sEVs, including size or morphology.

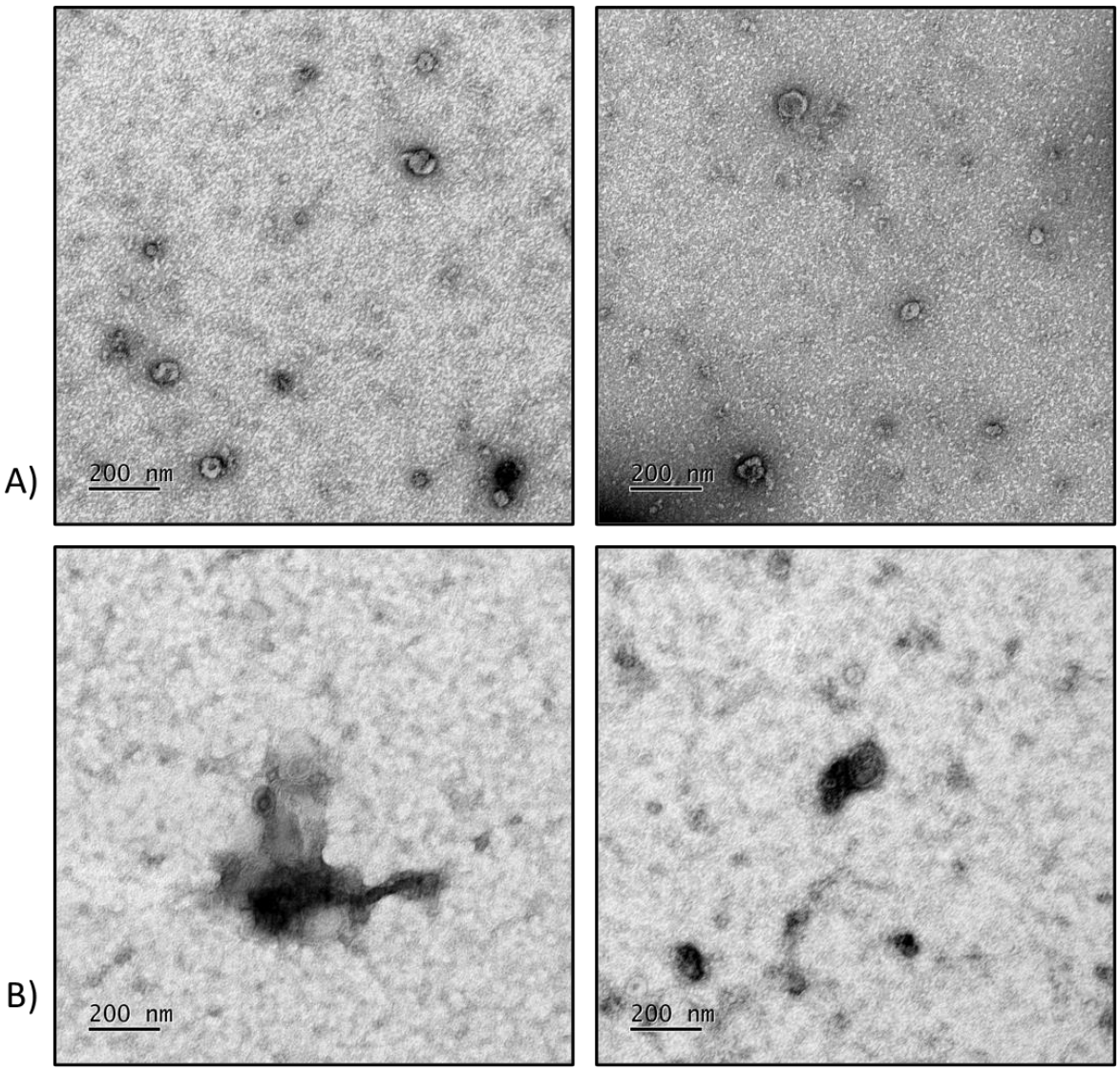

Figure 3.4. Brain derived samples display particles with the size and morphology of small extracellular vesicles

Images of isolated EVs taken by transmission electron microscopy. A) Representative images from neurological healthy control brain tissue. B) Representative images from AD brain tissue. Particles display lipid bilayer membranes and are smaller than 200 nm. Scale bar = 200 nm

3.4 Visualisation of small extracellular vesicle populations by nanoparticle tracking analysis

sEV populations isolated by SEC from fibroblasts and brain tissue were visualised by NTA, which captures scattered light by high resolution microscopy, with higher individual points of scattered light corresponding to higher concentrations. NTA determines the size of a particle through the Brownian motion of the particle in solution, where more motion corresponds with a smaller particle size (Figure 3.5).

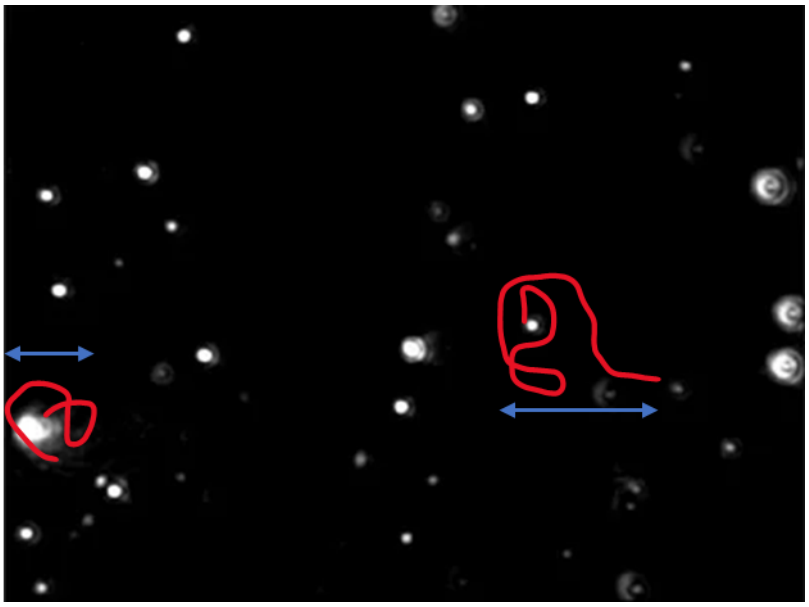

Figure 3.5. Nanoparticle tracking analysis – Brownian motion

Representative image taken from Zetaview nanoparticle tracking analysis (NTA) camera. Particles are inserted in solution into the NTA flow cell. A laser is directed into the flow cell and a camera detects the subsequent scatter of light which results from contact between the laser and particles in solution (white marks indicate scattered light detected by the camera). During imaging, the camera tracks the level of movement of a particle in solution and calculates its size, with smaller particles exhibiting larger Brownian motion (the motion of a particle within a fluid; highlighted by red line displaying the movement of the respective particle in a given time frame). Scale is not defined, though particles are measured through Brownian motion.

3.4.1 Nanoparticle tracking analysis of small extracellular vesicle populations derived from fibroblasts

In the fibroblasts, there was no observable difference in particle concentrations between neurological healthy control and AD samples, with mean particle concentrations of $5.9x10^{10}$ in the control samples and $6.5x10^{10}$ in the AD samples (Figure 3.6).

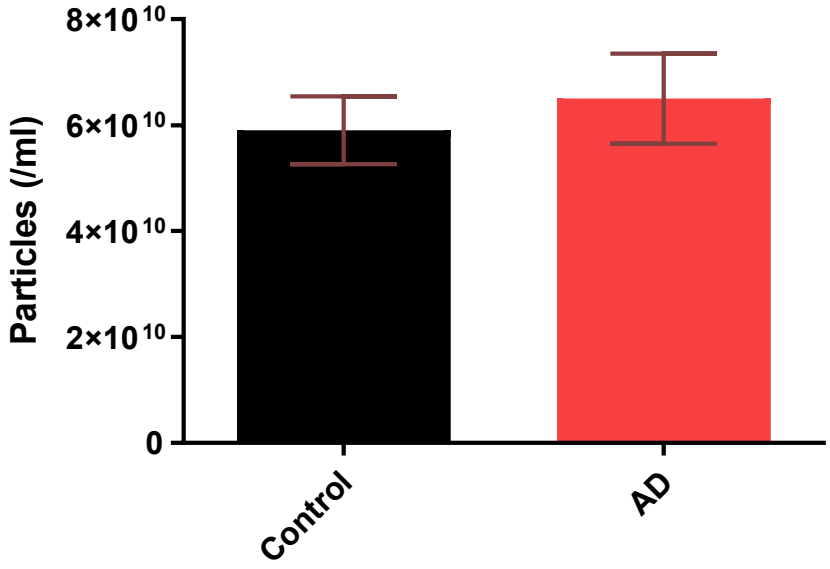

Figure 3.6. Concentration of secreted particles does not differ in AD and control fibroblasts

Concentration of secreted particles as measured by scattered light on the NTA. Samples were extracellular vesicles isolated from fibroblast cell cultures. Error bars = ±SD. N = 3 (Biological replicates). AD = Alzheimer's disease. T-test: NS.

3.4.2 Nanoparticle tracking analysis of small extracellular vesicle populations derived from brain tissue

There was no observable difference in particle concentrations between neurological healthy control and AD samples, with mean particle concentrations of $5.0x10^{10}$ in the control samples and $4.0x10^{10}$ in the AD samples (Figure 3.7).

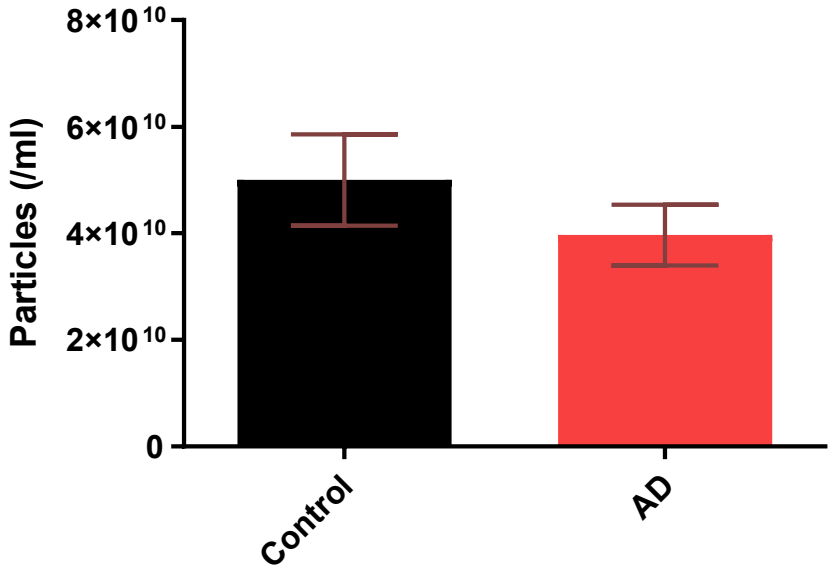

Figure 3.7. Concentration of secreted particles does not differ from AD brain tissue

Concentration of secreted particles as measured by scattered light on the NTA. Samples were extracellular vesicles isolated from brain tissue. Error bars = ±SD. N = 3 (Biological replicates). AD = Alzheimer's disease. T-test: NS.

3.5 Visualisation of small extracellular vesicle subpopulations by fluorescent nanoparticle tracking analysis

While NTA is capable of measuring particles that are within the size range of sEVs, it is unable to distinguish whether a particle is an sEV, lipoprotein, or another particle that was co-isolated based on size. Therefore, F-NTA has been used to measure different subpopulations within the total population, by tagging samples with sEV specific antibodies that are fluorescently conjugated. The population were measured in both scatter and fluorescent mode, where a 550 nm long-wave pass filter was placed in front of the camera to block the scattered light from the 520 nm laser, and so only dyes that emitted light at a higher wavelength passed.

Antibodies directed against the EV specific tetraspanin markers were used, including CD9, CD63, and CD81, which are involved in EV biogenesis and remain on their surface as described previously (Chapter 1.2.1). Tetraspanin stained particles were compared with CMO, a plasma membrane dye that emits above the 550 nm threshold, which provides

the ability to distinguish between biological particles and potential co-isolated salts and other factors that present at the same size.

3.5.1 F-NTA of small extracellular vesicle populations derived from fibroblasts

In the fibroblasts, there were no significant differences between neurological healthy control and AD groups in any of the staining conditions, CMO, CD9, CD63, CD81, or when the sample was stained simultaneously for all the tetraspanins, to determine the total population of tetraspanin stained particles in the sample (Figure 3.8). In the control samples, compared to scatter ($5.9x10^{10}$ particles) 88% of the particles were CMO positive ($5.2x10^{10}$ particles), 19% were CD9 positive ($1.1x10^{10}$ particles), 42% were CD63 positive ($2.5x10^{10}$ particles), 25% were CD81 positive ($1.5x10^{10}$ particles), and 54% were positive for a combination of tetraspanins ($3.2x10^{10}$ particles). In the AD samples, compared to scatter ($6.5x10^{10}$ particles), 89% of the particles were CMO positive ($5.8x10^{10}$ particles), 16% were CD9 positive ($0.9x10^{10}$ particles), 43% were CD63 positive ($2.5x10^{10}$ particles), 29% were CD81 positive ($1.7x10^{10}$ particles), and 60% were positive for a combination of tetraspanins ($3.5x10^{10}$ particles). In both groups, the isolated population of sEVs were predominantly CD63 positive. The results also suggest that the particles are presenting multiple tetraspanins on their surface, which is consistent with EVs, as the combined particle count of the individual tetraspanin stains (sum of CD9, CD63 and CD81 counts) are higher in control and AD samples ($5.1x10^{10}$ and $5.1x10^{10}$ particles, respectively) than the combined tetraspanin stain (CDMix counts; $3.2x10^{10}$ and $3.5x10^{10}$ particles, respectively). Overall, in both AD and control conditions, the relatively high percentages of CD positive particles indicates that there is an enrichment in EVs using SEC isolation.

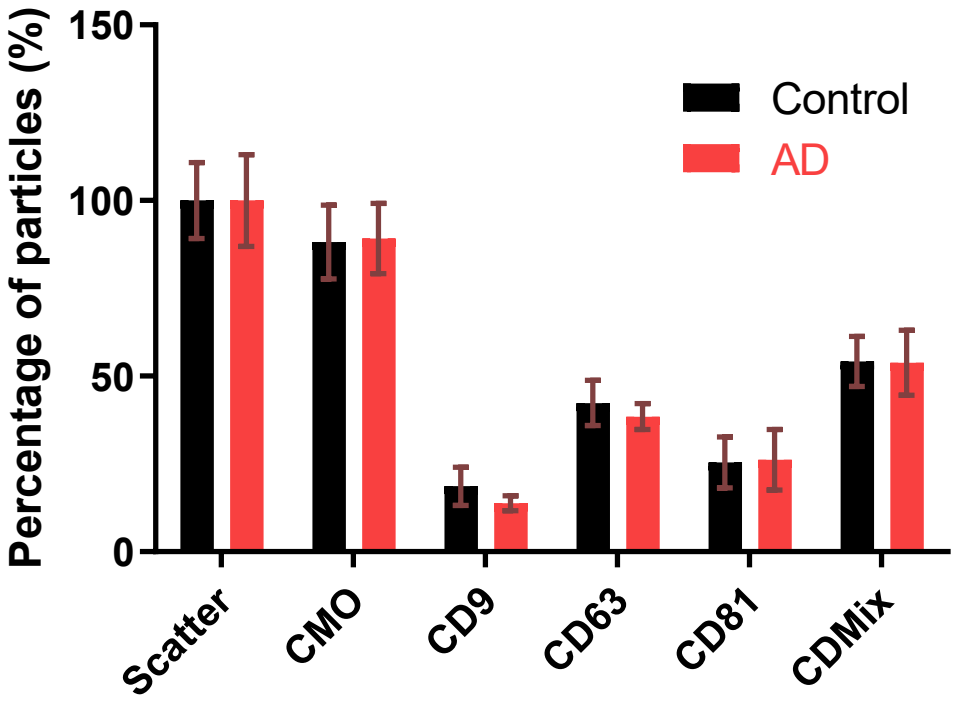

Figure 3.8. Concentrations of tetraspanin tagged particles does not differ in AD fibroblasts

Scatter - Concentration of all secreted particles as measured by scattered light on the NTA. CMO - Samples were incubated with cell mask orange (CMO) lipophilic dye to select for biological particles with lipid membranes. CD9/CD63/CD81 – Samples were incubated with antibodies raised against CD9/CD63/CD81 (cluster of differentiation), respectively, to select for particles which express the EV associated tetraspanin proteins. CDMix – Samples were incubated with an antibody cocktail of CD9/CD63/CD81, to select for particles which displayed at least one of the tetraspanin proteins. Samples were extracellular vesicles isolated from fibroblast cell cultures. Error bars = ±SD. N = 3 (Biological replicates). AD = Alzheimer's disease.

3.5.2 F-NTA of small extracellular vesicle populations derived from brain tissue

In the brain derived sEVs, there was a significant increase in CD63 positive particles in the AD samples compared to neurological healthy control (P = 0.018, Figure 3.9), suggesting that there is a alteration in secretion of EV subtypes in AD, particularly those associated with the CD63 pathways. Beyond CD63, there were no significant differences between control and AD groups in the staining conditions, CMO, CD9 or CD81, so any disease

associated changes do not seem to affect all the EV biogenesis machinery. In the control samples, compared to scatter ($5.9x10^{10}$ particles), 84% of the particles were CMO positive ($4.2x10^{10}$ particles), 17% of the particles were CD9 positive ($0.9x10^{10}$ particles), 20% were CD63 positive ($1.0x10^{10}$ particles), and 14% were CD81 positive ($0.7x10^{10}$ particles). In the AD samples, compared to scatter ($5.9x10^{10}$ particles) 116% of the particles were CMO positive ($4.6x10^{10}$ particles), 23% of the particles were CD9 positive ($0.9x10^{10}$ particles), 47% were CD63 positive ($1.9x10^{10}$ particles), and 24% were CD81 positive ($1.0x10^{10}$ particles). A higher amount of CMO stained particles than the observed particle count by scatter suggests that there was some aggregation of the CMO dye that was detected by the NTA, though CMO only controls did not get detected by NTA (appendix Figure 6.2). Notably, CD63 was not as predominant through the samples as with the fibroblast derived samples (Figure 3.9 vs Figure 3.8), though it still was the most expressed in the AD cases. Also, there is an increase in CD9 positive particles as a percentage of CMO (20.34% in the brain vs 18.10% in the fibroblasts). These differences in the composition of surface markers on EVs from brain and fibroblast origins corresponds with findings elsewhere that EV proteomes are distinctly related to their cell of origin (Haraszti et al, 2016; Kowal et al, 2016; Karimi et al, 2018). Therefore, characterisation of EVs require a broad set of markers, tailored on the expression of proteins in the cell of origin, particularly if using proteins that are associated in the different biogenesis pathways of EVs (Glebov et al, 2006; Frick et al, 2007; Karimi et al, 2018), as a pathway such as ESCRT may be preferentially used in one cell type, while a CD63 associated pathway is upregulated in another cell type (Columbo et al, 2013, Karimi et al, 2018). Overall, in both AD and control conditions, the relatively high percentages of CD positive particles indicates that there is an enrichment in EVs using SEC isolation.

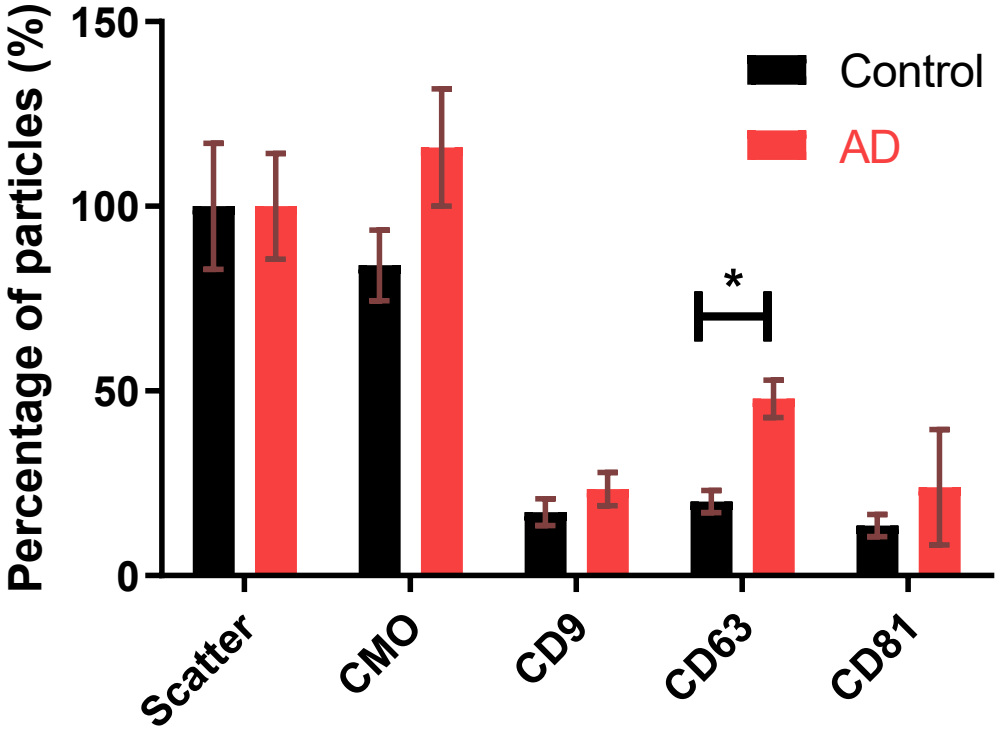

Figure 3.9. CD63 tagged particles derived from brain tissue are upregulated in Alzheimer's disease

*Scatter - Concentration of secreted particles as measured by scattered light on the NTA. CMO - Samples were incubated with cell mask orange (CMO) lipophilic dye to select for biological particles with lipid membranes. CD9/CD63/CD81 – Samples were incubated with antibodies raised against CD9/CD63/CD81 (cluster of differentiation), respectively, to select for particles which express the EV associated tetraspanin proteins. Samples were extracellular vesicles isolated from brain tissue. ANOVA + Dunnett's multiple comparisons: * = P < 0.05. Error bars = ±SD. N = 3 (Biological replicates). AD = Alzheimer's disease.*

3.6 Size profiling of small extracellular vesicle by fluorescent nanoparticle tracking analysis

3.6.1 Size of small extracellular vesicles derived from fibroblasts

Size profiles of fibroblast derived EVs, as observed by NTA, were within the range of small extracellular vesicles (<150 nm). Sizes of the sEVs did not differ between NTA scatter detection and CMO stained particles in either neurological healthy control or AD samples

(Figure 3.10; 147 ± 18 vs 144 ± 16.8 nm in controls, and 143 ± 17.5 vs 139 ± 11.2 nm in AD, respectively). In some cases, the CMO stain presented a higher particle size than the scatter results, which is potentially attributable to the accumulation of stain around the EV membrane. However, there is also a risk of dye aggregation with the 'no wash' staining procedure required for this technique. Therefore, CMO only controls were performed to ensure that the observed particles were due to stained EVs only, with CMO only readings showing minimum traces and therefore not contributing to the number of particles counted as EVs (Appendix Figure 6.2).

Optimisation of the tetraspanin staining procedure of sEVs is displayed in the appendix (appendix Figure 6.3). For both control and AD samples, the size of the particles were reduced in all the tetraspanin stained conditions, suggesting that they were corresponding to smaller subpopulations of sEV size ranges, such as exosomes and small microvesicles (Figure 3.10; Scatter vs CD9: $p = 0.008$, Scatter vs CD9=63: $p = 0.0001$, Scatter vs CD81: $p = 0.0002$, Scatter vs CDMix: $p = 0.0001$). In the control conditions, CD9 positive particles were 96 ± 15 nm, CD63 positive particles were 87 ± 12 nm, CD81 positive particles were 96 ± 18 nm, and combined tetraspanin positive particles were 82 ± 16 nm, on average. In the AD conditions, CD9 positive particles were 112 ± 22 nm, CD63 positive particles were 80 ± 10 nm, CD81 positive particles were 103 ± 17 nm, and combined tetraspanin positive particles were 87 ± 13 nm, on average. This suggests that the f-NTA detection can detect EV specific particles that display a size range in line with small EVs, and the population is distinct from the total isolated particles in all samples. Notably, given that 62% and 60% of control and AD particles, respectively, are positive when stained with the tetraspanin mix, it suggests that a significant population isolated from the fibroblasts are small EV associated. In all staining conditions, there were no significant differences in size of particles between control and AD samples, and given there are also no significant differences in concentration (Figure 3.8 (above)), it suggests any differences in sEV cargo will not be due to EV release and isolation from fibroblast culture medium.

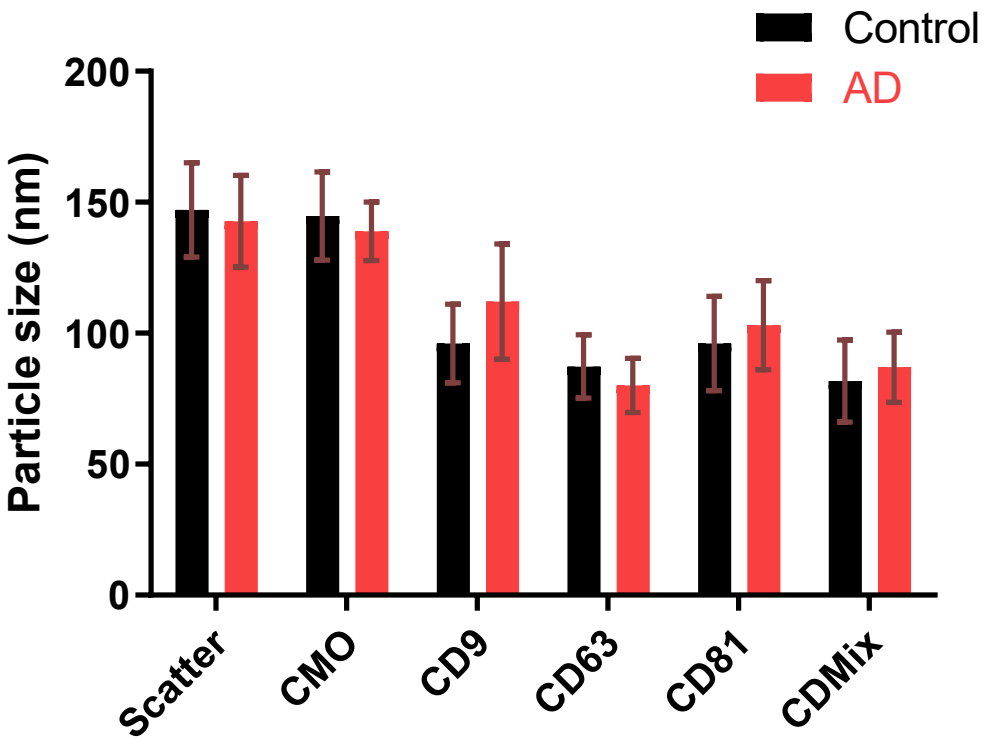

Figure 3.10. Fibroblast derived particles are in the size range of small extracellular vesicles

Scatter - Concentration of secreted particles as measured by scattered light on the NTA. CMO - Samples were incubated with cell mask orange (CMO) lipophilic dye to select for biological particles with lipid membranes. CD9/CD63/CD81 – Samples were incubated with antibodies raised against CD9/CD63/CD81 (cluster of differentiation), respectively, to select for particles which express the EV associated tetraspanin proteins. CDMix – Samples were incubated with an antibody cocktail of CD9/CD63/CD81, to select for particles which displayed at least one of the tetraspanin proteins. Samples were extracellular vesicles isolated from fibroblast cell cultures. The tetraspanin tagged (CD9, CD63, CD81, CDMix) samples were a smaller size range than the size range of secreted particles in the total samples (scatter), in both AD and control groups. Error bars = ±SD. N = 3 (Biological replicates). AD = Alzheimer's disease.

3.6.2 Size of small extracellular vesicles derived from brain tissue

Size profiles of brain derived sEVs, as observed by NTA, were generally within the range of small extracellular vesicles (<150 nm). Sizes of the populations did not differ between NTA scatter detection and CMO stained particles in either neurological healthy control or AD samples (Figure 3.11; 163 ± 18 vs 183 ± 25 nm in controls, and 152 ± 15 vs 173 ± 21 nm in AD, respectively). As in the fibroblast derived sEVs, the CMO stain presented a higher

particle size than the scatter results, though, the CMO only controls were performed to ensure that the observed particles were due to stained sEVs only and not aggregated dye (Appendix Figure 6.2).

There was a significant reduction in particle size in the CD9 positive particles ($p = 0.0064$; AD = 90 ± 6 nm, control = 118 ± 4 nm) and the CD63 positive particles ($p = 0.003$; AD = 118 ± 16 nm, control = 129 ± 19 nm) compared to scatter (AD = 163 ± 8 nm, control = 152 ± 14 nm), which was observed in both control and AD samples (Figure 3.11). The size of the other tetraspanin stained particle displayed a similar trend of reduction against the total and CMO stained particles. In the control conditions, CD81 positive particles were 123 ± 21 nm, on average. In the AD conditions, CD81 positive particles were 150 ± 11 nm, on average.

This suggests that the f-NTA detection is able to detect EV specific particles that display a size range in line with small EVs. While not as distinct as with the fibroblast derived sEVs, the brain derived sEVs robustly display expression of tetraspanin markers, particularly with the CD63 population, which showed a noticeable reduction in size compared to the total particle population, suggesting that a significant population isolated from the fibroblasts are small EV associated.

In all staining conditions, there were no significant differences in size of particles between control and AD samples, which is in line with previously observed literature (Cheng et al, 2020).

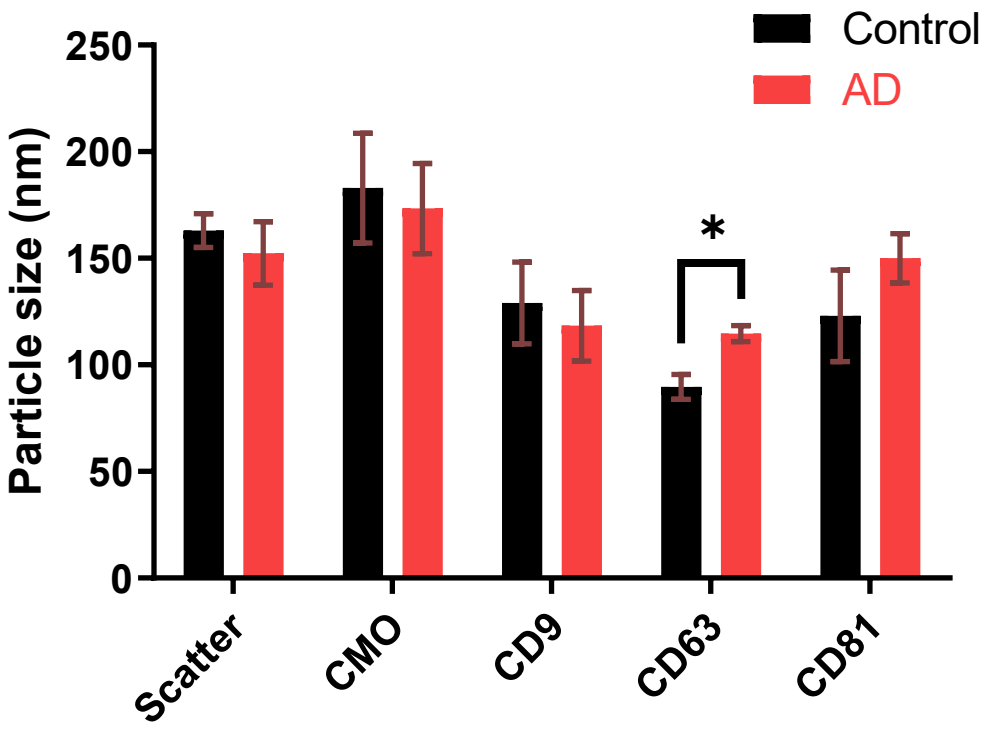

Figure 3.11. Tetraspanin tagged particles display size ranges consistent with small extracellular vesicles in AD brain derived sEVs

*Scatter - Concentration of secreted particles as measured by scattered light on the NTA. CMO - Samples were incubated with cell mask orange (CMO) lipophilic dye to select for biological particles with lipid membranes. CD9/CD63/CD81 – Samples were incubated with antibodies raised against CD9/CD63/CD81 (cluster of differentiation), respectively, to select for particles which express the EV associated tetraspanin proteins. Samples were extracellular vesicles isolated from brain tissue. Statistical comparisons show that CD63 tagged particles were larger in the AD groups. The tetraspanin tagged (CD9 and CD63, but not CD81) samples were a smaller size range than the size range of secreted particles in the total samples (scatter), in both AD and neurological healthy control groups. T-test = *: $P < 0.05$.. Error bars = ±SD. N = 3 (Biological replicates). AD = Alzheimer's disease.*

3.7 Protein profiling of small extracellular vesicles

3.7.1 Fibroblast-derived small extracellular vesicles display EV associated protein markers

While the combination of TEM and NTA visualisation techniques provides evidence for the EV associated nature of the isolated fibroblast derived samples, particularly with the

fluorescence tagging of tetraspanins, further confirmation of the samples sEV nature was sought using Western blotting. A comprehensive panel was performed, including the CD9, CD63, and CD81 tetraspanins, with further testing for non-tetraspanin proteins flotillin 1 and TSG-101, which are independently associated with EV biogenesis and are upregulated within EVs. Furthermore, samples were tested for calnexin and GM130, which are located in the endoplasmic reticulum and Golgi apparatus, respectively, and so are intracellular proteins that can be used as negative markers to determine whether the sEV isolations are pure or potentially contain cellular material that could affect downstream investigations.

In all investigations, sEV samples were compared against cell lysates (CL) from the fibroblast lines of origin, that expresses all the targeted proteins, including the negative markers. Protein was loaded in equal measure in all lanes, while sEV protein levels did not differ in AD conditions (appendix Figure 6.4). Figure 3.12 shows that sEV samples did not express GM130 or Calnexin, but they did express CD63, flotillin 1, TSG-101 and CD9, supporting the previous findings in suggesting that the isolated samples are sEV enriched and relatively pure of contaminants. CD63 appears to express more with the sEV samples than the other markers. Quantification was not performed on these samples due to the difficultly to measure against the cell lysate control, however, this observation is in line with the F-NTA observations (Figure 3.8, above) displaying CD63 as the predominantly tagged particle. The presence of expressed proteins from both tetraspanin and non-tetraspanin nature adds further robustness to our claims, as it covers more of the potential EV subtypes as observed in the MISEV guidelines (Théry *et al*, 2018).

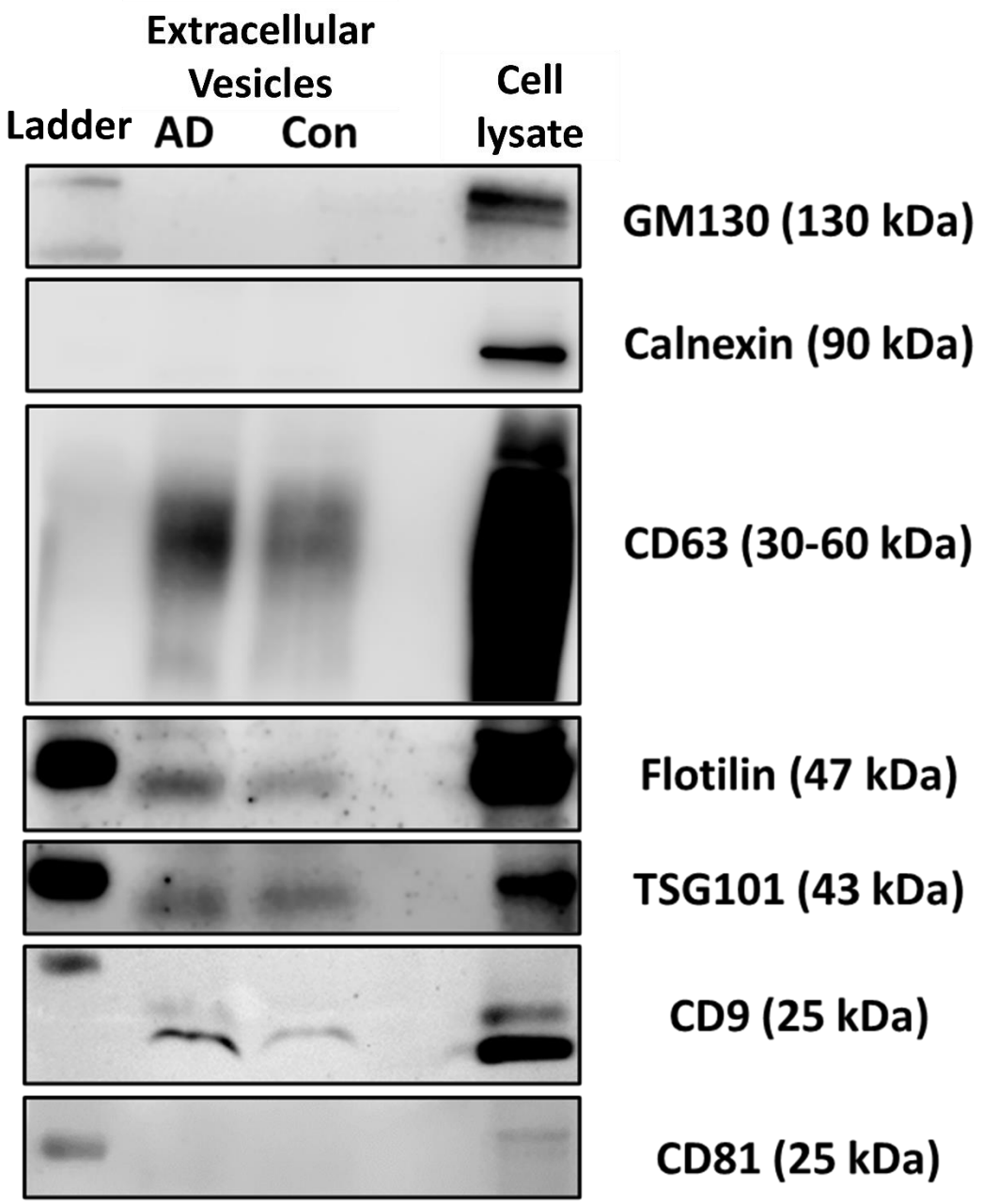

Figure 3.12. Fibroblast derived samples express extracellular vesicle associated proteins

*Western blot analysis of extracellular vesicles isolated from fibroblast cell culture. Tests for GM130 and Calnexin, associated with cell lysate fractions, were positive for cell lysate but did not express in the EV fractions. Tests for CD81, CD63, CD9, Flotillin, and TSG101, associated with EV fractions, were positive in both cell lysate and EV fractions, apart from CD81, which did not show for EVs. EV = extracellular vesicles, AD = Alzheimer's disease (AG05809), Con = control (AG08125), CL = cell lysate (Control - AG08125). Ladder (PageRuler Plus) = lane 1. All bands were identified at the expected kDa, presented in the brackets. Full blots are displayed in the Appendix (*Figure 6.6 - Figure 6.12*).*

Notably, in the fibroblast derived EVs, EV associated markers were displayed higher levels of expression in the AD case compared to the neurologically healthy control (Figure 3.13). In particular, the tetraspanin marker CD9 had 2.75-fold more expression in the AD case. However, this increase was not consistent with findings of the f-NTA analysis (Figure 3.6), though the methodology of the two techniques may result in different observations. Investigation of CD63 levels across all fibroblast sEVs did not show a significant difference between AD and neurologically healthy controls (Appendix Figure 6.13).

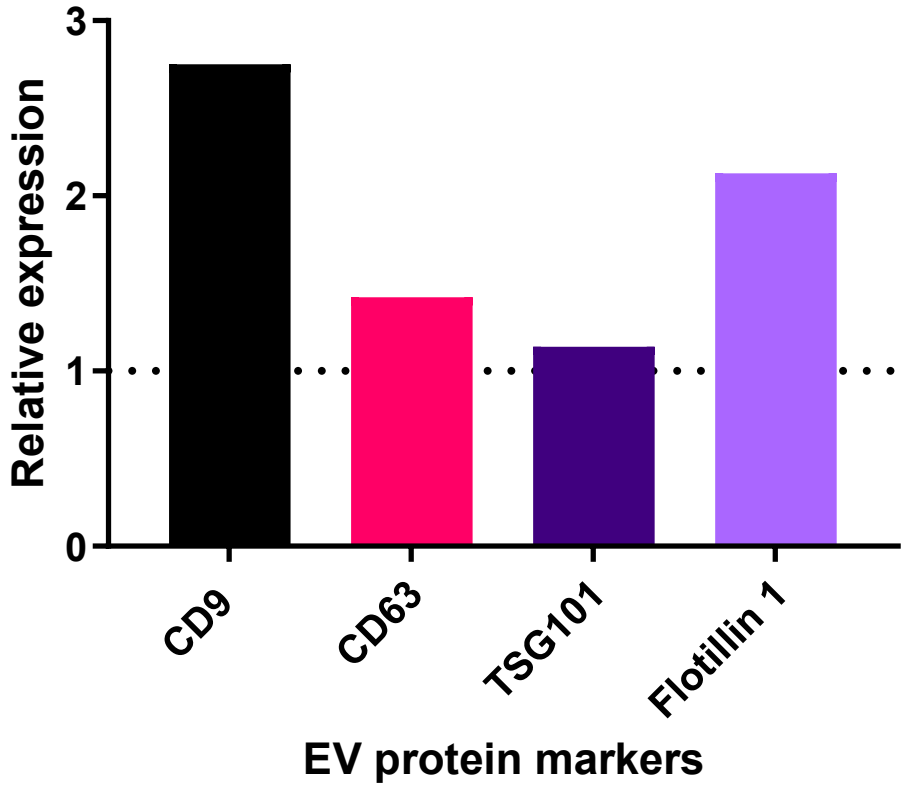

Figure 3.13. Extracellular vesicle associated proteins are enriched in fibroblast derived EVs, in AD

Western blot analysis of extracellular vesicles isolated from fibroblast cell culture. Quantification of Figure 3.12. Band intensities quantified using ImageJ, AD cases relative expression (fold change) of neurologically healthy controls. Relative expression: CD9 = 2.75, CD63 = 1.42, TSG101 = 1.14, Flotillin 1 = 2.13. N = 1.

3.7.2 Brain-derived small extracellular vesicles display EV associated protein markers

Brain derived sEV populations were also investigated with a comprehensive panel of western blotting markers, including the CD9, CD63, and CD81 tetraspanins, with further testing for non-tetraspanin proteins flotillin 1 and TSG-101. Furthermore, samples were tested for calnexin and GM130, used as the intracellular negative markers to determine whether the sEV isolations are pure or potentially contain cellular material that could affect downstream investigations. Protein was loaded in equal measure in all lanes, while sEV protein levels did not differ in AD conditions (appendix Figure 6.5).

In all investigations, sEV samples were compared against brain homogenates (BH), that expresses all the targeted proteins, including the negative markers. The sEV samples did not express GM130 or Calnexin, but they did express CD63, flotillin 1, TSG-101 and CD9 (Figure 3.14), supporting the previous findings in suggesting that the isolated samples are sEV enriched and relatively pure of contaminants. Brain derived sEVs displayed a more consistent expression of EV associated protein markers, where fibroblast derived sEVs showed lower abundance of protein. CD63 did not noticeably express more than the other markers, with all markers showing, as well as CD81 which did not express well in fibroblast derived sEVs. Highlighting the abundance of brain derived EV proteins, the displayed brain homogenates do not show as saturated, apart from CD81, to observe sEV protein expression. The consistent expression across all the tetraspanins is line with the F-NTA results, which did not show one marker as particularly dominant in the samples. With the challenges of isolating sEVs from tissue origin such as the brain, the characterisation displayed supports the ability of the methodology, with the additional clean up steps, to isolate abundant and pure sEVs.

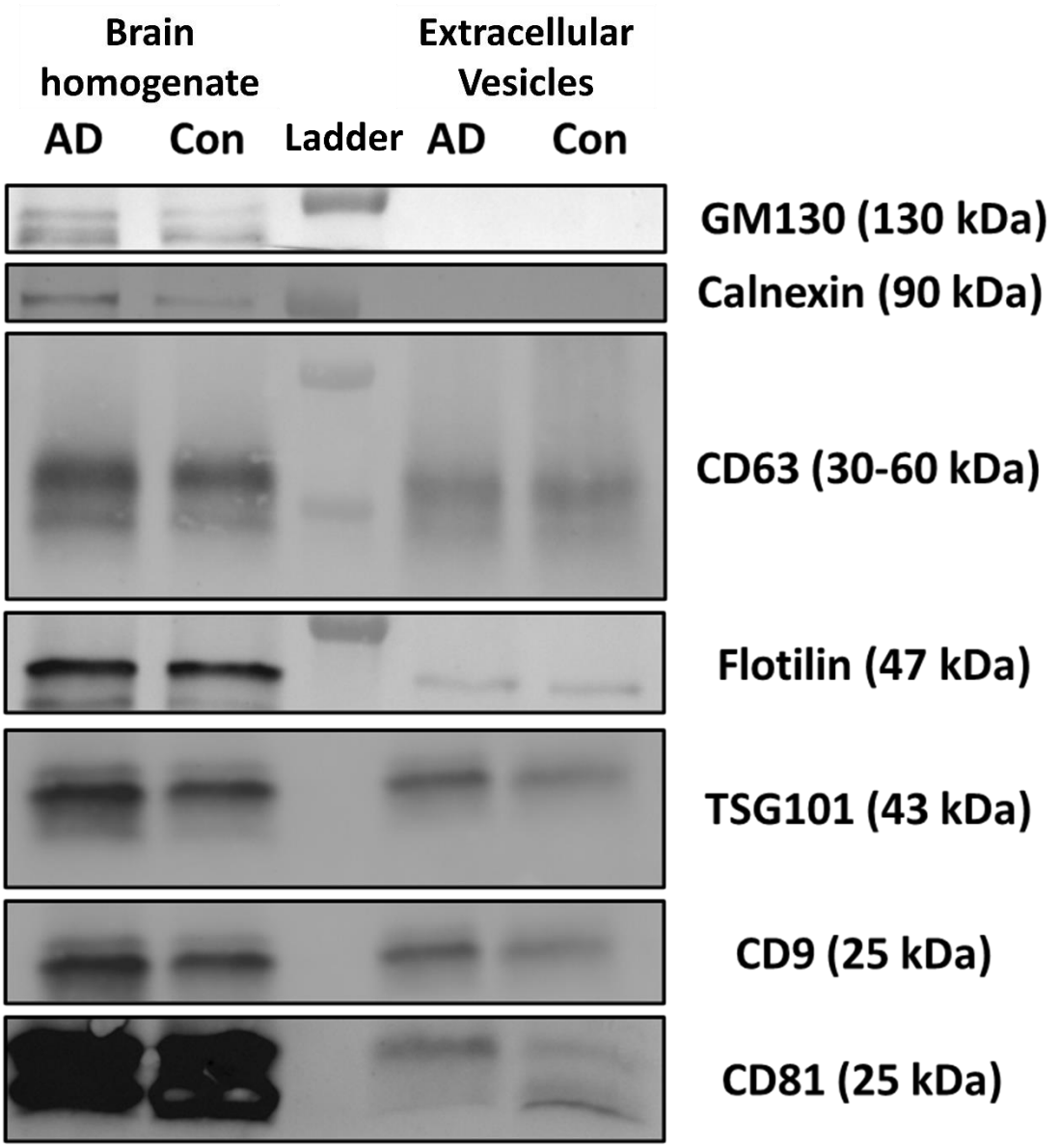

Figure 3.14. Brain derived samples express extracellular vesicle associated proteins

Western blot analysis of extracellular vesicles isolated from brain tissue. Tests for GM130 and Calnexin, associated with cell lysate fractions, were positive for brain homogenates but did not express in the EV fractions. Tests for CD81, CD63, CD9, Flotillin, and TSG101, associated with EV fractions, were positive in both brain homogenates and EV fractions. EV = extracellular vesicles, BH = brain homogenate, AD = Alzheimer's disease (Sample 1), Con = control (Sample 1). Ladder = Lane 3. All bands were identified at the expected kDa, presented in the brackets. Full blots are displayed in the Appendix (Figure 6.14 - Figure 6.20).

As with the fibroblast derived EVs, semi-quantification was performed on representative blots (Figure 3.15). Unlike in the fibroblast derived EVs, EV associated proteins are not as enriched in brain derived EVs, in AD conditions. CD81 showed the highest level of upregulation (Fold change = 1.85) in AD, relative to the neurologically healthy control. The increase in CD63 observed in the F-NTA analysis (Figure 3.9) was not observed in this case, though again the methodologies identify proteins in different topologies (F-NTA: Intact membrane, membrane proteins tagged; Western blot: Lysed EVs, protein measured both from membrane and internally).

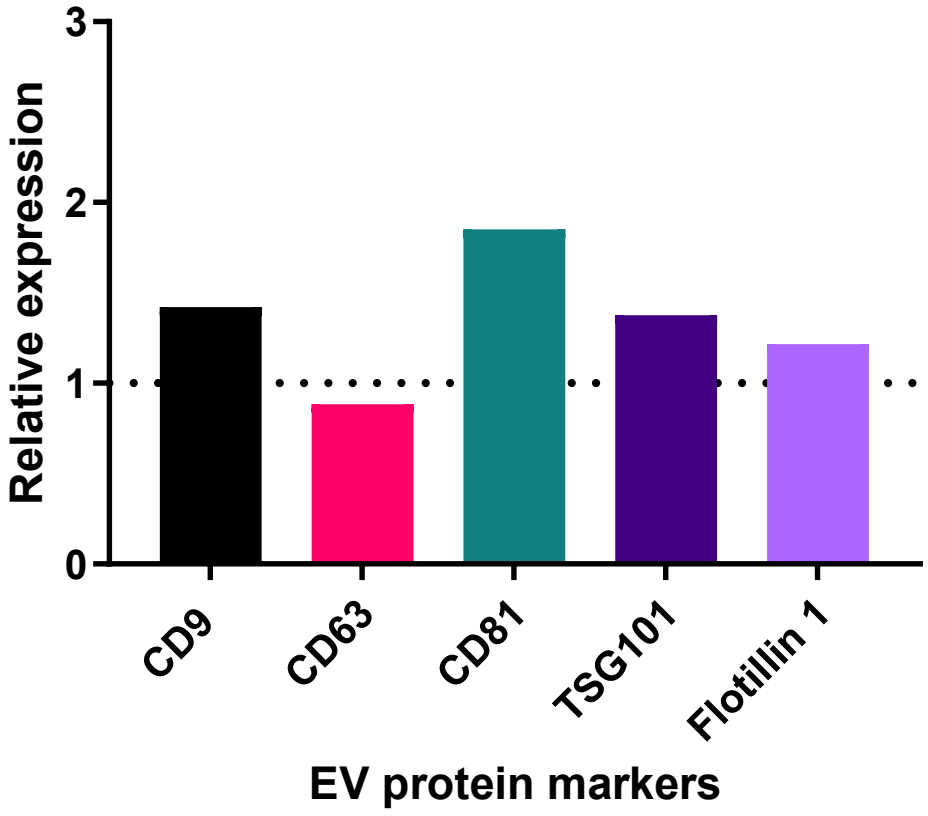

Figure 3.15. CD81 is upregulated in brain derived EVs in AD

Western blot analysis of extracellular vesicles isolated from brain tissue. Quantification of Figure 3.14. Band intensities quantified using ImageJ, AD cases relative expression (fold change) of neurologically healthy controls. Relative expression: CD9 = 1.42, CD63 = 0.88, CD81 = 1.85, TSG101 = 1.38, Flotillin 1 = 1.22. N= 1.

3.8 Discussion

EVs isolated from fibroblast culture media and brain tissue by SEC have been thoroughly characterised, with EV protein concentration, particle concentration, particle size and membrane markers being analysed. This is in line with the international consensus, which highlights the limitations of individual characterisation methods, and therefore recommends the implementation of multiple methods to support the overall claim of isolating EVs (Théry *et al*, 2018). For example, protein measurements tend to overestimate EVs as it will also measure any co-isolated RNPs and lipoproteins, although this is not as significant with EVs that are isolated by SEC, due to the higher resulting EV purity. The individual markers stained in the f-NTA, including the CD63+ and the mix of CD9+, CD63+ and CD81+ vesicles, provides a more specific characterisation of the isolated EVs. However, EVs that do not display one of these markers will not be picked up for analysis. Sizing of particles provides confidence that EVs are within the expected range, although alone it does not provide characteristics of isolated samples, and it is not currently possible to define the lower size limit of sensitivity. This is particularly true given the lack of reference materials to validate the size of the detected particles in the sample (Welsh *et al*, 2020). This study used a polystyrene size standard of 100 nm to calibrate the NTA, therefore there was some confidence in the subsequent measured particles, although more validated reference materials, including independent verification controls, are required in the future for full confidence of the measurement of EVs. Combined, these methods cover many of each other's limitations, for example the fluorescence tagging of specific EV markers being displayed at the expected size range for EVs that display such markers provides confidence in the visualisation of particles by NTA. Furthermore, the sensitivity of the protein concentration of EVs is complemented by specifically determining the individual CD9+, CD63+ and CD81+ EVs.

Based on these characterisation methods, no difference in protein concentration, particle number or particle size, between AD and neurological healthy control fibroblasts was observed in this study. This was as expected and corroborated with numerous studies (Saugstad *et al*, 2017; Gallart-Palau *et al*, 2020; Ruan *et al*, 2020), though further work remains to characterise a wider representation of samples from the study. Limitations do exist with expanding the characterisation to distinguishing between AD and controls, most

notably being that the methods of characterisation do not currently extend to provide a breakdown of the individual markers displayed by groups of EVs, therefore it misses the complexity of changes that are associated with AD. For example, Ruan *et al* did not observed any changes in EV concentration from AD brain tissue, however the AD EVs displayed a higher proportion of tau species and induced the accumulation of phosphorylated tau in recipient mice hippocampi (Ruan *et al*, 2020). This suggests that it is the EV cargo and not the EV pheotypes that are most affected by AD conditions.

4 Chapter 4: Investigation of small extracellular vesicle miRNAs in Alzheimer's disease

4.1 Introduction

With the study able to isolate sEVs from both cell culture medium and brain tissue, work progressed towards investigating the small RNA cargo of the isolated sEVs, with particular focus on miRNAs. Work in this chapter was performed on fibroblast and brain derived sEVs, as well as H_2O_2 treated SH-SY5Y cells, with analysis performed by qPCR and RNA sequencing. Differential analysis was categorised as fold change > 2 and P value < 0.05, unless stated otherwise.

4.1.1 Aims

The aims of this chapter were to investigate the RNA cargo of SEC isolated sEVs, in order to determine whether they were localised within the sEVs or as part of co-isolated non-EV molecules, such as RNPs. The study aimed to select a panel of candidate miRNA, which had either previously been associated with biological pathways in the brain or been implicated in AD, and to interrogate them in both fibroblast and brain derived sEVs in AD. Aims included investigating candidate miRNAs in H_2O_2 treated SH-SY5Y cells, to compare findings to a neuronal model that had AD associated molecular changes. The work also investigated the global changes of fibroblast and brain derived sEV miRNA in AD, utilising small RNA sequencing. Finally, the work aimed to analyse biological pathways associated with dysregulated miRNAs, to determine their functional relevance in AD.

4.2 RNA isolated from size exclusion chromatography was predominantly internalised within small extracellular vesicles and not associated with RNPs

An important analysis required for EV biomarker studies is determine whether miRNA is contained within, bound to the surface of the sEV or bound to co-isolated non-EV proteins (Théry *et al*, 2018).

Given that EVs have relative resistance to protease-based digestion due to their lipid bilayer (Shelke et al, 2014), a proteinase K and RNase A enzymatic digestion was performed on the sEV samples, based on the methodology of Diedronks et al (2020). The proteinase K would first degrade any proteins outside the sEVs (including on the sEV surface), which would expose any RNA that was bound to the sEV surface. Potentially more significant is the degradation of extracellular RNPs that can co-isolate with EVs (Turchinovich *et al*, 2011), that could influence the detected expression levels of miRNA in the study. Even with the observed separation of EVs and RNPs by SEC (Stranska *et al*, 2018), no isolation technique currently achieves completely pure EV populations.

Proteinase K based degradation of RNPs exposes any extracellular RNA, which is then degraded by RNase A treatment. Half of the sEV samples were treated with vesicle-free PBS as substitute to the enzymes, therefore any non-EV was not degraded and the difference in RNA concentration between the treated and untreated samples could be measured, which could indicate if the RNA isolated was sEV enclosed or not.

Currently, sEV samples from fibroblast cell cultures did not show any difference in RNA concentration between protease/RNase treatment and untreated controls (Figure 4.1). This suggests that most of the RNA co-isolated with sEVs through SEC is internalised within the sEVs, where it is protected from digestion. However, all subsequent isolations included a protease/RNase treatment to standardise any variations in isolation purity of EVs. This treatment was also performed on sEVs derived from brain tissue.

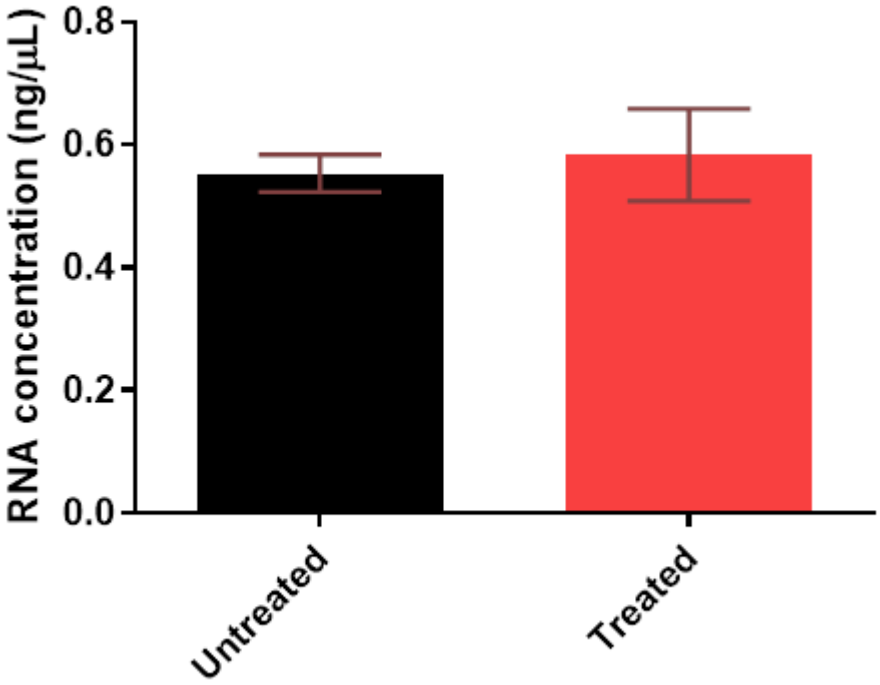

Figure 4.1. Total RNA concentration of fibroblast small extracellular vesicles does not change after proteinase K and RNase A treatment

Extracellular vesicles isolated from fibroblast cell cultures were treated with proteinase K and subsequently RNase A prior to RNA isolation, to determine whether RNA was EV associated (protected from the digestions). RNA concentration was measured by Qubit. N = 3 (technical repeats), error bars = ±SD. T-test: NS

Investigation of total RNA concentration between AD and healthy neuronal controls, was performed on both the fibroblast and brain derived sEVs, which were isolated using SEC and had undergone protease/RNase treatment prior to RNA isolation. In both cohorts, RNA concentrations of isolated sEVs did not change in AD conditions (Figure 4.2; Figure 4.3).

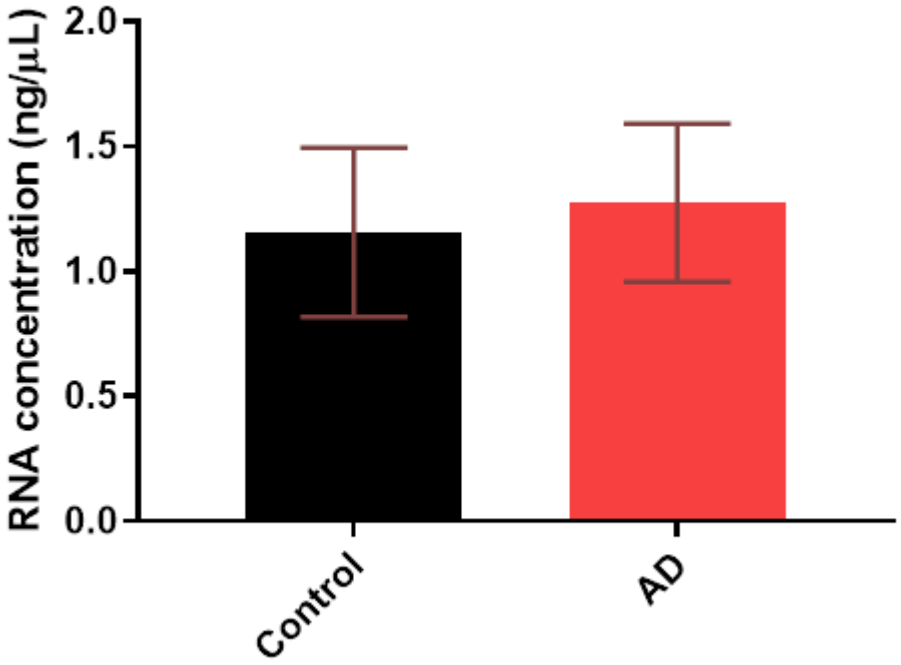

Figure 4.2. Total RNA concentration of fibroblast small extracellular vesicles does not differ in AD conditions

Extracellular vesicles isolated from fibroblast cell cultures showed no significant change in RNA content, between AD and neurological healthy control conditions. RNA concentration was measured by Qubit. N = 3 (Biological replicates), error bars = ±SD. Statistical test: T-test.

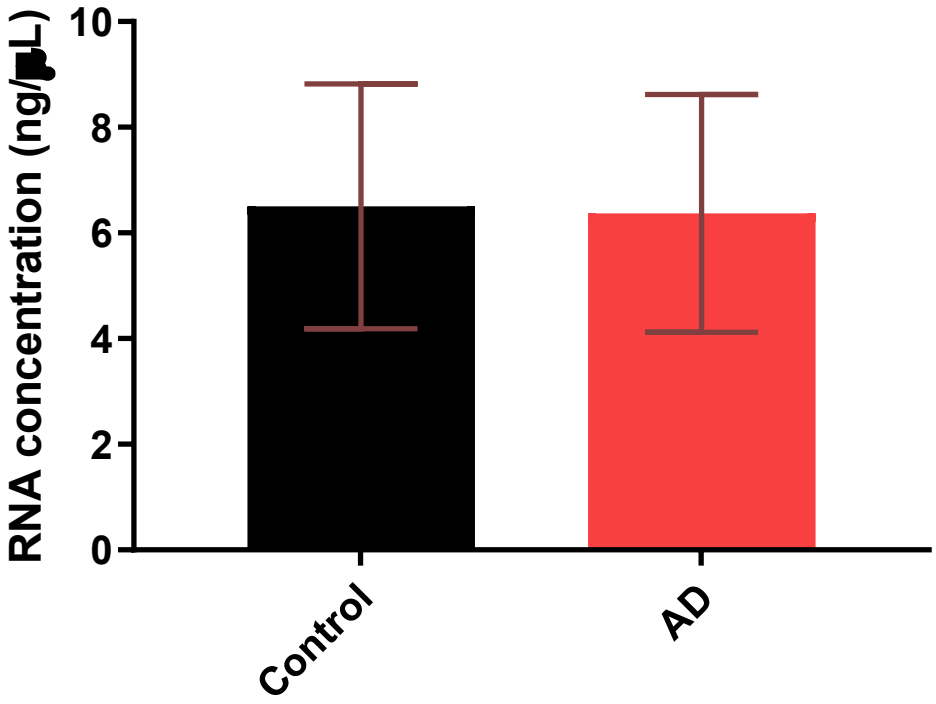

Figure 4.3. Total RNA concentration of brain derived small extracellular vesicles does not differ in AD conditions

Extracellular vesicles isolated from brain tissue showed no significant change in RNA content, between AD and neurological healthy control conditions. RNA concentration was measured by Qubit. N = 3 (Biological replicates), error bars = ±SD. Statistical test: T-test.

4.3 Interrogation of candidate miRNAs in small extracellular vesicles

4.3.1 Candidate miRNA expression in Alzheimer's disease fibroblasts

Investigation of candidate miRNAs, including the miRNAs in the chromosome 14 (C14) cluster was performed using SYBR-green based qPCR. From the candidate miRNAs outside of the C14 cluster, miR-92a and miR-146 were upregulated in the AD cell line, compared to neurological healthy controls (Figure 4.4). Within the C14 cluster, of the nine miRNAs that

were tested and expressed in the fibroblast cells, miR-655 and miR-134 were upregulated in the AD cell line, compared to neurological healthy controls (Figure 4.5). Notably, miRNAs analysed in the C14 cluster were both up- and downregulated, while the candidate AD associated miRNAs were showing a pattern of upregulation.

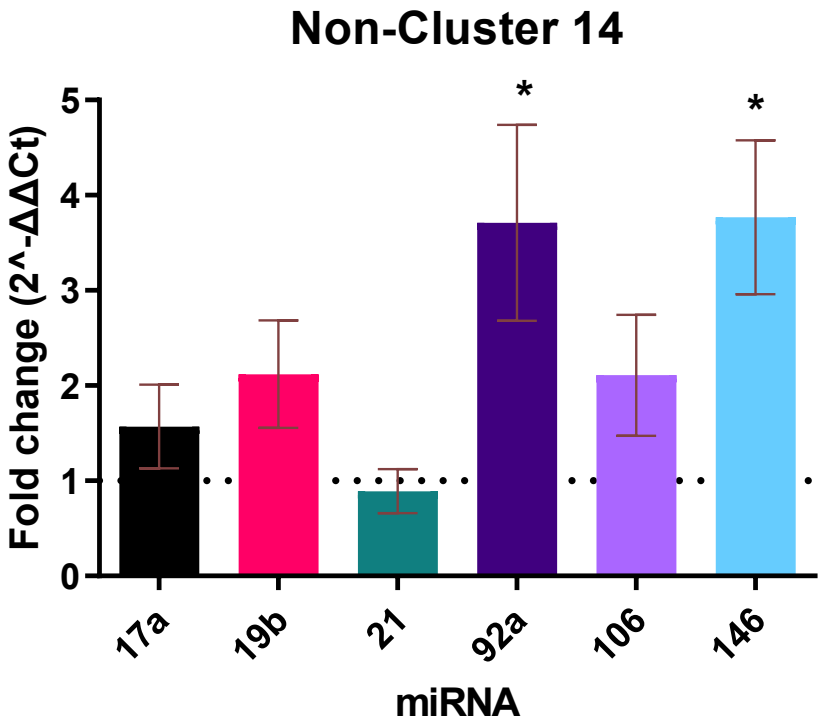

Figure 4.4. Mir-92a and Mir-146 are upregulated in AD fibroblasts compared to neurologically healthy controls

*Changes in expression of candidate miRNAs in AD fibroblasts as measured by qPCR, showing the relative increase or decrease in expression compared to neurological healthy controls. ΔΔCt = delta delta cycle threshold. Normalised to U6. Neurological healthy controls - normalised reference = dotted line (1). T-test: * = P < 0.05. Error bars = ±SD. N = 3 (Biological replicates).*

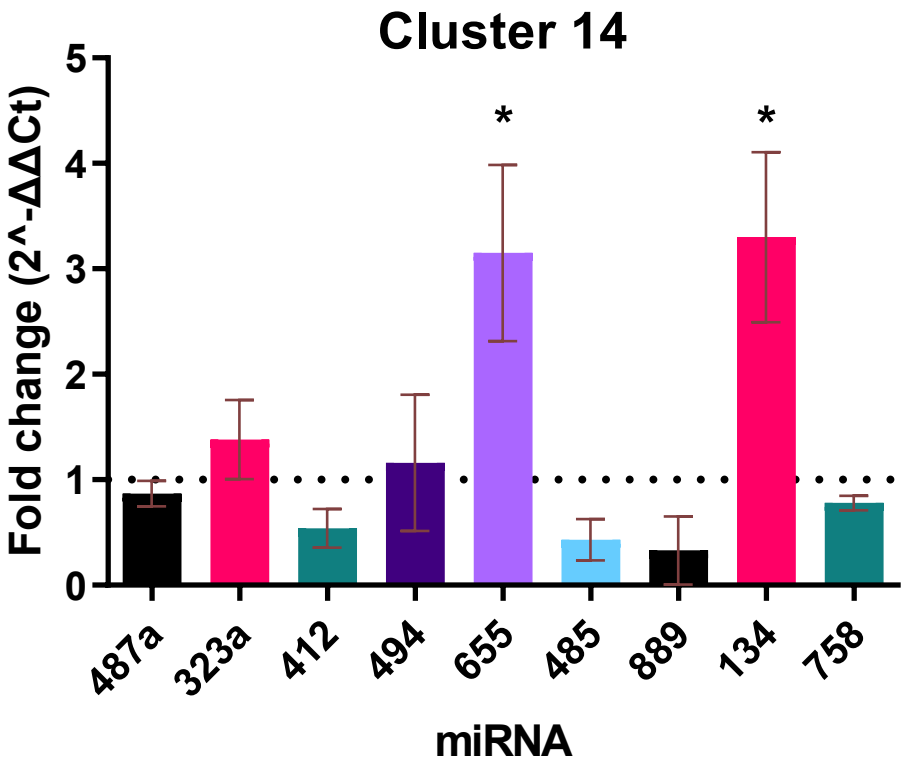

Figure 4.5. C14 Mir-655 and Mir-134 are upregulated in AD fibroblasts compared to neurologically healthy controls

*Changes in expression of chromosome cluster 14 miRNAs in AD fibroblasts as measured by qPCR, showing the relative increase or decrease in expression compared to neurological healthy controls. ΔΔCt = delta delta cycle threshold. Normalised to U6. Neurological healthy controls - normalised reference = dotted line (1). T-test: * = P < 0.05. Error bars = ±SD. N = 3 (Biological replicates).*

4.3.2 Alzheimer's disease fibroblast derived small extracellular vesicles display differentially expressed miRNAs

When the sEVs isolated from the fibroblasts were analysed for the candidate miRNAs, there was variation in whether the investigated miRNA showed a similar pattern of regulation as seen in the endogenous expression. From the candidate miRNAs outside of the C14 cluster, there was a trend of upregulation in the AD fibroblast derived sEVs compared to the neurological healthy controls, though only miR-106 was the only miRNA to show a

significant upregulation (Figure 4.6). This may partially be down to the level of biological variation observed between samples, while miR-92a and miR-146 also showed a level of upregulation in AD sEVs.

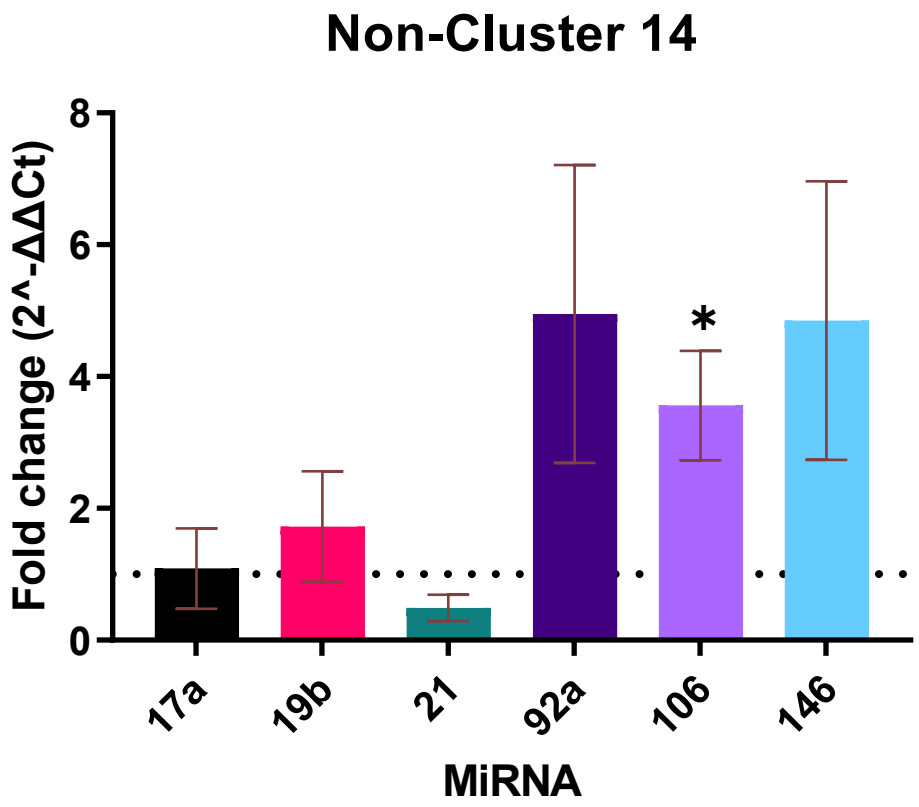

Figure 4.6. Mir-106 is upregulated in sEVs derived from AD fibroblasts compared to neurologically healthy controls

*Changes in expression of candidate miRNAs in AD sEVs derived from fibroblasts as measured by qPCR, showing the relative increase or decrease in expression compared to neurological healthy controls. ΔΔCt = delta delta cycle threshold. Normalised to Cel-39. Neurological healthy controls - normalised reference = dotted line (1). T-test: * = P < 0.05. Error bars = ±SD. N = 3(Biological replicates).*

Within the C14 cluster, of the nine miRNAs that were tested and expressed in the fibroblast sEVs, none displayed a significant difference in AD compared to neurological healthy control, however, there was a general population trend of upregulation in the cluster in AD (Figure 4.7). Interestingly, miR-134 was the most upregulated miRNA in fibroblast derived sEVs, which is also seen endogenously (Figure 4.5).

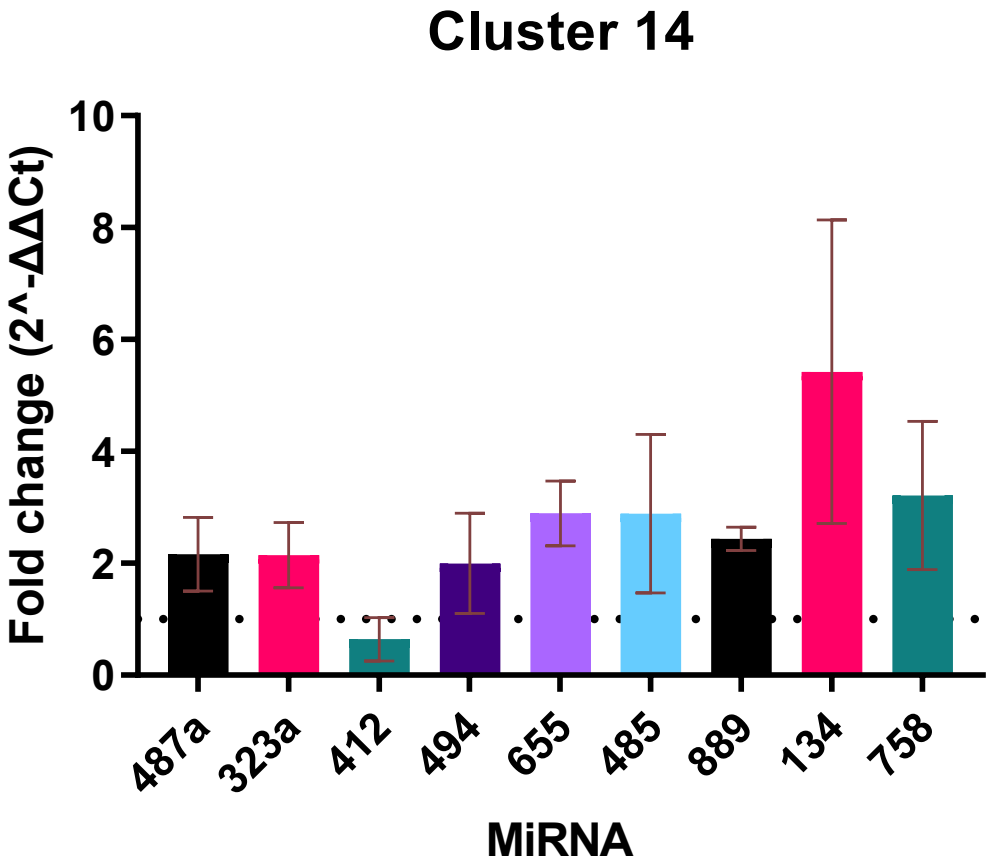

Figure 4.7. Chromosome 14 cluster miRNAs are not significantly different in sEVs derived from AD fibroblasts compared to neurologically healthy controls

Changes in expression of chromosome cluster 14 miRNAs in AD sEVs derived from fibroblasts as measured by qPCR, showing the relative increase or decrease in expression compared to neurological healthy controls. ΔΔCt = delta delta cycle threshold. Normalised to Cel-39. Neurological healthy controls - normalised reference = dotted line (1). Error bars = ±SD. N = 3 (Biological replicates). T-test: NS

Notably, though the preliminary size of the cohort reduced the statistical power of the findings, there were a number of dysregulated candidate miRNAs that warrant further investigation with an expanded cohort. Both the AD associated and C14 cluster miRNAs were primarily upregulated in both the cells and sEVs (Table 4.1). In the AD cohort, miR-92a and miR-146a showed a particularly increased expression in AD sEVs, though the prominent level of biological variation remains a limiting factor in these observations. In the C14 cluster, it is interesting to observe that AD had opposite effects on miR-485 and

miR-889 expression in the sEVs, compared to in the cells, suggesting that these miRNAs may be preferentially packaged in sEVs in AD conditions.

Table 4.1. Candidate miRNAs show upregulation in fibroblast sEVs

Tabular overview of changes in miRNA expression observed in AD, in both fibroblasts and fibroblast derived sEVs. MiRNA-92a, -106a, -146a, 655 and -134 were consistently upregulated in AD, while miRNA-485 and -889 were inversely dysregulated in AD, between fibroblasts and fibroblast derived sEVs.

miRNA		Fibroblast	
		Endogenous	sEV
Non-Cluster 14	17a	1.57	1.09
	19b	2.12	1.72
	21	0.89	0.49
	92a	3.71	4.95
	106a	2.11	3.56
	146a	3.77	4.85
Cluster 14	487a	0.87	2.16
	323a	1.38	2.14
	412	0.54	0.64
	494	1.16	2.00
	655	3.15	2.90
	485	0.43	2.89
	889	0.33	2.44
	134	3.30	5.42
	758	0.78	3.21

Red = upregulated (Fold change threshold > 2), green = downregulated (Fold change threshold < 0.5).

4.3.3 Chromosome 14 cluster miRNA – miR-134 is downregulated in SH-SY5Y derived EVs after H_2O_2 treatment

The differentiated SH-SY5Y cell line was also used as a neuronal model to compare findings of candidate miRNAs in the fibroblast sEVs.

Downregulation of miR-16 and miR-134 in EVs was observed in differentiated SH-SY5Y cells, treated with H_2O_2 to stimulate oxidative stress (Figure 4.8), interestingly this downregulation in miR-134 is inversed in the fibroblast sEVs, suggesting that AD might elicit different miRNA responses peripherally.

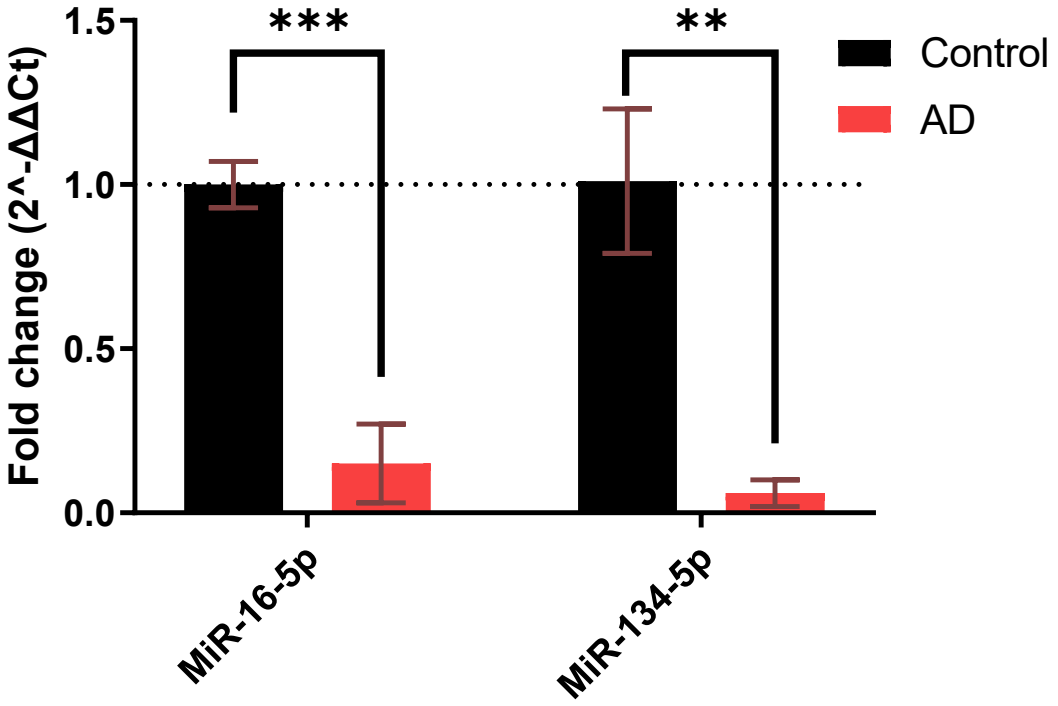

Figure 4.8. Candidate extracellular vesicle microRNA expression released from SH-SY5Y cells decreased after H_2O_2 treatment.

*Changes in expression of candidate miRNAs in EVs derived from H_2O_2 treated SH-SY5Y cells as measured by qPCR, showing the relative increase or decrease in expression compared to untreated SH-SY-5Y cells. ΔΔCt = delta delta cycle threshold. Normalised to Cel-39, normalised control reference = dotted line (1). T-test: **P < 0.01, ***P < 0.001, N=3 (technical repeats), error bars displayed as ±SD.*

4.3.4 Candidate miRNA expression in Alzheimer's disease brain derived small extracellular vesicles

Brain derived sEVs were also tested for candidate miRNA expression. Notably, only miR-146 and miR-155 displaying dysregulation, being downregulated in AD brain derived sEVs, compared to neurological healthy controls (Figure 4.9). Within the C14 miRNA cluster, there were no significantly dysregulated miRNAs in the brain derived sEVs (Figure 4.10).

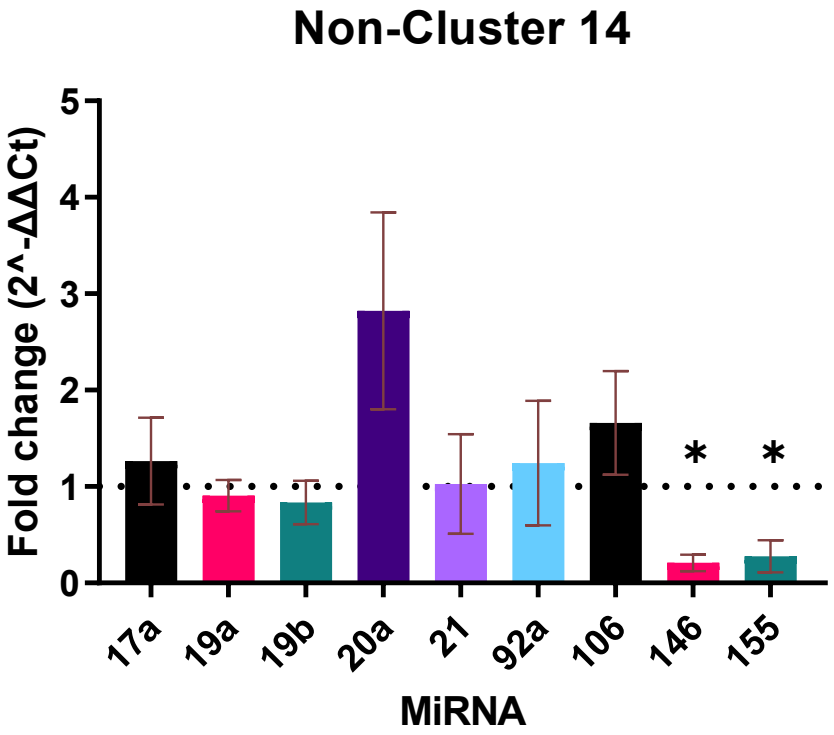

Figure 4.9. Mir-155 and Mir-146 are downregulated in brain derived sEVs in AD compared to neurologically healthy controls

*Changes in expression of candidate miRNAs in AD sEVs derived from brain tissue as measured by qPCR, showing the relative increase or decrease in expression compared to neurological healthy controls. ΔΔCt = delta delta cycle threshold. Normalised to Cel-39. Neurological healthy controls - normalised reference = dotted line (1). T-test: * = P < 0.05. Error bars = ±SD. N = 3(Biological replicates).*

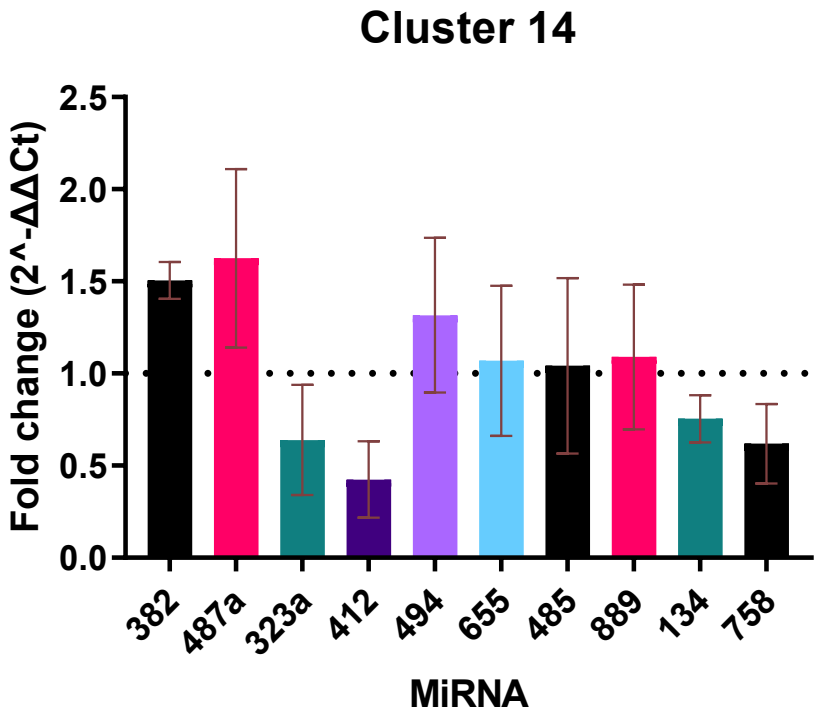

Figure 4.10. Chromosome 14 cluster miRNAs are not significantly different in brain derived sEVs in AD compared to neurologically healthy controls

*Changes in expression of chromosome cluster 14 miRNAs in AD sEVs derived from brain tissue as measured by qPCR, showing the relative increase or decrease in expression compared to neurological healthy controls. ΔΔCt = delta delta cycle threshold. Normalised to Cel-39. Neurological healthy controls - normalised reference = dotted line (1). Error bars = ±SD. N = 3(Biological replicates). T-test: * = NS*

4.3.5 Comparison of differentially expressed sEV miRNAs in Alzheimer's disease

Comparing the candidate miRNAs in central and peripheral models of AD, provides an opportunity to observe whether any specific changes that could be detected in a less invasive test are also present in the brain (Table 4.2). A direct comparison of the fold change (2^ΔΔ Ct) of miRNAs in AD conditions, that are present in both brain derived sEVs and fibroblast sEVs, shows that miR-106a is upregulated in both cases, while miR-146a is inversely regulated, with a downregulation seen in brain derived sEVs. Of the C14 cluster miRNAs, miR-487a is upregulated in both brain derived sEVs and fibroblast sEVs in AD.

Compared to the fibroblast endogenous expression, miR-106a and miR-146a are consistently upregulated, while miR-487a wad not observed to be dysregulated in the cell but could potentially be displaying EV specific dysregulation due to AD (Table 4.3). Combined, this highlights a panel of miRNAs that show potential as biomarkers in AD, which will require further testing.

Table 4.2. Comparison of candidate miRNA fold change in AD between brain derived sEVs and fibroblast sEVs

Tabular overview of changes in miRNA expression observed in AD, in both brain derived sEVs and fibroblast derived sEVs. MiRNA-146a was inversely dysregulated in AD, between brain derived sEVs and fibroblast derived sEVs.

miRNA		Brain tissue sEV	Fibroblast sEV
Non-Cluster 14	17a	1.27	1.09
	19a	0.91	
	19b	0.84	1.72
	20a	2.82	
	21	1.03	0.49
	92a	1.24	4.95
	106a	1.66	3.56
	146a	0.21	4.85
	155	0.28	
Cluster 14	382	1.51	
	487a	1.63	2.16
	323a	0.64	2.14
	412	0.43	0.64
	494	1.32	2.00
	655	1.07	2.90
	485	1.04	2.89
	889	1.09	2.44
	134	0.75	5.42
	758	0.62	3.21

Red = upregulated (Fold change threshold > 2), green = downregulated (Fold change threshold < 0.5), black = did not express.

Table 4.3. Comparison of candidate miRNA fold change in AD between brain and fibroblast derived sEVs and fibroblast cells

Tabular overview of changes in miRNA expression observed in AD, in both fibroblasts, fibroblast derived sEVs and brain derived sEVs. MiRNA-146a was inversely dysregulated in AD, between brain derived sEVs, compared to fibroblasts and fibroblast derived sEVs.

miRNA		Brain tissue	Fibroblast	
		sEV	sEV	Endogenous
Non-Cluster 14	106a	1.66	3.56	2.11
	146a	0.21	4.85	3.77

Red = upregulated (Fold change threshold > 2), green = downregulated (Fold change threshold < 0.5), black = did not express.

4.3.6 Pathway analysis of differentially expressed miRNAs in Alzheimer's disease

Comparing the experimentally validated targets of the differentially expressed miRNAs in Gene Ontology (GO) using miRPathDB (V2.0; Kehl et al, 2018), shows varied biological functions. The dysregulated miR-146a and miR-155 display functionality in inflammatory processes as well as responses to cellular stress and metabolism (Figure 4.11).

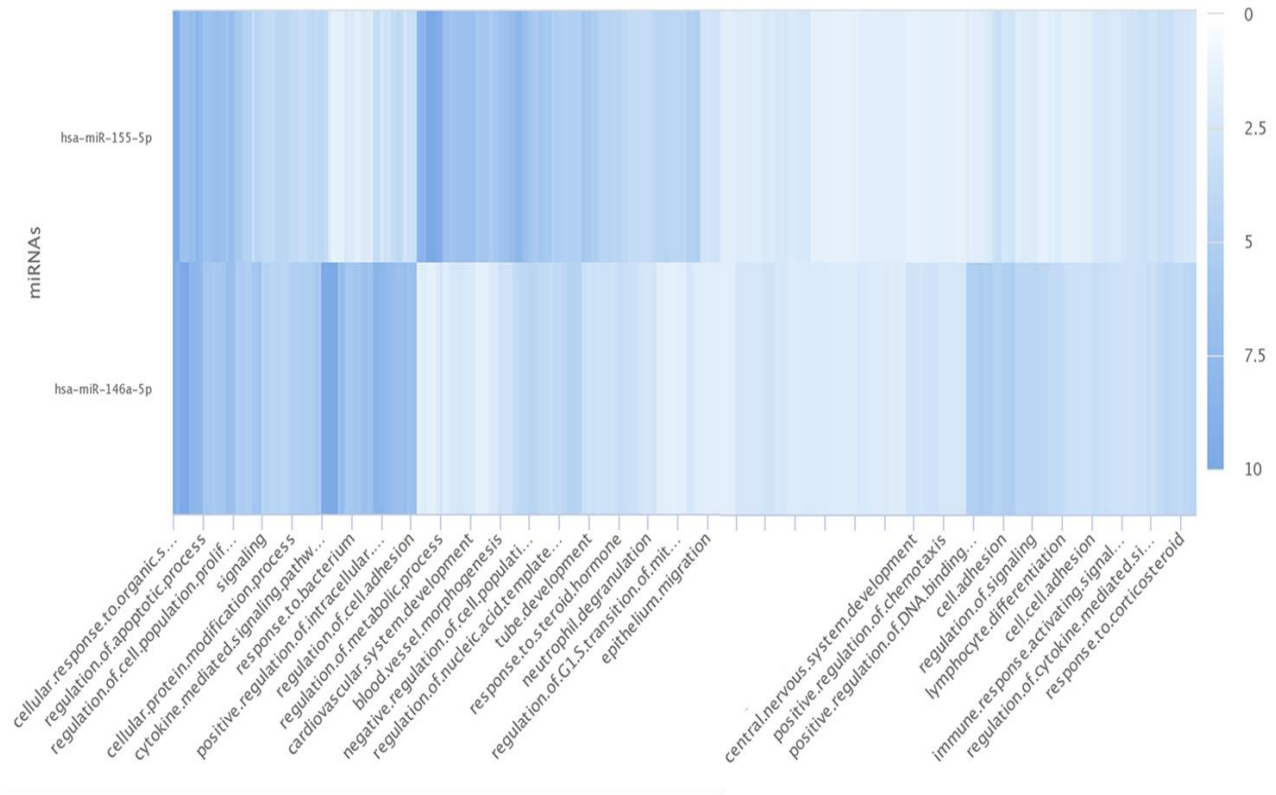

Figure 4.11. miR-146a and miR-155 show neuroinflammatory functions

Gene ontology analysis was performed using miRPathDB for miR-146a and miR-155. Pathways that are significant for miRNAs are displayed. Scale represents experimental significance. Darker = greater significance.

The cluster of upregulated miRNAs in fibroblast sEVs display functionality in responses to cellular death and metabolic changes, potentially suggesting a response to AD associated stress on the neuronal cells (Figure 4.12).

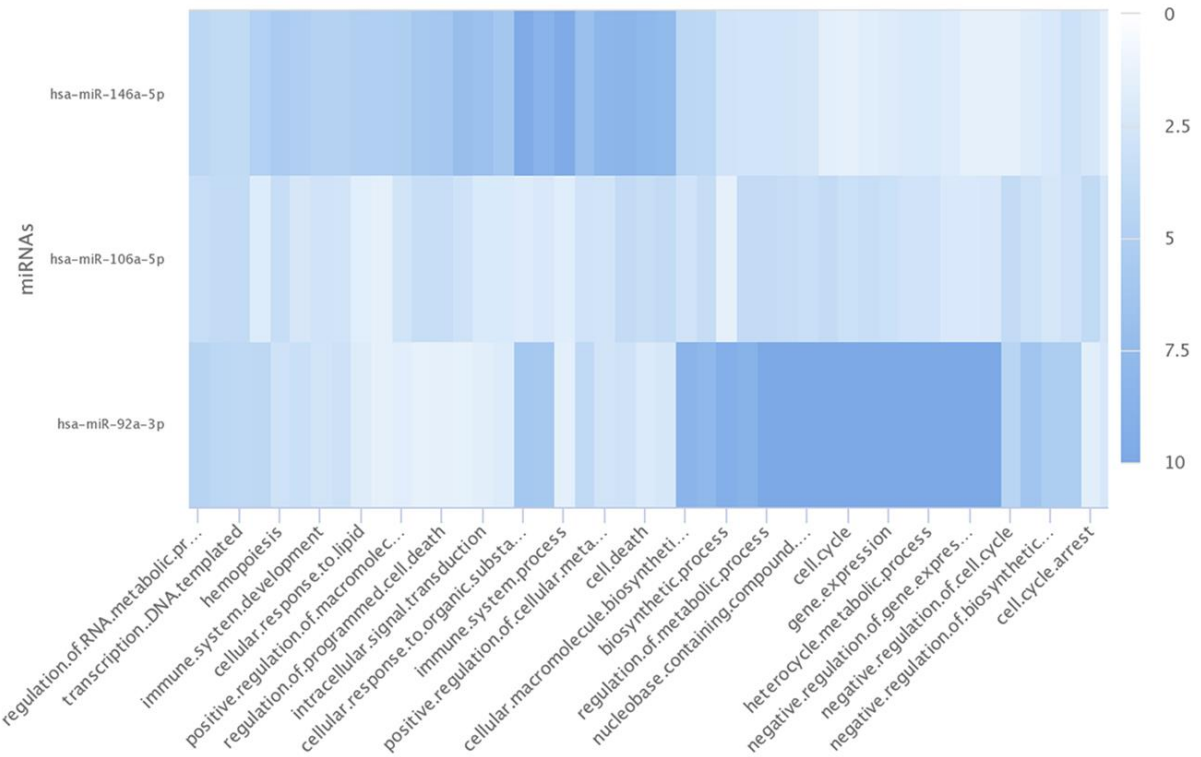

Figure 4.12. Upregulated miRNAs in fibroblast sEVs show function in regulation of cell death and metabolism

Gene ontology analysis was performed using miRPathDB for miR-146a, miR-106a and miR-92a. Pathways that are significant for miRNAs are displayed. Scale represents experimental significance. Darker = greater significance.

4.4 Small RNA sequencing of small extracellular vesicles in Alzheimer's disease

4.4.1 RNA sequencing workflow

Small RNA sequencing was performed in sequential steps with multiple quality check points (Figure 4.13) to ensure that the quality of reads was high enough to perform differential analysis on miRNAs derived from sEVs. Workflows were consistent for fibroblast derived and brain derived sEVs. The small RNA enriched fragment (Figure 4.13, 1) was isolated using the same methodology as for the RNA analysed via qPCR, to allow comparison between techniques. RNA was quantified prior to being converted into a cDNA library, to

normalise loading inputs. Ligation of the 3' and 5' adapters, converting the ligated RNA into cDNA and amplifying the cDNA to create libraries for sequencing (Figure 4.13, 2 and 3) was performed with the Lexogen Small RNA library preparation kit. The cDNA libraries were quantified and checked for their quality by measuring the size of the amplified products to confirm they were enriched in the miRNA fragment. Sequencing was performed using Illumina chemistry according to the protocols described (Figure 4.13, 4). Post sequencing quality checks were carried out, including analysing the number of reads generated between samples to determine whether further normalisation was required, as well as checking the quality scores of the reads to ensure that the reads generated could be confidently taken forward to align to the genome. Alignment of processed sequencing read counts was performed against the human genome and the miRbase miRNA annotations, to map reads to their designated miRNAs (Figure 4.13, 5). Alignments were checked for quality, including comparing alignment rates between the samples to check for differences in read quality, and to confirm the alignment confidence passed the quality checks. Read counts of miRNAs were compared between disease and neurological healthy control conditions in both fibroblast and brain derived sEVs, to determine whether miRNAs were differently expressed (Figure 4.13, 6). Differentially expressed miRNA were analysed with gene ontology (GO) using miRPathDB to analyse biological pathways in which they are involved.

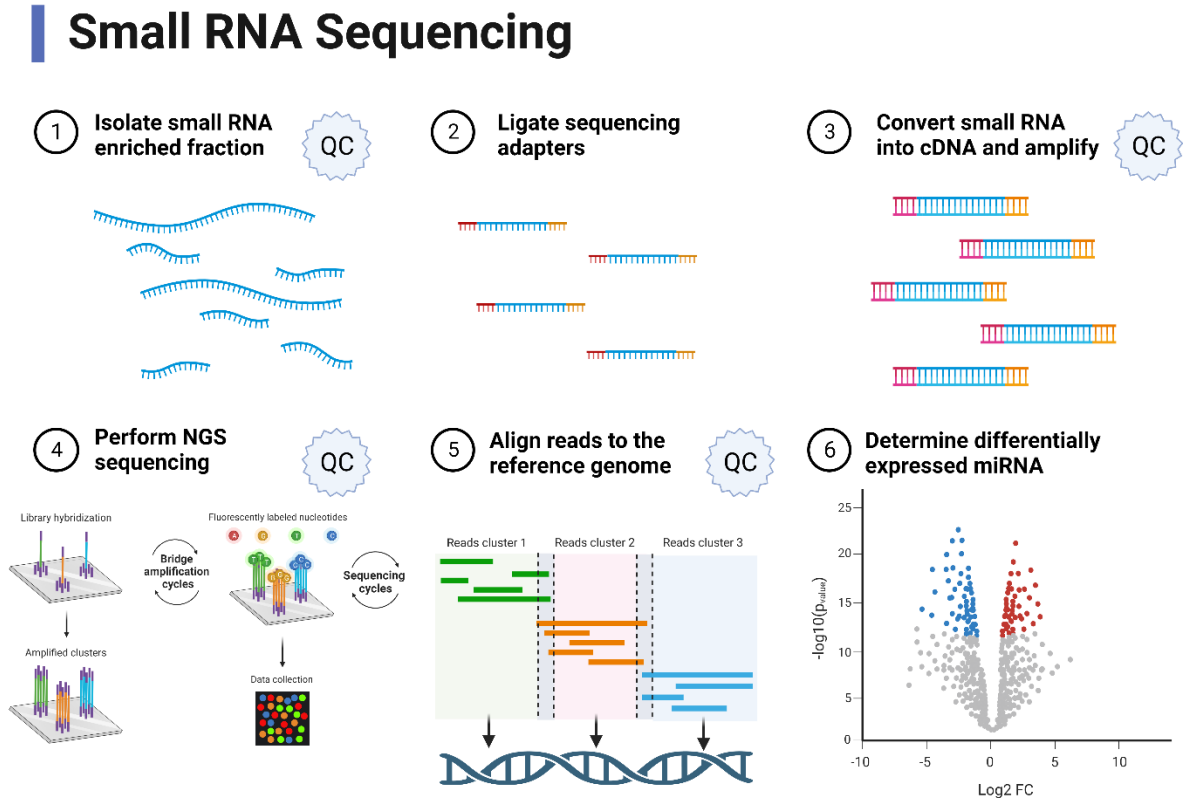

Figure 4.13. Small RNA sequencing workflow

Overview of the key stages of small RNA sequencing, including the quality check points for each step. 1) Isolate small RNA enriched fraction – quality check = quantification and normalisation of RNA for all samples. 2) Ligate sequencing adapters. 3) Convert small RNA into cDNA and amplification – quality check = quantification and size profiling of libraries to determine enriched RNA species. 4) Perform NGS sequencing – quality check = per base quality score cut off, trimming and removal of adapters and low quality reads. 5) Align reads to the reference genome – quality check = quantification of aligned reads and aligned miRNA read counts. 6) Determine differentially expressed miRNA. QC = quality check, FC = fold change.

4.4.2 Quality control of libraries for RNA sequencing

To ensure that the input RNA and subsequently converted cDNA libraries were of a sufficient quality to ensure that the RNA sequencing would correctly identify the respective populations, without bias from variable processing during the sequencing workflow, several quality checks were performed across the procedure. Firstly, RNA input was normalised to 6 and 10 ng for fibroblast derived and brain derived sEVs, respectively. The cDNA library preparation was performed according to the Lexogen Small RNA protocol,

without any amendments, to maintain consistency throughout between samples. The resultant libraries were quantified, and quality checked by Qubit and Tape station, respectively. Figure 4.14 and Figure 4.15 show the resultant size profiles of the cDNA libraries, with the enriched regions presenting in the small RNA ranges, and limited contamination by RNA fractions of different size profiles.

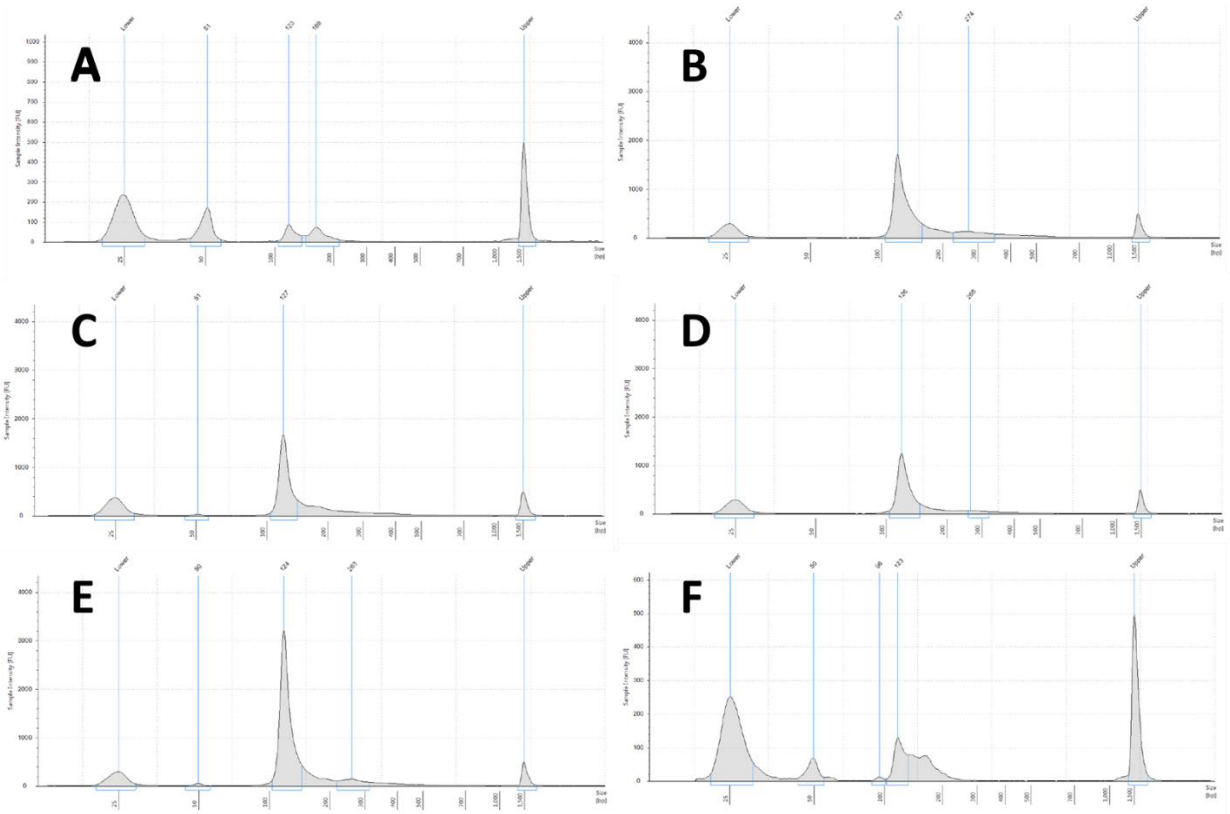

Figure 4.14. Lexogen cDNA libraries of fibroblast EV RNA is enriched in the small RNA fragment

Size profiling of the cDNA libraries generated from fibroblast derived sEVs by Tapestation. A-F represent biological replicates. X axis = size (bp), y axis = sample intensity (Fluorescence unit). In each graph, the first and last peaks represent the references (25 bp = lower, 1500 bp = upper). Samples showed enrichment in fractions in the size range of small RNA, peaks between 123 bp and 127 bp, with the expected size range of miRNA at 143 bp.

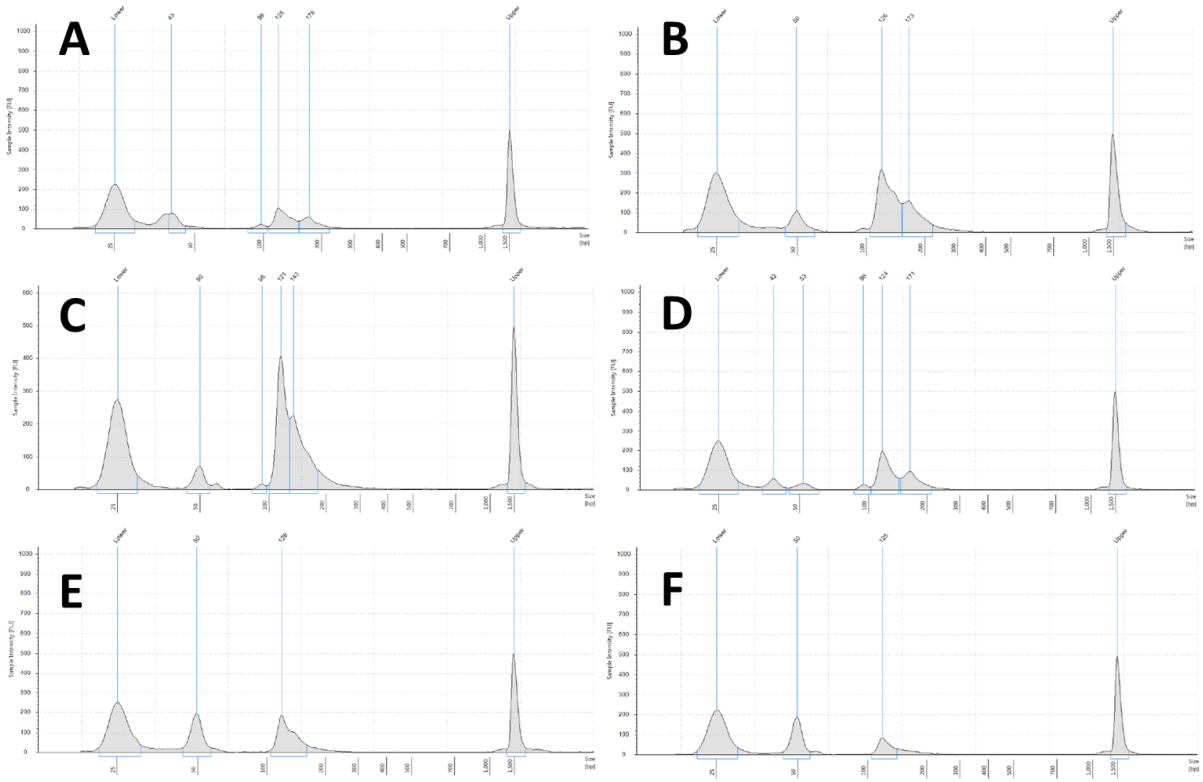

Figure 4.15. Lexogen cDNA libraries of brain derived EV RNA is enriched in the small RNA fragment

Size profiling of the cDNA libraries generated from brain tissue derived sEVs by Tapestation. A-F represent biological replicates. X axis = size (bp), y axis = sample intensity (Fluorescence unit). In each graph, the first and last peaks represent the references (25 bp = lower, 1500 bp = upper). Samples showed enrichment in fractions in the size range of small RNA, peaks between 121 bp and 127 bp, with the expected size range of miRNA at 143 bp.

All the average size profiles of the cDNA libraries were between 135 and 150 bp (Figure 4.16), indicating an enrichment of miRNA, which has an expected size profile of 143 bp with the ligated adapters. There was no observable input from fractions greater than 160 bp, which would indicate an enrichment in other RNA molecules, with smaller peaks at 120 bp, where adapter artifacts may present. However, any small peaks at this scale were indistinguishable from the larger miRNA peak. There were no differences in library sizes between AD and neurological healthy control samples in both conditions.

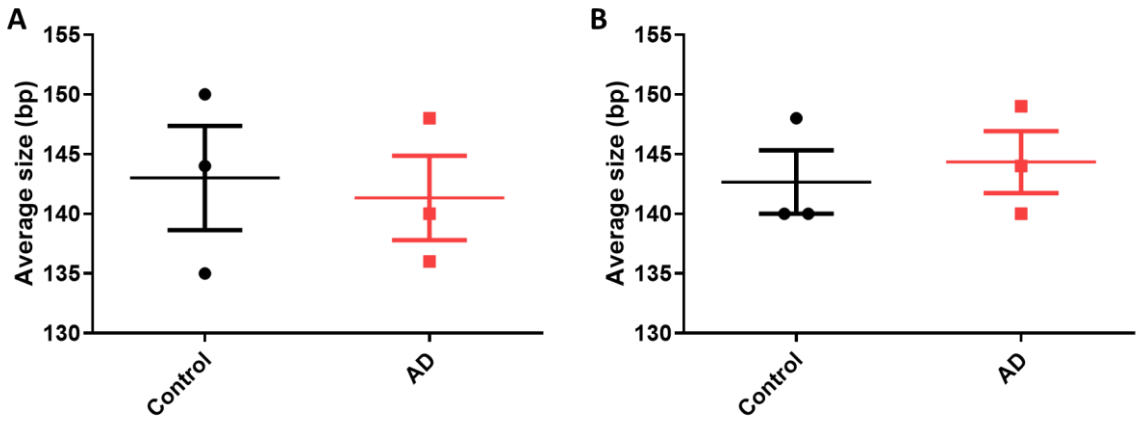

Figure 4.16. Average cDNA library sizes did not differ in AD compared to neurologically healthy controls

Quantification of average cDNA library size profiles, determined from the enriched regions in the Tapestation graphs. A) Fibroblast sEVs. B) Brain derived sEVs. AD = Alzheimer's disease. Mean ±SD. N = 3 (Biological replicates). T-test: NS

4.4.3 Analysis of sequencing reads and quality scores

With the cDNA libraries passing the preliminary quality checks, they were all processed for sequencing. Libraries were denatured and diluted to 8 pmol to maintain consistent input between all samples.

Initial sequencing results showed that read counts from the fibroblast sEVs ranged from 0.8 to 2.5 x 10^6, with no significant difference observed between AD and neurological healthy control populations (Figure 4.17, A). Similarly, read counts did not differ between AD and control populations in the brain derived sEVs, with counts ranging from 1.0 to 3.3 x10^6 (Figure 4.17, B).

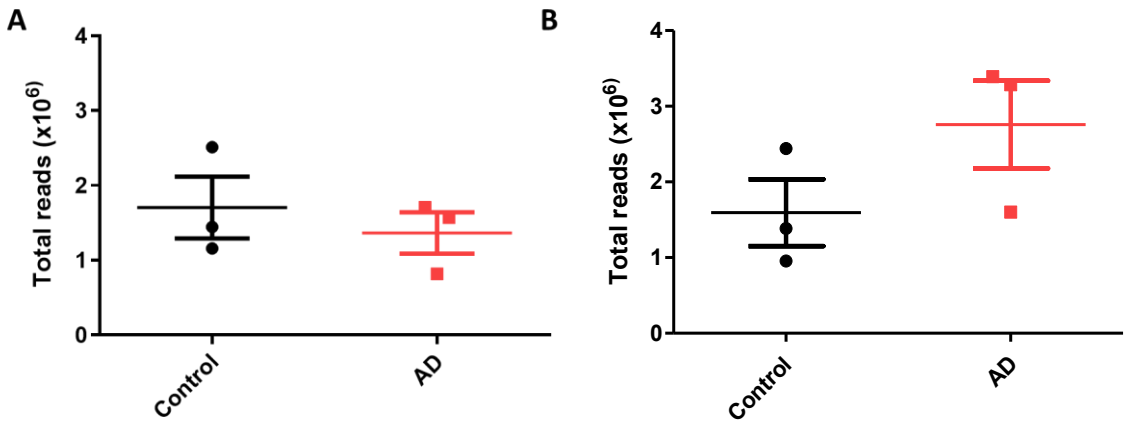

Figure 4.17. Total sequencing reads did not differ in AD compared to neurologically healthy controls

Average read counts of Illumina small RNA sequencing for AD and neurological healthy control samples in both cohorts. A) Fibroblast sEVs. B) Brain derived sEVs. AD = Alzheimer's disease. Mean ±SD. N = 3 (Biological replicates). T-test: NS

Across all the sequencing runs, over 90% of all reads passed the quality filter (lowest run = 92%), while over 93% of reads in all runs had a quality (Q) score of 30 or above and 80% with a Q score of 35 or above. The per base sequence qualities are displayed in Figure 4.18, highlighting that all the sequencing results were of a high quality, which limits any uncertainty when attributing reads to miRNAs. There were no differences between any groups, which reduces the risk of biased interpretation of downstream differential read counting.

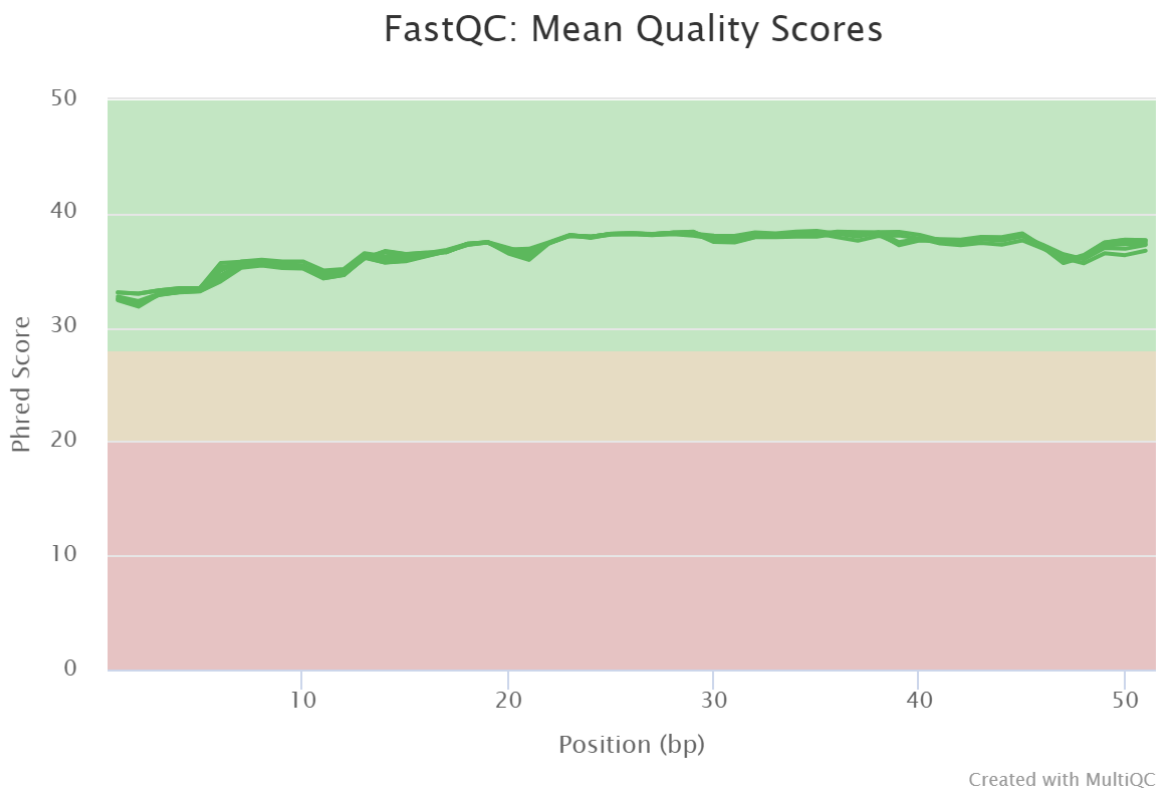

Figure 4.18. Visualisation of the average per base quality scores during sequencing

Average per base quality (Phred) scores were above the cut off of 30 (probability of a wrong base call is 1 in 1000) for all positions of the 50 bp sequencing run. Phred scores represent a log scale of the probability of a wrong base call, with higher scores indicating lower error rates. Bp = base pairs.

4.4.4 Clean up of sequencing reads and post trimming quality checks

Nonetheless, the sequencing runs required rigorous quality trimming and adaptor clipping to ensure that low quality reads were not included on any analysis. Given that the populations that underwent sequencing were enriched in miRNAs, which are around 22 bp in size, it is expected that there will be a lot of adapter content that was read during sequencing, as the smallest Illumina chemistry is the 50 bp read kit and so will continue to read into the 3' adapter. Therefore, reads were trimmed using Cutadapt, filtering the Lexogen 3' adapter, reads shorter than 16 bp (nonspecific product) and reads larger than 31 bp (other RNA types and fragments). A subsequent quality check was performed on all samples to ensure that the trimming and filtering was successful, and that only the reads of interest remained.

Figure 4.19 showed that after trimming, observable adapter content was removed from the remaining reads, as well as low quality reads and contaminant, which is displayed by a reduction in duplicated reads observed post trim (Figure 4.20). The trimmed reads resulted in a population of reads that were enriched in miRNA, as observed by the peaks at the 22 bp sequence length (Figure 4.21).

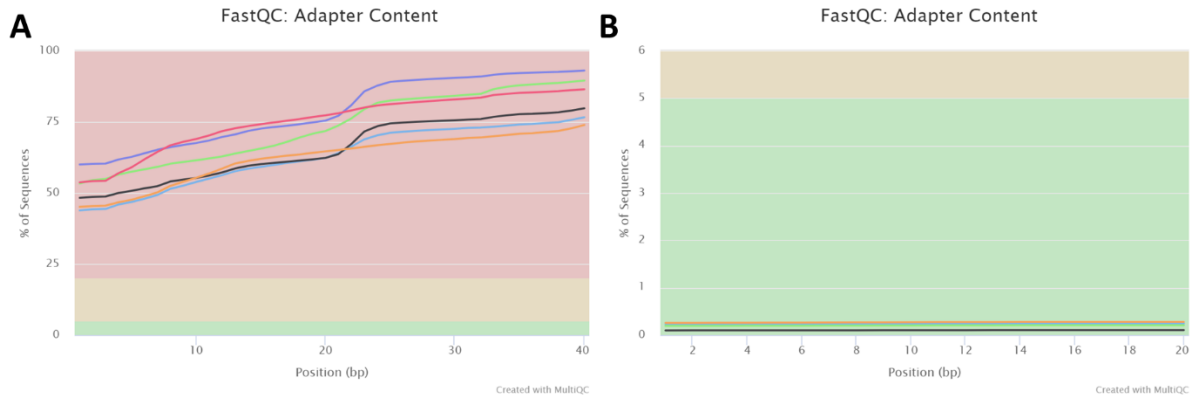

Figure 4.19. Filtering of sequencing reads removed adapter content

A) Pre-adapter trimming – adapter content: 50 – 90% of 50 bp run, depending on base position measured. B) Post-adapter trimming trimming – adapter content: 0% (negligible) of 50 bp run. Percent Illumina adapter content of sequencing reads. Adapter content was removed by trim of reads, which also reduced the size of reads to 20 bp on average.

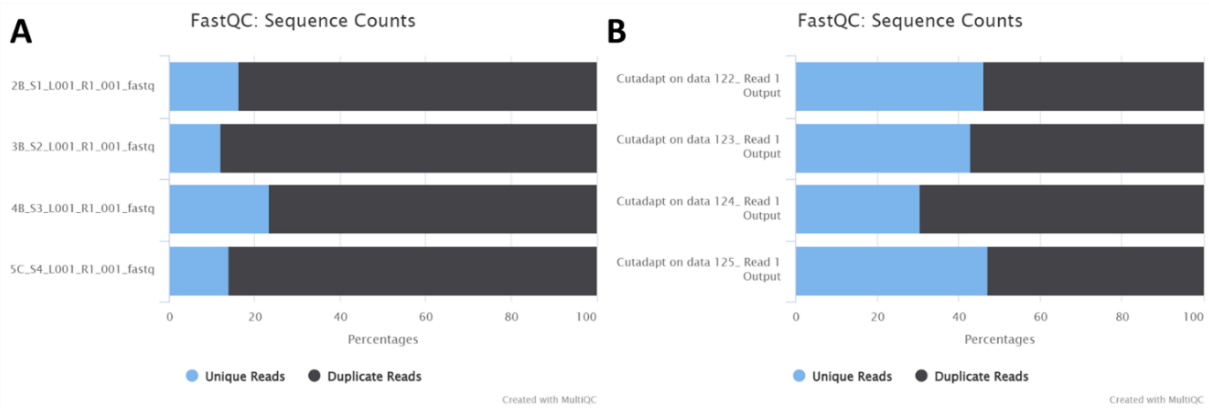

Figure 4.20. Filtering of sequencing reads removed duplicated content

A) Pre-adapter trimming. B) Post-adapter trimming. Percent duplicated reads were reduced by trimming and quality-based filtering of the reads.

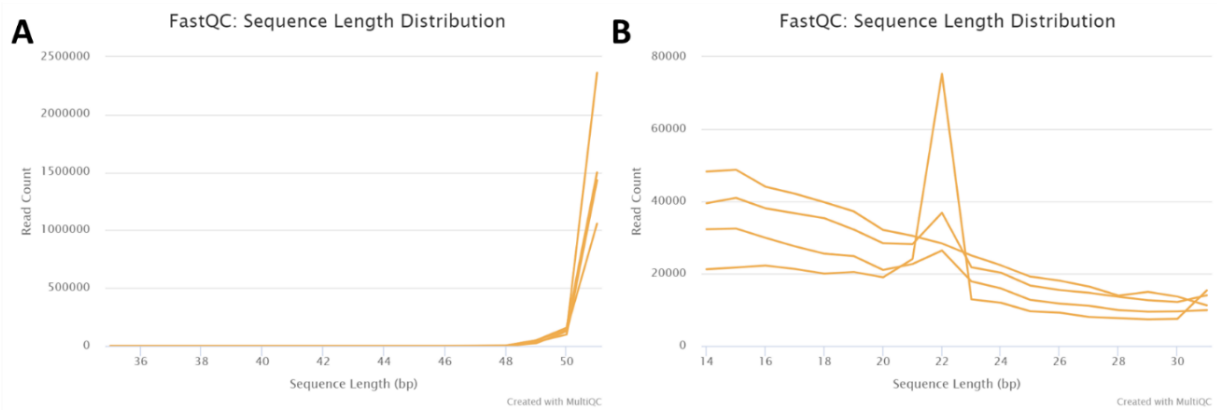

Figure 4.21. Filtering of sequencing reads results in sequencing reads enriched in miRNAs
A) Pre-adapter trimming – sequence length distribution of reads = 50 bp. B) Post-adapter trimming – sequence length distribution of reads = 14 - 36 bp, corresponding to lower and upper limits of reads passing filter after trimming adapters. Proportion of reads of miRNA specific sequence lengths were increased after trimming.

Trimming of the reads also cleaned up the nucleotide distributions observed per sequence, with the trimmed reads displaying a normalised distribution of GC content throughout (Figure 4.22), indicating a balanced composition of nucleotides that were not biased in specific overexpressed sequences. This was supported by the balancing of per base nucleotide proportions post trimming (Figure 4.23).

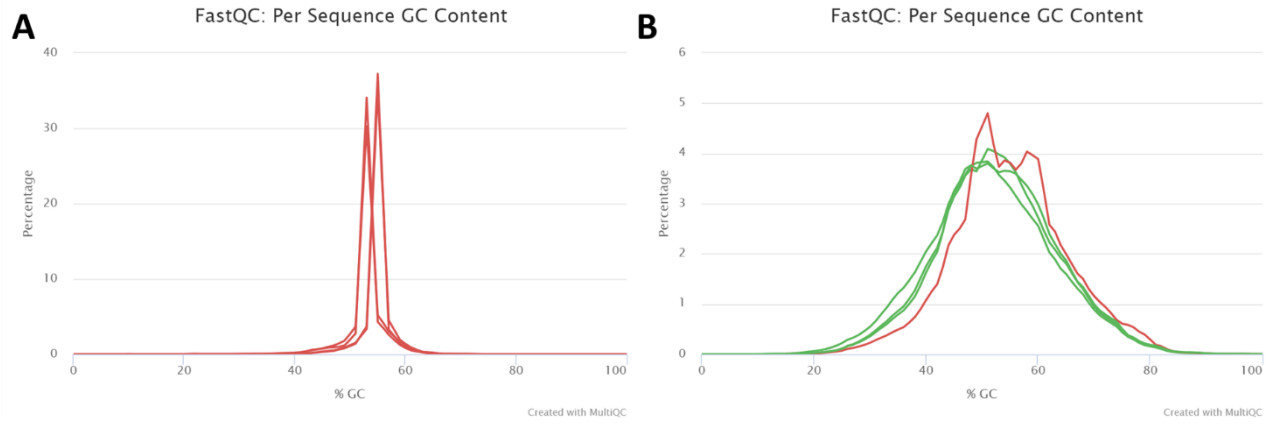

Figure 4.22. Samples expressed balanced GC content after filtering

A) Pre-adapter trimming. B) Post-adapter trimming. Percent GC nucleotide content of sequencing reads was normalised after trimming and filtering low quality reads.

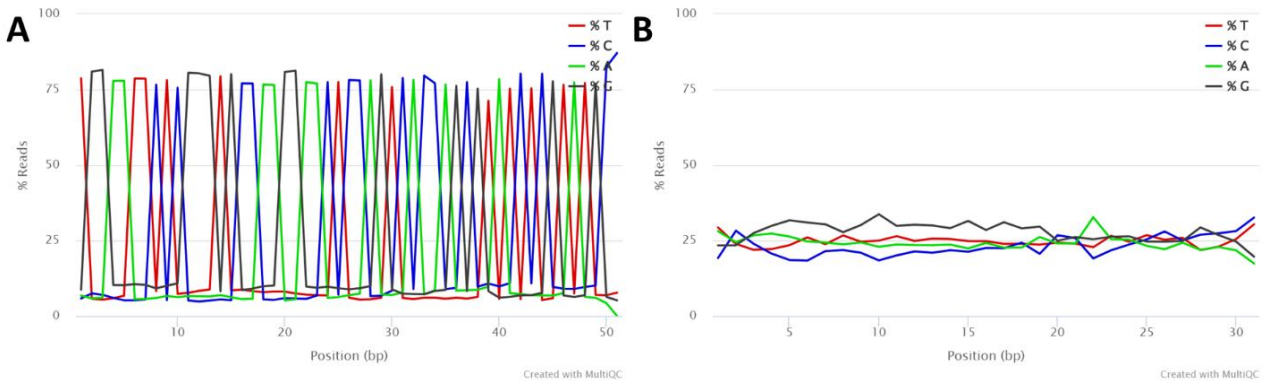

Figure 4.23. Samples expressed balanced nucleotide content after filtering

A) Pre-adapter trimming. B) Post-adapter trimming. Percentage of nucleotides that were read at each base were relatively equally distributed after trimming and quality filtering, with all nucleotides representing approximately 25% of each position. T (red) = Thymine, C (blue) = Cytosine, A (green) = Adenine, G (black) = Guanine.

4.4.5 Alignment and read count generation

Once trimmed reads had been quality checked, they were aligned to the reference human genome (Hg38) and the miRbase annotation of miRNAs, to determine the miRNA molecule the read represented. Quality checks of the alignment were performed, with alignment qualities above 20 on the Phred scale the cut-off for retaining reads for downstream read counting. The stringent quality checks and filtering resulted in approximately 10% of all initial reads being aligned to miRNA within the human genome. In the fibroblast sEVs (Figure 4.24, A), the aligned reads ranged from 0.3 to 1.7 x 10^5 in all the samples, while the brain derived sEVs (Figure 4.24, B) ranged from 0.9 to 4.6 x 10^5. In both cohorts, there were no significant differences between AD and neurological healthy control conditions, suggesting that the alignment rates would not influence observations of variations in miRNA expression.

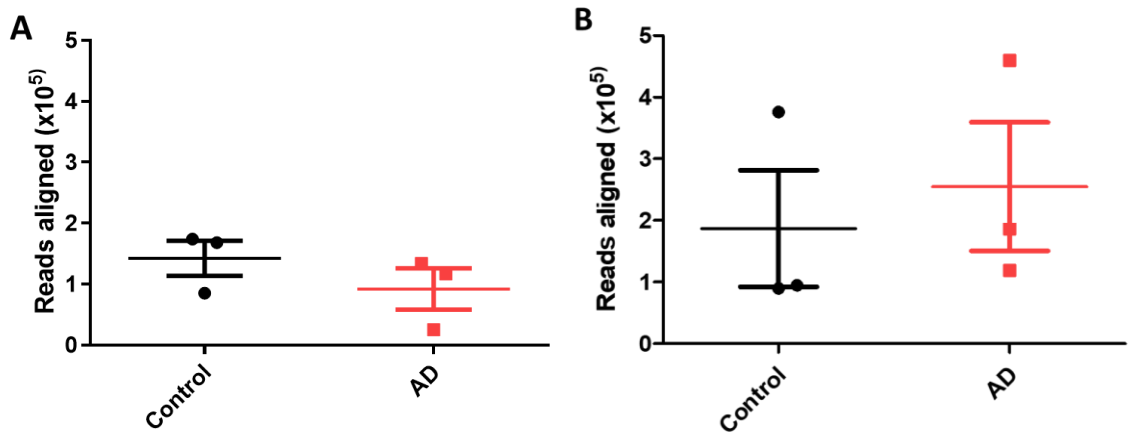

Figure 4.24. Reads aligning to the human genome post filtering did not differ in AD compared to neurologically healthy controls

Quantification of total reads that aligned to the human genome after filtering for low quality read alignments. A) Fibroblast sEVs. B) Brain derived sEVs. AD = Alzheimer's disease. Mean ±SD. N = 3 (Biological replicates). T-test: NS

4.4.6 Total variance of read counts

Differential gene expression analysis was performed using DESeq2, to determine whether the number of counts for a particular miRNA varied between the neurological healthy control and AD replicates. Total variance analysis was also performed on all samples to investigate whether they displayed patterns of expression between different subgroups, such as fibroblast neurological healthy control sEVs vs fibroblast AD sEVs.

Principal component analysis (PCA) was utilised to simplify and visualise the differential trends that are present in all the miRNA read counts between samples. It compiles groups of miRNAs that display similar trends of variability between samples and selects the two groups that provide the greatest statistical difference, plotting them in order on the X and Y axis. In both the fibroblast derived sEVs and the brain derived sEVs, PCA was unable to completely separate neurological healthy control and AD populations based on variation in miRNA populations (Figure 4.25). Noticeably, there is large variation between biological replicates, which, given that these samples are taken from individuals who will inevitably have different transcriptomic profiles, is not unexpected, though future consideration may be required on how to further control for variation. Even with the distinct inter-individual variability, there is a minor separation between neurological healthy control and AD in both

cohorts (Figure 4.25), though it is primarily based on the less variable PC2 plot, but it does suggest that there are some variable characteristics in miRNA expression.

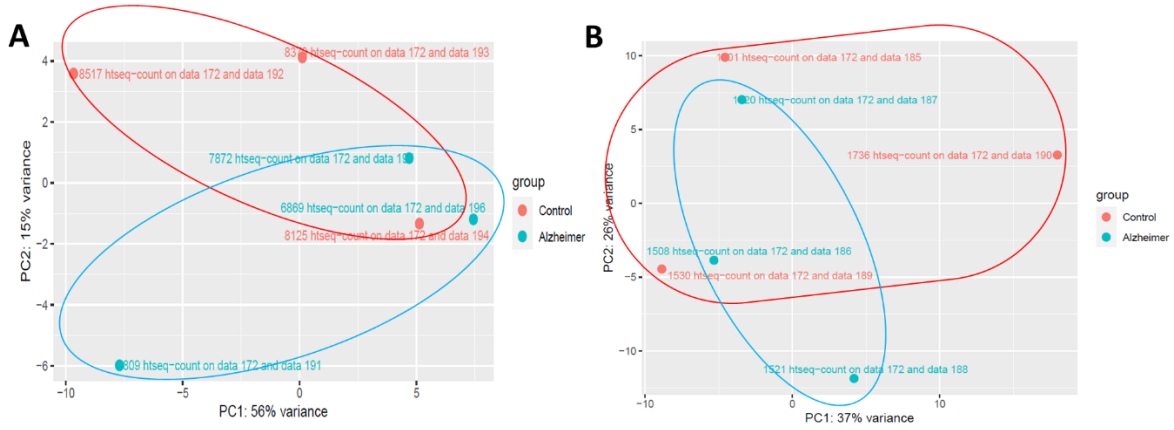

Figure 4.25. Population variation was not distinct between AD and neurological healthy control samples

Principal component analysis (PCA) of biological replicates in A) Fibroblast sEVs, and B) Brain derived sEVs. PC1 (x-axis) indicates the group of reads that displayed the highest level of variance across the samples, while PC2 (y-axis) indicates the second highest variance. Red = Neurological healthy control. Blue = Alzheimer's disease.

Observations of high inter-individual variation between samples in the PCA is also observed in the sample-sample distances plot, which attempts to group samples via hierarchical clustering based on similarities in their global expression. In the brain derived sEVs, the plot was unable to cluster samples based on disease profiles (Figure 4.26), with limited similarities seen across all individuals. The strongest correlation was between sample 1508 and 1530, from AD and neurological healthy control groups, respectively, which can also be observed by their close interaction on the PCA plot (Figure 4.25). Similar observations are found in the fibroblast derived sEVs (Appendix Figure 6.21).

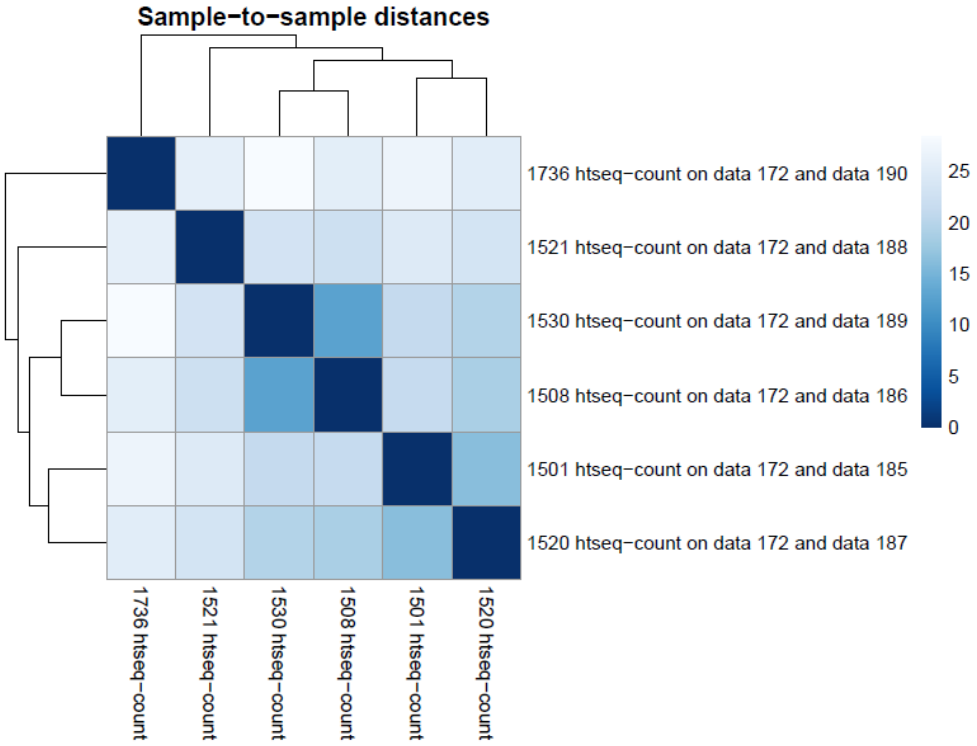

Figure 4.26. High levels of biological variation between samples limited clustering of groups in brain derived sEVs

Sample-sample distances plot displays the level of similarity between individual samples in a cohort, while attempting to perform hierarchical clustering on similar samples. Blue = correlation, darker shade = increased correlation.

Investigations of the spread of variability of individual miRNAs between samples was observed in the dispersion estimates plot, where miRNA dispersion levels correspond to their level of expression across samples. Higher expressed miRNAs are expected to have higher dispersion levels, and so the difference in expression is higher in miRNA that are relatively highly expressed, that display as statistically differentially expressed. Given the low abundance of miRNA in sEVs and small N number in the cohort, dispersion estimates will trend towards overestimated fitting of miRNA variation. Even so, the dispersion plot for the brain derived sEVs shows that samples do not diverge from the fitted relationship between expression and dispersion (Figure 4.27), suggesting that miRNA expression levels were not skewed by contaminants. Similar observations are found in the fibroblast derived sEVs (Appendix Figure 6.22).

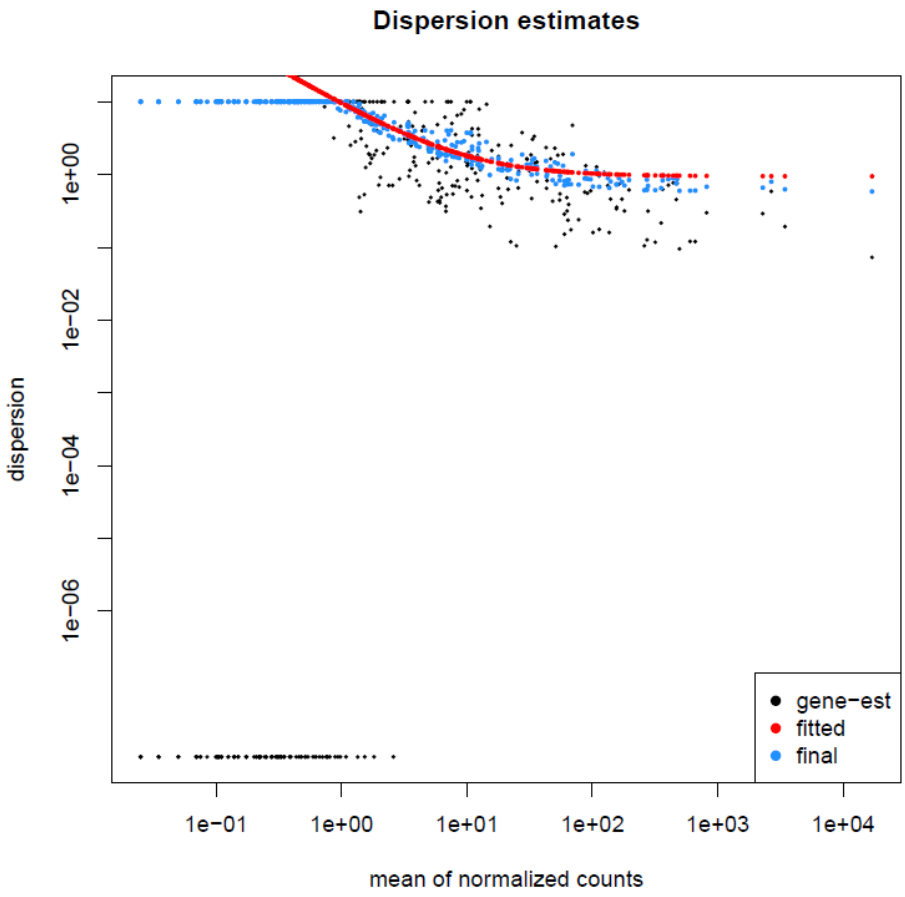

Figure 4.27. Dispersion estimates of sequencing reads from brain derived sEVs

Plot of amount of read counts observed for an individual miRNA against the variability/dispersion of the miRNA in the tested populations. One point = one miRNA. Black = unfitted comparisons, Red = fitted correlation based on all variances of miRNAs, Blue = fitted comparisons adjusted based on fitted correlation.

4.4.7 Differential analysis of Alzheimer's disease sEV miRNAs

4.4.7.1 Fibroblast derived small extracellular vesicles

Once the RNA sequencing data from both the fibroblast and brain derived sEV cohorts was processed, filtered and checked for quality scores as described above and in the small RNA sequencing workflow (Figure 4.13), the read counts of individual miRNAs could be compared between neurological healthy control and AD conditions. miRNAs were

categorised as differentially expressed if their fold change was greater than 2-fold (logFC > ±1), with a significance threshold of $p < 0.05$.

Counts of miRNAs detected in fibroblast derived sEVs ranged from 1240 to 6060, with no significant differences observed between neurological healthy control and AD conditions (Figure 4.28), the most abundant miRNAs in all samples were miR-221, miR-423 and miR-10b.

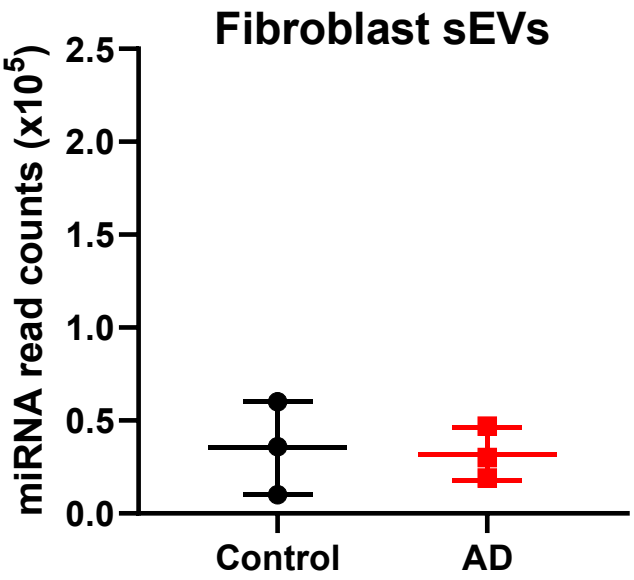

Figure 4.28. Aligned MiRNAs read counts did not differ in fibroblast derived sEVs

After aligning to the human genome, reads that corresponded with a miRNA annotation, based upon supplementary alignment to MiRBase, were quantified for all samples. AD = Alzheimer's disease. Mean ±SD. N = 3 (Biological replicates). T-test: NS

The miRNA content of fibroblast derived sEVs from AD groups did not significantly differ from neurologically healthy controls, as observed in the volcano plot (Figure 4.29). However, miR-146a shows a trend of upregulation in the AD fibroblast sEVs, with a fold change of greater than 4 ($p = 0.059$). This upregulation was also shown via qPCR, making it an interesting candidate for further investigation. Other miRNAs showed dysregulation in AD conditions, however without further replicates at this current stage, there is not enough statistical power to determine whether this will make viable candidates for further biomarker testing.

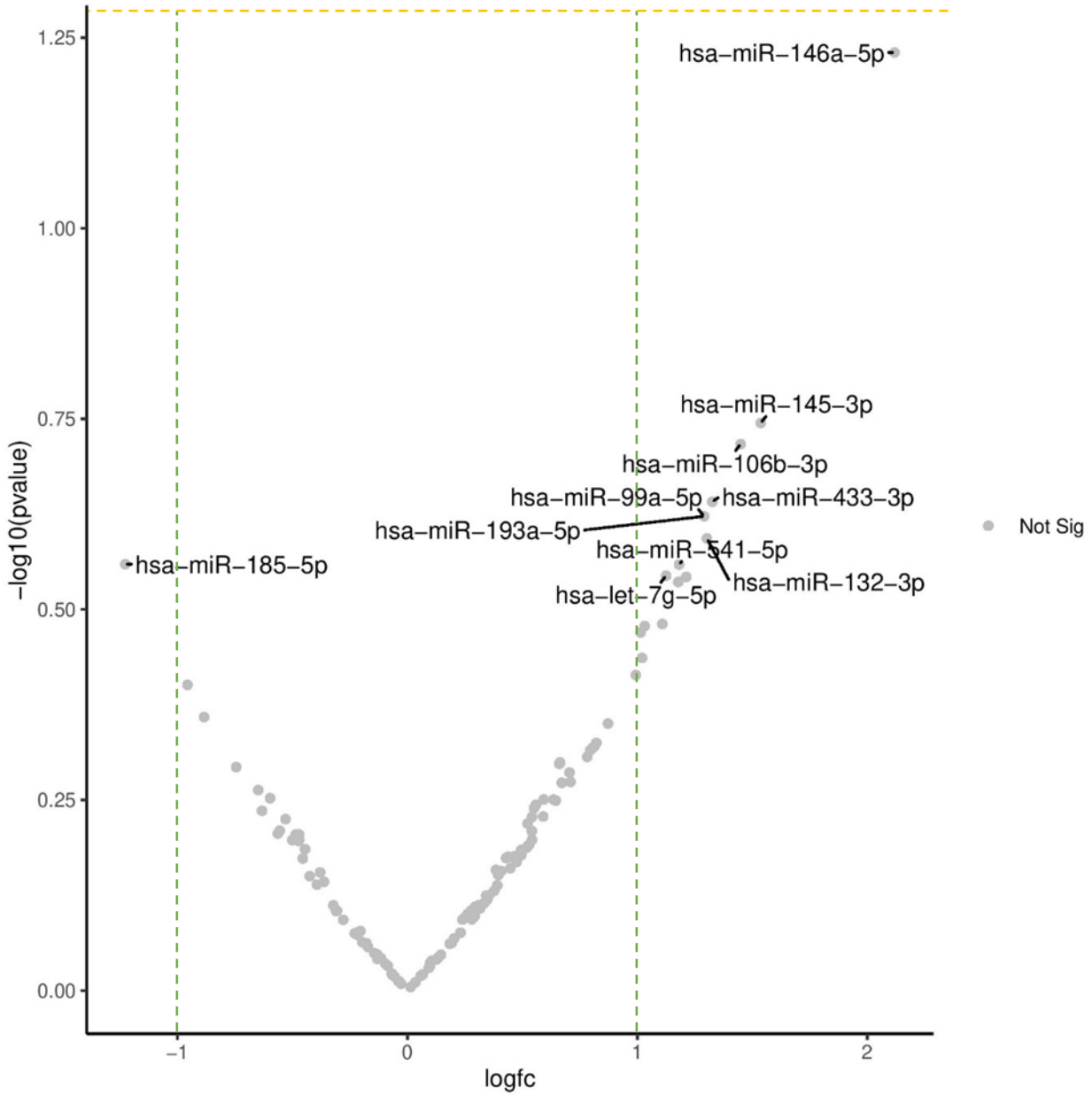

Figure 4.29. miR-146a was the most differentially expressed miRNA in fibroblast derived sEVs

Read counts of miRNAs for each group were compared using DESeq2 to identify differentially expressed genes, with logFC (log Fold change) plotted against -log (p value) on a volcano plot to visualise differences. The top 10 differentially expressed miRNA were annotated. Green broken line indicates logFC threshold = ±1. Significance threshold (yellow broken line) = 1.3 (log10(p-value), p <0.05. Grey = no significant change.

4.4.7.2 Brain derived small extracellular vesicles

In the brain derived sEVs, there was a significantly larger amount of read counts that aligned to the human genome than in the fibroblast derived sEVs, with read counts ranging from 49562 to 195889, with no significant differences observed between AD and neurological healthy control conditions (Figure 4.30). The most abundant miRNAs in all samples were let-7b, miR-30a and miR-143.

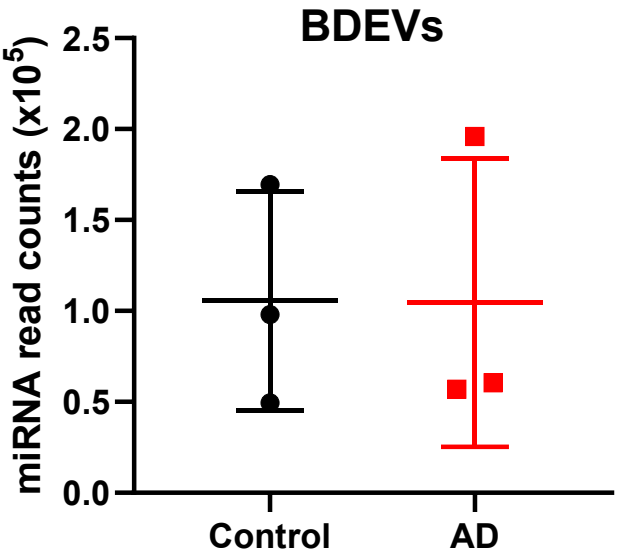

Figure 4.30. Aligned MiRNAs read counts did not differ in brain derived sEVs

After aligning to the human genome, reads that corresponded with a miRNA annotation, based upon supplementary alignment to MiRBase, were quantified for all samples. BDEVs: Brain derived small extracellular vesicles. AD = Alzheimer's disease. Mean ±SD. N = 3 (Biological replicates). T-test: NS

In the brain derived sEVs, there was a population of significantly dysregulated miRNAs in AD conditions. The highest level of dysregulation is observed with a group of upregulated miRNAs, consisting of miR-203a, miR-361, miR-141, miR-125b-1, and miR-30a, while miR-582 and miR-1248 were significantly downregulated (Figure 4.31).

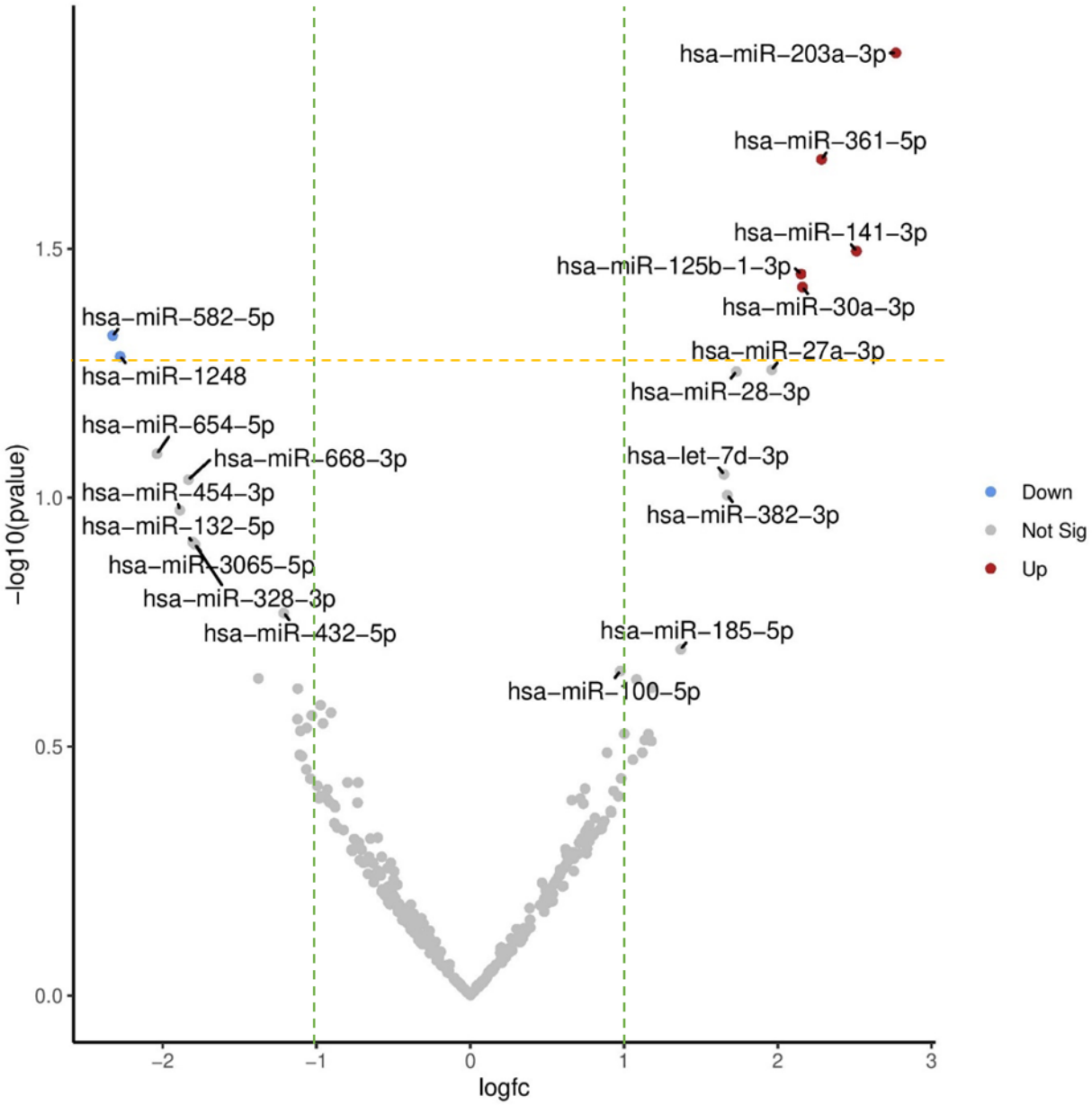

Figure 4.31. MiRNAs were differentially expressed in brain derived sEVs

Read counts of miRNAs for each group were compared using DESeq2 to identify differentially expressed genes, with log2 (FC) (Fold change) plotted against -log10 (p value) on a volcano plot to visualise differences. The top 10 differentially expressed miRNA were annotated. Green broken line indicates logFC threshold = ±1. Upregulated miRNAs: miR-203a, miR-361, miR-141, miR-125b, miR-30a. Downregulated miRNAs: miR-582, miR-1248. Significance threshold (yellow broken line) = 1.3 (log10(p-value), p <0.05. Red = upregulated, blue = downregulated, grey = no significant change.

4.4.8 Top differentially expressed miRNAs in Alzheimer's disease sEVs

The most differentially expressed miRNAs in AD for both fibroblast and brain derived sEVs are displayed in Table 4.4. While there is a lot of biological variation between samples, as previously highlighted, that makes it too difficult to distinguish differentially expressed miRNAs in the fibroblast sEVs with a lower N number, there are a panel of miRNA that show at least 2-fold differences in AD conditions, that will be interesting to investigate with an expanded cohort.

In the brain derived sEVs, beyond the significantly dysregulated candidates stated, there are other candidates that trend towards displaying significant variation that should not be discarded from further analysis. Notably, from the chromosome 14 cluster, miR-382 shows upregulation of the 3' strand and downregulation of the 5' strand, miR-323a is downregulated in both brain and fibroblast derived sEVs, though these are not statistically strong differences. Mir-668 (Log2(FC) = -1.832, p = 0.092) and miR-382 (Log2(FC) = 1.671, p = 0.099) of the cluster also shows a trend towards dysregulation, and present some of the statistically stronger trends within the c14 cluster.

The top differentially expressed miRNAs in both the fibroblast and brain derived sEV cohorts were compared (Figure 4.32), in order to determine whether there was any consistency between the groups and determine whether there were any miRNAs that were dysregulated in both groups.

Table 4.4. Top differentially expressed miRNA in fibroblast sEVs and brain derived sEVs

The top differentially expressed miRNA (log2(fold change)) as identified by DESeq2 and plotted on the volcano plot, with corresponding log2(fold change) and P values.

miRNA		Fibroblast sEV	
		log2 (FC)	P value
Up	hsa-miR-146a-5p	2.119	0.059
	hsa-miR-145-3p	1.537	0.180
	hsa-miR-106b-3p	1.450	0.192
	hsa-miR-433-3p	1.326	0.229
	hsa-miR-132-3p	1.303	0.255
	hsa-miR-193a-5p	1.291	0.239
	hsa-miR-99a-5p	1.291	0.239
	hsa-miR-370-3p	1.213	0.287
	hsa-miR-541-5p	1.182	0.276
Down	hsa-miR-152-3p	-0.555	0.617
	hsa-let-7f-5p	-0.563	0.623
	hsa-miR-1180-3p	-0.597	0.559
	hsa-miR-323a-3p	-0.632	0.581
	hsa-miR-30e-5p	-0.649	0.546
	hsa-miR-652-3p	-0.745	0.509
	hsa-miR-140-3p	-0.884	0.438
	hsa-let-7d-5p	-0.957	0.397
	hsa-miR-185-5p	-1.227	0.276

miRNA		BDEV	
		log2 (FC)	P value
Up	hsa-miR-203a-3p	2.768	0.013
	hsa-miR-141-3p	2.512	0.032
	hsa-miR-361-5p	2.284	0.021
	hsa-miR-30a-3p	2.161	0.038
	hsa-miR-125b-1-3p	2.151	0.036
	hsa-miR-181a-2-3p	2.051	0.051
	hsa-miR-27a-3p	1.960	0.055
	hsa-miR-28-3p	1.730	0.056
	hsa-miR-382-3p	1.671	0.099
	hsa-let-7d-3p	1.650	0.090
Down	hsa-miR-382-5p	-1.030	0.274
	hsa-miR-323a-5p	-1.039	0.367
	hsa-miR-132-3p	-1.063	0.290
	hsa-miR-92b-5p	-1.066	0.352
	hsa-miR-425-3p	-1.094	0.331
	hsa-miR-34a-5p	-1.104	0.294
	hsa-miR-1270	-1.109	0.329
	hsa-miR-421	-1.121	0.242
	hsa-miR-15a-5p	-1.123	0.279
	hsa-miR-432-5p	-1.212	0.171
	hsa-miR-339-3p	-1.377	0.231
	hsa-miR-3065-5p	-1.789	0.124
	hsa-miR-328-3p	-1.790	0.124
	hsa-miR-132-5p	-1.804	0.123
	hsa-miR-668-3p	-1.832	0.092
	hsa-miR-454-3p	-1.888	0.106
	hsa-miR-654-5p	-2.037	0.082
	hsa-miR-1248	-2.276	0.050
	hsa-miR-582-5p	-2.325	0.047

Left) Fibroblast sEVs. Right) Brain derived sEVs. P value threshold < 0.05. Red = upregulated, green = downregulated. BDEV: Brain derived small extracellular vesicle.

There were no positive correlations between brain and fibroblast derived sEV miRNAs in AD, which is not unexpected, given the transcriptomic differences that are present in both cellular origins, only 164 individual miRNAs displayed consistent expression in both cohorts

to be included in the analysis. Interestingly, two miRNAs came out as inversely dysregulated between brain and fibroblasts (cut-off = Log2(1)). This included miR-132 (Log2(FC): Brain = -1.063, Fibroblast = 1.303) and miR-185 (Log2(FC): Brain = 1.369, Fibroblast = -1.227), which both notably showed inverse patterns between brain and fibroblast (Figure 4.32). Neither miRNA showed statistically significant dysregulation, which makes it challenging to draw to many conclusions from this observation. However, miR-185 was the most downregulated miRNA in fibroblast derived sEVs and therefore, does display potential to be included in expanded investigation, to determine whether it has an interaction in AD pathways.

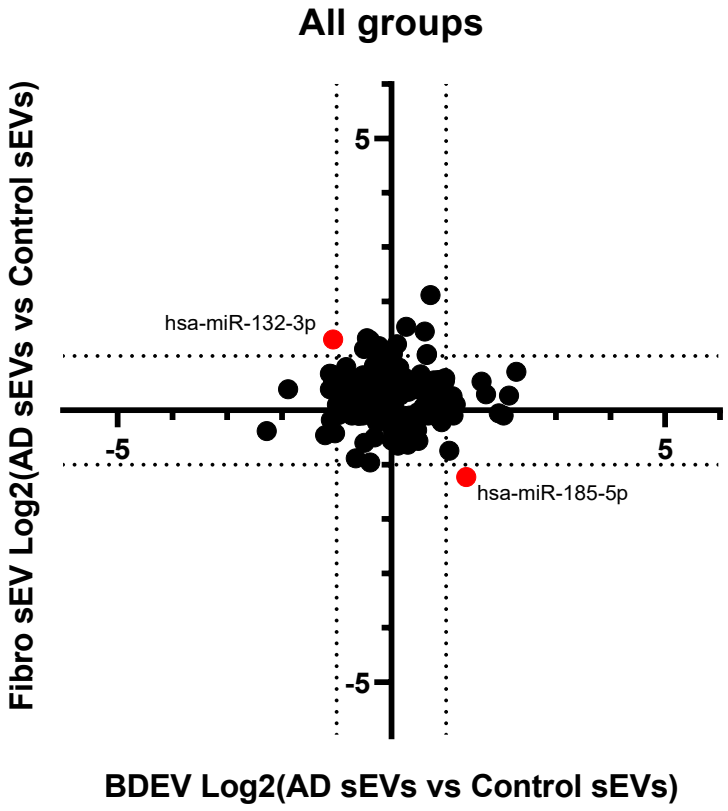

Figure 4.32. miR-132 and miR-185 display inverse regulation in sEVs in AD between fibroblast and brain derived sEVs

Dotted lines indicate a threshold of log2(FC) = ±1, where highlighted miRNA expressed a positive or negative fold change >2 in AD, in both fibroblast and brain derived sEVs. Green = miRNA fold change was positively correlated, red = miRNA fold change was negatively correlated. Black = miRNA did not pass one or more of the thresholds or did not have enough read counts (<5) to be analysed. BDEVs: Brain derived small extracellular vesicles. AD = Alzheimer's disease.

4.4.9 RNA sequencing identifies a sample of dysregulated chromosome 14 cluster miRNAs in Alzheimer's disease sEVs

As noted in Table 4.4 (above), the chromosome 14 cluster miRNAs are represented in some of the most differentially dysregulated miRNAs in the brain derived sEVs. Table 4.5 shows the other c14 candidates that showed a fold change >2 (note: Table 4.5 and Table 4.6 have been log transformed from the log2(FC) presentation above, in order to directly compare fold changes to observations from qPCR experiments). Most of the fold change, either up or down, is observed in the brain derived sEVs in AD, though mir-541 and miR-323b were downregulated over 2-fold in AD, in fibroblast derived sEVs.

Table 4.5. Candidate chromosome 14 cluster miRNAs were not dysregulated in AD

Visualisation of fold change values for chromosome 14 cluster miRNA in AD, in both brain-derived and fibroblast-derived sEVs. Split across pages 134 and 135.

miRNA	BDEV		miRNA	Fibroblast sEV	
	3p	5p		3p	5p
hsa-mir-656	0.94		hsa-mir-656	1.10	
hsa-mir-410	0.56		hsa-mir-410	0.57	
hsa-mir-369	0.80	1.07	hsa-mir-369	0.72	
hsa-mir-412		1.89	hsa-mir-412		1.16
hsa-mir-409	0.70		hsa-mir-409	0.63	
hsa-mir-541			hsa-mir-541		0.44
hsa-mir-377	1.74		hsa-mir-377		
hsa-mir-496			hsa-mir-496	0.77	
hsa-mir-154	1.54		hsa-mir-154		
hsa-mir-323b	0.82		hsa-mir-323b	0.46	
hsa-mir-485	0.91	0.61	hsa-mir-485	1.14	1.06
hsa-mir-668	0.28		hsa-mir-668		
hsa-mir-134		1.31	hsa-mir-134		1.13
hsa-mir-382	3.18	0.49	hsa-mir-382		1.32
hsa-mir-487a	0.82	0.70	hsa-mir-487a	0.77	
hsa-mir-655			hsa-mir-655		
hsa-mir-544a			hsa-mir-544a		
hsa-mir-889	0.66		hsa-mir-889	1.06	
hsa-mir-539		0.96	hsa-mir-539	0.77	
hsa-mir-487b	1.95		hsa-mir-487b	0.92	
hsa-mir-381	0.97		hsa-mir-381	0.57	
hsa-mir-1185-2			hsa-mir-1185-2		

hsa-mir-1185-1			hsa-mir-1185-1		
hsa-mir-300			hsa-mir-300		
hsa-mir-376a-1			hsa-mir-376a-1		
hsa-mir-376b			hsa-mir-376b		
hsa-mir-654	0.62	0.24	hsa-mir-654	0.72	
hsa-mir-376a-2			hsa-mir-376a-2		
hsa-mir-376c	1.83		hsa-mir-376c	0.76	
hsa-mir-495	0.53		hsa-mir-495	0.68	
hsa-mir-543		1.19	hsa-mir-543		1.23
hsa-mir-1193			hsa-mir-1193		
hsa-mir-494	0.53		hsa-mir-494	0.71	
hsa-mir-329-2			hsa-mir-329-2		
hsa-mir-329-1			hsa-mir-329-1		
hsa-mir-758			hsa-mir-758	0.77	
hsa-mir-323a	1.23	0.29	hsa-mir-323a	0.65	
hsa-mir-1197	0.72		hsa-mir-1197		
hsa-mir-380	1.50	0.79	hsa-mir-380	1.06	
hsa-mir-299	1.17		hsa-mir-299	0.68	
hsa-mir-411	2.26	1.05	hsa-mir-411	0.93	0.77
hsa-mir-379		0.80	hsa-mir-379	0.77	0.93

Red = upregulated (Fold change threshold > 2), green = downregulated (Fold change threshold < 0.5). Grey = not differentially expressed. Black = not expressed. BDEV: Brain derived small extracellular vesicle.

4.5 Comparison of candidate miRNA expression between qPCR and RNA sequencing

To validate the robustness of both the RNA sequencing and the qPCR experiments, candidate miRNAs that have been picked up by both methods were compared to see whether any observed dysregulation was consistent between them. Table 4.6 shows that there are more dysregulated miRNAs detected by qPCR than RNA sequencing. On one hand, this suggests that qPCR is more sensitive at picking up changes in the less abundant miRNA in the sample, with RNA sequencing predominantly creating clusters from the most expressed miRNA, and therefore, may miss miRNAs that do not reach the count threshold for inclusion in differential analysis. However, RNA sequencing works on a more rigorous statistical analysis than qPCR, for higher throughput analysis, in order to reduce the chance of picking up false positives. Even with these differences in mind, it is promising to see that in multiple cases where both techniques pick up differential miRNA expression, they trend

in the same direction. This is observed in miR-382 in the brain derived sEVs and miR-92a in the fibroblast derived sEVs, which were upregulated in AD, in all cases. miR-146a also showed consistent fold change differences in fibroblast sEVs, though the same miRNA also showed inverse results in the BDEVs, highlighting it as a candidate of interest that requires further investigation to accurately assess its role in sEVs in AD. Chromosome 14 miR-412 also showed inverse fold changes in brain derived sEVs in AD.

From the preliminary miRNA investigations, miRNAs miR-92a, miR-146a and miR-382 in the chromosome 14 cluster, are viable candidates for further biomarker testing.

Table 4.6 miR-92a and miR-146a display consistent expression changes in AD between qPCR and RNA sequencing, in brain derived sEVs

Comparison of fold change values, acquired from qPCR and RNA sequencing, for candidate miRNA in AD. Comparisons are shown for brain derived sEVs and fibroblast derived sEVs.

miRNA		BDEV		miRNA	Fibroblast sEV	
		qPCR	RNA Seq		qPCR	RNA Seq
Non-Cluster 14	17a	1.27	1.39	17a	1.09	0.93
	19a	0.91	0.59	19a		
	19b	0.84		19b	1.72	
	20a	2.82	0.68	20a		
	21	1.03	0.60	21	0.49	1.02
	92a	1.24	1.00	92a	4.95	2.04
	106a	1.66	1.15	106a	3.56	
	146a	0.21	1.64	146a	4.85	4.32
	155	0.28	0.69	155		
Cluster 14	382	1.51	3.18	382		1.32
	487a	1.63	0.82	487a	2.16	0.81
	323a	0.64	0.49	323a	2.14	0.65
	412	0.43	1.89	412	0.64	1.15
	494	1.32	0.53	494	2.00	0.71
	655	1.07		655	2.90	
	485	1.04	0.61	485	2.89	1.00
	889	1.09	0.66	889	2.44	1.06
	134	0.75	1.31	134	5.42	1.13
	758	0.62		758	3.21	

Red = upregulated (Fold change threshold > 2), green = downregulated (Fold change threshold < 0.5). Grey = not differentially expressed. Black = not expressed. BDEV: Brain derived small extracellular vesicle

4.6 miRNAs are differentially expressed in brain derived sEVs in AD females

The goal of developing an effective biomarker to improve the capability to intervene early in AD is made increasingly difficult by the noted heterogeneity of the disease. Whether that is due to a different accumulation of insults over a timeline or different presentation of genetic risk factors, or both, it is likely that future diagnostics will be aiming to target not just AD, but potential subtypes of AD based on individual circumstances. Sex is an under investigated but significant risk factor for the development of AD associated dementia (Nebel et al, 2018; Podcasy and Epperson, 2022), with vast sex-specific transcriptomic profiles observed in AD (Guo et al, 2022), though only a few have looked at miRNA profiles (Kodama et al, 2020), and fewer still in sEVs.

4.6.1 Fibroblast derived small extracellular vesicles

There were not any significantly differentially expressed miRNAs in the fibroblast derived sEVs in the female groups, as observed in the volcano plot (Figure *4.33*). However, while statistical power was reduced by analysing only an n = 2 per group, the general fold change trends increased, both in the most upregulated miRNA (miR-145, log2(FC) = 3.267) and most downregulated miRNA (miR-185, log2(FC) =-1.640). Which indicates that there may be miRNAs that are more dysregulated in AD within the female groups, though expanding this group is necessary to investigate this.

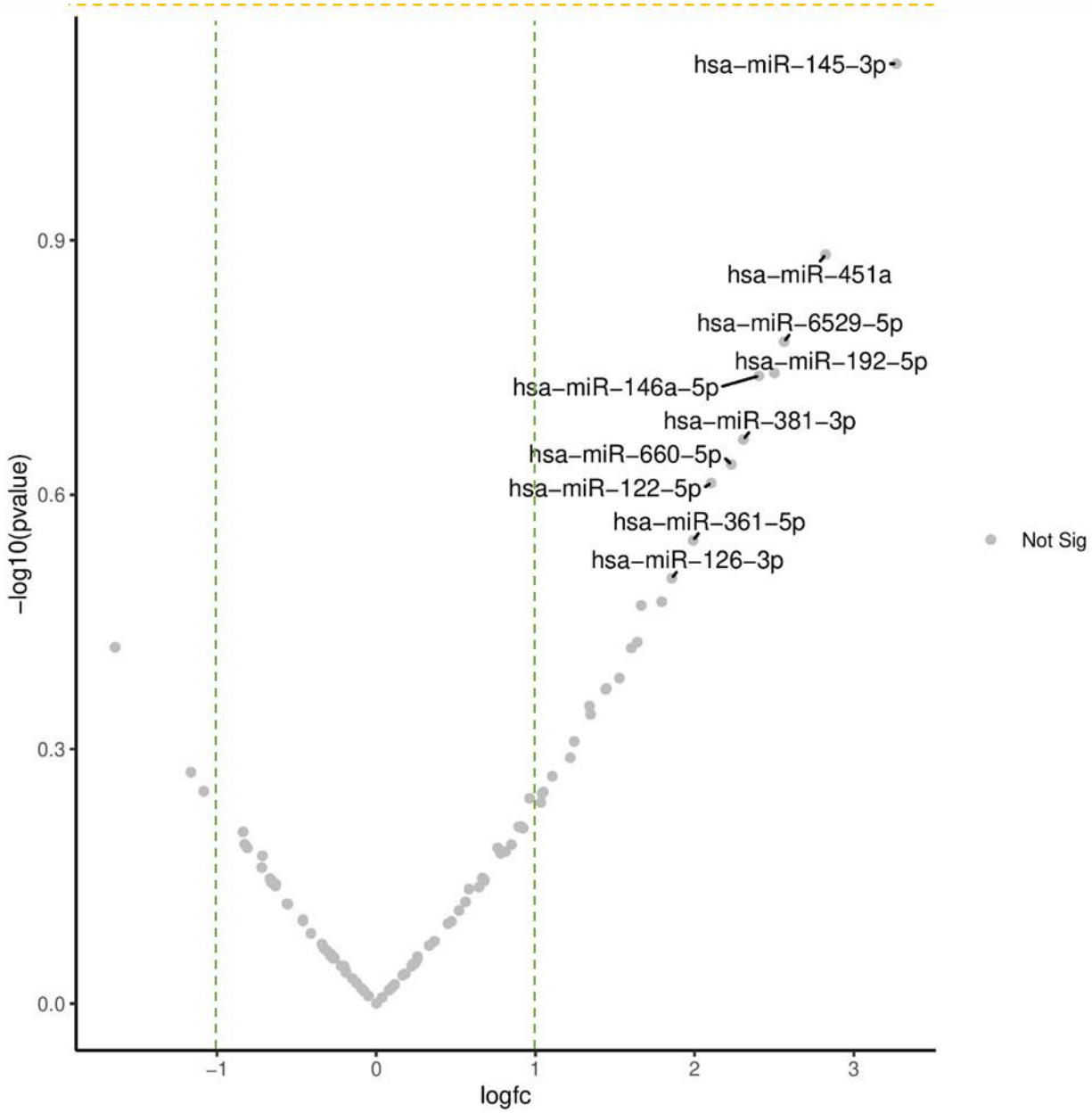

Figure *4.33*. miR-145 was the most differentially expressed miRNA in AD Fibroblast sEV AD in females

Cohorts were stratified to just compare females in each group (n=2 per group). Read counts of miRNAs for each group were compared using DESeq2 to identify differentially expressed genes, with logFC (log Fold change) plotted against -log (p value) on a volcano plot to visualise differences. The top 10 differentially expressed miRNA were annotated. Green broken line indicates logFC threshold = ±1. Significance threshold (yellow broken line) = 1.3 (log10(p-value), p <0.05. Grey = no significant change.

4.6.2 Brain derived small extracellular vesicles

Notably, in the brain derived sEVs, there was a population of significantly dysregulated miRNAs in the female AD groups, even with the reduced statistical power (Figure 4.34). Out of the observed differences, miR-203a remained as the most significantly dysregulated miRNA (Log2(FC) = 3.239, p = 0.015), as seen in the total population (Figure 4.31), which was also true of miR-125b-1 (Log2(FC) = 2.799, p = 0.038). Interestingly, miR-27a was significantly upregulated in brain derived sEVs in the AD female population (Log2(FC) = 2.878, p = 0.033), an observation that was not seen in the total population. The significantly downregulated miRNAs in the total population were not observed in the AD female group, however, miR-668 of the chromosome 14 cluster, did trend closer towards downregulation in AD and was the most downregulated miRNA (Log2(FC) = -2.515, p = 0.070).

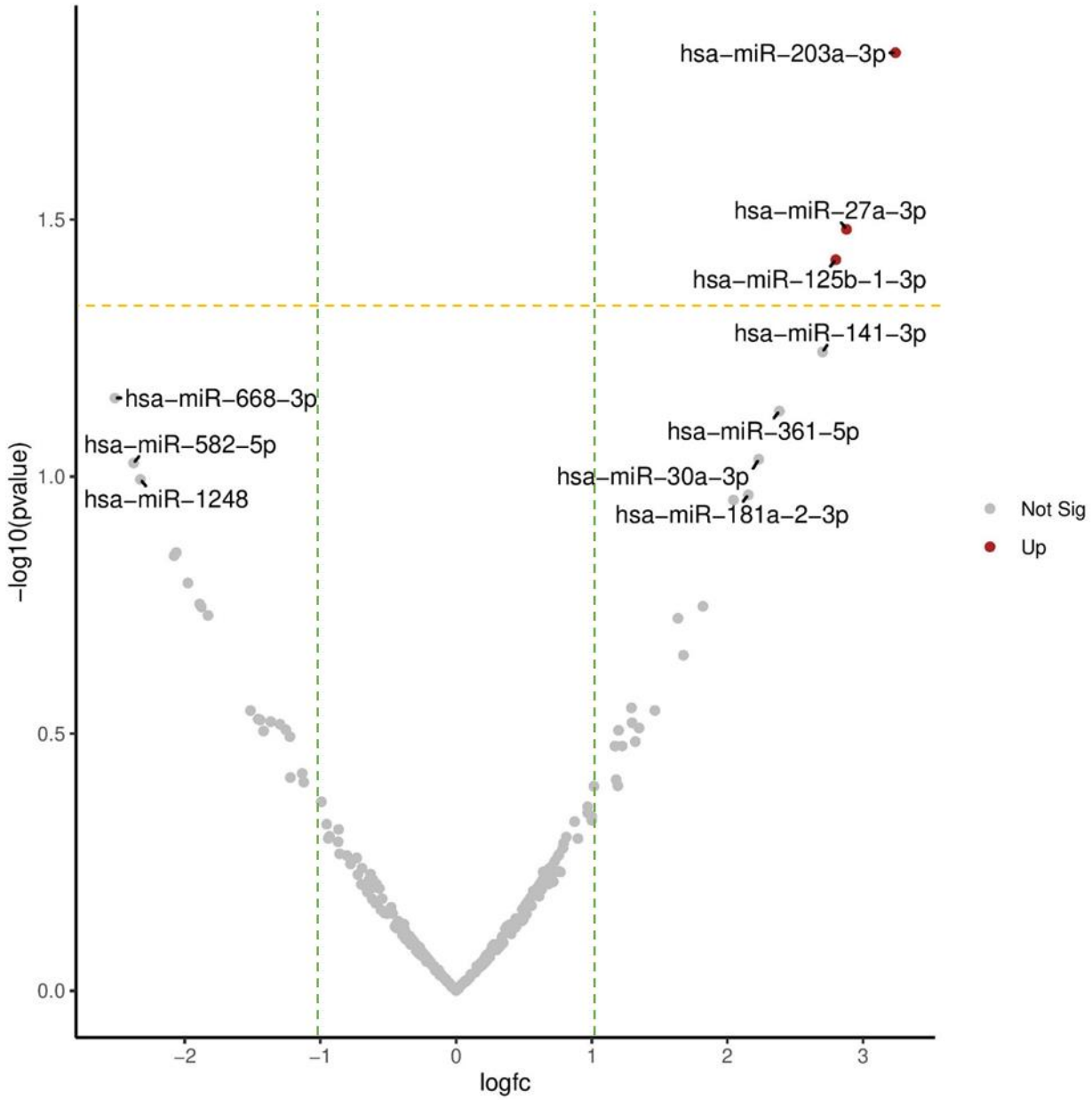

Figure 4.34. miR-27a is upregulated in AD brain derived sEVs in females

Cohorts were stratified to just compare females in each group (n=2 per group). Read counts of miRNAs for each group were compared using DESeq2 to identify differentially expressed genes, with logFC (log Fold change) plotted against -log (p value) on a volcano plot to visualise differences. The top 10 differentially expressed miRNA were annotated. Green broken line indicates logFC threshold = ±1. Upregulated miRNAs: miR-203a, miR-27a, miR-125b. Significance threshold (yellow broken line) = 1.3 (log10(p-value), p <0.05. Red = upregulated. Grey = no significant change.

4.6.3 Top differentially expressed miRNAs in Alzheimer's disease sEVs in females

The most differentially expressed miRNAs in the AD female groups for both fibroblast and brain derived sEVs are displayed in Table 4.7. As described above, the smaller group does not have the significant weight to distinguish significant differences in sEV miRNA expression, however there was a noticeable shift in the rankings of the top dysregulated miRNAs.

In the fibroblast derived sEVs, mir-145 has already been noted as the most dysregulated, though there are several candidates that also display a log2(FC) greater than 2, including miR-451a and miR-192. While no longer the most upregulated miRNA, miR-146a remains near the top of the most upregulated miRNAs in the AD female group.

In the brain derived sEVs, there are a group of miRNAs that are also trending towards up and downregulation in the AD female groups, including miR-141 (Log2(FC) = 2.702, p = 0.057) and miR-361 (Log2(FC) = 2.383, p = 0.075), as well as miR-582 (Log2(FC) =-2.378, p = 0.094).

Combined, there is a growing panel of miRNAs that have potential as biomarkers for AD, and with expanded testing, may show some differential expression based on populations including sex.

Once again, the top differentially expressed miRNAs in the AD female groups were compared between the fibroblast and brain derived sEV cohorts, in order to determine whether there were any correlations between dysregulated miRNAs (cut-off = Log2(1)).

Notably, there were more observed correlations, both positive and inverse, between the brain and fibroblast cohorts in the female AD groups, than in the total population (Figure 4.35). The group including miR-361 (Log2(FC): Brain = 2.383, Fibroblast = 2.307), miR-487b (Log2(FC): Brain = 1.180, Fibroblast = 1.245) and miR-335 (Log2(FC): Brain = 1.348, Fibroblast = 1.035) were upregulated in both fibroblast and brain derived sEVs in AD. Another miRNA previously highlighted in both qPCR and RNA sequencing is miR-146a, which was also upregulated in both AD female groups (Log2(FC): Brain = 1.171, Fibroblast = 2.404).

Table 4.7 miRNAs were upregulated in brain derived sEVs in AD females

The top differentially expressed miRNA (log2(fold change)), between females, as identified by DESeq2 and plotted on the volcano plot, with corresponding log2(fold change) and P values.

miRNA		Fibroblast sEV	
		log2 (FC)	P value
Up	hsa-miR-145-3p	3.267	0.078
	hsa-miR-451a	2.823	0.131
	hsa-miR-6529-5p	2.562	0.166
	hsa-miR-192-5p	2.502	0.181
	hsa-miR-146a-5p	2.404	0.182
	hsa-miR-381-3p	2.307	0.216
	hsa-miR-660-5p	2.231	0.231
	hsa-miR-122-5p	2.104	0.243
	hsa-miR-361-5p	1.991	0.284
	hsa-miR-126-3p	1.857	0.315
Down	hsa-miR-1180-3p	-0.826	0.649
	hsa-miR-30a-5p	-0.836	0.627
	hsa-let-7d-5p	-1.082	0.562
	hsa-let-7f-5p	-1.163	0.533
	hsa-miR-185-5p	-1.640	0.380

miRNA		BDEV	
		log2 (FC)	P value
Up	hsa-miR-203a-3p	3.239	0.015
	hsa-miR-27a-3p	2.878	0.033
	hsa-miR-125b-1-3p	2.799	0.038
	hsa-miR-141-3p	2.702	0.057
	hsa-miR-361-5p	2.383	0.075
	hsa-miR-30a-3p	2.231	0.093
	hsa-miR-181a-2-3p	2.154	0.109
	hsa-let-7d-3p	2.045	0.111
	hsa-miR-382-3p	1.820	0.179
	hsa-miR-185-5p	1.676	0.223
Down	hsa-miR-15a-5p	-1.830	0.186
	hsa-miR-3065-5p	-1.878	0.179
	hsa-miR-328-3p	-1.891	0.177
	hsa-miR-144-3p	-1.978	0.161
	hsa-miR-454-3p	-1.978	0.161
	hsa-miR-338-5p	-2.063	0.141
	hsa-miR-654-5p	-2.080	0.143
	hsa-miR-1248	-2.327	0.101
	hsa-miR-582-5p	-2.378	0.094
	hsa-miR-668-3p	-2.515	0.070

P value threshold < 0.05. Red = upregulated, green = downregulated. BDEV: Brain derived small extracellular vesicle

There was a select population of miRNAs that were inversely dysregulated in the AD female group, between brain and fibroblast derived sEVs (Figure 4.35). This included miR-660 (Log2(FC): Brain = -1.515, Fibroblast = 2.231), miR-15a (Log2(FC): Brain = -1.830, Fibroblast = 1.441) and miR-99a (Log2(FC): Brain = -1.1348, Fibroblast = 1.603), which were upregulated in fibroblasts but downregulated in the brain. Conversely, miR-185 (Log2(FC): Brain = 1.676, Fibroblast = -1.640) was upregulated in the brain but downregulated in fibroblast sEVs.

As before there are limitations on drawing these comparisons without further investigation, but given the specific correlation in female groups, they display potential for biomarkers in stratified cohorts. Further, miR-361 was one of the most dysregulated miRNAs in both groups and was trending towards significance in the brain derived sEVs.

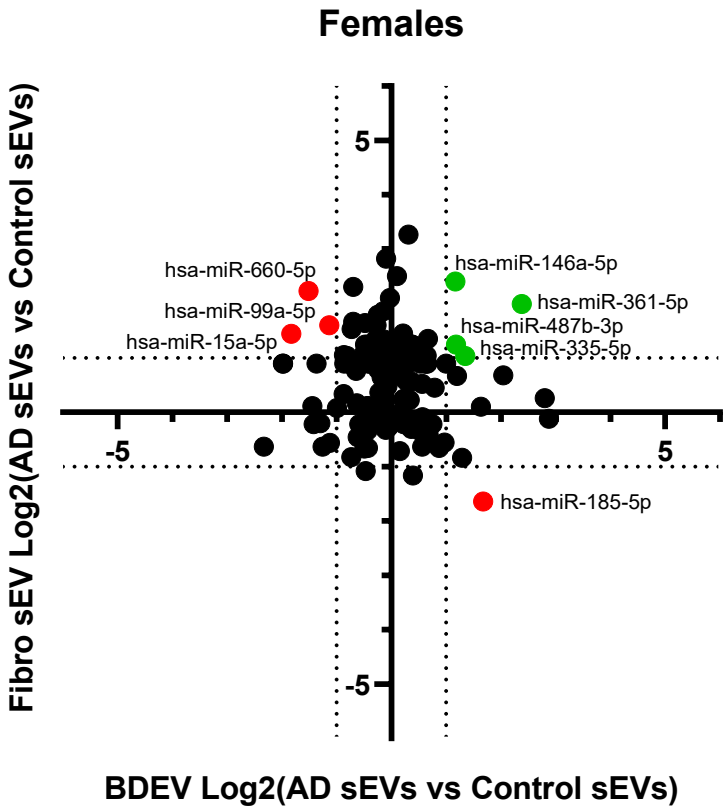

Figure 4.35. Different miRNA groups are positively and negatively correlated between fibroblast and brain derived sEVs, in AD females

Dotted lines indicate a threshold of log2(FC) = ±1, where highlighted miRNA expressed a positive or negative fold change >2 in AD, in both fibroblast and brain derived sEVs. Green = miRNA fold change was positively correlated, red = miRNA fold change was negatively correlated. Black = miRNA did not pass one or more of the thresholds or did not have enough read counts (<5) to be analysed. BDEVs: Brain derived small extracellular vesicles. AD = Alzheimer's disease.

4.6.4 Correlation of miRNA fold changes in AD sEVs between sexes

In both the fibroblast and brain derived sEV cohorts, the male and female groups were separated and analysed separately (i.e. Fibroblast cohort: AD male vs Control male, AD females vs control females). The fold changes in miRNAs observed in the sex stratified groups were then compared against each other, in order to observe whether there were any sex specific miRNA changes in AD.

The purpose of this comparison is to display the relative contribution of both sexes on the differential expression profiles of sEV miRNA derived from both fibroblasts and brain tissue, respectively. Given that there is only an n = 1 for the male groups in both the fibroblast and brain derived sEV cohorts, these observations are based on log2(FC) > 1. It is shown that there are a group of miRNAs that are inversely changed in AD fibroblast derived sEVs, between the sexes (Figure 4.36). The group consisting of miR-660 (Log2(FC): Male = -1.874, Female = 2.231), miR-21 (Log2(FC): Male = -1.585, Female = 1.441) and miR-192 (Log2(FC): Male = -1.1348, Female = 1.603), are upregulated in the female AD group but downregulated in the male AD group.

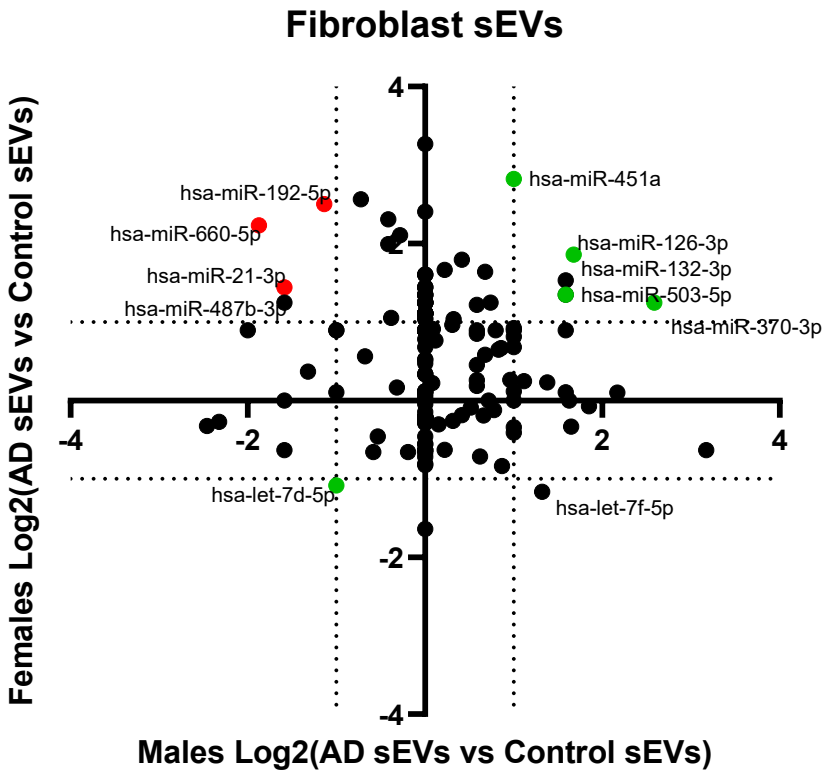

Figure 4.36. Sex displays different contributions to miRNA changes in sEVs in AD fibroblasts

Dotted lines indicate a threshold of log2(FC) = ±1, where highlighted miRNA from fibroblast derived sEVs expressed a positive or negative fold change >2 in AD, in both males and females. Green = miRNA fold change was positively correlated, red = miRNA fold change was negatively correlated. Black = miRNA did not pass one or more of the thresholds or did not have enough read counts (<5) to be analysed. BDEVs: Brain derived small extracellular vesicles. AD = Alzheimer's disease.

In the brain derived sEVs (Figure 4.37), miR-99a (Log2(FC): Male = 1.285, Female = -1.135) and miR-1307 (Log2(FC): Male = 1.170, Female = -1.221), are downregulated in the female AD group but upregulated in the male AD group. Conversely, miR-148b (Log2(FC): Male = -1.087, Female = 1.000) is upregulated in the female AD group but downregulated in the male AD group.

Notably, miR-660 (Log2(FC): Male = 1.273, Female = -1.516) was downregulated in the female AD group but upregulated in the male AD group, a relationship which was reversed in the fibroblast derived sEVs (Figure 4.36). Chromosome 14 cluster miR-382 is upregulated in both male and female AD groups (Log2(FC): Male = 2.002, Female = 1.820), an

observation which is consistent with its trend towards upregulation in the total population in AD.

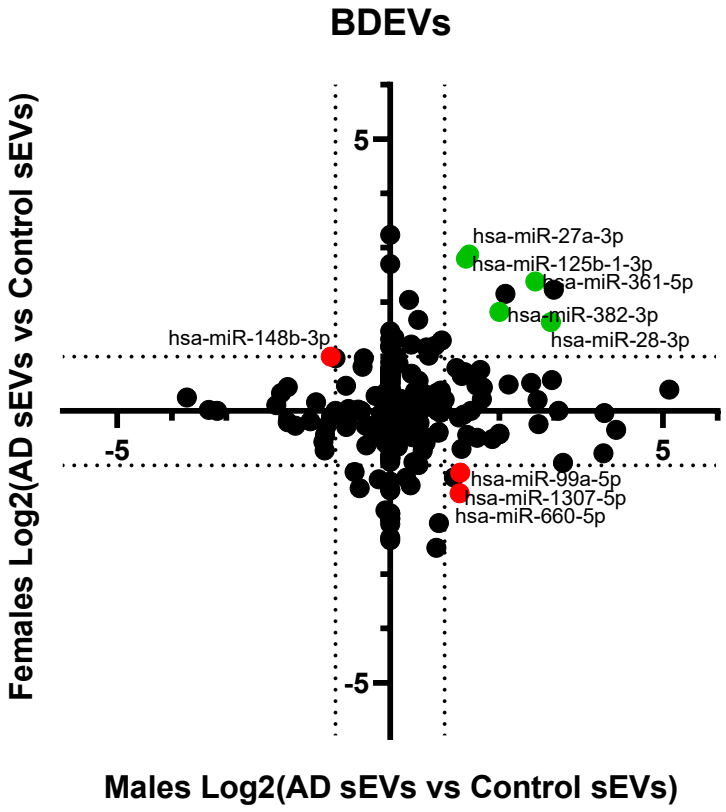

Figure 4.37. Sex displays different contributions to miRNA changes in sEVs in AD brain tissue

Dotted lines indicate a threshold of log2(FC) = ±1, where highlighted miRNA from brain derived sEVs expressed a positive or negative fold change >2 in AD, in both males and females. Green = miRNA fold change was positively correlated, red = miRNA fold change was negatively correlated. Black = miRNA did not pass one or more of the thresholds or did not have enough read counts (<5) to be analysed. BDEVs: Brain derived small extracellular vesicles. AD = Alzheimer's disease.

4.7 Pathway analysis of differentially expressed miRNAs in Alzheimer's disease

In order to determine the functional relevance of the miRNAs that have been identified in both qPCR and RNA sequencing analysis, differentially expressed miRNAs ($log2(FC) > 1$, $p < 0.05$) were ran through biological pathway resources, including GO, Reactome and KEGG (Kyoto Encyclopaedia of Genes and Genomes), using miRPathDB (V2.0). Trending miRNAs ($log2(FC) > 1$), including those to distinguish between AD sex differences were ran individually through GO. All biological pathways are based on experimental evidence, with statistically significant associations shown.

4.7.1 Fibroblast derived small extracellular vesicles

Given the small group of differentially expressed miRNA in fibroblast derived sEVs in AD, the grouping of miRNAs for pathway analysis was limited, with different pathway analysis tools only having specific information for individual miRNAs. Though some interesting observations were still made. In the full fibroblast sEV cohort, miR-146a-5p was the most differentially expressed, which has several neuroinflammatory associations that are relevant in AD, including interleukin signalling pathways (Chapter 4.3.6 - GO analysis - Figure 4.11 and Figure 4.12). This is part of a wider range of peripheral immunomodulatory functions, as well as regulation of protein phosphorylation and growth factor responses.

Other miRNAs which trended towards upregulation in AD fibroblast sEVs, particularly when looking at the female groups, included miR-451a, which is also associated in interleukin signalling responses, as well as MAPK signalling and WNT and NOTCH signalling, important for cellular differentiation and wound healing, but also implicated in neurogenesis in the brain (Figure 4.38).

As previously stated, miR-146a and miR-92a observed to be upregulated in fibroblast sEVs in AD, by both qPCR and RNA sequencing. These two miRNAs make particularly interesting candidates for further biomarker investigations. Figure 4.11 has already made observations about the association of miR-146a and immune signalling, however, there are several other pathways that both miRNAs have been investigated against. These include regulating

multiple cellular metabolic processes, as well as responding to cellular stress, apoptotic signalling pathways and regulation of cell cycle signalling (Figure 4.39).

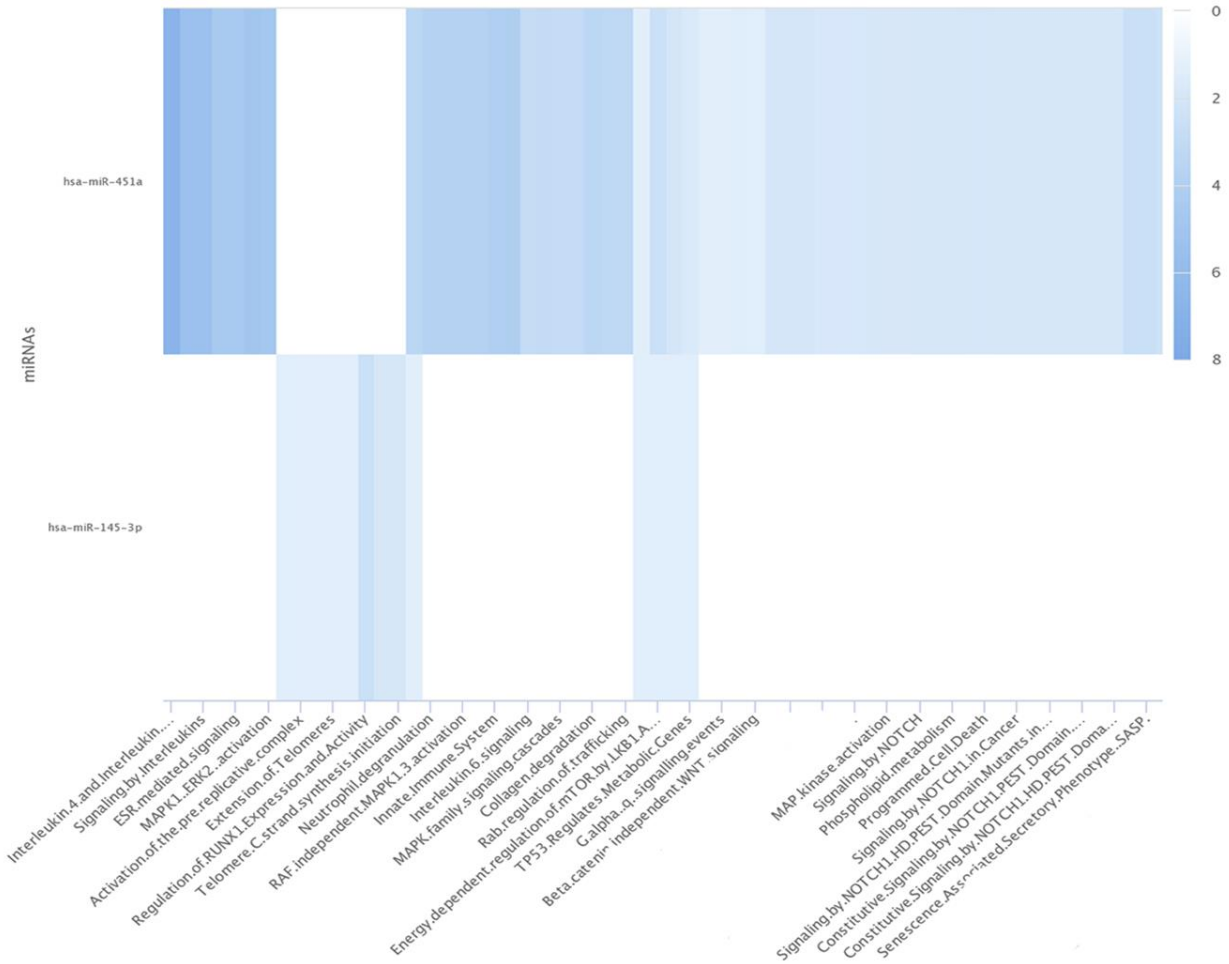

Figure 4.38. Reactome pathways implicated by miR-451a include interleukin, WNT and NOTCH signalling

Reactome analysis was performed using miRPathDB for miR-451a and miR-145. Pathways that are significant for miRNAs are displayed. Scale represents experimental significance. Darker = greater significance.

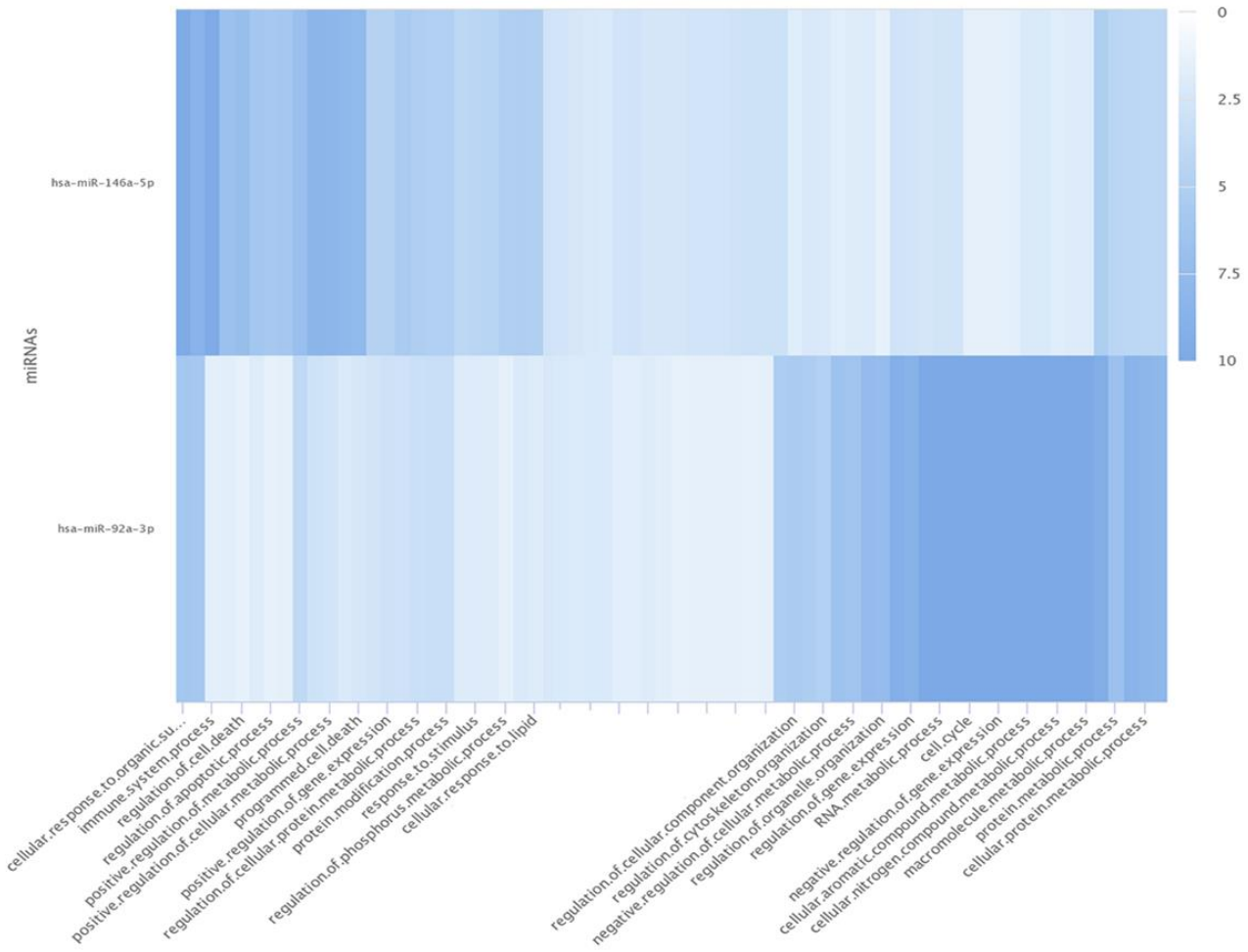

Figure 4.39. Gene ontology of upregulated miR-146a and miR-92a in fibroblast sEVs in AD

Gene ontology analysis was performed using miRPathDB for miR-146a, and miR-92a. Pathways that are significant for miRNAs are displayed. Scale represents experimental significance. Darker = greater significance.

4.7.2 Brain derived small extracellular vesicles

In brain derived sEVs, there was a cohort of upregulated miRNAs in AD. When the biological processes of these miRNA were investigated using GO (Figure 4.40) and Reactome (Figure 4.41), they were observed to be associated with several cell death pathways, including apoptosis pathways and responses to cellular stress. Notably, there was a common association with responses to oxidative stress in cells, a significant molecular change in AD. Other pathways included regulation of metabolism and cytokine signalling.

Figure 4.40. Gene ontology of upregulated miRNAs in brain derived sEVs in AD

Gene ontology analysis was performed using miRPathDB for miR-30a, miR-125b, miR-141, miR-361 and miR-203a. Pathways that are significant for miRNAs are displayed. Scale represents experimental significance. Darker = greater significance.

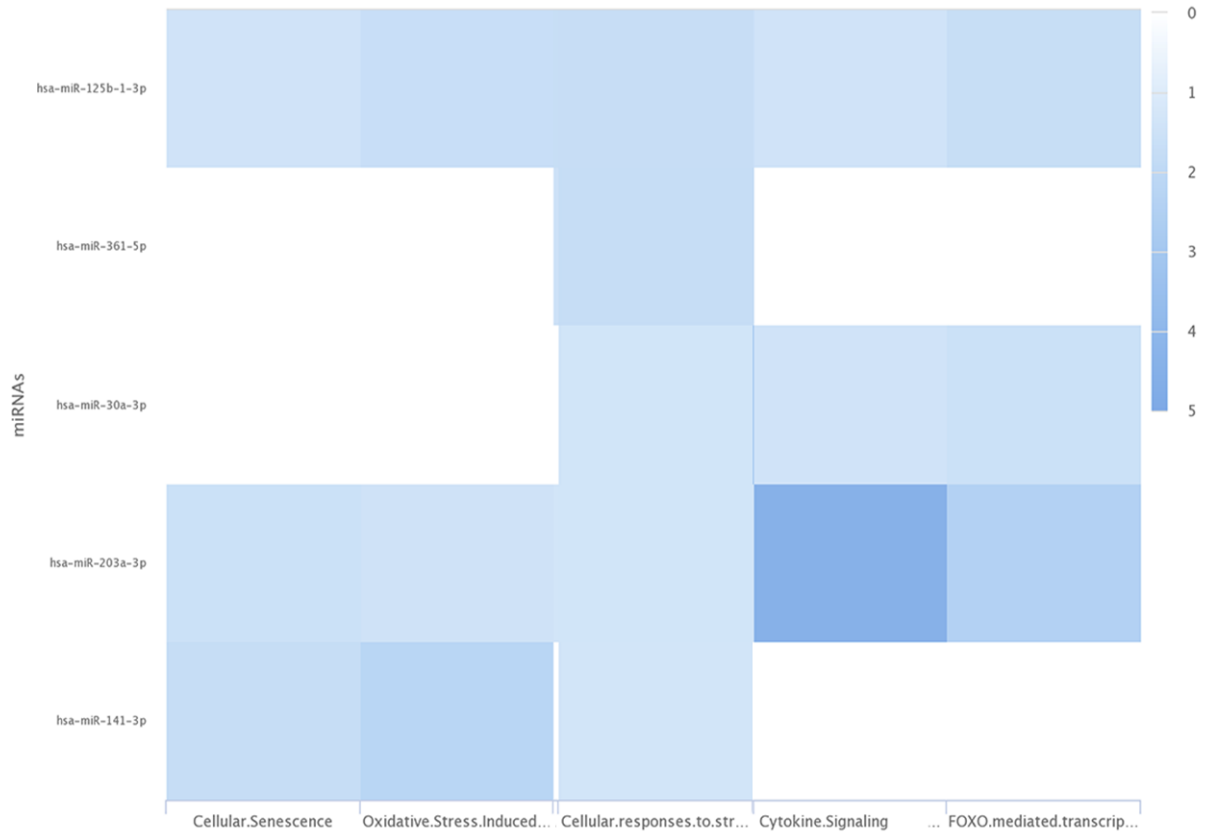

Figure 4.41. Reactome pathways implicated by multiple upregulated miRNAs in BDEVs include oxidative stress responses

Reactome analysis was performed using miRPathDB for miR-125a, miR-361, miR-30a, miR-203a and miR-141. Pathways that are significant for miRNAs are displayed. Scale represents experimental significance. Darker = greater significance.

When the brain derived sEV cohort was stratified for the female groups, miR-27a was observed as upregulated, unlike in the total population, alongside miR-203a. GO pathway analysis found that both miRNAs were associated with neurogenesis and brain development (Figure 4.42). They were also implicated in responses to cellular stress and oxidative stress, as well as regulation of protein phosphorylation.

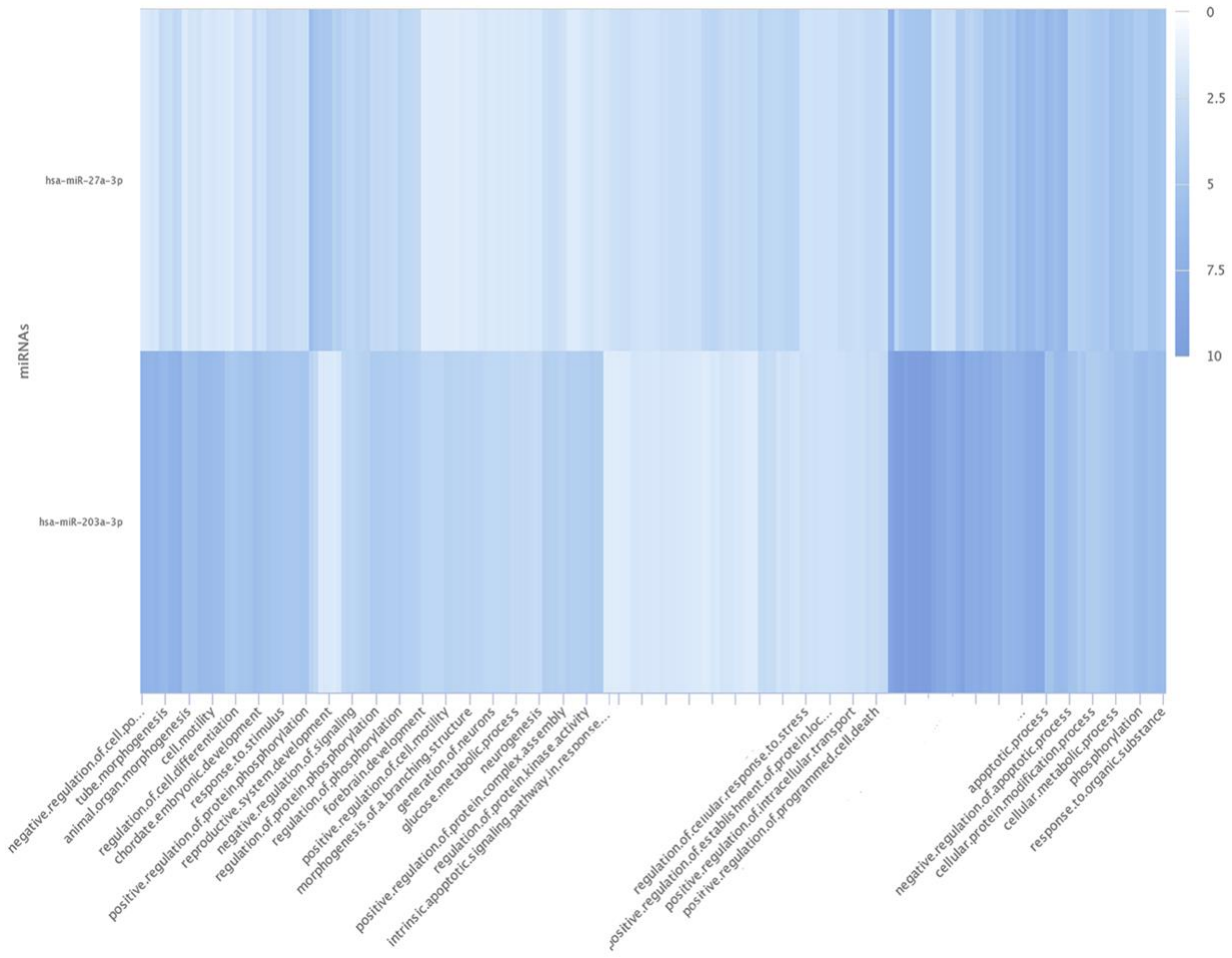

Figure 4.42. Female specific miRNA upregulation in brain derived sEVs identified neurogenesis and protein phosphorylation pathways

Gene ontology analysis was performed using miRPathDB for miR-27a and miR-203a. Pathways that are significant for miRNAs are displayed. Scale represents experimental significance. Darker = greater significance.

4.7.3 Differentially regulated miRNA between brain and fibroblast derived sEVs

When directly comparing the fibroblast and brain derived sEV cohorts, in order to observe whether any miRNAs showed dysregulation in AD both groups, it was noted that miR-132 and miR-185 showed inverse dysregulation in AD, between fibroblast and brain. When looking at these miRNAs, we see both neuronal and peripheral biological pathways that have been experimentally associated (Figure 4.43). Peripherally, both are associated with

cellular migration and differentiation, as well as vascular development. Pathways associated with the brain and AD include responses to reactive oxygen species, hypoxia, WNT signalling and neurogenesis, and protein phosphorylation mechanisms.

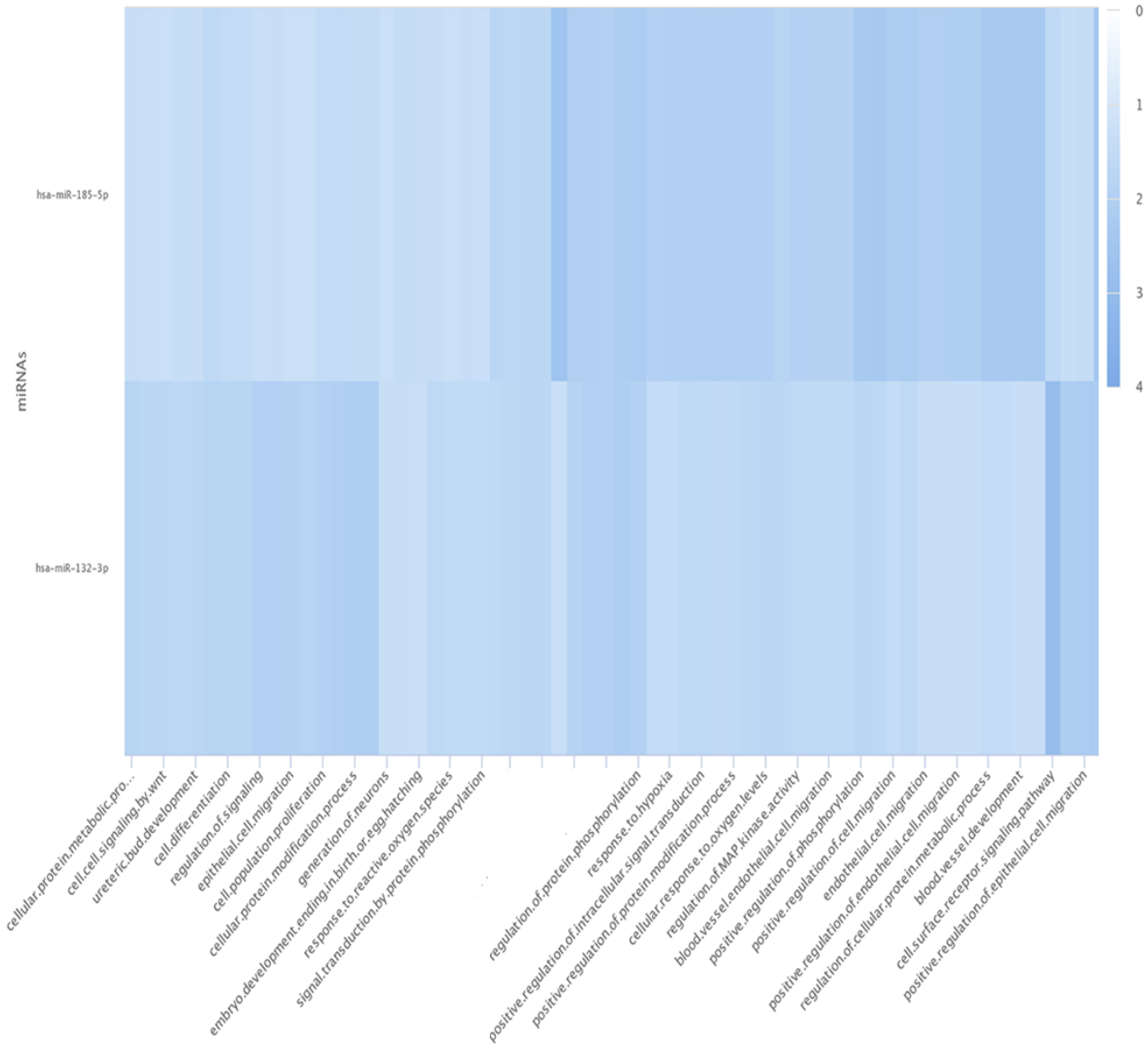

Figure 4.43. Gene ontology of inversely regulated miR-185 and miR-132 between brain and fibroblast derived sEVs

Gene ontology analysis was performed using miRPathDB for miR-185 and miR-132. Pathways that are significant for miRNAs are displayed. Scale represents experimental significance. Darker = greater significance.

Interestingly, when the population was stratified by sex, there were more miRNAs that were dysregulated in both the brain and fibroblast derived sEVs. When these miRNAs were

plotted into GO analysis, it was observed that they were associated with several metabolic processes, including regulating metabolism on cellular, protein and nuclear levels (Figure 4.44). They were also associated with cell cycle regulation, apoptosis, and responses to cellular stress, as well as regulation of phosphorylation and signalling pathways associated with ageing.

When just the miRNAs that were upregulated in the fibroblast derived sEVs and downregulated in brain derived sEVs were plotted into GO analysis, the same pathways as above were observed. However, the most significant pathways shifted towards regulation of cell cycle and included WNT signalling and cellular development pathways (Figure 4.45).

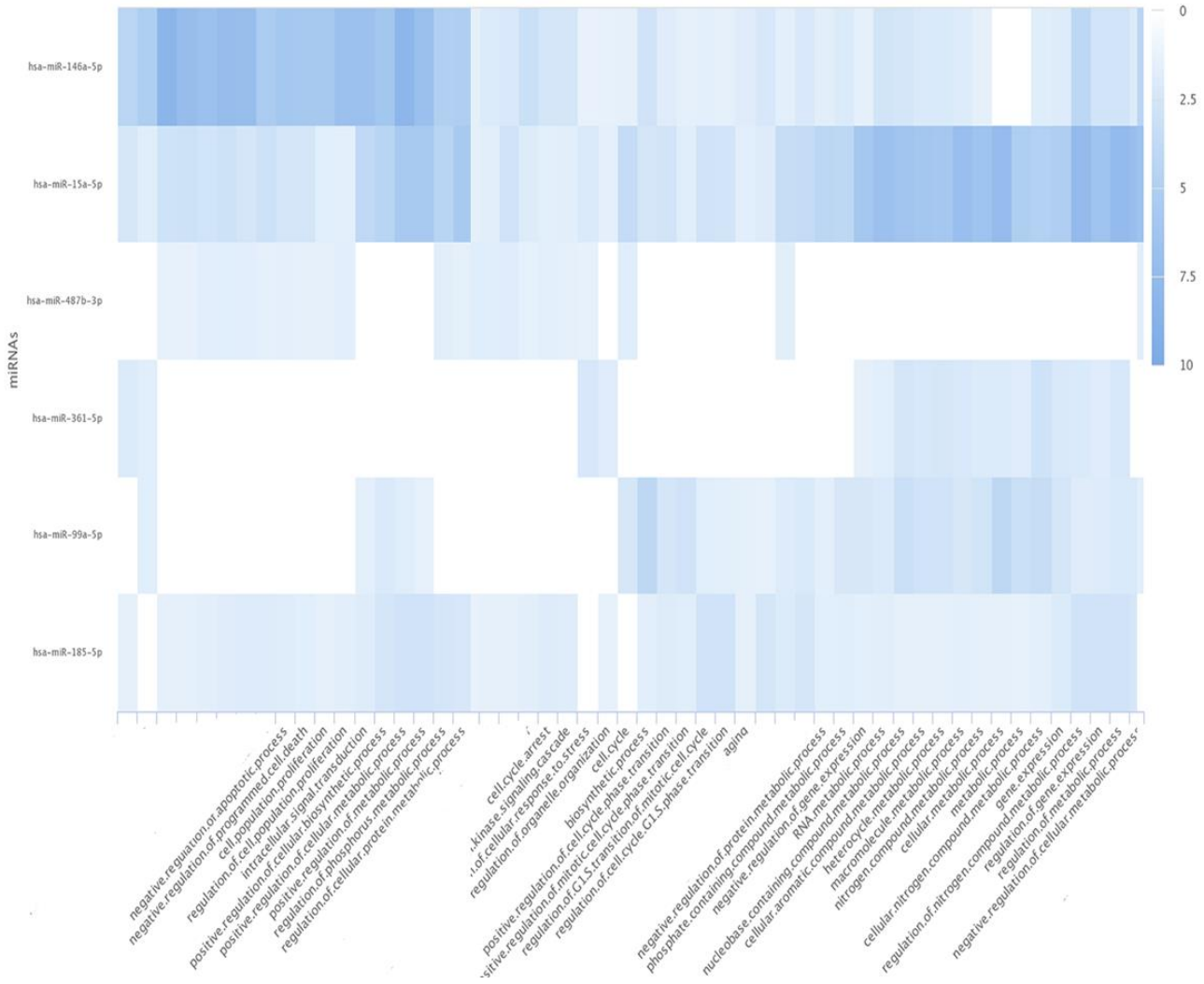

Figure 4.44. Gene ontology of consistently dysregulated miRNAs between brain and fibroblast derived sEVs in AD females

Gene ontology analysis was performed using miRPathDB for miR-146a, miR-15a, miR-487b, miR-361, miR-99a and miR-185. Pathways that are significant for miRNAs are displayed. Scale represents experimental significance. Darker = greater significance.

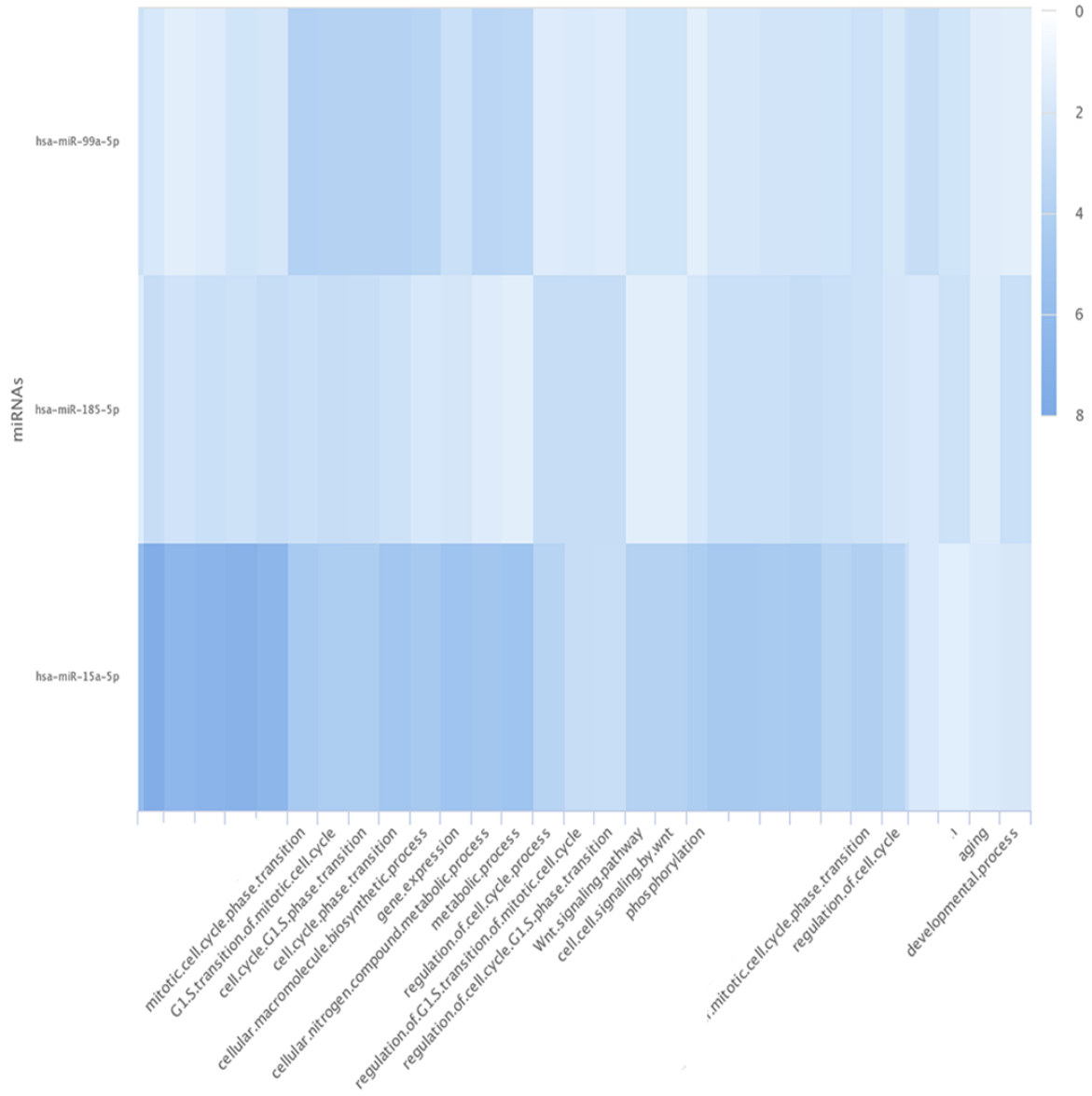

Figure 4.45. Gene ontology of inversely regulated miRNAs between fibroblast and brain derived sEVs in AD females

Gene ontology analysis was performed using miRPathDB for miR-99a, miR-185 and miR-15a. Pathways that are significant for miRNAs are displayed. Scale represents experimental significance. Darker = greater significance.

4.7.4 Sex dependent differentially regulated miRNA in Alzheimer's disease

In both the fibroblast and brain derived sEV cohorts, the male and female groups were separated and analysed separately (i.e. Fibroblast cohort: AD male vs Control male, AD

females vs control females). The fold changes in miRNAs observed in the sex stratified groups were then compared against each other, in order to observe whether there were any sex specific miRNA changes in AD.

In the fibroblast derived sEVs, miR-192, miR-21 and miR-660 were upregulated (log2(FC) > 1) in the female AD group but downregulated (log2(FC) > -1) in the male AD group. When these miRNAs were analysed in GO, the contributions primarily came from miR-192, however, miR-660 was associated with cellular differentiation, being experimentally observed in noradrenergic neuronal and smooth muscle cell differentiation (Figure 4.46). miR-192 was most significantly associated with cell cycle regulation, showing several hits across the GO analysis.

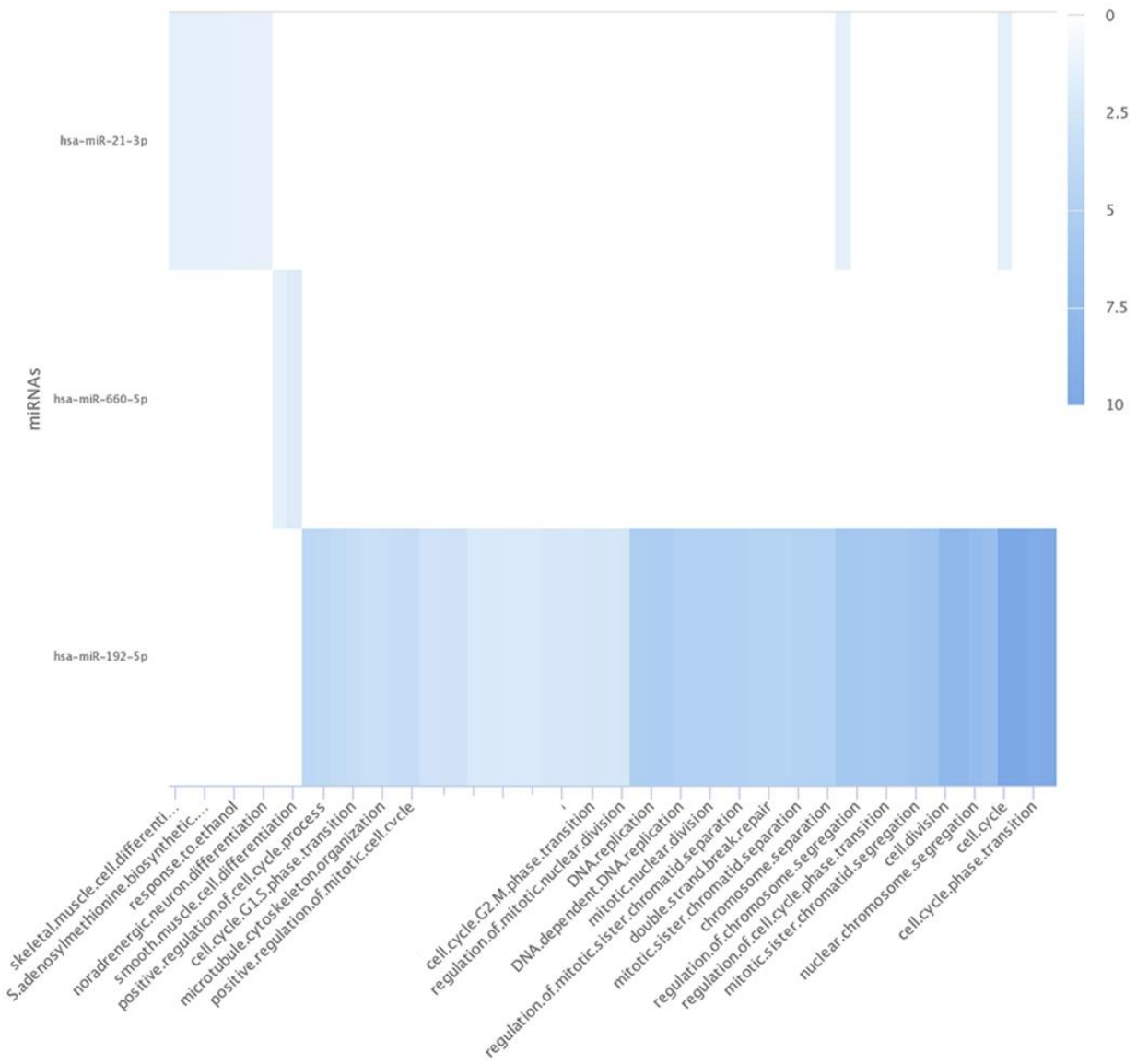

Figure 4.46. Gene ontology of inversely regulated miRNAs in fibroblast derived sEVs between males and females

Gene ontology analysis was performed using miRPathDB for miR-21, miR-660 and miR-192. Pathways that are significant for miRNAs are displayed. Scale represents experimental significance. Darker = greater significance.

In the brain derived sEVs (Figure 4.47), miR-99a, miR-1307 and miR-660 were upregulated (log2(FC) > 1) in the male AD group but downregulated (log2(FC) > -1) in the female AD group. miR-148b was downregulated (log2(FC) > -1) in the male AD group but upregulated (log2(FC) > 1) in the female AD group. GO analysis for these miRNAs found that miR-99a was associated with Schwann cell differentiation and development, as well as implications

in cellular ageing and oxidative pathways. miR-148b was associated with neurogenesis and lysosomal pathways.

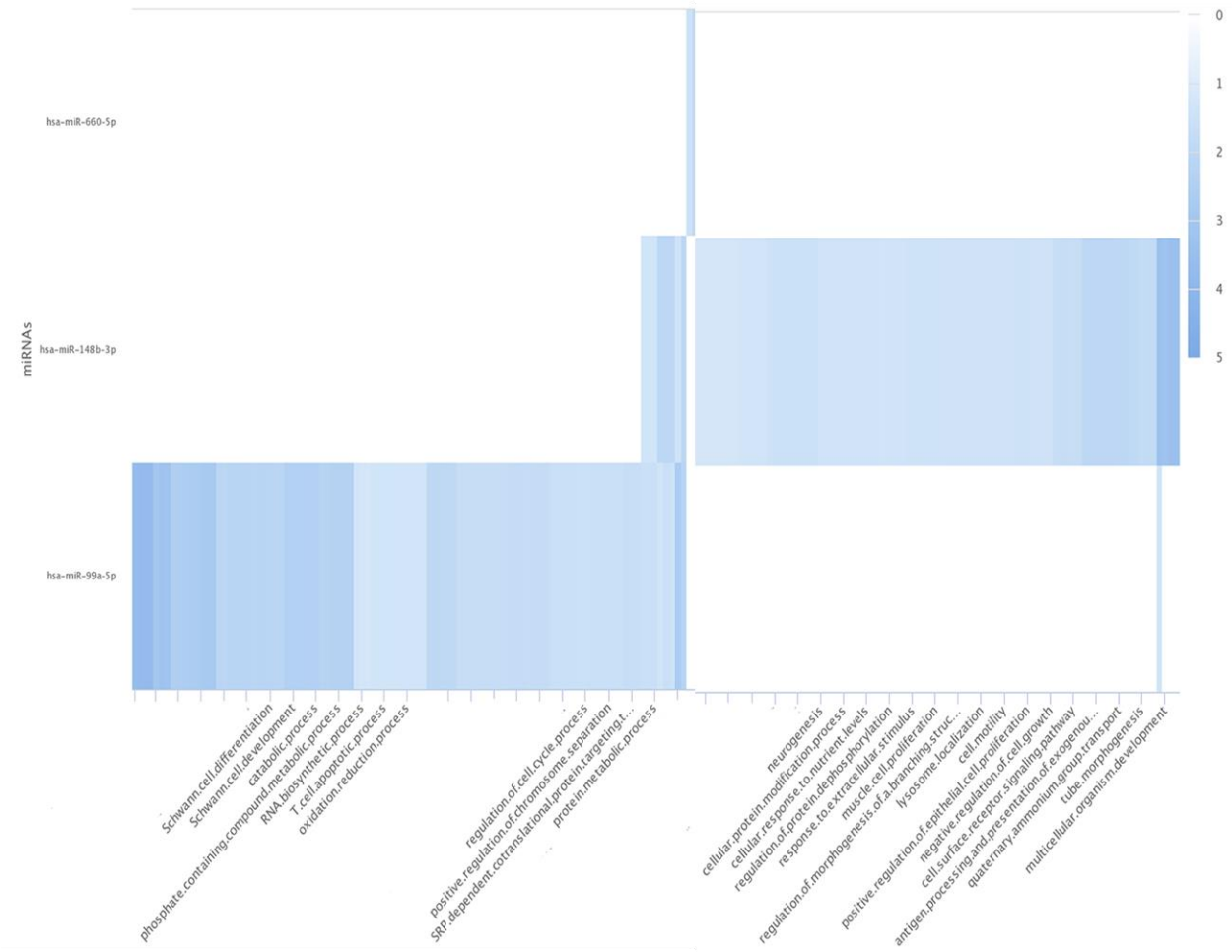

Figure 4.47. Gene ontology of inversely regulated miRNAs in brain derived sEVs between males and females

Gene ontology analysis was performed using miRPathDB for miR-660, miR-148b and miR-99a. Pathways that are significant for miRNAs are displayed. Scale represents experimental significance. Darker = greater significance.

4.8 Discussion

In this chapter, the study interrogated miRNA cargo of sEVs from fibroblast cell culture and human brain tissue, in order to determine whether there were changes in AD conditions. The study observed that RNA concentrations of sEVs was unchanged after a proteinase K and RNase A digestion, which suggested that RNA isolated as part of the sEV isolation was internalised within sEVs. This added confidence to the specificity of the downstream

measurements which intended to analyse EV associated miRNA, though to ensure there was no variation during different sEV isolation, the study continued to use the proteinase K/ RNase A digestion prior to all RNA isolations.

The study analysed two cohorts of miRNAs that were considered interesting candidates for differential analysis in AD conditions. Firstly, the chromosome 14 cluster (C14), which has previously been implicated as enriched within the brain, having multiple functions in neurogenesis and regulation of neurotrophic factors (Cavaillé et al, 2002; Glazov et al, 2008; Winter, 2014). Further, C14 has previously been implicated in brain disorders, including glioblastoma and medulloblastoma (Nayak et al, 2018; Kumar et al, 2018), as well as schizophrenia (Hollins et al, 2014). It has not previously been implicated in Alzheimer's disease, however several miRNAs from the cluster are dysregulated in biofluids across different neurodegenerative diseases (Brennan et al, 2019), which combined with its association with neuronal signalling pathways, warrants investigation. The second cohort of miRNAs had previously been observed to be dysregulated in AD or had been shown to regulate important AD signalling pathways. The miR-17 family (miR-17, miR-18a, miR-19a, miR-20a, miR-19b-1, miR-92a, miR-106a and miR-106b), for example, have been shown to target AD protein APP (Patel et al, 2008; Hébert et al, 2009) and is dysregulated in response to Aβ insult (Schonrock et al, 2010). Other candidate miRNAs, such as miR-155 and miR-146 have been linked to AD through inflammatory responses to the cellular stress underlying AD progression (Delay et al, 2012; Guedes et al, 2014; Song and Lee, 2015). Combined, the candidates are associated with AD via divergent signalling pathways and so provide a wide window of observation into potentially differentially expressed miRNAs in sEVs that could be measurable peripherally.

Small RNA sequencing of sEV miRNAs provides a higher throughput comparison of AD associated effects than qPCR, therefore interesting miRNAs could potentially be discovered that were not considered in the initial cohort of candidates to be tested. This study founds a cluster of upregulated miRNA in the BDEVs, miR-203a, miR-361, miR-141, miR-125b-1, and miR-30a, while miR-582 and miR-1248 were significantly downregulated. In the fibroblast derived sEVs, small RNA sequencing identified miR-146, miR-145, miR-106b and miR-132 as some of the most upregulated miRNAs in AD. Through the small RNA

sequencing data, this study was able to investigate miRNAs that showed potential to be able to distinguish changes in AD between sexes, including miR-23a, miR-668 and miR-660.

In conclusion, in this chapter the study found multiple cohorts of interesting miRNA expression patterns, which will individually be discussed in the next chapter, but combined they provide a promising panel for further investigation of EV derived biomarkers for AD, both from candidate AD associated miRNA, as well as novel miRNA that so far have limited investigations in AD.

5 Chapter 5: General discussion

5.1 Project summary

The aims of this project were to investigate the feasibility of isolating sEVs from cell culture medium and the extracellular space of human brain tissue. The work required a robust characterisation of isolated particles, by visualisation and protein specific methodology, to confirm that any isolations were indeed small EVs. The second set of aims was to measure the miRNA cargo of sEVs, in order to determine whether there were changes in this cargo in AD conditions, both in a peripheral model (fibroblast cell culture) and human frontal cortex tissue. The objectives of this aim were to measure miRNA expression in a targeted qPCR approach and analyse the global miRNA expression profile of isolated sEVs. The aims of this project were set out with the goal of investigating whether miRNA cargo of sEVs derived from AD specific models could be used as a biomarker for the detection of AD.

5.2 Isolation and characterisation of EVs

This project isolated sEVs from two cohorts, a fibroblast cell culture model from AD patients and neurological healthy controls, and a human brain tissue cohort, donated post-mortem by AD patients and neurologically healthy controls. Given the novelty of isolating sEVs from these sources, a robust characterisation was performed to ensure that the isolated samples were just sEVs and no other secreted factors such as RNPs (Shelke et al, 2014) were present.

There is consensus about the requirements for characterising EVs from a wide range on biological sources, published as the minimal information for studies of extracellular vesicles (MISEV guidelines; Théry et al, 2018), which is the current international standard for EV studies. This includes the need for visual confirmation of EVs, to determine that they are in the size range of the EV population of interest as well as observing the typical bilayer enclosed morphology of an EV. The current gold standard for visualisation is TEM, which has the resolution to visualise particles in detail on the nanometre scale and is consequently able to determine whether particles present with EV associated lipid bilayer

membranes (van der Pol, 2014; Höög and Lötvall, 2015). This study imaged sEVs isolated from both fibroblast cultures and brain tissue with TEM. It was observed that there were particles in the size range of sEVs (<150 nm), which also had the EV associated lipid bilayer membranes.

NTA is another recommended technique for visualising the size more representative of the entire population of particles isolated, compared to the single particle visualisation of TEM. Its capabilities have expanded with current models now able to target subpopulations of particles by fluorescently conjugated antibody tagging, that can target the surface proteins of EVs. This process allows for more in depth analysis of the relative contribution of different EV populations to the total particle numbers isolated in a sample, as well as being able to distinguish the size profiles of tagged particles from the entire sample (Arab et al, 2021). Within this study, sEVs were tagged for the transmembrane tetraspanins CD9, CD63 and CD81, as well as staining the entire groups of lipid-bilayer membrane bound particles for CMO membrane stain. This allows for the differentiation of biologically sourced particles from the entire milieu of secreted factors, which may include salts and factors that are co-isolated during processing of samples. One step beyond this, the specific tetraspanin tagging of particles allows for distinguishing the sEV associated particles from co-isolated biomolecules that could include similarly sized lipoproteins (Stranska et al, 2018). As the tetraspanin associated pathways are well characterised in the release of EVs from MVBs (Andreu and Yáñez-Mó, 2014), the high abundance of these particles that are observed in the SEC based isolations from both fibroblast and brain tissue derived samples suggest that the sEV populations will have a degree of exosomal contribution. However, distinguishing subpopulations of EVs based on their biogenesis cannot be concluded without direct visualisation of their release in the cell of origin through fluorescence imaging (Théry et al, 2018), and so the better terminology for characterising EVs in this study is based on size, hence the use of small (s)EVs, which are defined as 50-200 nm. Given that most of the CMO stained particles and particularly the tetraspanin tagged particles are observed in this size range, the study concludes that the isolated particles are sEVs derived from brain tissue and fibroblast cultures.

Confirmation that the EV associated protein “barcodes” are present in isolated samples is also necessary. MISEV provides recommendations on the protein signatures of EVs,

including the tetraspanins CD9, CD63, and CD81, which contribute to EV biogenesis and secretion from multivesicular bodies, and are highly abundant, particularly in small EVs as discussed (Andreu and Yáñez-Mó, 2014). Given that there are multiple EV secretion pathways, also the tetraspanin independent ESCRT (endosomal sorting complex required for transport; Columbo et al, 2013, Karimi et al, 2018), it is preferential to analysis EV samples from multiple sorting pathways. TSG-101 was used in this study aside the tetraspanins as it is part of the ESCRT machinery, and flotillin 1 is a well characterised membrane protein that promotes vesicle release and is abundant in EV preparations (Glebov et al, 2006; Frick et al, 2007; Karimi et al, 2018). Importantly, the EV field is relatively new and therefore continues to adjust criteria of EV characterisation as new data emerges, as with the debate about whether markers are truly indicative of EVs or potentially they are present in a larger population of secreted particles (Liao et al, 2019). Therefore, this study selected these pathway independent and well characterised proteins for EV analysis.

5.3 Human brain tissue, patient derived fibroblasts and SH-SY5Y neuronal models – Investigating AD

One of the major challenges in AD research, which is true of many neurodegenerative diseases, is the lack of consensus of the best models to use to best represent the changes that occur in the disease, whether that is human brain tissue (Clement et al, 2016), animal models (Drummond and Wisniewski, 2017), or cellular models (Arber, Lovejoy and Wray, 2017). There is no one complete model currently and since there is large heterogeneity in onset of AD, there is not likely to be in the future. A more realistic approach is to base the model on the goal of the research. For this study, it is the investigation of EV miRNA biomarkers for AD, therefore there are specific reasons for using both cohorts in the study. As discussed, research into EVs and by extension EV miRNAs in AD is a growing field, so the understanding of what is expected to be released from the brain is limited. Therefore, it is important to expand the knowledge of EV miRNA that are associated with the onset of AD in the brain by looking at human brain tissue, through this there will hopefully be a larger

database of AD miRNAs that are secreted in the brain that research can refer to in the future.

Conversely, given the difficultly of directly visualising the changes that occur in the brain during progression of the disease, emphasis should also be directed towards the use of less invasive biological samples that may also display changes as a result of AD. A promising avenue is the analysis of biofluids such as blood and CSF (Riancho et al, 2019; Milà-Alomà et al, 2022; Teunissen et al, 2022), which is truly relevant for EV associated biomarkers since EVs can cross the blood-brain barrier (Chen et al, 2016; Morad et al, 2019). The question remains for biofluids that since they involve complex mixtures of molecules that can be derived from vast number of tissues and cells, what is the relative contribution from an individual cell type to this molecular profile.

There is evidence that fibroblasts mirror some of the physiological changes that can occur in the brain in diseases such as AD, for example, with altered mitochondrial function (Wang et al, 2008). AD, despite being a disease of the brain, causes systemic changes across the body, which has been observed in various peripheral tissues. Examples include dysregulated expression of $A\beta_{1-42}$, one of the hallmark neuropathological proteins, in skeletal muscle of AD patients (Kuo et al, 2000) as well as in primary skin fibroblasts of FAD patients with a Swedish FAD mutation, where the change can be observed prior to the onset of neuronal symptoms (Citron et al, 1994). Changes within the brain can also influence the peripheral tissues, as while AD is predominantly associated with areas of the brain specific to memory, the disease progression also causes dysregulation to areas that have not been as well investigated. The hypothalamus exerts control of metabolic function in the periphery and is one such region that is impaired by AD, including through AD associated oxidative stress (Gomes et al, 2014). The dysregulation to this region is observed to contribute to the increases in glucose intolerance observed in AD patients (Clarke et al, 2015). AD research has moved towards induced pluripotent stem cell (IPSC) models, which have incredible potential to elucidate the molecular mechanisms of the disease (Arber et al, 2017). However, IPSCs are transformed from cells, such as fibroblasts, which have either a relevant genetic mutation or have been extensively characterised with disease associated changes, such as Ca2+ channel deficits (Ito et al, 1994). Furthermore, AD fibroblasts display an oxidative stress phenotype, with increased protein phosphorylation, apoptosis, and

DNA damage (Ramamoorthy et al, 2012). Other AD phenotypic changes that occur in fibroblasts derived from AD patients include lysosomal dysfunction (Coffey et al, 2014), autophagy dysfunction (Martín-Maestro, 2017), alterations to circadian rhythm and DNA methylation (Cronin et al, 2017) and mitochondrial dysfunction (Pérez et al, 2017).

Finally, using the differentiated SH-SY5Y model, which maintains the health and adherence of the SH-SY5Y neuronal cells as they differentiate towards mature neurons, provides a different insight into biomarker analysis of AD, as it can be modulated to simulate the pathways that occur in early AD. The differentiated SH-SY5Y model is a useful model to investigate how EVs changes with AD associated stresses, as they closely resemble the phenotype of mature neurons, and with the proliferative neuroblastoma stage they can provide a relatively high throughput and homogenous cellular assay (Encinas et al, 2002). Furthermore, they are a well validated model for neurodegenerative diseases, with varying differentiation methods resulting in the production of different neuronal subtypes, which display physiologically relevant tau isoforms (Agholme et al, 2010; Chalatsa et al, 2019; Medeiros et al, 2019).

5.4 Extracellular vesicles in AD

As the understanding of EVs develops, so too does the knowledge of their roles in the balance between homeostasis and disease, and this relationship is nowhere more apparent than in neurodegenerative disorders. Investigation is beginning to unravel EVs potential to propagate neuropathology, such as Aβ and tau, but inversely, they could also betray diseases of the brain, which even today is a notoriously difficult organ to observe. From the initial observations that EVs carried Aβ (Rajendran et al, 2006), multiple groups have identified AD associated changes in EV cargoes, including more disease specific isoforms of the classic hallmark pathology, including $A\beta_{1-42}$ and phosphorylated tau species (pS396 and pT181; Fiandaca et al, 2015; Muraoka et al, 2020).

This study found that there was an upregulation in EV associated markers in AD sEVs, with f-NTA analysis identifying that CD63 tagged particles were upregulated in brain derived sEVs, in AD compared to neurologically healthy controls. Similarly, western blots of fibroblast sEVs observed that there was a 2.75-fold increase in CD9 expression in AD. Given

that CD63 and CD9 are important proteins in EV biogenesis from endosomal pathways, these changes could align with disruptions in endosomal processing in AD, which is particularly apparent in *ApoE-e4* cases which includes dysregulation of Rab GTPases (Nuriel et al, 2017). Notably, EV associated TSG-101 has also previously been found to be dysregulated in *ApoE-e4* cases, highlighting the common pathways of AD and EV biogenesis (Peng et al, 2018), though TSG-101 wasn't dysregulated in this study.

While evaluating AD cargo, particularly miRNA, was the main aim of this study, these observations make it clear that biomarkers for AD require multitargeted approaches, which compare hallmark protein changes with novel markers, including proteins and RNAs.

5.5 Transcriptomic approaches in AD

This study compared RNA yields from different EV isolation techniques, namely the Qiagen membrane affinity columns to SEC, with focus on SEC and precipitation combination methods to produce a relatively high yield while maintaining purity within the samples, as advised in MISEV guidelines (Théry et al, 2018). In this study, it was observed that the RNA concentration isolated from fibroblast derived EVs was 10-fold higher in membrane affinity columns, in comparison to SEC. However, NTA analysis found that the isolations from SEC, from both fibroblasts and brain tissue, were enriched in a population of particles which expressed EV associated proteins, suggesting the SEC based isolation used in this study was relatively pure. Other studies have also directly compared SEC and membrane affinity based methods, to determine which is a better method for purer EV isolations, and have found that membrane affinity columns isolate numerous non-EV particles and contaminants (Stranska et al, 2018). Therefore, combining the information from this study and others, it was determined that the higher RNA concentration from the membrane affinity columns had a high risk of being associated with other extracellular factors as well as EVs.

Debate remains as to the importance and feasibility of isolating extremely pure EVs for biomarker studies, as EVs only make up a small proportion of extracellular molecules, and so a miRNA change that could provide a useful insight into AD might be missed by ignoring the total extracellular RNA content (Tosar et al, 2021). Therefore, work will progress by

looking at the extracellular RNA, isolated by membrane affinity columns and SEC (which was not treated by proteinase K and RNase A), in order to compare the differences observed in EVs in AD conditions.

5.6 Oxidative stress and extracellular vesicle miRNA

It is well categorised that oxidative stress is abundant in the pre-symptomatic stages of AD and may be a driver of the pathogenesis of the disease (Wang et al, 2014). Testing oxidative stress responses in the SH-SY5Y model will help us understand whether its contribution to the pathogenesis is mediated by an altered EV response, for example with the transport of miRNAs which promote further oxidative stress or neuroinflammation. Moreover, there is overlap with oxidative stress and perturbed autophagic function, which in turn might affect the endosomal pathways and therefore, EV secretion and packaging (Hamlett et al, 2017).

This study has investigated a panel of miRNAs, including C14MC miRNAs, in the isolated EVs from SH-SY5Y cells which have undergone oxidative stress. It was observed that mir-16-5p and mir-134-5p were downregulated in oxidative stress conditions. Notably, mir-16-5p was previously suggested as a reference for EV miRNA analysis given it had previously been measured as stable in EVs, with EV miRNA isolation kits such as the Qiagen exoRNeasy Serum/Plasma kit including it for reference. Though more recently, it has been found to be differentially expressed in EVs from various disorders, including being downregulated in the CSF of AD patients (Gui et al, 2015), which is supported by our observations in oxidative stress. Other work has reported that mir-16-5p is downregulated in the hippocampus of late stage AD patients, though this is not mirrored in the CSF (Müller et al, 2014), however, this change could be measured in EVs in young onset AD (McKeever et al, 2018) and AD (Gui et al, 2015), suggesting that EVs in the CSF may more closely resemble changes in the brain. Functionally, mir-16-5p targets the APP gene, therefore reduction in mir-16-5p expression results in increased production of APP and subsequently Aβ (Lui et al, 2012). In addition, mir-16-5p inhibits the expression of inflammatory markers in the brain, as well as other AD associated proteins, including BACE1 and phosphorylated tau isoforms, indicating that mir-16-5p plays an important role in CNS and could be utilised as a therapeutic intervention (Parsi et al, 2015). Interestingly, Parsi and colleagues identified that proteins

associated with oxidative phosphorylation were the most altered after mir-16-5p treatment, after AD and Parkinson's disease associated proteins. Given that this study found a reduction in mir-16-5p with oxidative stress, further work needs to be performed to understand the nature of this relationship. One previous study did not find an association with H_20_2 treatment and mir-16 expression in endothelial cells (Magenta et al, 2011), highlighting that oxidative stress alone may not be enough to alter mir-16 expression as in AD, and that it is more likely a result of multiple AD associated changes that could be observed in AD derived cells.

5.7 Dysregulated miRNAs in sEVs in AD

5.7.1 Fibroblast derived sEV miRNAs regulate pathways in AD

In the fibroblast derived sEVs, small RNA sequencing identified miR-146, miR-145, miR-106b and miR-132 as some of the most upregulated miRNAs in AD. Interestingly, two of the candidate miRNAs (miR-146 and miR-106b), were identified as candidate miRNA, supporting the studies interest into their association with AD, moreover with both also being upregulated in qPCR, highlighting that independent methodology observed the same response.

The most upregulated miRNA in fibroblast sEVs in AD was miR-146, which has been well categorised as displaying an important role in AD and is a noted regulator of inflammation (Rusca and Monticelli, 2011). Our GO analysis displayed functionality in inflammatory processes as well as responses to cellular stress and metabolism. In transgenic mouse models of AD, miR-146a has been observed to be consistently upregulated, with particularly high expression in both the Tg2576 and 5xFAD models, but specifically only after the onset of neuropathology had occurred (Li et al, 2011). The study corroborated this by showing that in human brain tissue, miR-146a was raised in the hippocampal CA1 region and the superior temporal lobe neocortex, in patients with mid- and late-stage AD. The inflammatory role of miR-146a was tested in a co-culture model of human glial and neuronal cells, where miR-146a was raised following the incubation of IL-1β (Li et al, 2011). Genetic testing of miR-146a found that a rare allele of the single nucleotide polymorphism

(SNP) – rs2910164, found in the coding region of pri-miR-146a, was associated with AD (Zhang et al, 2015). The allele displayed reduced miR-146a levels in the serum of both AD patients and healthy controls, and subsequent testing showed upregulation of Toll-like receptor (TLR)2 and TNF-α, both noted targets of miR-146a, in HEK293 cells transfected with the rare allele. TNF-α and TLR2 are both well characterised markers for neuroinflammation, with TLR2 triggering neuroinflammatory feedback in response to $A\beta_{1-42}$ (Liu et al, 2012), therefore reduced miR-146a may exacerbate a potentially overactive and neurodegenerative inflammatory response. In the hippocampus of down syndrome (DS) patients with AD as well as a mouse models of DS and AD, miR-146a was increased alongside a downregulation of IRAK-1 (Interleukin-1 receptor-associated kinase 1) and TRAF6 (TNF receptor associated factor), suggesting further mechanisms by which miR-146a modulates inflammation in AD (Arena et al, 2017). Given that inflammaging is an underlying driver of numerous diseases, including AD (Zuo et al, 2019), it is interesting to note that miR-146a dysregulation occurs during ageing (Vasa-Nicotera et al, 2011; Jiang et al, 2011), where miR-146a dysregulation attenuates the physiological function of immune responses. This was also observed in osteoarthritis, where the age-associated damage to cartilage were exacerbated in a loss of miR-146a model, via the subsequent dysregulation of inflammatory cytokines such as IL-6 (Guan et al, 2018). Neuroinflammatory pathways have also been elucidated in relation to miR-146a, through targeting IRAK1 and TRAF6, also as shown previously, and RhoA/NF-κB in brain endothelial cells, which dysregulates downstream VCAM1, linked to T-cell adhesion in neuroinflammation (Wu et al, 2015). There may be a NF-κB/miR-146a signalling loop in the brain that triggers oxidative stress in AD, as it has also been observed that in a human hippocampal neuron cell model, that NF-κB upregulated miR-146a and a miR-146a dependent ROS response. TP53-induced glycolysis and apoptosis regulator (TIGAR) was proposed as a pathway by which miR-146a induces oxidative stress in the brain (Lei et al, 2021). The discord in observations of regulation patterns of miR-146a AD (Brennan et al, 2019) highlights that the complexity of the mechanisms underlying miRNA regulation of brain physiology and pathophysiology is not understood, and further investigation in relevant models will support more specificity in their associations with AD. Understanding the physiology will also provide context to the pathophysiological findings, so it is interesting to find that miR-146a is also associated with supporting early neurogenesis, and guides neuronal differentiation and lineage of H9

human neural stem cells (Nguyen et al, 2018). Given that adult hippocampal neurogenesis has also been observed to be dysregulated in AD (Moreno-Jiménez et al, 2019), this may elucidate another AD associated miR-146a pathway.

While previous studies identified miR-146a as a marker in later stage AD, a more recent study found that in patients with MCI, an increase in miR-146a expression in the plasma was associated with progression to AD (Ansari et al, 2019). Though it was noted that at baseline testing, that miR-146a was negatively correlated with Aβ concentration in the CSF as well as hippocampal volumes, increased miR-146a was seen in ApoE-ε4 carriers, therefore the question remains whether peripheral miR-146a reflects the changes of the brain in AD (Ansari et al, 2019). With AD, patients that displayed worse cognitive performance had lower serum miR-146a, suggesting that the dysregulated neuroinflammation in response to neuropathology is driving further neuronal interference (Maffioletti et al, 2020). miR-146a, as part of a miRNA panel, was able to predict the ratio of phosphorylated tau to $A\beta_{1-42}$ in the CSF of AD patients, suggesting it has capability as a biomarker for AD (Jia et al, 2021). Lower miR-146a was observed in AD in the CSF, which may correspond closer to our finding of decreased miR-146a in the BDEVs rather than the increase in the fibroblast sEVs, which may suggest that responses to AD in fibroblasts do not directly mirror the impact of AD on the brain. One unexplored consideration is whether responses in peripheral tissues could be directed to meet demands in the brain, for example, an increase in shuttling miR-146a from fibroblasts and other peripheral sources could compensate for a potential disease associated reduction in miR-146a in the brain. An upregulation in miR-146a in skin fibroblasts has been observed in other neuronal disorders, suggesting that a signature of neuronal dysregulation can be recorded peripherally (Nguyen et al, 2016). Currently, only one study has functionally observed miR-146a in EVs in the brain, in which microglial derived EVs were transferred to recipient neuronal cells. MiR-146a-5p selectively represses the translation of Synaptotagmin 1 and Neuroligin 1, essential in dendritic spine formation and synapse stability, respectively, which was shown in morphological loss of neuronal dendritic spine density and reduction in the strength of synaptic currents (Prada *et al*, 2018). This finding suggests that EVs can mediate the detrimental neuroinflammatory effects that occur in AD.

The miR-17 family (miR-17, miR-18a, miR-19a, miR-20a, miR-19b-1, miR-92a, miR-106a and miR-106b), for example, have been shown to target AD protein APP (Patel et al, 2008; Hébert et al, 2009) and is dysregulated in response to Aβ insult (Schonrock et al, 2010). GO analysis found functionality in responses to cellular death and metabolic changes, potentially suggesting a response to AD associated stress on the neuronal cells.

Within the miR-17 family, this study observed that miR-106a was upregulated in fibroblast and brain derived sEVs in AD, via qPCR, while miR-106b, paralogous to miR-106a with the same seed sequence (Mir-106a-5p - U**AAAGUG**CUUACAGUGCAGGUAG; Mir-106b-5p – U**AAAGUG**CUGACAGUGCAGUA, seed sequence in bold), was upregulated in fibroblast sEVs, via RNA sequencing. The miR-106a and miR-106b paralogs are well characterised in brain tumours, showing consistent overexpression in neuroblastoma (Schulte et al, 2007; Fontana et al, 2008), glioblastoma (Ernst et al, 2010; Li et al, 2017), medulloblastoma (Northcott et al, 2009), and pilocytic astrocytoma (Ho et al, 2013; Jones et al, 2015), which is modulated by the c-Myc oncogene (O'Donnell et al, 2005; Gruszka and Zakrzewska, 2018).

The upregulation of miR-106a in glioblastoma targets tissue inhibitor of metalloproteinases-2 (TIMP-2), which fittingly inhibits metalloproteinases, therefore promoting tumour invasiveness (Wang et al, 2014). Interestingly, metalloproteinases have long been associated with AD and interact with APP (Miyazaki et al, 1993), and are important for numerous neuronal physiological functions, including plasticity, and blood-brain barrier maintenance (Michaluk and Kaczmarek, 2007; Barr et al, 2009; Wiera et al, 2013; Lech et al, 2019; Qin et al, 2019), therefore the regulation of through miR-106a and potentially the miR-17 family presents a potential route for biomarker investigation. Circulating metalloproteinase levels have been correlated to AD (Tuna et al, 2018), however measuring regulatory miRNAs in EVs may further improve the specificity and provide a more accessible route to investigate these pathways. Upregulation of miR-106a in AD could be a defence mechanism against oxidative stress damage, as in a mouse model of stroke, it was observed that miR-106a targets PH domain leucine-rich repeat protein phosphatase 2 (PHLPP2), which inhibits the ability of PHLPP2 to supress the antioxidant Response Element / Nuclear factor-erythroid 2 p45-related factor 2 (ARE/Nrf2) pathway (Rizvi et al, 2015; Tang et al, 2022). With relevance to AD, miR-106a targets the 3'UTR of

APP and have been found to be able to downregulate APP translation potentially through the interaction with this site (Patel et al, 2008). Given this target, miR-106a has been investigated as a biomarker of AD with mixed results. Initial studies found no difference in miR-106a in AD in plasma (Kumar et al, 2013), however more recently, miR-106a was found as part of a miRNA panel that was differentially expressed in AD in whole blood, and was the most predictive of AD (93% specificity and 68% sensitivity, Yilmaz et al, 2016). The variation in results between studies shows how differential preparations (Serum vs whole blood) and population parameters will affect outcomes of biomarker analysis, and will remain a challenge in the field to corroborate findings. One study identified miR-106a as having the most ability to distinguish AD in ROC (Receiver operating characteristic) analysis, and subsequently found that it was downregulated in the 5XFAD mouse model (Zhang et al, 2021). Another finding in ALS, showed upregulation of miR-106a in serum (Taguchi and Wang, 2018), showing that even though the two diseases share similar molecular pathways, the distinctly opposite profiles of miR-106a suggest divergent baseline characteristics.

Regarding miR-106b, as with miR-106a, there is the same predicted target site in APP, but notably in a study that compared both paralogs, APP was only downregulated in the miR-106b transfected cell line. Further patterns of regulation were shown in the developing mouse brain, primary mouse cortical neurons, and glutamatergic mouse neurons, where, as the mouse aged or the cells were passaged, the expression levels of miR-106b reduced, and the protein expression levels of APP subsequently increased. Following this, the study investigated miR-106b in the human brain, finding decreased miR-106b in AD (Hébert et al, 2009). ATP-binding cassette transporter A1 (ABCA1), has also been found to be a target of miR-106b (Kim et al, 2012), which is implicated in cholesterol transport onto apoA and apoE, and a regulator of Aβ (Wahrle et al, 2008). Kim and colleagues found that miR-106b suppressed ABCA1 expression in mouse Neuro2a cells and rat cortical neurons. The transfection of miR-106b also dysregulated cholesterol efflux in Neuro2a cells, and downregulated the secretion and clearance of Aβ (Kim et al, 2012). Alternatively, miR-106b presents a neuroprotective effect by inhibiting thioredoxin-interacting protein (TXNIP), which upregulates oxidative responses in disease (Yoshihara et al, 2014; Pan et al, 2021). Circulating biomarkers using miR-106b have been investigated, finding that a 9-miRNA

panel could distinguish between AD and control in the serum (Guo et al, 2017). One of the first studies to measure serum EV miRNA biomarkers in AD, found that both miR-106a and miR-106b were upregulated (Cheng et al, 2015), which corresponds with the findings in this study. The study was performed in the early stage of EV research and uses an affinity column to isolate EVs from serum, which, as discussed in this study, may not separate out EV miRNA from the other extracellular RNA factors, therefore, further work to differentiate these would provide valuable information for biomarker design.

The upregulation of miR-134 in fibroblast sEVs was interesting, combined with this studies observation of a downregulation of miR-134 in SH-SY5Y cells, upon oxidative stress induction. This brings into question whether miR-134 is displaying tissue specific responses to oxidative stress in AD. Investigation into mir-134-5p, and the other miRNAs in the C14 cluster, and AD is not extensive, although they have been shown to maintain neuronal homeostasis, with dysregulation of the cluster associated with brain cancers including oligodendrogliomas and glioblastoma (Kumar et al, 2018; Nayak et al, 2018). The role of mir-134 in the brain is multifaceted, which is mediated through its targeting of CREB and BDNF, two essential proteins involved in numerous neuronal functions, including regulating synaptic plasticity and neurogenesis (Gao et al, 2010). The relationship between mir-134-5p and CREB has been observed in animal models (Shen et al, 2018) as well as SH-SY5Y cells (Feng et al, 2020). The CREB/BDNF pathway is also associated with protecting against oxidative stress, some studies have observed that inhibiting mir-134 reduced the apoptotic response of retinol ganglion cells after H202 treatment, which was attributed to an upregulation of CREB (Shao et al, 2015). Inhibiting mir-134 has been found to attenuate damage caused by oxidative stress in other models, including from ischemic injury in hippocampal neurons (Huang et al, 2014), as well as in animal models of epilepsy (Sun et al, 2017; Gao et al, 2019). Sun and colleagues also noted that mir-134 inhibition improved mitochondrial function, with reduced reactive oxygen species, as well as reducing the levels of the autophagy associated Atg5, LC3B II and beclin 1, indicating a wider protective response of the mir-134/CREB pathway (Sun et al, 2017). Potential for mir-134 to be utilised as a biomarker for AD has been suggested previously (Sheinerman et al, 2013), with observations that measuring the mir-134 family in the plasma provided a high sensitivity and specificity for differentiating MCI from age matched controls. This was supported by

studies of the CSF, showing mir-134 is differentially expressed between AD and control samples (Burgos et al, 2014), however, this dysregulation did not translate to extracellular vesicles that were isolated from the CSF (Riancho et al, 2017). Given the close relationship between oxidative stress and AD, it is not surprising to see that inhibition of mir-134 restored the deficits in synaptic plasticity (including in LTP) that are associated with AD and Aβ 1-42 accumulation, in a similar manner to the oxidative stress models (Baby et al, 2020). These interactions indicate that there is a lot still to understand about the influence of mir-134, as well as the rest of the C14 cluster, in AD.

5.7.2 Brain derived sEV miRNAs regulate pathways in AD

In the brain derived sEVs, small RNA sequencing identified two panels of miRNAs, miR-203a, miR-361, miR-141, miR-125b-1, and miR-30a were upregulated in AD, while miR-582 and miR-1248 were downregulated. In pathway analysis, the panel were associated with several cell death pathways, including apoptosis pathways and responses to cellular stress. Notably, there was a common association with responses to oxidative stress in cells, a significant molecular change in AD. Other pathways included regulation of metabolism and cytokine signalling

The most upregulated miRNA in the BDEVs was miR-203a, which is relatively unexplored in AD. It has previously been characterised as anti-oncogenic, including the suppression of hepatocellular carcinoma migration and angiogenesis, through targeting the vascular endothelial growth factor receptor (VEGFR; Wang et al, 2018). Alternatively, in breast cancer, miR-203a expression correlates with poor prognosis (He et al, 2016), where it targets suppressor of cytokine signalling 3 (SOCS3), known as an insulin-induced regulator of cytokines (Emanuelli et al, 2000), which inhibits cancer progression (Xu et al, 2019). In the brain cancer, glioblastoma, miR-203a inhibited tumour migration and activated interferon signalling by targeting ataxia-telangiectasia mutated (ATM), a regulator of interferons (Yang et al, 2017). Interestingly, all three of these downstream targets of miR-203a have previously been implicated in AD. With VEGFR, it is established that AD has a component of cerebrovascular dysfunction, partially attributable to cerebral amyloid angiopathy (CAA) (Rovelet-Lecrux et al, 2006). Increased $A\beta_{1-42}$ oligomers caused downstream dysregulation of VEGFR1/2 in brain endothelial cells. In particular, VEGFR1

upregulation in response to $A\beta_{1-42}$ oligomers induced a p53 mediated senescence, which provides a pathway in which cerebrovascular dysregulation occurs in AD (Angom et al, 2018). SOCS3 has been observed to be a potential intermediary between diabetes and AD (Vieira et al, 2018), both responding to Aβ and triggering insulin signalling that can regulate APP processing and neuroinflammation (Cao et al, 2018), while insulin signalling dysregulation in diabetes associated insulin resistance in AD is still under investigated. Finally, neuronal ATM is downregulated in the AD frontal cortex and downstream ATM signalling is reduced in neurons in regions sensitive to AD, potentially due to a reduced DNA damage response to oxidative stress (Shen et al, 2016). In a study investigating the effect of B vitamins on inhibiting neuroinflammation induced by 1,2 diacetyl benzene (DAB), which has been hypothesised to be detrimental to cognitive performance, through increased oxidative stress and hyperphosphorylation of tau (Kang et al, 2017), miR-203a was observed to be dysregulated by DAB (Nguyen et al, 2022). In SY-SY5Y cells, DAB induced inflammatory upregulation, including increased IL-6 and NF-κB, as well as GSK-3β induced tau phosphorylation, was attenuated by vitamins B1, B2 and B3. The study identified miRNAs predicted to interact with DAB induced genes (NFKB1, IL1B, IL10, IL6, and TNF), and subsequently found that miR-203a was downregulated in response to DAB, but then upregulated in SH-SY5Ys that were pre-incubated with vitamins B1, B2 and B3 (Nguyen et al, 2022). In a mouse traumatic brain injury (TBI) model, miR-203a was increased in response to TBI and induced the phosphorylation of tau and triggered neuronal apoptosis, suggesting that it could mediate between neuronal stress and progression of neurodegeneration (Zhao et al, 2021). Supporting this, miR-203a was observed to be dysregulated in brain derived EVs in a mouse TBI model (Ko et al, 2020). Only one study so far has tested miR-203a as a biomarker for AD, which used a machine learning method called adaptive boosting for miRNA disease association (ABMDA) to find that miR-203a was predicted the third most differentially expressed circulating miRNA in AD (Yuen et al, 2021).

Other upregulated miRNAs in BDEVs in AD included miR-141 and miR-361. MiR-141 is a mitochondria-related miRNA that regulates mitochondrial function, including the production of ATP, as well as inducing oxidative stress and damage responses (Ji et al, 2015). Inflammatory cytokine IL-6 was also observed to be upregulated in response to miR-

141. The study found that the miR-141 predicted target PTEN was downregulated in response to, as well as mediating the effect of miR-141 on mitochondrial dysfunction. In a model of Parkinson's disease, 1-methyl-4-phenylpyridinium (MPP+, a dopaminergic neurotoxin) caused an upregulation of miR-141 in PC12 cells, which in turn downregulated SIRT1 (sirtuin 1: silent information regulator 1) activity and promoted apoptosis and oxidative stress (Rostamian et al, 2018). Mir-141 has been observed as an astrocyte EV associated biomarker for neuroinflammation, where endogenous astrocyte miR-141 was greatly increased and only expressed in EVs in response to IL-1β treatment (Gayen et al, 2020), which suggests that the upregulation observed in this study may be due to AD associated neuroinflammation. This is supported by other studies observing miR-141 increases after stroke induced neuroinflammation (Verma et al, 2018). Mir-141 has been found to be downregulated in the plasma EVs in AD (Lugli et al, 2015), which is the opposite of what was observed in this study and could highlight the complexity of biofluid EVs from multiple cell sources, which could reduce the specificity of miRNA dysregulation in AD. Therefore, further understanding of the specific peripheral tissue responses in AD will greatly support findings in biofluids.

Mir-361 has been observed to regulate zinc finger gene 217 (ZNF217), which had been suggested to moderate Aβ induced neurotoxicity (Gao et al, 2020). The miRNA is downregulated in AD brains and APPswe transfected SH-SY5Y cell, and has been found to target BACE1, where miR-361 induction reduced BACE1 protein levels and rescuing cognitive function in an AD mouse model (Ji et al, 2019). When comparing major depressive disorder and AD, miR-361 was one of 7 miRNAs that was dysregulated in both conditions (Mendes-Silva et al, 2016), which considering the emerging risk of untreated depression for AD (Livingston et al, 2020), might make miR-361 a unique biomarker for stratifying groups at risk of AD progression. One study has found miR-361 to be upregulated in serum EVs in AD, which corresponds to this study, interestingly there was also an upregulation in MCI, suggesting an avenue for early AD biomarker testing (Cheng et al, 2015).

The final two upregulated miRNA in BDEVs were miR-30a and miR-125b. MiR-30a is upregulated in the brain in hypoxic conditions following ischaemic injury, but downregulated upon reperfusion/reoxygenation. It was observed to target beclin 1 and therefore miR-30a downregulation in reperfusion/reoxygenation conditions promoted

beclin 1 mediated autophagy and cell survival (Wang et al, 2014). In this study, since miR-30a was upregulated in BDEVs in AD, it could point to a dysregulation in autophagy in AD conditions. Mir-30a is upregulated in the serum of Parkinson's disease patients (Burgos et al, 2014), however, the only observation in AD showed a downregulation of miR-30a in CSF (Lusardi et al, 2017).

Mir-125b has been more thoroughly investigated in AD, probably due to it being one of the most enriched miRNA in the brain (Sempere et al, 2004), though this did not translate to it being one of the highest expressed miRNA in this study's BDEV samples. It has been characterised as an essential regulator of cellular stress responses through its targeting of p53, and supresses apoptosis in neuronal and peripheral cells (Le et al, 2009). Through targeting of TNF-α, miR-125b also regulates innate immune responses (Tili et al, 2007). The more neuronal specific functions of miR-125b include the regulation of synapse morphology through the targeting of the NDMA receptor NR2A (Edbauer et al, 2010). MiR-125b also regulates VEGF-induced angiogenesis in glioblastomas (Smits et al, 2012), which suggests that it could also be a more specific marker of cerebrovascular disfunction in AD, similar to miR-203b (Angom et al, 2018). In AD, miR-125b has observed in independent studies to be increased in the temporal cortex (Cogswell, 2008; Absalon et al, 2013), frontal cortex (Banzhaf-Strathmann et al, 2014), and the CSF (Alexandrov et al, 2012), suggesting it may interact with AD associated pathways. Mir-125b has also been observed to be increased in EVs derived from the CSF in AD patients, which highlights that EV expression can mirror the changes occurring in the brain, particularly when they are brain derived (McKeever et al, 2018).

When miR-125b is overexpressed in hippocampal neurons, it induces the phosphorylation of multiple epitopes on tau, including S202/T205 and T231/S235, through the regulation of tau kinases and phosphatases, such as Bcl-2-like protein 2 (Bcl-W). Consequently, miR-125b overexpression impairs neuronal viability and cognitive function (Banzhaf-Strathmann et al, 2014). In a cerebral hypoxia injury model, miR-125b regulation was protective against reduced cerebral function by modulating apoptotic (BCL-2) and ROS pathways (Shen et al, 2018). MiR-125b may also be protective in an AD model, as induction of miR-125b attenuated the neuronal damage caused by Aβ-induced apoptosis and oxidative stress, which is like the findings in the cerebral injury model (Shen et al, 2018),

but this study also found that miR-125b targets BACE1, and may regulate AD through this interaction (Li et al, 2020).

MiR-125b was downregulated in the serum of AD patients, which is converse to the findings in the brain and CSF (Tan et al, 2014), though this may indicate why, in this study, miR-125b was upregulated in the BDEVs but not in the fibroblast sEVs. The findings of downregulated serum miR-125b were corroborated in a more recent study (Li et al, 2020), though they also found that miR-125b was also reduced in neuronal cells upon Aβ-induction. Notably, even though miR-125b levels were divergent between the brain and blood, serum miR-125b was still capable of predicting AD in a test population (sensitivity/specificity: 80.8%/68.3%), and higher miR-125b levels were correlated with worse cognitive performance by MMSE (Mini-Mental State Examination; Tan et al,2014). This highlights that since AD has influences across the whole body (Wang et al, 2017), that a biomarker does not necessarily have to mirror the changes occurring in the brain, even in a neurodegenerative disease like AD.

In this study, there were two miRNAs that were inversely regulated between fibroblast and brain derived sEVs in AD, miR-132 (Log2(FC): Brain = -1.063, Fibroblast = 1.303) and miR-185 (Log2(FC): Brain = 1.369, Fibroblast = -1.227). Pathway analysis found that, peripherally, both are associated with cellular migration and differentiation, as well as vascular development. Pathways associated with the brain and AD include responses to reactive oxygen species, hypoxia, WNT signalling and neurogenesis, and protein phosphorylation mechanisms. MiR-132 has previously been observed to be consistently downregulated in the human brain, through the hippocampus, temporal cortex and frontal cortex in AD (Lau et al, 2013; Salta and De Strooper, 2017; Pichler et al, 2017; Li and Cai, 2021). It modulates multiple AD associated pathways, including targeting MAPK and BACE1 in neuropathological pathways, FOXO3a and PTEN in neurotoxicity pathways, CREB and methyl CpG-binding protein 2 (MeCP2) in neurogenesis pathways, IRAK1 in neuroinflammatory pathways, and vascular signaling pathways (Figure 5.1; Salta and De Strooper, 2017; Qian et al, 2017), which situates miR-132 as a central mediator of AD and as target for therapeutics and biomarkers.

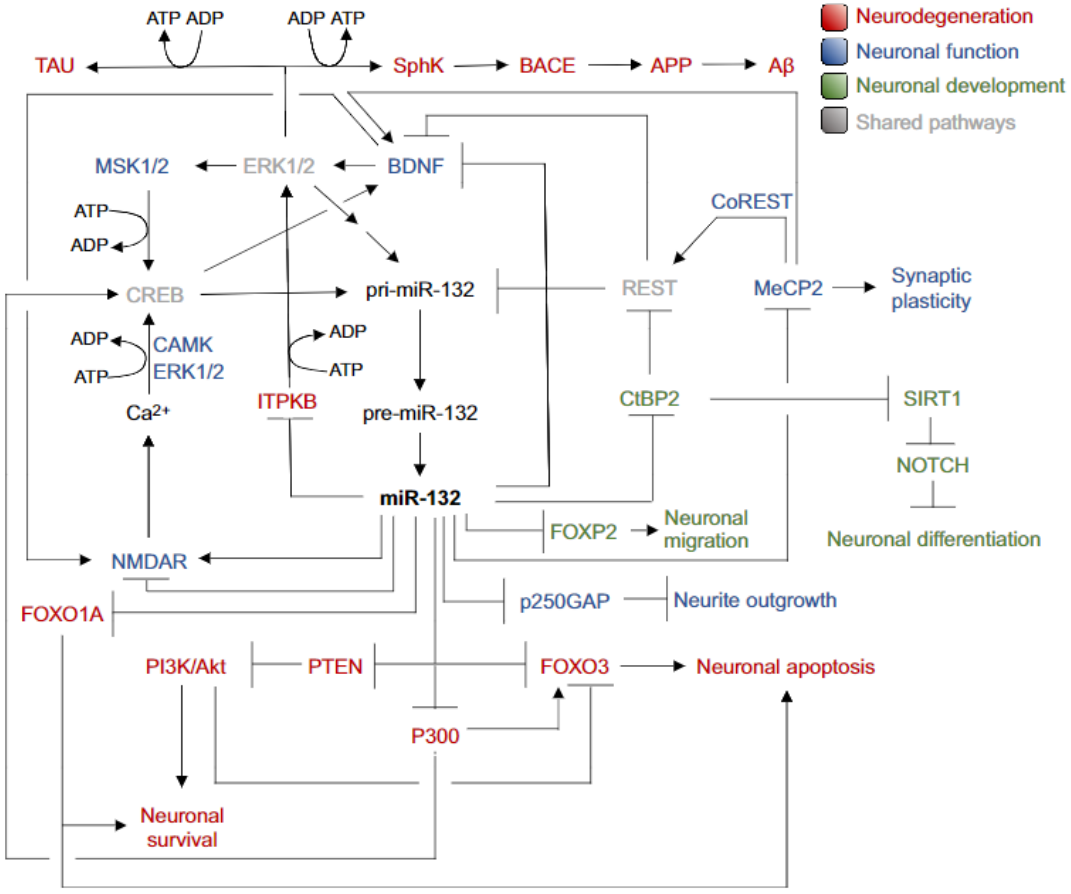

Figure 5.1. miR-132 is a central regulator of molecular pathways in the brain

Mir-132 is involved in numerous pathways in the brain, including those involved in neuronal development (green), neuronal function (blue), and neurodegeneration (red), as well as pathways involved in multiple processes (grey). Taken from (Salta and De Strooper, 2017)

Downregulation of miR-132 in the AD brain upregulates various Aβ isoforms, including increasing plaque burden in the hippocampal regions and increasing $Aβ_{1-42}$ and $Aβ_{1-40}$ oligomers. The downregulation also increases tau phosphorylation on sites such as AT8 and AT270. Some of these regulatory patterns were observed to be mediated through miR-132 targeting the kinase inositol 1,4,5-trisphosphate 3-kinase B (ITPKB), which has independent regulatory mechanisms for both pathologies (Salta et al, 2016). Tau phosphorylation has also been observed to be regulated by miR-132/NOS1 (nitric oxide synthase 1), including Ser396, Ser404, and Ser202 sites (Wang et al, 2017). Deletion of miR-132 and the homolog miR-212 also promotes $Aβ_{1-42}$ production and plaque load in the mouse hippocampus and temporal cortex, through the regulation of SIRT1, a protein deacetylase that is well

categorised in AD (Ng et al, 2015; Hernandez-Rapp et al, 2016). MiR-132 targeting of MAPK appears to be neuroprotective by attenuating multiple downstream functional responses to MAPK in rats, reducing downstream oxidative stress and improving cognitive function (Deng et al, 2020). Adult hippocampal neurogenesis has been observed to be regulated by miR-132, which was expressed in neuronal precursor and progenitor cells in mice, and is shown to be required for the induction of neurogenesis. MiR-132 was also found to increase during neuronal differentiation, being increased over 300-fold in mature neurons compared to primary human embryonic stem cells. When adult neurogenesis is impaired in an AD mouse model, induction of miR-132 was able to ameliorate the deficits and the subsequent AD associate memory impairment (Walgrave et al, 2021).

Since miR-132 has been observed to interact with numerous pathways, the complexity of its role in the brain is high, and so it is unsurprising to find observations that also show that downregulated miR-132 is also neuroprotective (in contrast to the previous studies). The miR-132/SIRT1 axis was also dysregulated in lymphoblast cell lines (LCLs) from AD patients (miR132: Up, SIRT1: Down). Interestingly, this study also observed the opposite pattern in the LCLs of a population of neurologically healthy centenarians, against the population aged 56-82 years (miR132: Down, SIRT1: Up), suggesting that this axis may also be protective during healthy ageing (Hader et al, 2018). The study supported this with observations that miR-132 was negatively correlated with MMSE scores and age of onset in AD. Whether the changes in LCLs mirror the brain or not, the study also observed a decrease of miR-132 in the olfactory bulb and hippocampus in AD. This suggests that age should be considered when using miR-132, as with other factors in AD, as a biomarker, though the differences in observation of miR-132 levels in AD to a lot of literature should be investigated further. One study has investigated miR-132 in EVs derived from the plasma of AD patients, using an L1CAM based separation method to select for EVs of neuronal origin in the complex biofluid (Cha et al, 2019). The study found that miR-132 was downregulated in neuronally derived EVs from the plasma of AD patients, and was able to moderately discriminate control populations from AD with dementia populations (ROC: AUC = 0.84), though it could not separate control and AD-MCI groups as well (ROC: AUC = 0.68). It is promising to see that the findings in this study correspond with our findings from BDEVs, and supports further investigation of EV miR-132 as a biomarker for AD, particularly

to investigate whether the inverse upregulation in Fibroblast sEVs is rigorous, as it could be the underpinning for a less invasive test for AD.

Of the most downregulated BDEV miRNAs in AD, miR-582 has limited investigated associations in AD. In cancer, miR-582 has been seen to regulate TGF-β through targeting TGF-β receptors (TGFBR) and SMAD (Huang et al, 2019), suggesting that it has regulatory roles in apoptosis signalling. In fact, inhibition of miR-582 has been shown to inhibit apoptosis in a brain oxygen-glucose deprivation post injury model, where miR-582 targeted NOS. The study also observed that miR-582 inhibition attenuated the increases in TNF-a and IL-1β (Zhang and Zhang, 2020). MiR-582 is neuroprotective in an SH-SY5Y model, where its overexpression protected cell viability and reduced caspase 3 and caspase 9, to reduce apoptosis from propofol induced neurotoxicity (Zhang et al, 2020). In AD, mir-582 was predicted to be a regulator of APP and target FERMT2, associated with APP metabolism. In HEK293 cells, miR-582 transfection increase expression of Aβ and sAPPα, and in primary neuronal cultures, it was primarily associated with neurons in comparison to astrocytes, though there were no differences in miR-582 expression in AD derived cells. The study used pathway analysis to predict that miR-582 influences axon guidance and maintenance (Eysert et al, 2021). Upregulation of miR-582 has also been seen to increase in APP in a CAA model (Nicholas et al, 2016). So far, biomarker tests for miR-582 have provided mixed results, with one study finding higher expression in the EVs derived from serum of AD patients (Cheng et al, 2015), while another found no changes (Li et al, 2020), and our study found lower expression in BDEVs. The isolation methods of EVs for all three studies were different (affinity columns vs precipitation vs SEC), which could influence the extent that the studies were EV specific and are therefore it is difficult to directly compare, though the contrast in findings means that further investigation into the tissue specific roles of miR-582 may help to unravel the observed differences.

The other downregulated miRNA, miR-1248, has been observed to be differentially expressed in disorders like asthma, regulating the inflammatory cytokine IL-5 (Panganiban et al, 2012). Other inflammatory pathways associated with miR-1248 have been observed in the autoimmune disorder, Sjögren's syndrome, where it directly regulated RIG-1/ IFN-β signalling, as well as ITPR3, which is involved in calcium signalling (Jang et al, 2019). MiR-1248 was decreased in the human adipose-derived stem cells from diabetes mellitus

patients and targets the CITED2/HIF-1a pathway, which is associated with cellular proliferation, growth factor signalling and oxidative stress signalling (Xiao et al, 2020). In the brain, miR-1248 was upregulated in response to oxidative stress induction of human primary astrocytes, with a reduction in its predicted target, 8-deoxyguanosine DNA glycosylase 1 (OGG1), which is protective against oxidative DNA damage in the brain (Nwokwu et al, 2022). This regulatory pathway was tested, with miR-1248 inhibition resulting in an upregulation of OGG1, highlighting a novel DNA repair axis in the brain. MiR-1248 has not previously been observed as differentially expressed in AD, though it was found to be downregulated in the serum with age, and was observed to negatively regulate IL-6 and TNFα, suggesting it has a role in inflammaging (Hooten et al, 2013). Potentially, downregulation of miR-1248 in AD could be indicating that there is dysregulated neuroinflammatory pathways in the AD group.

Of the chromosome 14 miRNAs, miR-382 was interesting as the -3p strand was upregulated in AD BDEVs while the -5p strand was downregulated, which suggests that miR-382 has divergent regulatory effects in AD. The role of miR-382 in the brain is not well studied, though based on observations in other diseases, it has roles in regulating inflammatory and as an oncogene. In a cellular model of cardiovascular disease, miR-382 targets nuclear factor IA (NFIA), which has functional roles in regulation of cholesterol homeostasis and adipocyte differentiation (Hu et al, 2010; Waki et al, 2011), as well as promoting the development of glia in the developing brain (Deneen et al, 2006). The study found that miR-382 induction upregulated TNF-a, IL-1β and IL-6, while dysregulating cholesterol efflux (Hu et al, 2014). In a cell culture model for hypoxia, downregulated miR-382 was associated with reduced endothelial cell migration and proliferation, which are required for angiogenesis. MiR-382 targeted PTEN and inhibition of this pathway was observed to reduce hypoxia induced angiogenesis (Seok et al, 2014), though given that PTEN also regulates axon formation and regeneration (Park et al, 2010), miR-382 could also regulate these pathways. In the brain, miR-382 is expressed in hippocampal and cortex synaptosomes (Pichardo-Casas et al, 2012), is upregulated in the olfactory epithelial cells of schizophrenia patients (Mor et al, 2013), while miR-382 upregulation inhibits ventricular enlargement in the brains of a schizophrenia mouse model (Eom et al, 2020), though ventricular enlargement has also been observed in the AD brain (Nestor et al, 2008). MiR-

382 has been found to regulate BDNF and the downstream PI3K/AKT signalling pathway (Song et al, 2017), which are important in neurogenesis and the maintenance of synaptic plasticity (Gao et al, 2010; Zimbone et al, 2018). Previous biomarker studies have found that plasma miR-382/ miR-370 was able to distinguish MCI from healthy controls with 74%-88% sensitivity and 80-92% specificity (Sheinerman et al, 2013), and that miR-382 was downregulated in the grey matter in AD (Wang et al, 2011). In neurological models that relate to AD, miR-382 was upregulated in the hippocampus of a rat model of depression (Zhou et al, 2018) and in plasma EVs in an aged population (Rani et al, 2017).

5.8 Future considerations – Sex associated differences in sEV miRNA cargo in AD

When investigating EV miRNA changes in AD between the female groups, in the fibroblasts the most upregulated miRNA was miR-145 (log2(FC) = 3.267) and the most downregulated was miR-185 (log2(FC) =-1.640).

MiR-145 has been observed to be a regulator of oxidative stress apoptosis and inflammation through targeting NF-κB, the downregulation of miR-145 corresponded to an upregulation of caspase-3, IL-1β, TNF-α, IL-6 and ROS (Xue et al, 2021). In contrast to AD, miR-145 was downregulated in the brain metastasis from lung cancer, and induction of miR-145 inhibited brain tumour invasion and cell migration through the targeting of OCT-4, EGFR, and c-MYC (Donzelli et al, 2015), such inverse patterns between cancer and AD have previously been proposed (Driver et al, 2012), so it would be interesting to see whether miRNAs such as miR-145, with their broad targets, could be an intermediary in this. MiR-145, for example, has shown that it inhibits pro-cell survival pathways (Donzelli et al, 2015), and whether this could be detrimental over time in AD could be further investigated. In glaucoma, a downregulation of miR-145 also promoted cell viability and reduced apoptosis responses, through targeting the TRIM2 (tripartite motif-containing 2)-PI3K/AKT signaling pathway (Xu et al, 2021). Interestingly, TRIM2 regulates several neuroprotective pathways, including regulation of neurofilament light subunit (NF-L) ubiquitination (Balastik et al, 2008) and Bcl-2-interacting Mediator of Cell Death (Bim) E3 Ligase, associated with apoptosis (Thompson, 2011). Therefore, an upregulation of miR-

145 may be indicative of neurodegeneration as it inhibits the neuroprotective TRIM2. In biomarker analysis, miR-145 has been observed to be differentially expressed in the neuroinflammatory disorders, neuropsychiatric systemic lupus erythematosus (NPSLE) and multiple sclerosis (MS), suggesting that it may contribute peripherally and neuronally to neuronal disorders (Sharif-Eldin et al, 2017; Mansourian et al, 2017). So far in AD, miR-145 has shown mixed responses, being upregulated in young-onset (YO)AD (McKeever et al, 2018), but downregulated in general AD patients (Lusardi et al, 2017). Notably, the study that saw an upregulation of miR-145 investigated in the EVs derived from CSF, which may indicate that there is an EV specific upregulation in AD, as this corresponded with the findings in this study. However, it did not find the same response in late-onset AD, so it may not be a general marker for AD, but warrants further investigation for its ability to differentiate subpopulations.

MiR-185, the most downregulated miRNA in both females and the total population, is associated with regulating autophagy and apoptosis, through targeting the AMPK/mTOR signalling pathway (Wen et al, 2017). In an SH-SY5Y model, treated with 1-methyl-4-phenyl-1,2,3,6-tetrahydropyridine (MPTP) to induce a PD phenotype, miR-185 was downregulated. However, on induction of miR-185 overexpression, the number of apoptotic cells, beclin-1 mediated autophagy and upregulation of AMPK/mTOR signaling, triggered by MPTP, was reversed, suggesting a neuroprotective role for miR-185. In AD, miR-185 targets APP and can inhibit expression in a neuronal cell model (Ding et al, 2022). Interestingly, the study also found that miR-185 and APP form an axis, as APP overexpression also could inhibit miR-185, which corresponds with the finding that miR-185 was downregulated in the EVs of serum from AD patients, which was also in line with this study. Reduced amounts of miR-185 have been found in blood (Sabaie et al, 2022), and in the EVs derived from plasma, in AD patients (Lugli et al, 2015), as well as in the serum in PD (Ding et al, 2015). There are consistent findings of downregulated miR-185 in biofluids of AD, though in contrast, miR-185 was observed to be upregulated in the temporal cortex in AD (Sabaie et al, 2022), which may indicate why this study only found downregulation of miR-185 in the fibroblast derived EVs. The contrast between the central and peripheral findings needs further investigation, but miR-185 could have potential as a peripheral specific biomarker of AD.

When investigating EV miRNA changes in AD between the female groups, in the brain, miR-27a was significantly upregulated (log2(FC) = 2.878), where it did not show as strong an upregulation in the total population in AD, even if it was still high (log2(FC) = 1.960). GO pathway analysis found that it was associated with neurogenesis and brain development, and implicated in responses to cellular stress and oxidative stress, as well as regulation of protein phosphorylation. Strikingly, this was one finding in this study that was particularly in contrast to the findings published elsewhere so far. In multiple studies, miR-27a was found to be reduced in the CSF (Frigerio et al, 2013) and the blood (Su et al, 2019), or unchanged in the neocortex (Culpan et al, 2011) or cell-free CSF (Müller et al, 2016), of AD patients. Müller et al (2016) noticed that if cell-free CSF was spiked with blood, that the expression of miR-27a increased quickly, suggesting that there is a significant cellular component of miR-27a that is different to the extracellular expression. Functionally, miR-27a maintains brain endothelial structure and is positively correlated to claudin-5 and occluding expression through targeting GSK3ß (Hammad et al, 2022) and aquaporin-11 (Xi et al, 2018). MiR-27a has also been observed to target apoptotic protease activating factor-1 (Apaf-1) to regulate neuronal apoptosis in hypoxic conditions (Chen et al, 2014). Inhibition of miR-27a was protective in a model of TBI through targeting DRAM2 (DNA damage regulated autophagy modulator 2), and reducing the LC3II/LC3I autophagic response, as well as TNF-α, IL-6, and IL-1β inflammatory responses (Li et al, 2020). This finding suggests that the higher miR-27a observed in our study could correspond with increase AD associated neuroinflammation.

Therefore, miR-27a remains as an interesting biomarker for AD, though this study requires further testing to determine the differences in observations to the consensus. One potential reason is whether miR-27a is differentially packaged into EVs in AD, it has been observed that BDEVs contain a different miRNA transcriptome to the brain (Vella et al, 2017), though specific information on miR-27a is not certain. Notably, one study that compared the expression levels of miRNAs in AD, between EVs and brain homogenates, found that miR-27a was upregulated in AD in the BDEVs, but they did not find any changes in the brain homogenate (Cheng et al, 2020), this supports the conclusion that miR-27a could be an interesting EV associated biomarker in AD.

MiR-668, a chromosome 14 cluster miRNA, was the most downregulated miRNA in BDEVs (log2(FC) =-2.515), in AD females. MiR-668 was found to be upregulated in replicative senescence model in normal human keratinocytes, while overexpression of miR-668 increased the percent of β-galactosidase positive cells and induced the expression of p53. However, miR-668 was not observed to change with age (Shin et al, 2011). In AD, miR-668 was observed to be downregulated in the prefrontal cortex in LOAD, which corresponds to our findings of a downregulation in prefrontal cortex derived EVs (Lau et al, 2013). However, in a (female) mouse model of AD, miR-668 was upregulated in response to $A\beta_{1-42}$ and corresponded to oxidative stress responses, including production of ROS. Notably, the study also observed an increase in p53 in AD mice as found in the keratinocyte senescence model (Shin et al, 2011). MiR-668 was observed to target oxidation resistance 1 (OXR1), which influences p53-p21 signalling, and inhibition of miR-668 countered the oxidative stress and apoptosis induced by $A\beta_{1-42}$ (Li et al, 2022). In down syndrome, which as previously discussed has genetic links to AD (Arena et al, 2017), miR-668 was downregulated. Interestingly, the study found that miR-668 was overexpressed in females compared to males, but miR-668 remained downregulated in down syndrome, when just looking at females (Biselli et al, 2022). This supports our suggestion that some miRNAs have a sex-linked bias, and that miR-668 may be a candidate for further analysis of this. In fact, the C14 cluster may be a novel target for sex-linked differences in diseases, as one study observed 10 miRNAs from the cluster, including miR-668, to be upregulated in multiple sclerosis, but only in males (Baulina et al, 2022). It was only miRNAs in the DLK1-DIO3 locus that displayed this difference, and no other locus associate genes, including DLK1, DIO3 and RTL1, which brings into question whether there is any miRNA specific machinery that is differently regulated between sexes.

From a perspective of sex specific changes in AD, miR-660 was particularly interesting in this study. When looking at just females, miR-660 was inversely expressed in AD between the brain and fibroblast derived sEVs (Log2(FC): Brain = -1.515, Fibroblast = 2.231). Moreso, when the analysis looked for differences between the sexes, miR-660 was inversely expressed in AD, between males and females, both in the fibroblast derived sEVs (Log2(FC): Male = -1.874, Female = 2.231) and the brain derived sEVs (Log2(FC): Male = 1.273, Female = -1.516), a pattern that was switched between tissue of origin (Figure 5.2).

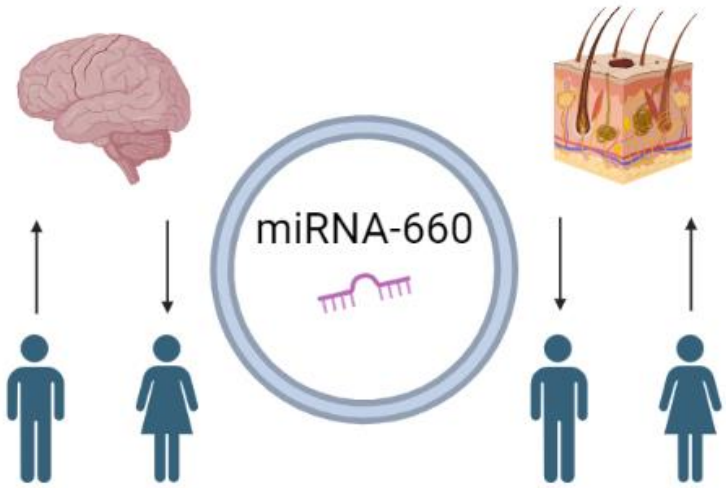

Figure 5.2. miR-660 displayed sex specific regulation in AD, in both fibroblast and brain derived sEVs.

This study found miR-660 to be a candidate for sex specific changes in AD. In brain derived sEVs, miR-660 was upregulated in males but downregulated in females, in AD. The opposite was observed in fibroblast derived sEVs, where miR-660 was downregulated in males but upregulated in females, in AD. Created in Biorender.

In GO analysis, miR-660 was associated with cellular differentiation, being experimentally observed in noradrenergic neuronal and smooth muscle cell differentiation. It was also regulation of cell cycle and included WNT signalling and cellular development pathways. MiR-660 is upregulated in Chronic Myeloid Leukaemia (CML), where it is observed to be protective against oxidative stress through the targeting of EPAS1, also known as HIF2a (hypoxia-inducible factor 2 alpha), which is neuroprotective in ischaemic conditions (Barteczek et al, 2016; Salati et al, 2017). In renal cell carcinoma, miR-660 is downregulated and associated with the inhibition of cell migration, proliferation and apoptosis (He et al, 2017). Alternatively, miR-660 has also been found to be oncogenic, through targeting FOXO1 (Feng et al, 2020), which has also been identified as a therapeutic pathway for AD (Zhao et al, 2022). Other studies have found that miR-660 upregulates PI3K/AKT/mTOR signalling through targeting TET2, thereby promoting cell survival responses (Peng et al, 2020).

Two previous studies have identified miR-660 as an AD biomarker, one showing that as part of 9-miRNA panel in the serum, it could distinguish AD from healthy controls (Guo et

al, 2017). In another study, miR-660 was downregulated in the blood of AD patients (Satoh, et al, 2015). The same findings are not observed in this study in the total population, given that there are counteracting patterns between the sexes, furthermore, the statistical power of this observation is severely limiting, however, given the exploratory nature of this study to identify new candidates for further testing, miR-660 shows novel promise as a sex specific biomarker for AD.

5.9 Towards biomarkers for AD

So where do these findings fit into the outlook for biomarkers for AD?

At the start of 2022, scientific outputs in the field described AD as a disease with no confirmed therapies that could halt or slow the progression of onset. As discussed, this is predominantly due to the vast amount of contributing factors that lead towards the accumulation of neuropathology and the currently irreversible damage to neurons and the brain (Scheltens et al, 2021). A considerable proportion of these risk factors have the most effect at early and mid-life, including several modifiable factors that vary from individual to individual (Livingston, 2020). It is increasingly apparent that these variations can trigger molecular changes at least 20 years in advance of symptom onset, which contribute to the respective onset (Preische et al, 2019; O'Conner et al, 2021). It is apparent that if therapies are to be effective in modifying AD onset, then they need to be applied within this pre-symptomatic window, where there is the best chance to intervene in neuropathology development and limit neuronal damage. In the first trial to observe a targeted therapy that shows any modification of cognitive decline in AD, Lecanemab – a human IgG1 monoclonal antibody targeting and reducing the levels of Aβ soluble protofibrils compared to controls over an 18-month time course, at time of writing (van Dyck et al, 2022), the eligibility criteria was specifically early Alzheimer's, with mild cognitive impairment or mild dementia onset based of the National Institute on Aging–Alzheimer's Association criteria (McKhann et al, 2011). While this antibody may target soluble Aβ more effective than previously unsuccessful trials, it is notably more successful due to the specific design to target early AD and future redesigned trials will be more successful following the same targeted approach (Veitch et al, 2018; Reiss et al, 2021). Therefore, advances into

biomarker testing in the early stages of AD are essential in supporting the success of future clinical trials.

There is great promise in the development of peripheral biomarkers for AD, with exciting results from the CSF and the blood. But, with all complex biofluids, there is difficulty in determining the specificity of the results. EVs have been shown to display an insight of the molecular changes within their cell of origin, and therefore have great potential as more specific biomarkers of multiple diseases, including AD, when measured in biofluids. However, there are still a lot of challenges in the field before we can get to an EV biomarker, including the need for a consensus on the balance of a pure EV only biomarker against missing out on changes in secreted factors by narrowing the field of view too far. Analysis of EV associated miRNA changes from multiple tissues in an individual disease will greatly improve insight into relative contribution of tissues to EVs in biofluids. Furthermore, they could help further understand the systemic changes that occur in AD, leading to developing more personalised diagnostics and therapies.

5.10 Limitations

This project has a few limitations that need to be addressed to put the findings in context and to guide the progression of further work into implementing these findings towards the goal of improving AD biomarkers.

Firstly, there are low n numbers used, n = 3 per AD and control groups, in both cohorts. While the design of this pilot study requires initial investigation into smaller groups to determine whether there is potential for the work to progress, it also means that all findings will not be representative of AD, especially since this work emphasises the requirement for future therapies to be targeted to the multiple presentations of AD. This limitation is most apparent in the attempt to preliminarily stratify groups based on sex, resulting in a comparison of n=1 per group in males. While that analysis was performed to provide visualisation of trending patterns between sexes, and to provide a basis for candidate miRNAs that could be investigated in an expanded cohort, there will be no statistical robustness to those observations until the cohort is expanded.

As the age difference between AD patients and neurologically healthy controls were significantly different in the brain tissue cohort, consideration needs to be taken as to how this might influence the findings of the results. It has been observed that concentrations of EVs decrease in the plasma with age (Eitan et al, 2017), however EV secretion increases in response to cellular senescence (Takahashi et al, 2017). In senescent fibroblasts, the EV secretion associated RAB27B is upregulated (Fujii et al, 2006), highlighting that EV associated pathways may be 'switched on' to increase clearance of waste products from senescent cells.

Also, to consider, miRNA cargo of EVs can be dysregulated with ageing, including the increase of miR-183 in bone derived EVs (Davies et al, 2017). One candidate within this study has previously been associated with inflammaging is miR-146a, which is downregulated in aging endothelial cells (Vasa-Nicotera, 2011). In this study, in the brain tissue cohort, the neurologically healthy group were older than the AD group, though miR-146a was downregulated in AD. Whether this was in spite of age-associated changes in the neurologically healthy group, or whether the relationship with ageing differs in different tissues in the brain, remains to be understood. Further, there are multiple other candidates that don't have any known association with age, however, this is could be down to the tests not being performed to date. Therefore, current findings of miRNA changes in EVs in AD, will be taken with the uncertainty of whether age differences influence relative expression levels. However, future work will endeavour to use a larger cohort that is better matched for age, and candidates will be reassessed to determine their association with AD in a more controlled study.

Regarding the fibroblast model, while some points have been addressed to support the use of these cells in AD, there are still questions over the ability of fibroblasts to represent the changes to the extracellular vesicle biogenesis and packaging of miRNAs that may occur in the brain during AD. Further investigation will be needed to support this studies claims that fibroblast derived EVs can contribute as a biomarker for AD.

A challenge in the SH-SY5Y H2O2 model involves the amount of cell death as a result of oxidative stress, and the impact on EV release. As it is well characterised that oxidative stress triggers cell death due to apoptotic pathways (Ryter et al, 2006), and there is increasing understanding that cells release EVs under apoptotic and other cell death

conditions (Poon et al, 2019). While the concentration of H2O2 was optimised to produce a lower level of cell death (Zhang et al, 2007; Harvey et al, 2012), any release of apoptotic bodies may skew the characterisation of EVs (Frey and Gaipl, 2010), as well as their RNA content (Crescitelli et al, 2013), therefore, this must be taken into consideration against current findings.

Given that the SH-SY5Y cells were used in this study for initial trials of EV isolations, miRNA findings in this model are currently only from EVs isolated using membrane affinity columns. Therefore, as previously discussed, until these experiments are repeated using SEC based isolations with further characterisation, the changes in miRNAs may be more indicative of extracellular changes rather than just EV specific changes. Though, the findings remain interesting for supporting candidate biomarker analysis.

Conversely, the use of SEC as an isolation method for future biomarker testing in a clinical scenario is currently limited, given the number of hours required to get samples isolated from patients to a point where downstream testing can begin. Future methodology may aim for a compromise between purity and feasibility, where the biomarker candidate of interest is readily retained but not hidden behind contaminants. One example of promise is the use of microfluidics as a higher throughput affinity based isolation, in a 'lab on a chip' format, which would also increase accessibility to areas that do not have access to specialised equipment (Guo et al, 2018). Work will need to be done to compare constantly emerging isolation methodologies with robust protocols such as SEC to ensure that differences in findings due to methodology are limited.

5.11 Further work and future directions

Work continues to expand the n numbers of the cohorts involved in the study, to provide an increased representation of the heterogeneity of people living with AD and increase the power of the analysis to improve the ability to stratify populations based on factors such as sex.

The study will investigate an expanded panel of miRNA candidates, initially by validating the miRNAs that were identified in the RNA sequencing analysis with qPCR. This will add

further robustness to the findings, particularly in miRNAs that were trending towards dysregulation but not statistically powered. Furthermore, an extended set of samples will be run through small RNA sequencing, to expand the cohort's capability to probe for less expressed miRNAs that may not reach the reads count threshold to be investigated for differential analysis.

While this study had focused on fibroblast cell culture, expanding our use of the SH-SY5Y model would help investigate AD associated pathways further in relevance to EV miRNA markers, and would allow us to validate further some of the markers observed in the study. It is well categorised that oxidative stress is abundant in the pre-symptomatic stages of AD and may be a driver of the pathogenesis of the disease (Wang et al, 2014). Testing oxidative stress responses in the model will help us understand whether its contribution to the pathogenesis is mediated by an altered EV response, for example with the transport of miRNAs which promote further oxidative stress or neuroinflammation. Moreover, there is overlap with oxidative stress and perturbed autophagic function, which in turn might affect the endosomal pathways and therefore, EV secretion and packaging (Hamlett et al, 2017).

Other markers that will be tested in both fibroblast and SH-SY5Y models include tau and Aβ isoforms, to determine whether the AD fibroblasts do produce hallmark pathology as previously described (Citron et al, 1994), and if so, whether it is released in EVs, and whether it influences the secretion of EV associated cargo, including miRNAs.

Also, trialling a 3D SH-SY5Y culture set up may improve the ability of the cell model to recapitulate the brain in healthy and disease conditions (Taylor-Whiteley *et al*, 2019). Further, the physiological function of cells, including EV biogenesis, appears to alter in a 3D environment with more exposure to ECM (Thippabholta *et al*, 2019). Therefore, this could support any findings, and add a further dimension to investigation of EV miRNA changes in AD associated conditions.

A limiting factor in this study is that the fibroblast cultures and brain tissue were from different cohorts, therefore, it is difficult to determine whether changes in AD are comparable neuronally and peripherally, or whether the differences were due to biological variation between individuals. Therefore, biomarker studies can be enhanced by investigating multiple tissues/biofluids from the same individuals, and comparing whether

changes in EV biomarkers are consistent across the body. Developing a bank of peripheral tissue that supports current brain banks would greatly support these studies.

Furthermore, utilising other peripheral sources in this study would progress investigation of the candidate miRNA identified as dysregulated in AD conditions. Blood derived EVs have been presented as a good candidate for targeting future AD biomarkers, given they are a less invasive source of EVs and contain sub-populations of neuronally derived EVs (Kapogiannis et al, 2019). Potentially, longitudinal testing of neuronally derived EVs from the blood of individuals at risk of developing AD may identify specific changes that prelude disease onset.

Finally, several the candidate miRNAs identified in this study have been observed to interact with different pathways that are associated with increased risk of developing AD. Utilisation of some of these candidates in future studies may support stratification of populations within AD, which could support more specific drug targeting of different disease pathways, potentially improving clinical trial outcomes.

5.12 Conclusion

Overall, this project has been able to identify a set of miRNAs that are dysregulated in AD, which have potential to contribute as biomarkers. Interestingly, a subsection of miRNAs (miR-27a, miR-668 and miR-660) showed different expression patterns in AD between males and females. Whether they can contribute to diagnosis of AD in stratified populations, further investigation is required, however, given the association of these miRNAs with AD specific pathways, there is capability to support the future of personalised interventions.

6 Appendix

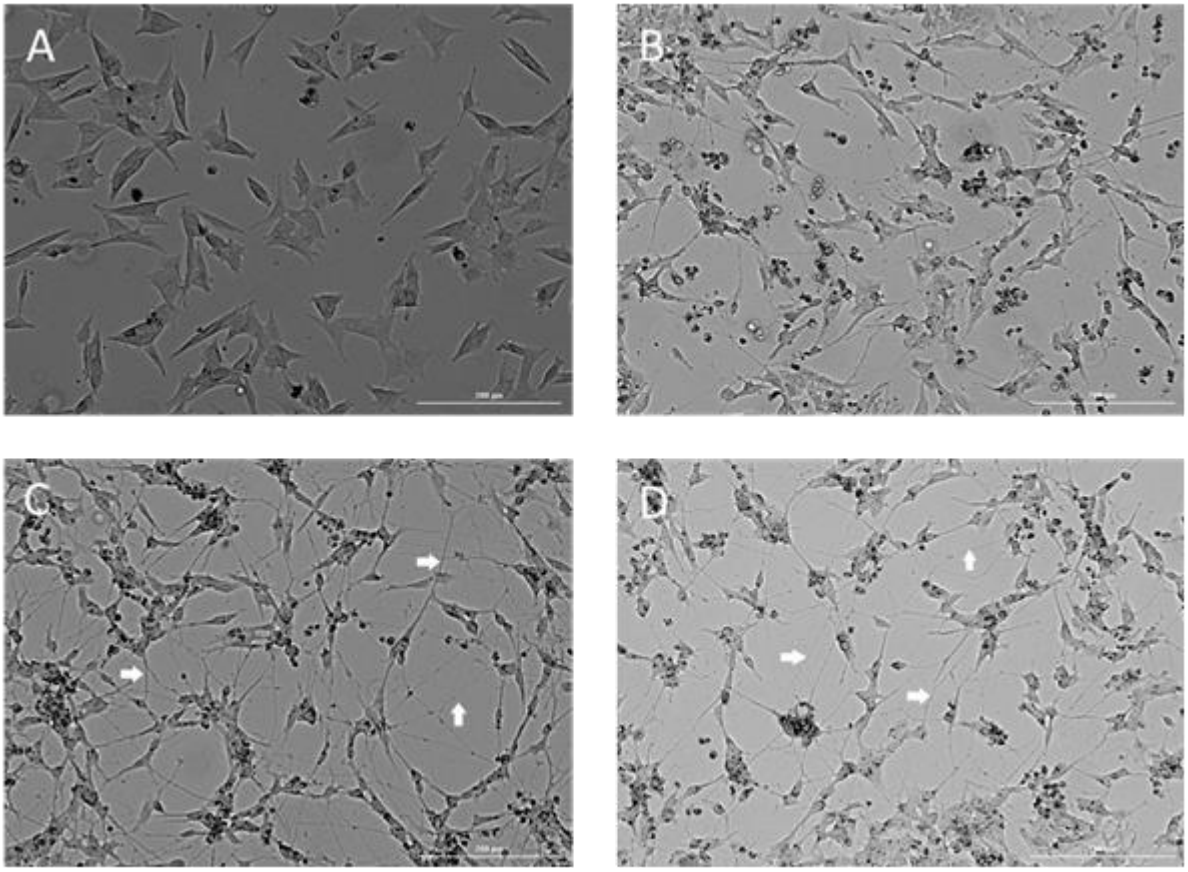

Figure 6.1. Morphological appearance of SH-SY5Y cells during the 21-day retinoic acid-based differentiation procedure.

A) Day 1, cells maintain the short, rounded phenotype of the neuroblastoma cell line. B) Day 10, cells show a more elongated body with some branching of neurites. C) Day 18, cells show further connection of neurites, arrows indicate examples of extended neurites. D) Day 21, cells display thorough connection of elongated neurites, arrows indicate examples of extended neurites. Scale-200 µm.

Table 6.1. Candidate miRNAs upregulated in EVs released from differentiated SH-SY5Y cells versus undifferentiated SH-SY5Y cells

Differentiated vs undifferentiated SH-SY5Y cells	
miRNAs Upregulated	Fold Change
miR-155-5p	5.17
miR-379-5p	4.08
miR-377-5p	4.69
miR-134-5p	2.03
miR-17-5p	7.26

Note: Values were normalised to miR-16-5p

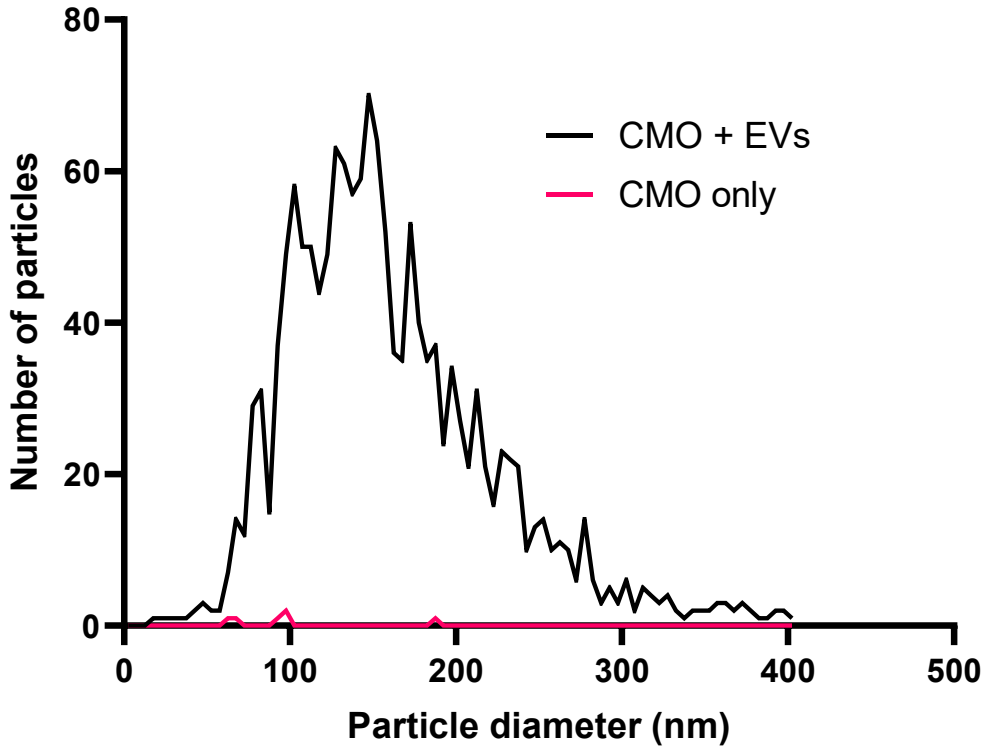

Figure 6.2. Comparison of size profiles of CMO only control vs CMO stained fibroblast EVs

Figure displays the control experiment of injecting CMO stain with PBS into NTA, compared against CMO and EV mix. Blue = CMO and EV mix, Grey = CMO only. Figure shows that CMO did not appear to aggregate during the timeframe that CMO staining of EVs took place in (1 hour).

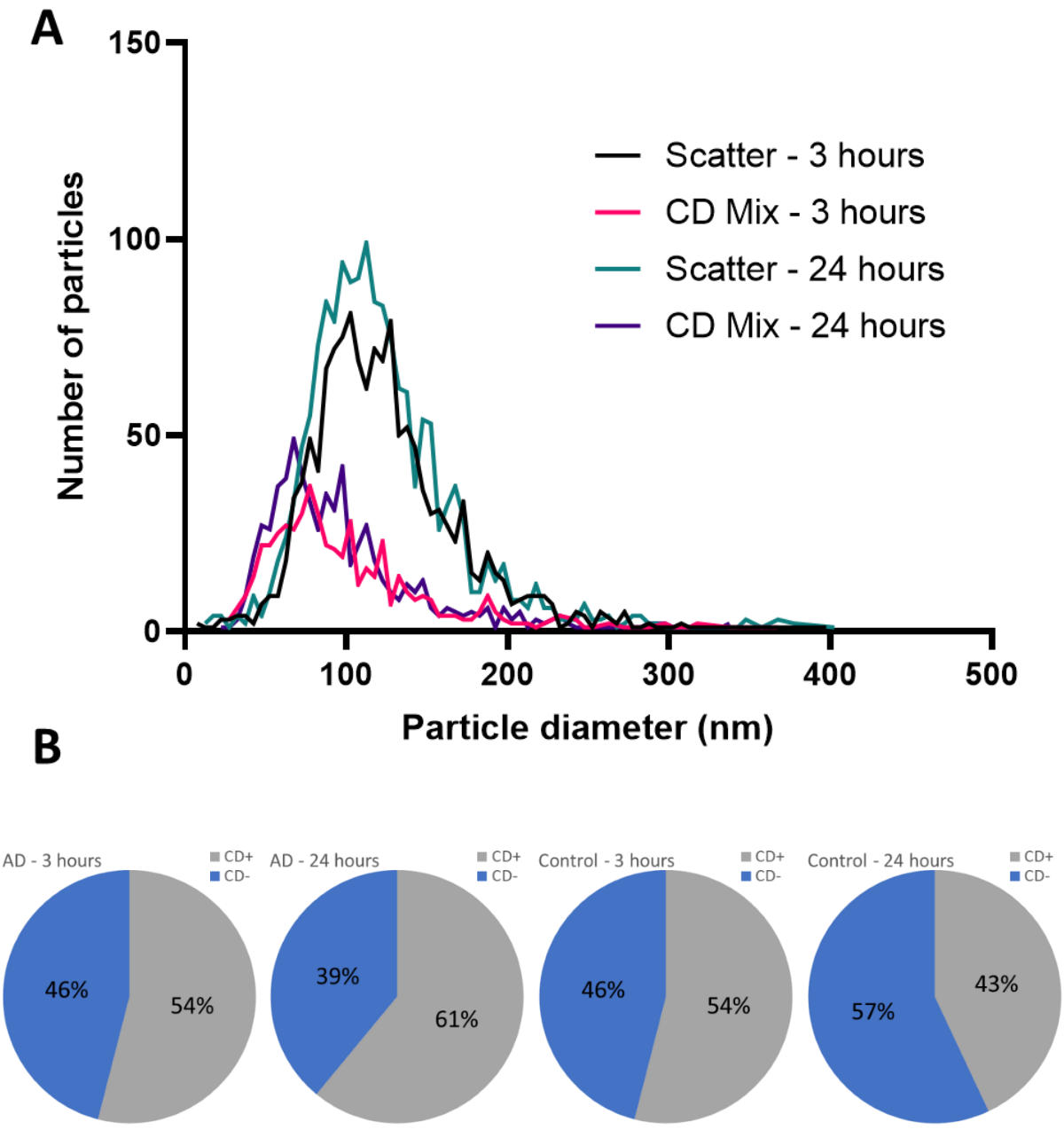

Figure 6.3. The CD9/63/81 antibody mix saturated the binding sites of the extracellular vesicles after 24 hours, though the majority of sites were tagged after 3 hours

NTA profile (Top) is shown in AD fibroblasts derived EVs. Bottom: AD - CD9/63/81 positive rate: 3 hours = 54%, 24 hours = 61%. EVs derived from neurological healthy control fibroblasts exhibiting no increase in percentage of CD9/63/81 positive EVs after 24 hours incubation (NTA profile not shown, CD9/63/81 positive rate: 3 hours = 54%, 24 hours = 43%). CD mix = CD9/63/81 positive EVs. Number absolute = absolute number of particles detected at each size threshold, increasing in 5 nm increments.

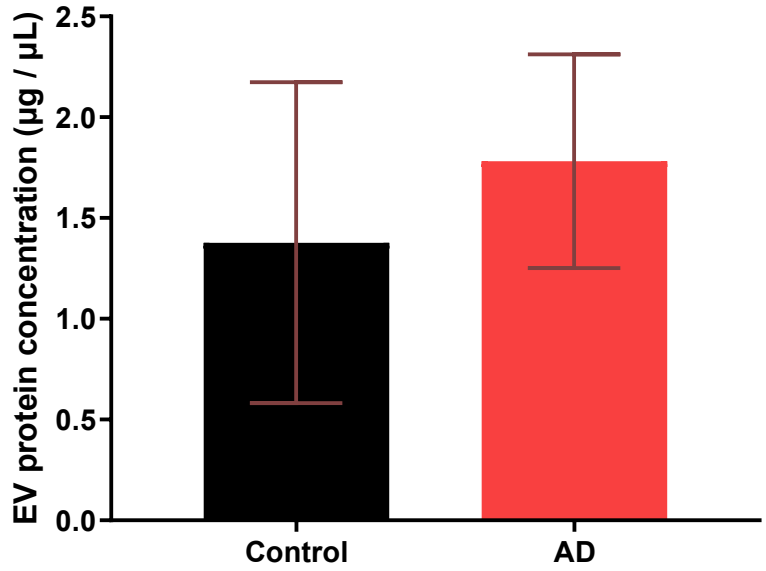

Figure 6.4. Total protein concentration of extracellular vesicles does not differ in Alzheimer's disease and neurological healthy control fibroblasts

EV protein concentration was measure by BCA assay. N = 3 (neurological healthy control) and 3 (AD) (Biological replicates). NS = not significant, P < 0.05, error bars = ±SD.

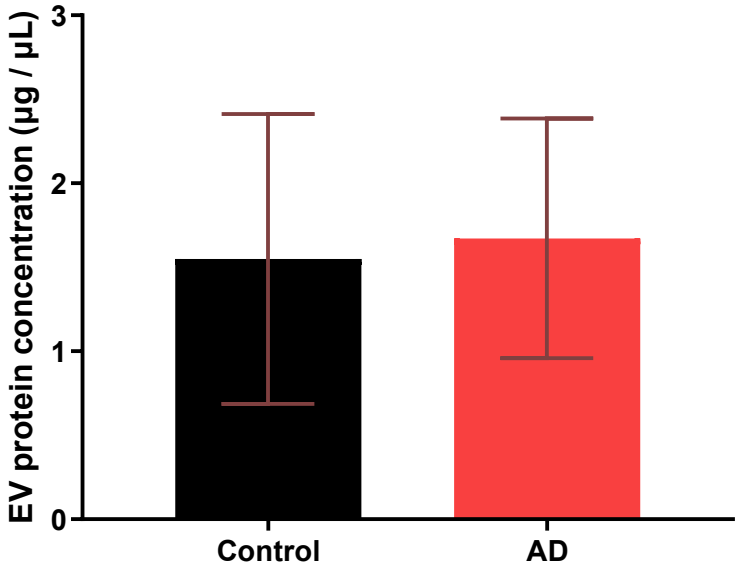

Figure 6.5. Total protein concentration of extracellular vesicles does not differ in Alzheimer's disease and neurological healthy control brain tissue

EV protein concentration was measure by BCA assay. N = 3 (control) and 3 (AD) (Biological replicates). NS = not significant, P < 0.05, error bars = ±SD.

Figure 6.6. Western blot – GM130 is not expressed in fibroblast derived sEVs

GM130 is observed below the 250 kDa band of the protein ladder. Lane 1) PageRuler Plus ladder. Lane 2) sEV – AG05809. Lane 3) sEV – AG08125. Lane 4) Gap. Lane 7) Cell lysate - AG08125.

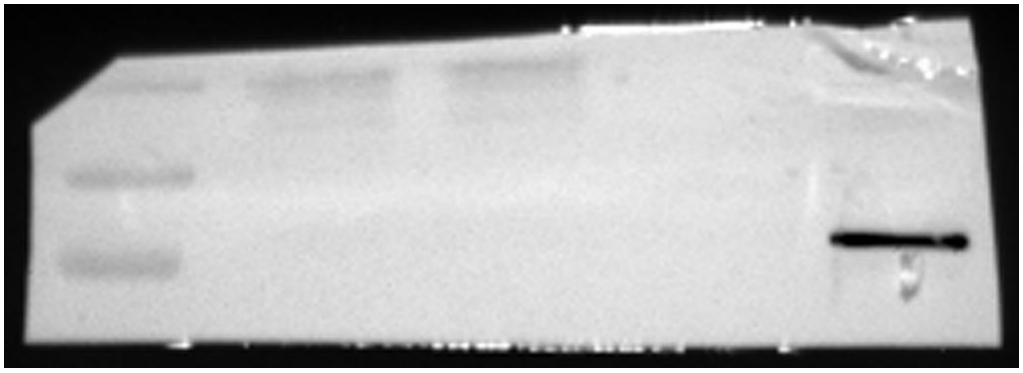

Figure 6.7. Western blot – Calnexin is not expressed in fibroblast derived sEVs

Calnexin is observed next to the 100 kDa band of the protein ladder. Lane 1) PageRuler Plus ladder. Lane 2) sEV – AG05809. Lane 3) sEV – AG08125. Lane 4) Gap. Lane 7) Cell lysate - AG08125.

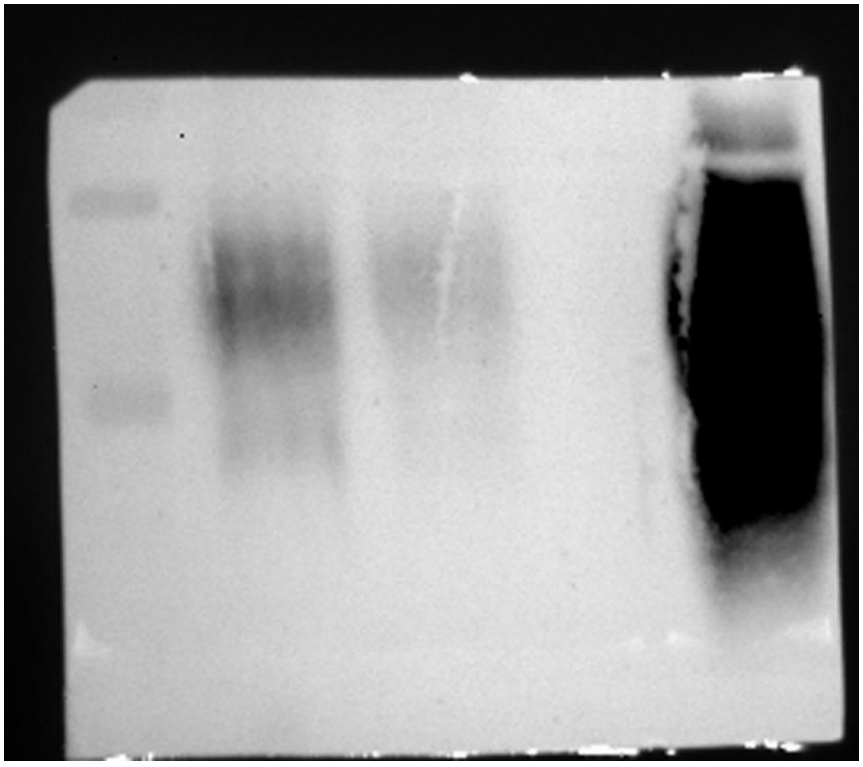

Figure 6.8. Western blot – CD63 expression in fibroblast derived sEVs

CD63 is observed between the 55 and 35 kDa bands of the protein ladder. Lane 1) PageRuler Plus ladder. Lane 2) sEV – AG05809. Lane 3) sEV – AG08125. Lane 4) Gap. Lane 7) Cell lysate - AG08125.

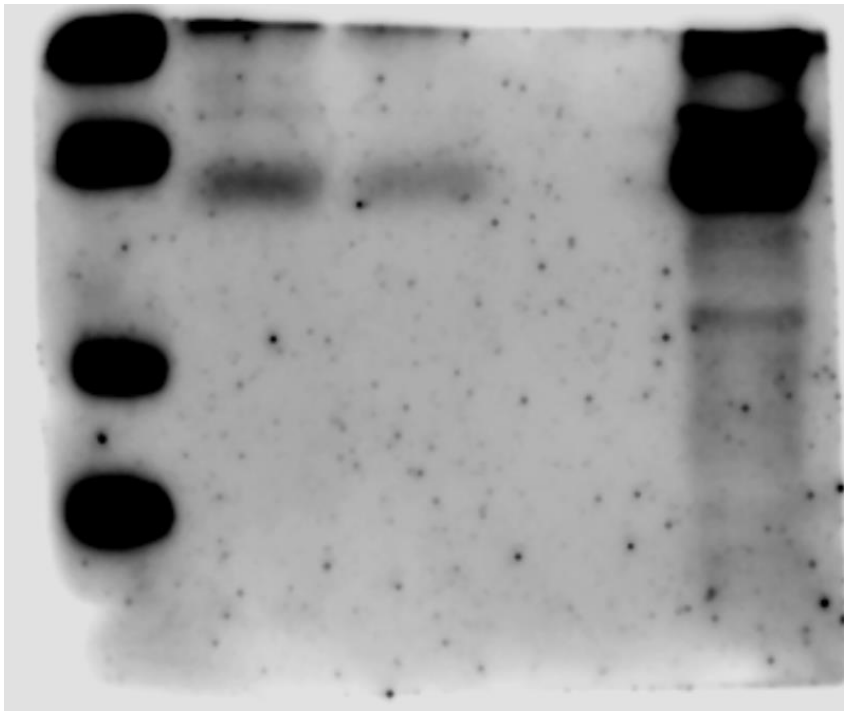

Figure 6.9. Western blot – Flotillin 1 expression in fibroblast derived sEVs

Flotillin 1 is observed below the 55 kDa band of the protein ladder. Lane 1) PageRuler Plus ladder. Lane 2) sEV – AG05809. Lane 3) sEV – AG08125. Lane 4) Gap. Lane 7) Cell lysate - AG08125.

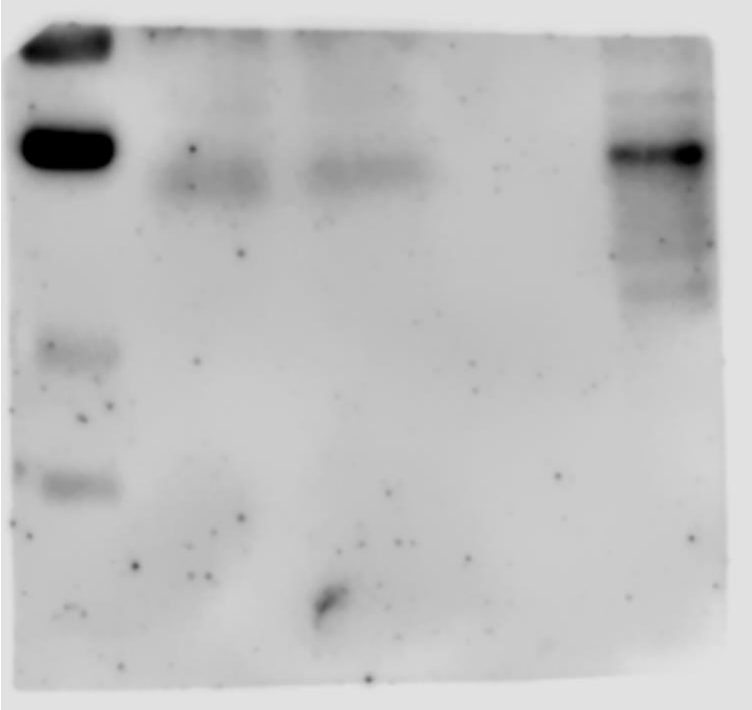

Figure 6.10. Western blot – TSG-101 expression in fibroblast derived sEVs

TSG-101 is observed below the 55 kDa band of the protein ladder. Lane 1) PageRuler Plus ladder. Lane 2) sEV – AG05809. Lane 3) sEV – AG08125. Lane 4) Gap. Lane 7) Cell lysate - AG08125.

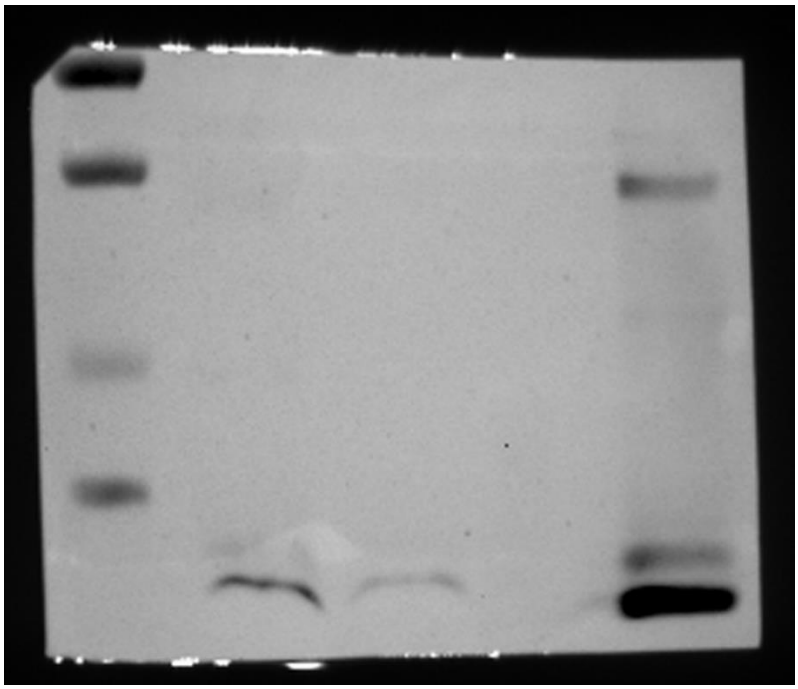

Figure 6.11. Western blot – CD9 expression in fibroblast derived sEVs

CD9 is observed below the 25 kDa band of the protein ladder. Lane 1) PageRuler Plus ladder. Lane 2) sEV – AG05809. Lane 3) sEV – AG08125. Lane 4) Gap. Lane 7) Cell lysate - AG08125.

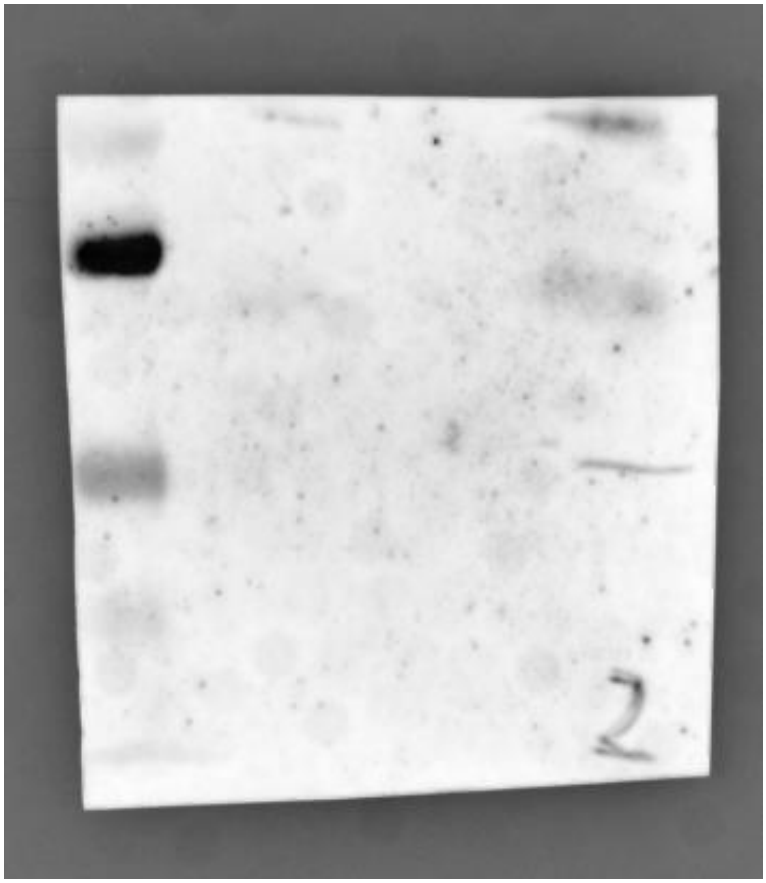

Figure 6.12. Western blot – CD81 was not expressed in fibroblast derived sEVs

CD81 is observed below the 25 kDa band of the protein ladder. Lane 1) PageRuler Plus ladder. Lane 2) sEV – AG05809. Lane 3) sEV – AG08125. Lane 4) Gap. Lane 7) Cell lysate - AG08125.

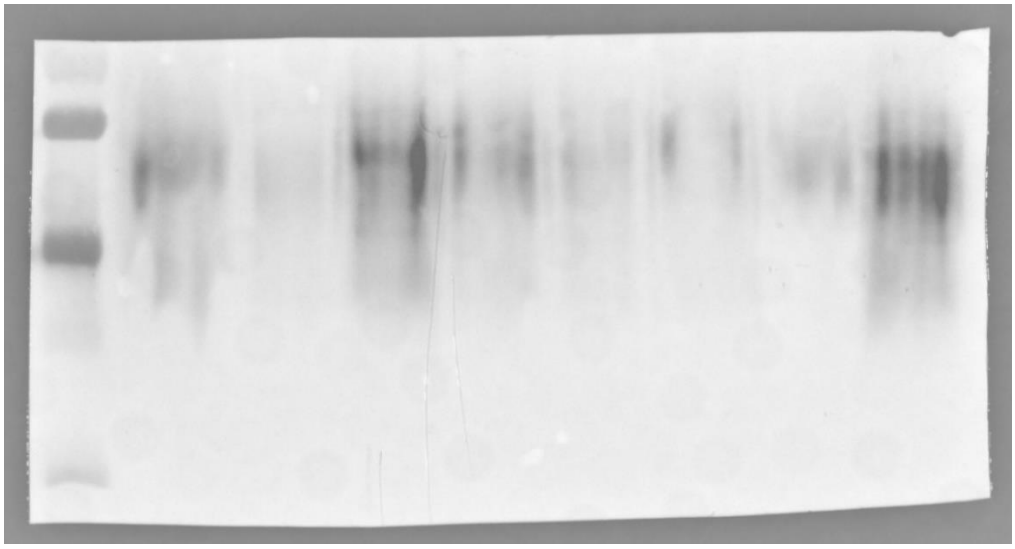

Figure 6.13. CD63 expresses in sEVs derived from fibroblasts from all cases, but is not differentially expressed in AD

CD63 is observed between the 55 and 35 kDa bands of the protein ladder. Lane 1) PageRuler Plus ladder. Lane 2) sEV – AG05809. Lane 3) sEV – AG06869. Lane 4) sEV – AG07872. Lane 5) sEV – AG08125. Lane 6) sEV – AG08379. Lane 7) sEV – AG08517. Lane 8) Cell lysate – AG05809. Lane 9) Cell lysate – AG08125. Band intensities quantified using ImageJ, AD cases relative expression was 1.58 (±0.79) fold greater than neurological healthy control cases (1 ± 0.41). T-test: P = 0.16.

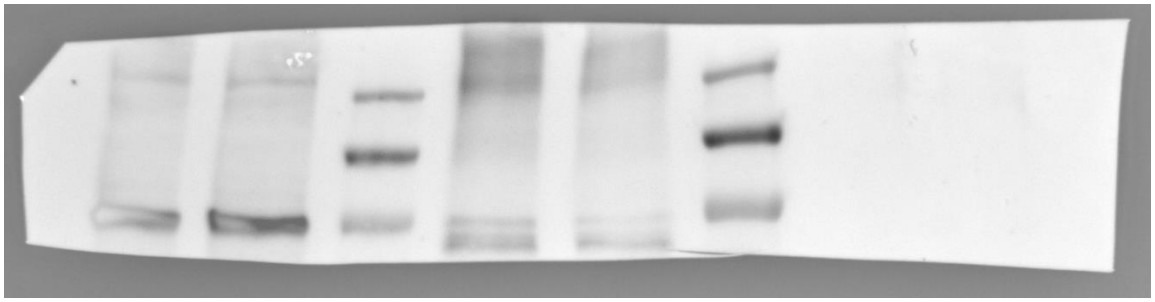

Figure 6.14. Western blot – GM130 is not expressed in brain derived sEVs

GM130 is observed below the 250 kDa band of the protein ladder. Lane 1) Brain homogenate + collagenase – AD sample 1. Lane 2) Brain homogenate + collagenase – control sample 1. Lane 3) PageRuler Plus ladder. Lane 4) Brain homogenate – AD sample 1. Lane 5) Brain homogenate – control sample 1. Lane 6) PageRuler Plus ladder. Lane 7) sEV – AD sample 1. Lane 8) sEV– Control sample 1.

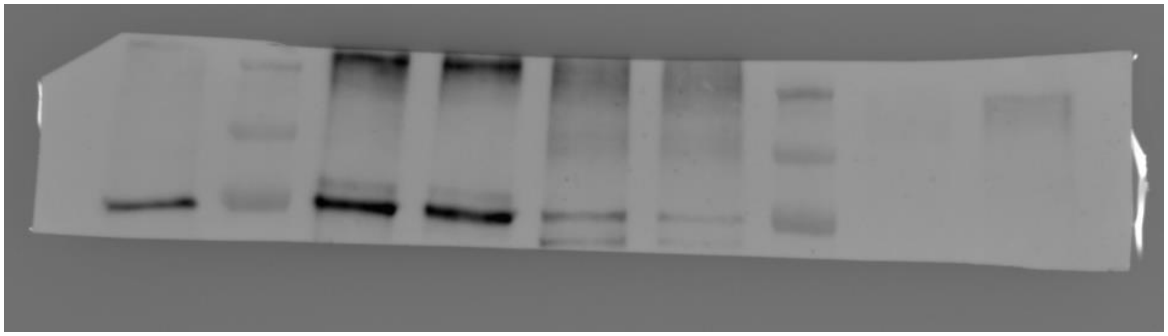

Figure 6.15. Western blot – Calnexin is not expressed in brain derived sEVs

Calnexin is observed next to the 100 kDa band of the protein ladder. Lane 1) Fibroblast cell lysate – AG08125 (used for initial loading control). Lane 2) PageRuler Plus ladder. Lane 3) Brain homogenate + collagenase – AD sample 1. Lane 4) Brain homogenate + collagenase – Control sample 1. Lane 5) Brain homogenate – AD sample 1. Lane 6) Brain homogenate – Control sample 1. Lane 7) PageRuler Plus ladder. Lane 8) sEV – AD sample 1. Lane 9) sEV– Control sample 1.

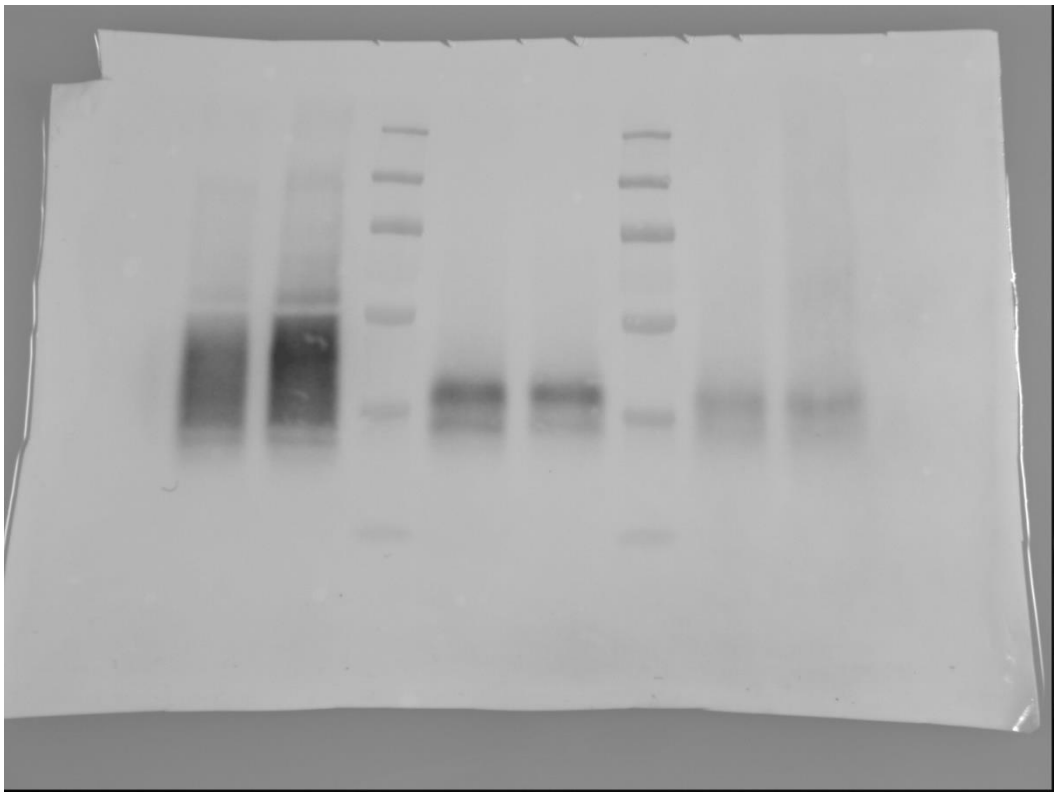

Figure 6.16. Western blot – CD63 expression in brain derived sEVs

CD63 is observed between the 55 and 35 kDa bands of the protein ladder. Lane 1) Brain homogenate + collagenase – AD sample 1. Lane 2) Brain homogenate + collagenase – Control sample 1. Lane 3) PageRuler Plus ladder. Lane 4) Brain homogenate – AD sample 1. Lane 5) Brain homogenate – Control sample 1. Lane 6) PageRuler Plus ladder. Lane 7) sEV – AD sample 1. Lane 8) sEV– Control sample 1.

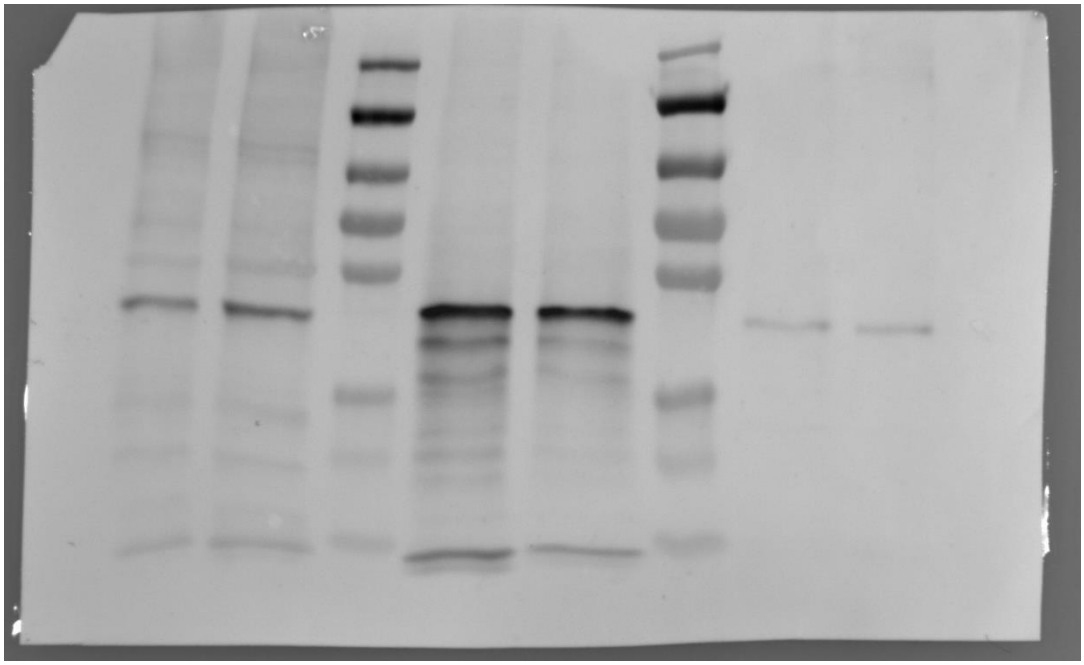

Figure 6.17. Western blot – Flotillin 1 expression in brain derived sEVs

Flotillin 1 is observed below the 55 kDa band of the protein ladder. Lane 1) Brain homogenate + collagenase – AD sample 1. Lane 2) Brain homogenate + collagenase – Control sample 1. Lane 3) PageRuler Plus ladder. Lane 4) Brain homogenate – AD sample 1. Lane 5) Brain homogenate – Control sample 1. Lane 6) PageRuler Plus ladder. Lane 7) sEV – AD sample 1. Lane 8) sEV– Control sample 1.

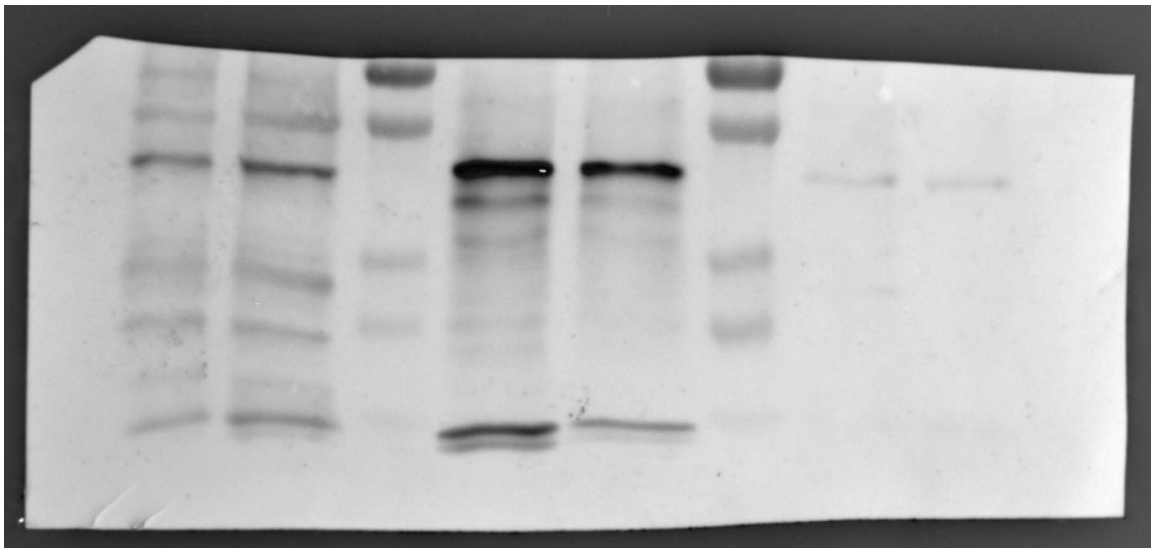

Figure 6.18. Western blot – TSG-101 expression in brain derived sEVs

TSG-101 is observed below the 55 kDa band of the protein ladder. Lane 1) Brain homogenate + collagenase – AD sample 1. Lane 2) Brain homogenate + collagenase – Control sample 1. Lane 3) PageRuler Plus ladder. Lane 4) Brain homogenate – AD sample 1. Lane 5) Brain homogenate – Control sample 1. Lane 6) PageRuler Plus ladder. Lane 7) sEV – AD sample 1. Lane 8) sEV– Control sample 1.

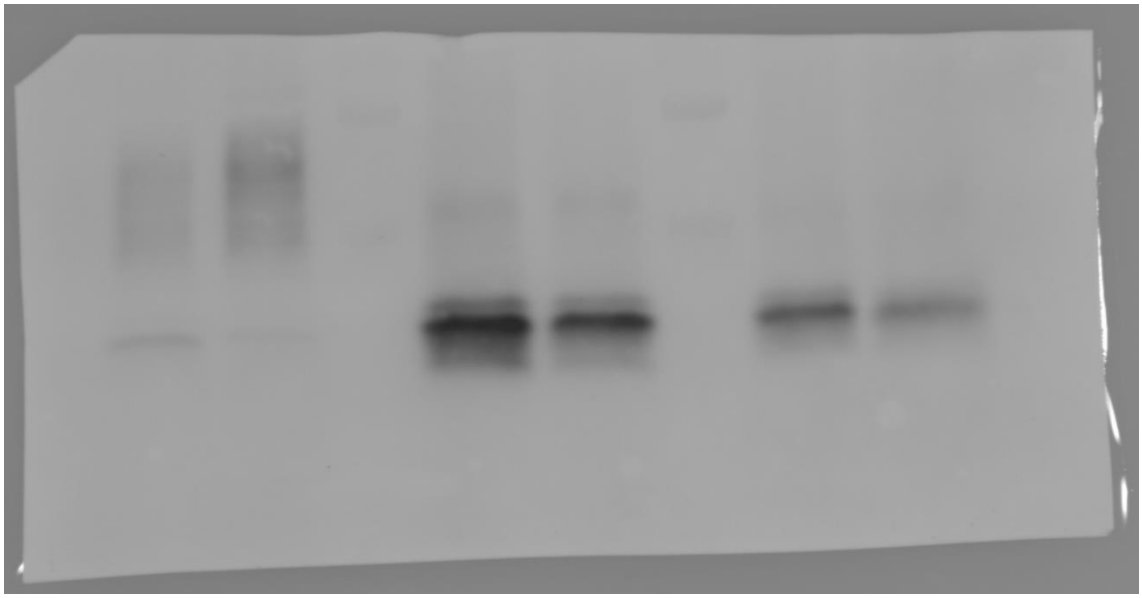

Figure 6.19. Western blot – CD9 expression in brain derived sEVs

CD9 is observed below the 25 kDa band of the protein ladder. Lane 1) Brain homogenate + collagenase – AD sample 1. Lane 2) Brain homogenate + collagenase – Control sample 1. Lane 3) PageRuler Plus ladder. Lane 4) Brain homogenate – AD sample 1. Lane 5) Brain homogenate – Control sample 1. Lane 6) PageRuler Plus ladder. Lane 7) sEV – AD sample 1. Lane 8) sEV– Control sample 1.

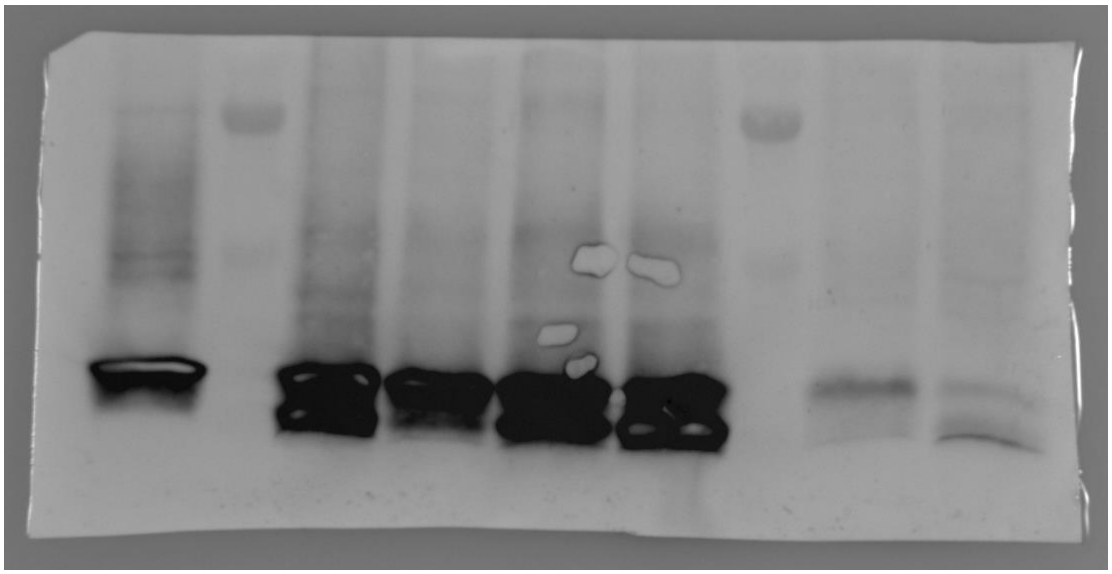

Figure 6.20. Western blot – CD81 expression in brain derived sEVs

CD81 is observed below the 25 kDa band of the protein ladder. Lane 1) Fibroblast cell lysate – AG08125 (used for initial loading control). Lane 2) PageRuler Plus ladder. Lane 3) Brain homogenate + collagenase – AD sample 1. Lane 4) Brain homogenate + collagenase – Control sample 1. Lane 5) Brain homogenate – AD sample 1. Lane 6) Brain homogenate – Control sample 1. Lane 7) PageRuler Plus ladder. Lane 8) sEV – AD sample 1. Lane 9) sEV– Control sample 1.

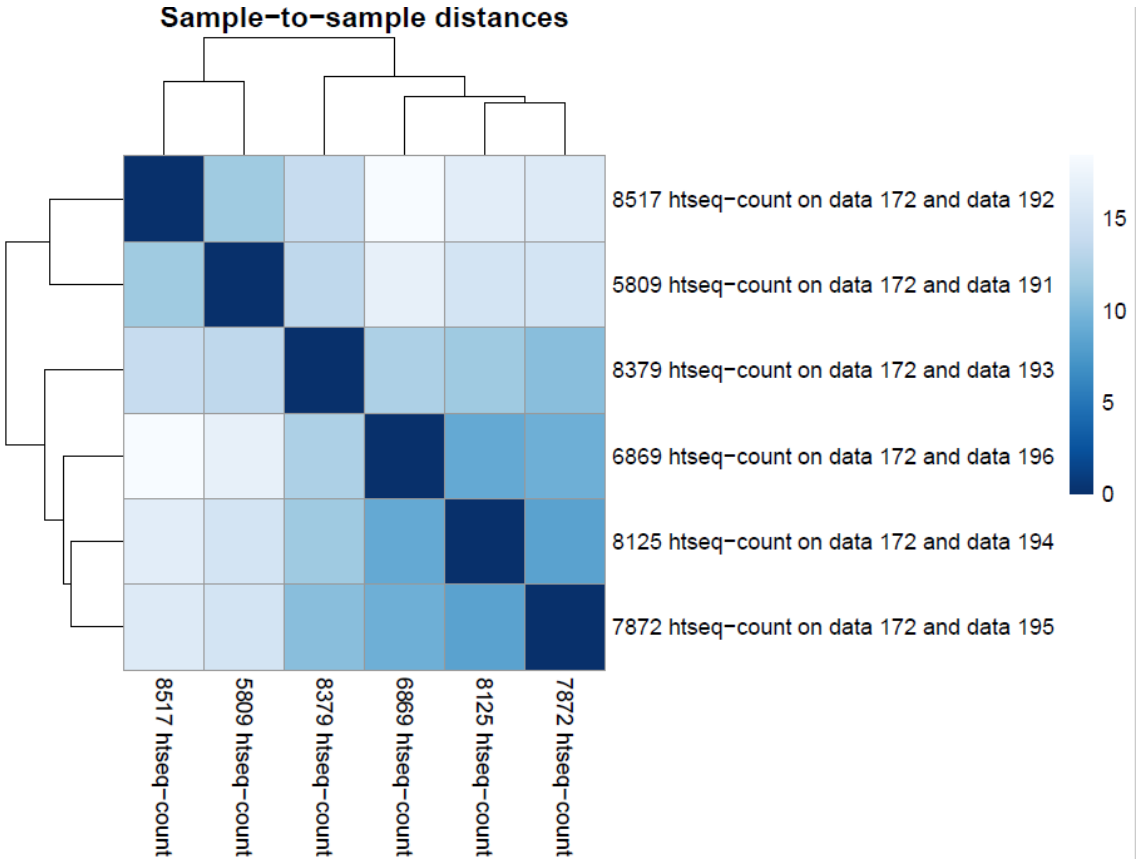

Figure 6.21. Biological variation between individual fibroblast sEV samples was high

Sample-sample distances plot displays the level of similarity between individual samples in a cohort, while attempting to perform hierarchical clustering on similar samples. Blue = correlation, darker shade = increased correlation.

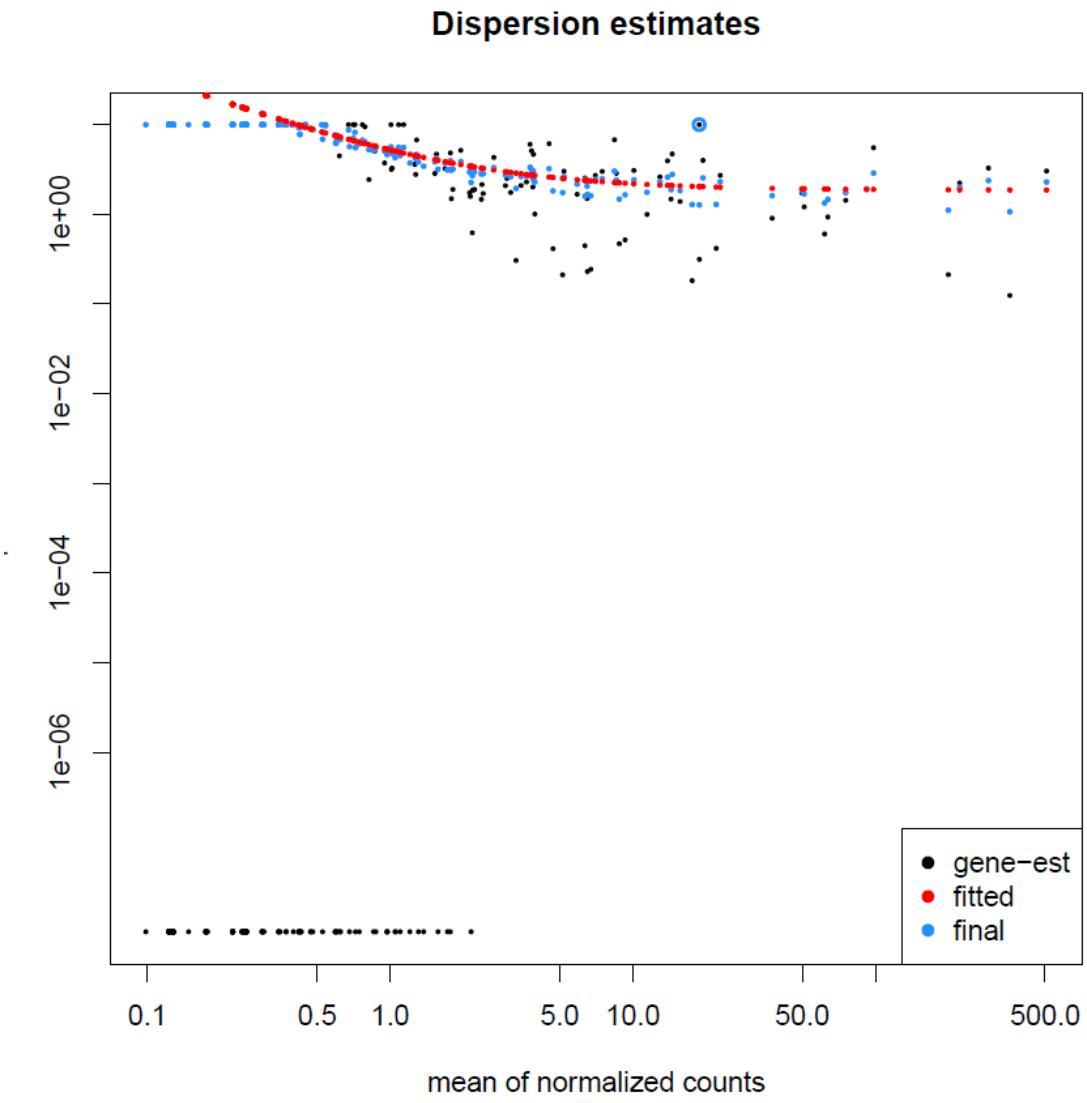

Figure 6.22. Dispersion estimates of sequencing reads of fibroblast sEVs

Plot of amount of read counts observed for an individual miRNA against the variability/dispersion of the miRNA in the tested populations. One point = one miRNA. Black = unfitted comparisons, Red = fitted correlation based on all variances of miRNAs, Blue = fitted comparisons adjusted based on fitted correlation.

7 References

2018 Alzheimer's disease facts and figures. (2018). Alzheimer's & Dementia, 14(3), 367–429. https://doi.org/10.1016/j.jalz.2018.02.001

Abdulrahman, B. A., Abdelaziz, D. H., & Schatzl, H. M. (2018). Autophagy regulates exosomal release of prions in neuronal cells. The Journal of Biological Chemistry, 293(23), 8956–8968. https://doi.org/10.1074/jbc.RA117.000713

Alois Alzheimer (1907), Translated by L. Jarvik and H. Greenson (1987). About a peculiar disease of the cerebral cortex. Alzheimer disease and associated disorders, 1(1), 3–8.

Absalon, S., Kochanek, D. M., Raghavan, V., & Krichevsky, A. M. (2013). MiR-26b, Upregulated in Alzheimer's Disease, Activates Cell Cycle Entry, Tau-Phosphorylation, and Apoptosis in Postmitotic Neurons. The Journal of Neuroscience, 33(37), 14645–14659. https://doi.org/10.1523/JNEUROSCI.1327-13.2013

Agholme, L., Lindström, T., Kågedal, K., Marcusson, J., & Hallbeck, M. (2010). An In Vitro Model for Neuroscience: Differentiation of SH-SY5Y Cells into Cells with Morphological and Biochemical Characteristics of Mature Neurons. Journal of Alzheimer's Disease, 20(4), 1069–1082. https://doi.org/10.3233/JAD-2010-091363

Agosta, F., Libera, D. D., Spinelli, E. G., Finardi, A., Canu, E., Bergami, A., Chiavetto, L. B., Baronio, M., Comi, G., Martino, G., Matteoli, M., Magnani, G., Verderio, C., & Furlan, R. (2014). Myeloid microvesicles in cerebrospinal fluid are associated with myelin damage and neuronal loss in mild cognitive impairment and Alzheimer disease. Annals of Neurology, 76(6), 813–825. https://doi.org/10.1002/ana.24235

Agostini, M., Tucci, P., Steinert, J. R., Shalom-Feuerstein, R., Rouleau, M., Aberdam, D., Forsythe, I. D., Young, K. W., Ventura, A., Concepcion, C. P., Han, Y.-C., Candi, E., Knight, R. A., Mak, T. W., & Melino, G. (2011). MicroRNA-34a regulates neurite outgrowth, spinal morphology, and function. Proceedings of the National Academy of Sciences of the United States of America, 108(52), 21099–21104. https://doi.org/10.1073/pnas.1112063108

Albanese, M., Chen, Y.-F. A., Hüls, C., Gärtner, K., Tagawa, T., Mejias-Perez, E., Keppler, O. T., Göbel, C., Zeidler, R., Shein, M., Schütz, A. K., & Hammerschmidt, W. (2021). MicroRNAs are minor constituents of extracellular vesicles that are rarely delivered to target cells. PLOS Genetics, 17(12), e1009951. https://doi.org/10.1371/journal.pgen.1009951

Alexandrov, P. N., Dua, P., Hill, J. M., Bhattacharjee, S., & Zhao, Y. (n.d.). MicroRNA (miRNA) speciation in Alzheimer's disease.

Ali, T., Kim, T., Rehman, S. U., Khan, M. S., Amin, F. U., Khan, M., Ikram, M., & Kim, M. O. (2018). Natural Dietary Supplementation of Anthocyanins via PI3K/Akt/Nrf2/HO-1 Pathways Mitigate Oxidative Stress, Neurodegeneration, and Memory Impairment in a Mouse Model of Alzheimer's Disease. Molecular Neurobiology, 55(7), 6076–6093. https://doi.org/10.1007/s12035-017-0798-6

Alvarez-Erviti, L., Seow, Y., Yin, H., Betts, C., Lakhal, S., & Wood, M. J. A. (2011). Delivery of siRNA to the mouse brain by systemic injection of targeted exosomes. Nature Biotechnology, 29(4), 341–345. https://doi.org/10.1038/nbt.1807

An, K., Klyubin, I., Kim, Y., Jung, J. H., Mably, A. J., O'Dowd, S. T., Lynch, T., Kanmert, D., Lemere, C. A., Finan, G. M., Park, J. W., Kim, T.-W., Walsh, D. M., Rowan, M. J., & Kim, J.-H. (2013). Exosomes neutralize synaptic-plasticity-disrupting activity of Aβ assemblies in vivo. Molecular Brain, 6, 47. https://doi.org/10.1186/1756-6606-6-47

Andreu, Z., & Yáñez-Mó, M. (2014). Tetraspanins in Extracellular Vesicle Formation and Function. Frontiers in Immunology, 5. https://www.frontiersin.org/articles/10.3389/fimmu.2014.00442

Angelopoulou, E., Paudel, Y. N., Shaikh, M. F., & Piperi, C. (2020). Flotillin: A Promising Biomarker for Alzheimer's Disease. Journal of Personalized Medicine, 10(2), Article 2. https://doi.org/10.3390/jpm10020020

Angom, R. S., Wang, Y., Wang, E., Pal, K., Bhattacharya, S., Watzlawik, J. O., Rosenberry, T. L., Das, P., & Mukhopadhyay, D. (2019). VEGF receptor-1 modulates amyloid β 1–42 oligomer-induced senescence in brain endothelial cells. The FASEB Journal, 33(3), 4626–4637. https://doi.org/10.1096/fj.201802003R

Annese, A., Manzari, C., Lionetti, C., Picardi, E., Horner, D. S., Chiara, M., Caratozzolo, M. F., Tullo, A., Fosso, B., Pesole, G., & D'Erchia, A. M. (2018). Whole transcriptome profiling of Late-Onset Alzheimer's Disease patients provides insights into the molecular changes involved in the disease. Scientific Reports, 8(1), 4282. https://doi.org/10.1038/s41598-018-22701-2

Ansari, A., Maffioletti, E., Milanesi, E., Marizzoni, M., Frisoni, G. B., Blin, O., Richardson, J. C., Bordet, R., Forloni, G., Gennarelli, M., & Bocchio-Chiavetto, L. (2019). MiR-146a and miR-181a are involved in the progression of mild cognitive impairment to Alzheimer's disease. Neurobiology of Aging, 82, 102–109. https://doi.org/10.1016/j.neurobiolaging.2019.06.005

Arab, T., Mallick, E. R., Huang, Y., Dong, L., Liao, Z., Zhao, Z., Gololobova, O., Smith, B., Haughey, N. J., Pienta, K. J., Slusher, B. S., Tarwater, P. M., Tosar, J. P., Zivkovic, A. M., Vreeland, W. N., Paulaitis, M. E., & Witwer, K. W. (2021). Characterization of extracellular vesicles and synthetic nanoparticles with four orthogonal single-particle analysis platforms. Journal of Extracellular Vesicles, 10(6), e12079. https://doi.org/10.1002/jev2.12079

Arakhamia, T., Lee, C. E., Carlomagno, Y., Kumar, M., Duong, D. M., Wesseling, H., Kundinger, S. R., Wang, K., Williams, D., DeTure, M., Dickson, D. W., Cook, C. N., Seyfried, N. T., Petrucelli, L., Steen, J. A., & Fitzpatrick, A. W. P. (2020). Posttranslational Modifications Mediate the Structural Diversity of Tauopathy Strains. Cell, 180(4), 633-644.e12. https://doi.org/10.1016/j.cell.2020.01.027

Arber, C., Lovejoy, C., & Wray, S. (2017). Stem cell models of Alzheimer's disease: Progress and challenges. Alzheimer's Research & Therapy, 9(1), 42. https://doi.org/10.1186/s13195-017-0268-4

Arena, A., Iyer, A. M., Milenkovic, I., Kovacs, G. G., Ferrer, I., Perluigi, M., & Aronica, E. (2017). Developmental Expression and Dysregulation of miR-146a and miR-155 in Down's Syndrome and Mouse Models of Down's Syndrome and Alzheimer's Disease. Current Alzheimer Research, 14(12), 1305–1317. https://doi.org/10.2174/1567205014666170706112701

Arimon, M., Takeda, S., Post, K. L., Svirsky, S., Hyman, B. T., & Berezovska, O. (2015). Oxidative stress and lipid peroxidation are upstream of amyloid pathology. Neurobiology of Disease, 84, 109–119. https://doi.org/10.1016/j.nbd.2015.06.013

Asai, H., Ikezu, S., Tsunoda, S., Medalla, M., Luebke, J., Haydar, T., Wolozin, B., Butovsky, O., Kügler, S., & Ikezu, T. (2015). Depletion of microglia and inhibition of exosome synthesis halt tau propagation. Nature Neuroscience, 18(11), 1584–1593. https://doi.org/10.1038/nn.4132

Aswad, H., Jalabert, A., & Rome, S. (2016). Depleting extracellular vesicles from fetal bovine serum alters proliferation and differentiation of skeletal muscle cells in vitro. BMC Biotechnology, 16(1), 32. https://doi.org/10.1186/s12896-016-0262-0

Badhwar, A., & Haqqani, A. S. (2020). Biomarker potential of brain-secreted extracellular vesicles in blood in Alzheimer's disease. Alzheimer's & Dementia : Diagnosis, Assessment & Disease Monitoring, 12(1), e12001. https://doi.org/10.1002/dad2.12001

Bahrini, I., Song, J., Diez, D., & Hanayama, R. (2015). Neuronal exosomes facilitate synaptic pruning by up-regulating complement factors in microglia. Scientific Reports, 5. https://doi.org/10.1038/srep07989

Baker, S., Polanco, J. C., & Götz, J. (2016). Extracellular Vesicles Containing P301L Mutant Tau Accelerate Pathological Tau Phosphorylation and Oligomer Formation but Do Not Seed Mature Neurofibrillary Tangles in ALZ17 Mice. Journal of Alzheimer's Disease, 54(3), 1207–1217. https://doi.org/10.3233/JAD-160371

Balaj, L., Atai, N. A., Chen, W., Mu, D., Tannous, B. A., Breakefield, X. O., Skog, J., & Maguire, C. A. (2015). Heparin affinity purification of extracellular vesicles. Scientific Reports, 5, 10266. https://doi.org/10.1038/srep10266

Balastik, M., Ferraguti, F., Pires-da Silva, A., Lee, T. H., Alvarez-Bolado, G., Lu, K. P., & Gruss, P. (2008). Deficiency in ubiquitin ligase TRIM2 causes accumulation of neurofilament light chain and neurodegeneration. Proceedings of the National Academy of Sciences, 105(33), 12016–12021. https://doi.org/10.1073/pnas.0802261105

Balusu, S., Wonterghem, E. V., Rycke, R. D., Raemdonck, K., Stremersch, S., Gevaert, K., Brkic, M., Demeestere, D., Vanhooren, V., Hendrix, A., Libert, C., & Vandenbroucke, R. E. (2016). Identification of a novel mechanism of blood–brain communication during peripheral inflammation via choroid plexus-derived extracellular vesicles. EMBO Molecular Medicine, e201606271. https://doi.org/10.15252/emmm.201606271

Banzhaf-Strathmann, J., Benito, E., May, S., Arzberger, T., Tahirovic, S., Kretzschmar, H., Fischer, A., & Edbauer, D. (2014). MicroRNA-125b induces tau hyperphosphorylation and cognitive deficits in Alzheimer's disease. The EMBO Journal, 33(15), 1667–1680. https://doi.org/10.15252/embj.201387576

Barr, T. L., Latour, L. L., Lee, K.-Y., Schaewe, T. J., Luby, M., Chang, G. S., El-Zammar, Z., Alam, S., Hallenbeck, J. M., Kidwell, C. S., & Warach, S. (2010). Blood–Brain Barrier Disruption in Humans Is Independently Associated With Increased Matrix Metalloproteinase-9. Stroke, 41(3), e123–e128. https://doi.org/10.1161/STROKEAHA.109.570515

Barteczek, P., Li, L., Ernst, A.-S., Böhler, L.-I., Marti, H. H., & Kunze, R. (2017). Neuronal HIF-1α and HIF-2α deficiency improves neuronal survival and sensorimotor function in the early acute phase after ischemic stroke. Journal of Cerebral Blood Flow & Metabolism, 37(1), 291–306. https://doi.org/10.1177/0271678X15624933

Basso, M., & Bonetto, V. (2016). Extracellular Vesicles and a Novel Form of Communication in the Brain. Frontiers in Neuroscience, 10. https://doi.org/10.3389/fnins.2016.00127

Bastida, E., Ordinas, A., Escolar, G., & Jamieson, G. A. (1984). Tissue factor in microvesicles shed from U87MG human glioblastoma cells induces coagulation, platelet aggregation, and thrombogenesis. Blood, 64(1), 177–184.

Baulina, N., Kiselev, I., Kozin, M., Kabaeva, A., Boyko, A., & Favorova, O. (2022). Male-specific coordinated changes in expression of miRNA genes, but not other genes within the DLK1-DIO3 locus in multiple sclerosis. Gene, 836, 146676. https://doi.org/10.1016/j.gene.2022.146676

Bays, H. E., Ballantyne, C. M., Braeckman, R. A., Stirtan, W. G., & Soni, P. N. (2013). Icosapent Ethyl, a Pure Ethyl Ester of Eicosapentaenoic Acid: Effects on Circulating Markers of Inflammation from the MARINE and ANCHOR Studies. American Journal of Cardiovascular Drugs, 13(1), 37–46. https://doi.org/10.1007/s40256-012-0002-3

Bellingham, S. A., Coleman, B. M., & Hill, A. F. (2012). Small RNA deep sequencing reveals a distinct miRNA signature released in exosomes from prion-infected neuronal cells. Nucleic Acids Research, 40(21), 10937–10949. https://doi.org/10.1093/nar/gks832

Belloy, M. E., Napolioni, V., & Greicius, M. D. (2019). A Quarter Century of APOE and Alzheimer's Disease: Progress to Date and the Path Forward. Neuron, 101(5), 820–838. https://doi.org/10.1016/j.neuron.2019.01.056

Ben Khedher, M. R., Haddad, M., Laurin, D., & Ramassamy, C. (2021). Effect of APOE ε4 allele on levels of apolipoproteins E, J, and D, and redox signature in circulating extracellular vesicles from cognitively impaired

with no dementia participants converted to Alzheimer's disease. Alzheimer's & Dementia: Diagnosis, Assessment & Disease Monitoring, 13(1), e12231. https://doi.org/10.1002/dad2.12231

Bennett, R. E., DeVos, S. L., Dujardin, S., Corjuc, B., Gor, R., Gonzalez, J., Roe, A. D., Frosch, M. P., Pitstick, R., Carlson, G. A., & Hyman, B. T. (2017). Enhanced Tau Aggregation in the Presence of Amyloid β. The American Journal of Pathology, 187(7), 1601–1612. https://doi.org/10.1016/j.ajpath.2017.03.011

Benussi, L., Ciani, M., Tonoli, E., Morbin, M., Palamara, L., Albani, D., Fusco, F., Forloni, G., Glionna, M., Baco, M., Paterlini, A., Fostinelli, S., Santini, B., Galbiati, E., Gagni, P., Cretich, M., Binetti, G., Tagliavini, F., Prosperi, D., … Ghidoni, R. (2016). Loss of exosomes in progranulin-associated frontotemporal dementia. Neurobiology of Aging, 40, 41–49. https://doi.org/10.1016/j.neurobiolaging.2016.01.001

Bhatt, D. L., Hull, M. A., Song, M., Van Hulle, C., Carlsson, C., Chapman, M. J., & Toth, P. P. (2020). Beyond cardiovascular medicine: Potential future uses of icosapent ethyl. European Heart Journal Supplements, 22(Supplement_J), J54–J64. https://doi.org/10.1093/eurheartj/suaa119

Bhatt, D. L., Steg, P. G., Miller, M., Brinton, E. A., Jacobson, T. A., Ketchum, S. B., Doyle, R. T., Juliano, R. A., Jiao, L., Granowitz, C., Tardif, J.-C., & Ballantyne, C. M. (2019). Cardiovascular Risk Reduction with Icosapent Ethyl for Hypertriglyceridemia. New England Journal of Medicine, 380(1), 11–22. https://doi.org/10.1056/NEJMoa1812792

Bianco, F., Pravettoni, E., Colombo, A., Schenk, U., Möller, T., Matteoli, M., & Verderio, C. (2005). Astrocyte-Derived ATP Induces Vesicle Shedding and IL-1β Release from Microglia. The Journal of Immunology, 174(11), 7268–7277. https://doi.org/10.4049/jimmunol.174.11.7268

Biselli, J. M., Zampieri, B. L., Biselli-Chicote, P. M., de Souza, J. E. S., Bürger, M. C., da Silva Jr, W. A., Goloni-Bertollo, E. M., & Pavarino, É. C. (2022). Differential microRNA expression profile in blood of children with Down syndrome suggests a role in immunological dysfunction. Human Cell, 35(2), 639–648. https://doi.org/10.1007/s13577-022-00672-x

Blandford, S. N., Galloway, D. A., & Moore, C. S. (2018). The roles of extracellular vesicle microRNAs in the central nervous system. Glia, 66(11), 2267–2278. https://doi.org/10.1002/glia.23445

Booth, A. M., Fang, Y., Fallon, J. K., Yang, J.-M., Hildreth, J. E. K., & Gould, S. J. (2006). Exosomes and HIV Gag bud from endosome-like domains of the T cell plasma membrane. The Journal of Cell Biology, 172(6), 923–935. https://doi.org/10.1083/jcb.200508014

Brennan, S., Keon, M., Liu, B., Su, Z., & Saksena, N. K. (2019). Panoramic Visualization of Circulating MicroRNAs Across Neurodegenerative Diseases in Humans. Molecular Neurobiology, 56(11), 7380–7407. https://doi.org/10.1007/s12035-019-1615-1

Brites, D., & Fernandes, A. (2015). Neuroinflammation and Depression: Microglia Activation, Extracellular Microvesicles and microRNA Dysregulation. Frontiers in Cellular Neuroscience, 9. https://doi.org/10.3389/fncel.2015.00476

Brookmeyer, R., & Abdalla, N. (2018). Estimation of lifetime risks of Alzheimer's disease dementia using biomarkers for preclinical disease. Alzheimer's & Dementia, 14(8), 981–988. https://doi.org/10.1016/j.jalz.2018.03.005

Buschmann, D., Haberberger, A., Kirchner, B., Spornraft, M., Riedmaier, I., Schelling, G., & Pfaffl, M. W. (2016). Toward reliable biomarker signatures in the age of liquid biopsies—How to standardize the small RNA-Seq workflow. Nucleic Acids Research, 44(13), 5995–6018. https://doi.org/10.1093/nar/gkw545

Butterfield, D. A., Bader Lange, M. L., & Sultana, R. (2010). Involvements of the lipid peroxidation product, HNE, in the pathogenesis and progression of Alzheimer's disease. Biochimica et Biophysica Acta (BBA) - Molecular and Cell Biology of Lipids, 1801(8), 924–929. https://doi.org/10.1016/j.bbalip.2010.02.005

Calkins, M. J., Manczak, M., Mao, P., Shirendeb, U., & Reddy, P. H. (2011). Impaired mitochondrial biogenesis, defective axonal transport of mitochondria, abnormal mitochondrial dynamics and synaptic degeneration in a mouse model of Alzheimer's disease. Human Molecular Genetics, 20(23), 4515–4529. https://doi.org/10.1093/hmg/ddr381

Cao, L., Wang, Z., & Wan, W. (2018). Suppressor of Cytokine Signaling 3: Emerging Role Linking Central Insulin Resistance and Alzheimer's Disease. Frontiers in Neuroscience, 12. https://www.frontiersin.org/articles/10.3389/fnins.2018.00417

Cataldo, A. M., Petanceska, S., Terio, N. B., Peterhoff, C. M., Durham, R., Mercken, M., Mehta, P. D., Buxbaum, J., Haroutunian, V., & Nixon, R. A. (2004). Aβ localization in abnormal endosomes: Association with earliest Aβ elevations in AD and Down syndrome. Neurobiology of Aging, 25(10), 1263–1272. https://doi.org/10.1016/j.neurobiolaging.2004.02.027

Cavaillé, J., Seitz, H., Paulsen, M., Ferguson-Smith, A. C., & Bachellerie, J.-P. (2002). Identification of tandemly-repeated C/D snoRNA genes at the imprinted human 14q32 domain reminiscent of those at the Prader–Willi/Angelman syndrome region. Human Molecular Genetics, 11(13), 1527–1538. https://doi.org/10.1093/hmg/11.13.1527

Cha, D. J., Mengel, D., Mustapic, M., Liu, W., Selkoe, D. J., Kapogiannis, D., Galasko, D., Rissman, R. A., Bennett, D. A., & Walsh, D. M. (2019). MiR-212 and miR-132 Are Downregulated in Neurally Derived Plasma Exosomes of Alzheimer's Patients. Frontiers in Neuroscience, 13. https://www.frontiersin.org/articles/10.3389/fnins.2019.01208

Chartier-Harlin, M.-C., Crawford, F., Houlden, H., Warren, A., Hughes, D., Fidani, L., Goate, A., Rossor, M., Roques, P., Hardy, J., & Mullan, M. (1991). Early-onset Alzheimer's disease caused by mutations at codon 717 of the β-amyloid precursor protein gene. Nature, 353(6347), Article 6347. https://doi.org/10.1038/353844a0

Cheignon, C., Faller, P., Testemale, D., Hureau, C., & Collin, F. (2016). Metal-catalyzed oxidation of Aβ and the resulting reorganization of Cu binding sites promote ROS production. Metallomics : Integrated Biometal Science, 8(10), 1081–1089. https://doi.org/10.1039/c6mt00150e

Cheignon, C., Jones, M., Atrián-Blasco, E., Kieffer, I., Faller, P., Collin, F., & Hureau, C. (2017). Identification of key structural features of the elusive Cu–Aβ complex that generates ROS in Alzheimer's disease †Electronic supplementary information (ESI) available: Fluorescence data, UV-vis curves, XANES and EPR data, EPR parameters table, 1H NMR data and a proposed mechanism of O2 reduction. See DOI: 10.1039/c7sc00809k Click here for additional data file. Chemical Science, 8(7), 5107–5118. https://doi.org/10.1039/c7sc00809k

Cheignon, C., Tomas, M., Bonnefont-Rousselot, D., Faller, P., Hureau, C., & Collin, F. (2018). Oxidative stress and the amyloid beta peptide in Alzheimer's disease. Redox Biology, 14, 450–464. https://doi.org/10.1016/j.redox.2017.10.014

Chen, C. C., Liu, L., Ma, F., Wong, C. W., Guo, X. E., Chacko, J. V., Farhoodi, H. P., Zhang, S. X., Zimak, J., Ségaliny, A., Riazifar, M., Pham, V., Digman, M. A., Pone, E. J., & Zhao, W. (2016). Elucidation of Exosome Migration Across the Blood–Brain Barrier Model In Vitro. Cellular and Molecular Bioengineering, 9(4), 509–529. https://doi.org/10.1007/s12195-016-0458-3

Chen, F.-Z., Zhao, Y., & Chen, H.-Z. (2019). MicroRNA-98 reduces amyloid β-protein production and improves oxidative stress and mitochondrial dysfunction through the Notch signaling pathway via HEY2 in Alzheimer's disease mice. International Journal of Molecular Medicine, 43(1), 91–102. https://doi.org/10.3892/ijmm.2018.3957

Chen, H., Yang, J., Low, P. S., & Cheng, J.-X. (2008). Cholesterol Level Regulates Endosome Motility via Rab Proteins. Biophysical Journal, 94(4), 1508–1520. https://doi.org/10.1529/biophysj.106.099366

Chen, J., Zhao, B., Zhao, J., & Li, S. (2017). Potential Roles of Exosomal MicroRNAs as Diagnostic Biomarkers and Therapeutic Application in Alzheimer's Disease. Neural Plasticity, 2017. https://doi.org/10.1155/2017/7027380

Cheng, L., Doecke, J. D., Sharples, R. A., Villemagne, V. L., Fowler, C. J., Rembach, A., Martins, R. N., Rowe, C. C., Macaulay, S. L., Masters, C. L., & Hill, A. F. (2015). Prognostic serum miRNA biomarkers associated with Alzheimer's disease shows concordance with neuropsychological and neuroimaging assessment. Molecular Psychiatry, 20(10), Article 10. https://doi.org/10.1038/mp.2014.127

Cheng, L., Vella, L. J., Barnham, K. J., McLean, C., Masters, C. L., & Hill, A. F. (n.d.). Small RNA fingerprinting of Alzheimer's disease frontal cortex extracellular vesicles and their comparison with peripheral extracellular vesicles. Journal of Extracellular Vesicles, 9(1), 1766822. https://doi.org/10.1080/20013078.2020.1766822

Chen-Plotkin, A. S., Unger, T. L., Gallagher, M. D., Bill, E., Kwong, L. K., Volpicelli-Daley, L., Busch, J. I., Akle, S., Grossman, M., Deerlin, V. V., Trojanowski, J. Q., & Lee, V. M.-Y. (2012). TMEM106B, the Risk Gene for Frontotemporal Dementia, Is Regulated by the microRNA-132/212 Cluster and Affects Progranulin Pathways. Journal of Neuroscience, 32(33), 11213–11227. https://doi.org/10.1523/JNEUROSCI.0521-12.2012

Chevillet, J. R., Kang, Q., Ruf, I. K., Briggs, H. A., Vojtech, L. N., Hughes, S. M., Cheng, H. H., Arroyo, J. D., Meredith, E. K., Gallichotte, E. N., Pogosova-Agadjanyan, E. L., Morrissey, C., Stirewalt, D. L., Hladik, F., Yu, E. Y., Higano, C. S., & Tewari, M. (2014). Quantitative and stoichiometric analysis of the microRNA content of exosomes. Proceedings of the National Academy of Sciences of the United States of America, 111(41), 14888–14893. https://doi.org/10.1073/pnas.1408301111

Christ, L., Raiborg, C., Wenzel, E. M., Campsteijn, C., & Stenmark, H. (2017). Cellular Functions and Molecular Mechanisms of the ESCRT Membrane-Scission Machinery. Trends in Biochemical Sciences, 42(1), 42–56. https://doi.org/10.1016/j.tibs.2016.08.016

Citron, M., Oltersdorf, T., Haass, C., McConlogue, L., Hung, A. Y., Seubert, P., Vigo-Pelfrey, C., Lieberburg, I., & Selkoe, D. J. (1992). Mutation of the beta-amyloid precursor protein in familial Alzheimer's disease increases beta-protein production. Nature, 360(6405), 672–674. https://doi.org/10.1038/360672a0

Citron, M., Vigo-Pelfrey, C., Teplow, D. B., Miller, C., Schenk, D., Johnston, J., Winblad, B., Venizelos, N., Lannfelt, L., & Selkoe, D. J. (1994). Excessive production of amyloid beta-protein by peripheral cells of symptomatic and presymptomatic patients carrying the Swedish familial Alzheimer disease mutation. Proceedings of the National Academy of Sciences of the United States of America, 91(25), 11993–11997.

Clarke, J. R., Lyra e Silva, N. M., Figueiredo, C. P., Frozza, R. L., Ledo, J. H., Beckman, D., Katashima, C. K., Razolli, D., Carvalho, B. M., Frazão, R., Silveira, M. A., Ribeiro, F. C., Bomfim, T. R., Neves, F. S., Klein, W. L., Medeiros, R., LaFerla, F. M., Carvalheira, J. B., Saad, M. J., … De Felice, F. G. (2015). Alzheimer-associated Aβ oligomers impact the central nervous system to induce peripheral metabolic deregulation. EMBO Molecular Medicine, 7(2), 190–210. https://doi.org/10.15252/emmm.201404183

Clement, C., Hill, J. M., Dua, P., Culicchia, F., & Lukiw, W. J. (2016). Analysis of RNA from Alzheimer's Disease Post-mortem Brain Tissues. Molecular Neurobiology, 53(2), 1322–1328. https://doi.org/10.1007/s12035-015-9105-6

Cleveland, D. W., Hwo, S.-Y., & Kirschner, M. W. (1977). Physical and chemical properties of purified tau factor and the role of tau in microtubule assembly. Journal of Molecular Biology, 116(2), 227–247. https://doi.org/10.1016/0022-2836(77)90214-5

Coffey, E. E., Beckel, J. M., Laties, A. M., & Mitchell, C. H. (2014). Lysosomal alkalization and dysfunction in human fibroblasts with the Alzheimer's disease-linked presenilin 1 A246E mutation can be reversed with cAMP. Neuroscience, 263, 111–124. https://doi.org/10.1016/j.neuroscience.2014.01.001

Cogswell, J. P., Ward, J., Taylor, I. A., Waters, M., Shi, Y., Cannon, B., Kelnar, K., Kemppainen, J., Brown, D., Chen, C., Prinjha, R. K., Richardson, J. C., Saunders, A. M., Roses, A. D., & Richards, C. A. (2008). Identification

of miRNA Changes in Alzheimer's Disease Brain and CSF Yields Putative Biomarkers and Insights into Disease Pathways. Journal of Alzheimer's Disease, 14(1), 27–41. https://doi.org/10.3233/JAD-2008-14103

Cohen, M. L., Kim, C., Haldiman, T., ElHag, M., Mehndiratta, P., Pichet, T., Lissemore, F., Shea, M., Cohen, Y., Chen, W., Blevins, J., Appleby, B. S., Surewicz, K., Surewicz, W. K., Sajatovic, M., Tatsuoka, C., Zhang, S., Mayo, P., Butkiewicz, M., … Safar, J. G. (2015). Rapidly progressive Alzheimer's disease features distinct structures of amyloid-β. Brain, 138(4), 1009–1022. https://doi.org/10.1093/brain/awv006

Colombo, M., Moita, C., van Niel, G., Kowal, J., Vigneron, J., Benaroch, P., Manel, N., Moita, L. F., Théry, C., & Raposo, G. (2013). Analysis of ESCRT functions in exosome biogenesis, composition and secretion highlights the heterogeneity of extracellular vesicles. Journal of Cell Science, 126(24), 5553–5565. https://doi.org/10.1242/jcs.128868

Colombo, M., Raposo, G., & Théry, C. (2014). Biogenesis, Secretion, and Intercellular Interactions of Exosomes and Other Extracellular Vesicles. Annual Review of Cell and Developmental Biology, 30(1), 255–289. https://doi.org/10.1146/annurev-cellbio-101512-122326

Corder, E., Saunders, A., Strittmatter, W., Schmechel, D., Gaskell, P., Small, G., Roses, A., Haines, J., & Pericak-Vance, M. (1993). Gene dose of apolipoprotein E type 4 allele and the risk of Alzheimer's disease in late onset families. Science, 261(5123), 921–923. https://doi.org/10.1126/science.8346443

Cordonnier, M., Nardin, C., Chanteloup, G., Derangere, V., Algros, M.-P., Arnould, L., Garrido, C., Aubin, F., & Gobbo, J. (2020). Tracking the evolution of circulating exosomal-PD-L1 to monitor melanoma patients. Journal of Extracellular Vesicles, 9(1), 1710899. https://doi.org/10.1080/20013078.2019.1710899

Cosín-Tomàs, M., Senserrich, J., Arumí-Planas, M., Alquézar, C., Pallàs, M., Martín-Requero, Á., Suñol, C., Kaliman, P., & Sanfeliu, C. (2019). Role of Resveratrol and Selenium on Oxidative Stress and Expression of Antioxidant and Anti-Aging Genes in Immortalized Lymphocytes from Alzheimer's Disease Patients. Nutrients, 11(8), Article 8. https://doi.org/10.3390/nu11081764

Court, F. A., Midha, R., Cisterna, B. A., Grochmal, J., Shakhbazau, A., Hendriks, W. T., & Minnen, J. V. (2011). Morphological evidence for a transport of ribosomes from Schwann cells to regenerating axons. Glia, 59(10), 1529–1539. https://doi.org/10.1002/glia.21196

Coyle, J. T., Oster-Granite, M. L., Reeves, R. H., & Gearhart, J. D. (1988). Down syndrome, Alzheimer's disease and the trisomy 16 mouse. Trends in Neurosciences, 11(9), 390–394. https://doi.org/10.1016/0166-2236(88)90075-6

Crescitelli, R., Lässer, C., Jang, S. C., Cvjetkovic, A., Malmhäll, C., Karimi, N., Höög, J. L., Johansson, I., Fuchs, J., Thorsell, A., Gho, Y. S., Olofsson Bagge, R., & Lötvall, J. (2020). Subpopulations of extracellular vesicles from human metastatic melanoma tissue identified by quantitative proteomics after optimized isolation. Journal of Extracellular Vesicles, 9(1), 1722433. https://doi.org/10.1080/20013078.2020.1722433

Crescitelli, R., Lässer, C., Szabó, T. G., Kittel, A., Eldh, M., Dianzani, I., Buzás, E. I., & Lötvall, J. (2013). Distinct RNA profiles in subpopulations of extracellular vesicles: Apoptotic bodies, microvesicles and exosomes. Journal of Extracellular Vesicles, 2, 10.3402/jev.v2i0.20677. https://doi.org/10.3402/jev.v2i0.20677

Crimins, J. L., Rocher, A. B., & Luebke, J. I. (2012). Electrophysiological changes precede morphological changes to frontal cortical pyramidal neurons in the rTg4510 mouse model of progressive tauopathy. Acta Neuropathologica, 124(6), 777–795. https://doi.org/10.1007/s00401-012-1038-9

Croese, T., & Furlan, R. (2018). Extracellular vesicles in neurodegenerative diseases. Molecular Aspects of Medicine, 60, 52–61. https://doi.org/10.1016/j.mam.2017.11.006

Cronin, P., McCarthy, M. J., Lim, A. S. P., Salmon, D. P., Galasko, D., Masliah, E., De Jager, P. L., Bennett, D. A., & Desplats, P. (2017). Circadian alterations during early stages of Alzheimer's disease are associated with aberrant cycles of DNA methylation in BMAL1. Alzheimer's & Dementia : The Journal of the Alzheimer's Association, 13(6), 689–700. https://doi.org/10.1016/j.jalz.2016.10.003

Culpan, D., Kehoe, P. G., & Love, S. (n.d.). Tumour necrosis factor-α (TNF-α) and miRNA expression in frontal and temporal neocortex in Alzheimer's disease and the effect of TNF-α on miRNA expression in vitro.

Cummings, J., Lee, G., Nahed, P., Kambar, M. E. Z. N., Zhong, K., Fonseca, J., & Taghva, K. (2022). Alzheimer's disease drug development pipeline: 2022. Alzheimer's & Dementia : Translational Research & Clinical Interventions, 8(1), e12295. https://doi.org/10.1002/trc2.12295

Cunha, C., Gomes, C., Vaz, A. R., & Brites, D. (2016). Exploring New Inflammatory Biomarkers and Pathways during LPS-Induced M1 Polarization [Research article]. Mediators of Inflammation. https://doi.org/10.1155/2016/6986175

Dang, C., Harrington, K. D., Lim, Y. Y., Ames, D., Hassenstab, J., Laws, S. M., Yassi, N., Hickey, M., Rainey-Smith, S., Robertson, J., Sohrabi, H. R., Salvado, O., Weinborn, M., Villemagne, V. L., Rowe, C. C., Masters, C. L., Maruff, P., & Group, for the A. R. (2018). Relationship Between Amyloid-β Positivity and Progression to Mild Cognitive Impairment or Dementia over 8 Years in Cognitively Normal Older Adults. Journal of Alzheimer's Disease, 65(4), 1313–1325. https://doi.org/10.3233/JAD-180507

Davis, C., Dukes, A., Drewry, M., Helwa, I., Johnson, M. H., Isales, C. M., Hill, W. D., Liu, Y., Shi, X., Fulzele, S., & Hamrick, M. W. (2017). MicroRNA-183-5p Increases with Age in Bone-Derived Extracellular Vesicles, Suppresses Bone Marrow Stromal (Stem) Cell Proliferation, and Induces Stem Cell Senescence. Tissue Engineering. Part A, 23(21–22), 1231–1240. https://doi.org/10.1089/ten.TEA.2016.0525

de Rivero Vaccari, J. P., Brand, F., Adamczak, S., Lee, S. W., Barcena, J. P., Wang, M. Y., Bullock, M. R., Dietrich, W. D., & Keane, R. W. (2016). EXOSOME-MEDIATED INFLAMMASOME SIGNALING AFTER CENTRAL NERVOUS SYSTEM INJURY. Journal of Neurochemistry, 136(0 1), 39–48. https://doi.org/10.1111/jnc.13036

Dehghan, E., Zhang, Y., Saremi, B., Yadavali, S., Hakimi, A., Dehghani, M., Goodarzi, M., Tu, X., Robertson, S., Lin, R., Chudhuri, A., & Mirzaei, H. (2017). Hydralazine induces stress resistance and extends C. elegans lifespan by activating the NRF2/SKN-1 signalling pathway. Nature Communications, 8(1), Article 1. https://doi.org/10.1038/s41467-017-02394-3

Dehghani, R., Rahmani, F., & Rezaei, N. (2018). MicroRNA in Alzheimer's disease revisited: Implications for major neuropathological mechanisms. Reviews in the Neurosciences, 29(2), 161–182. https://doi.org/10.1515/revneuro-2017-0042

Dellar, E. R., Hill, C., Melling, G. E., Carter, D. R. F., & Baena-Lopez, L. A. (2022). Unpacking extracellular vesicles: RNA cargo loading and function. Journal of Extracellular Biology, 1(5), e40. https://doi.org/10.1002/jex2.40

Deneen, B., Ho, R., Lukaszewicz, A., Hochstim, C. J., Gronostajski, R. M., & Anderson, D. J. (2006). The Transcription Factor NFIA Controls the Onset of Gliogenesis in the Developing Spinal Cord. Neuron, 52(6), 953–968. https://doi.org/10.1016/j.neuron.2006.11.019

Deng, Y., Zhang, J., Sun, X., Ma, G., Luo, G., Miao, Z., & Song, L. (2020). MiR-132 improves the cognitive function of rats with Alzheimer's disease by inhibiting the MAPK1 signal pathway. Experimental and Therapeutic Medicine, 20(6), 1–1. https://doi.org/10.3892/etm.2020.9288

De Strooper, B., & Karran, E. (2016). The Cellular Phase of Alzheimer's Disease. Cell, 164(4), 603–615. https://doi.org/10.1016/j.cell.2015.12.056

DeVos, S. L., Miller, R. L., Schoch, K. M., Holmes, B. B., Kebodeaux, C. S., Wegener, A. J., Chen, G., Shen, T., Tran, H., Nichols, B., Zanardi, T. A., Kordasiewicz, H. B., Swayze, E. E., Bennett, C. F., Diamond, M. I., & Miller, T. M. (2017). Tau reduction prevents neuronal loss and reverses pathological tau deposition and seeding in mice with tauopathy. Science Translational Medicine, 9(374), eaag0481. https://doi.org/10.1126/scitranslmed.aag0481

Di Domenico, F., Tramutola, A., & Butterfield, D. A. (2017). Role of 4-hydroxy-2-nonenal (HNE) in the pathogenesis of alzheimer disease and other selected age-related neurodegenerative disorders. Free Radical Biology and Medicine, 111, 253–261. https://doi.org/10.1016/j.freeradbiomed.2016.10.490

Dickens, A. M., Tovar-y-Romo, L. B., Yoo, S.-W., Trout, A. L., Bae, M., Kanmogne, M., Megra, B., Williams, D. W., Witwer, K. W., Gacias, M., Tabatadze, N., Cole, R. N., Casaccia, P., Berman, J. W., Anthony, D. C., & Haughey, N. J. (2017). Astrocyte-shed extracellular vesicles regulate the peripheral leukocyte response to inflammatory brain lesions. Sci. Signal., 10(473), eaai7696. https://doi.org/10.1126/scisignal.aai7696

Ding, H., Huang, Z., Chen, M., Wang, C., Chen, X., Chen, J., & Zhang, J. (2016). Identification of a panel of five serum miRNAs as a biomarker for Parkinson's disease. Parkinsonism & Related Disorders, 22, 68–73. https://doi.org/10.1016/j.parkreldis.2015.11.014

Ding, L., Yang, X., Xia, X., Li, Y., Wang, Y., Li, C., Sun, Y., Gao, G., Zhao, S., Sheng, S., Liu, J., & Zheng, J. C. (2022). Exosomes Mediate APP Dysregulation via APP-miR-185-5p Axis. Frontiers in Cell and Developmental Biology, 10, 793388. https://doi.org/10.3389/fcell.2022.793388

Doll, S., Proneth, B., Tyurina, Y. Y., Panzilius, E., Kobayashi, S., Ingold, I., Irmler, M., Beckers, J., Aichler, M., Walch, A., Prokisch, H., Trümbach, D., Mao, G., Qu, F., Bayir, H., Füllekrug, J., Scheel, C. H., Wurst, W., Schick, J. A., … Conrad, M. (2017). ACSL4 dictates ferroptosis sensitivity by shaping cellular lipid composition. Nature Chemical Biology, 13(1), Article 1. https://doi.org/10.1038/nchembio.2239

Donzelli, S., Mori, F., Bellissimo, T., Sacconi, A., Casini, B., Frixa, T., Roscilli, G., Aurisicchio, L., Facciolo, F., Pompili, A., Carosi, M. A., Pescarmona, E., Segatto, O., Pond, G., Muti, P., Telera, S., Strano, S., Yarden, Y., & Blandino, G. (2015). Epigenetic silencing of miR-145-5p contributes to brain metastasis. Oncotarget, 6(34), 35183–35201.

Driedonks, T. A. P., Mol, S., de Bruin, S., Peters, A.-L., Zhang, X., Lindenbergh, M. F. S., Beuger, B. M., van Stalborch, A.-M. D., Spaan, T., de Jong, E. C., van der Vries, E., Margadant, C., van Bruggen, R., Vlaar, A. P. J., Groot Kormelink, T., & Nolte-'T Hoen, E. N. M. (2020). Y-RNA subtype ratios in plasma extracellular vesicles are cell type- specific and are candidate biomarkers for inflammatory diseases. Journal of Extracellular Vesicles, 9(1), 1764213. https://doi.org/10.1080/20013078.2020.1764213

Driver, J. A., Beiser, A., Au, R., Kreger, B. E., Splansky, G. L., Kurth, T., Kiel, D. P., Lu, K. P., Seshadri, S., & Wolf, P. A. (2012). Inverse association between cancer and Alzheimer's disease: Results from the Framingham Heart Study. BMJ, 344, e1442. https://doi.org/10.1136/bmj.e1442

Drummond, E., & Wisniewski, T. (2017). Alzheimer's disease: Experimental models and reality. Acta Neuropathologica, 133(2), 155–175. https://doi.org/10.1007/s00401-016-1662-x

Duc Nguyen, H., Hee Jo, W., Hong Minh Hoang, N., & Kim, M.-S. (2022). Anti-inflammatory effects of B vitamins protect against tau hyperphosphorylation and cognitive impairment induced by 1,2 diacetyl benzene: An in vitro and in silico study. International Immunopharmacology, 108, 108736. https://doi.org/10.1016/j.intimp.2022.108736

Dunning, C. J. R., George, S., & Brundin, P. (2013). What's to like about the prion-like hypothesis for the spreading of aggregated α-synuclein in Parkinson disease? Prion, 7(1), 92–97. https://doi.org/10.4161/pri.23806

Edbauer, D., Neilson, J. R., Foster, K. A., Wang, C.-F., Seeburg, D. P., Batterton, M. N., Tada, T., Dolan, B. M., Sharp, P. A., & Sheng, M. (2010). Regulation of Synaptic Structure and Function by FMRP-Associated MicroRNAs miR-125b and miR-132. Neuron, 65(3), 373–384. https://doi.org/10.1016/j.neuron.2010.01.005

Eitan, E., Green, J., Bodogai, M., Mode, N. A., Bæk, R., Jørgensen, M. M., Freeman, D. W., Witwer, K. W., Zonderman, A. B., Biragyn, A., Mattson, M. P., Noren Hooten, N., & Evans, M. K. (2017). Age-Related Changes in Plasma Extracellular Vesicle Characteristics and Internalization by Leukocytes. Scientific Reports, 7(1), Article 1. https://doi.org/10.1038/s41598-017-01386-z

Eitan, E., Hutchison, E. R., Marosi, K., Comotto, J., Mustapic, M., Nigam, S. M., Suire, C., Maharana, C., Jicha, G. A., Liu, D., Machairaki, V., Witwer, K. W., Kapogiannis, D., & Mattson, M. P. (2016). Extracellular vesicle-associated Aβ mediates trans-neuronal bioenergetic and Ca2+-handling deficits in Alzheimer's disease models. Npj Aging and Mechanisms of Disease, 2, 16019. https://doi.org/10.1038/npjamd.2016.19

Eitan, E., Zhang, S., Witwer, K. W., & Mattson, M. P. (2015). Extracellular vesicle–depleted fetal bovine and human sera have reduced capacity to support cell growth. Journal of Extracellular Vesicles, 4(1), 26373. https://doi.org/10.3402/jev.v4.26373

Elahi, F. M., & Miller, B. L. (2017). A clinicopathological approach to the diagnosis of dementia. Nature Reviews Neurology, 13(8), 457–476. https://doi.org/10.1038/nrneurol.2017.96

Emanuelli, B., Peraldi, P., Filloux, C., Sawka-Verhelle, D., Hilton, D., & Obberghen, E. V. (2000). SOCS-3 Is an Insulin-induced Negative Regulator of Insulin Signaling *. Journal of Biological Chemistry, 275(21), 15985–15991. https://doi.org/10.1074/jbc.275.21.15985

Eom, T.-Y., Han, S. B., Kim, J., Blundon, J. A., Wang, Y.-D., Yu, J., Anderson, K., Kaminski, D. B., Sakurada, S. M., Pruett-Miller, S. M., Horner, L., Wagner, B., Robinson, C. G., Eicholtz, M., Rose, D. C., & Zakharenko, S. S. (2020). Schizophrenia-related microdeletion causes defective ciliary motility and brain ventricle enlargement via microRNA-dependent mechanisms in mice. Nature Communications, 11(1), Article 1. https://doi.org/10.1038/s41467-020-14628-y

Ernst, A., Campos, B., Meier, J., Devens, F., Liesenberg, F., Wolter, M., Reifenberger, G., Herold-Mende, C., Lichter, P., & Radlwimmer, B. (2010). De-repression of CTGF via the miR-17-92 cluster upon differentiation of human glioblastoma spheroid cultures. Oncogene, 29(23), Article 23. https://doi.org/10.1038/onc.2010.83

Evdokimova, V., Ruzanov, P., Gassmann, H., Zaidi, S. H., Peltekova, V., Heisler, L. E., McPherson, J. D., Orlic-Milacic, M., Specht, K., Steiger, K., Schober, S. J., Thiel, U., McKee, T. D., Zaidi, M., Spring, C. M., Lapouble, E., Delattre, O., Burdach, S., Stein, L. D., & Sorensen, P. H. (2019). Exosomes transmit retroelement RNAs to drive inflammation and immunosuppression in Ewing Sarcoma (p. 806851). bioRxiv. https://doi.org/10.1101/806851

Falcão, A. S., Carvalho, L. A. R., Lidónio, G., Vaz, A. R., Lucas, S. D., Moreira, R., & Brites, D. (2017). Dipeptidyl Vinyl Sulfone as a Novel Chemical Tool to Inhibit HMGB1/NLRP3-Inflammasome and Inflamma-miRs in Aβ-Mediated Microglial Inflammation. ACS Chemical Neuroscience, 8(1), 89–99. https://doi.org/10.1021/acschemneuro.6b00250

Fauré, J., Lachenal, G., Court, M., Hirrlinger, J., Chatellard-Causse, C., Blot, B., Grange, J., Schoehn, G., Goldberg, Y., Boyer, V., Kirchhoff, F., Raposo, G., Garin, J., & Sadoul, R. (2006). Exosomes are released by cultured cortical neurones. Molecular and Cellular Neuroscience, 31(4), 642–648. https://doi.org/10.1016/j.mcn.2005.12.003

Fedeli, C., Filadi, R., Rossi, A., Mammucari, C., & Pizzo, P. (2019). PSEN2 (presenilin 2) mutants linked to familial Alzheimer disease impair autophagy by altering Ca2+ homeostasis. Autophagy, 15(12), 2044–2062. https://doi.org/10.1080/15548627.2019.1596489

Feng, Z., Chen, R., Huang, N., & Luo, C. (2020). Long non-coding RNA ASMTL-AS1 inhibits tumor growth and glycolysis by regulating the miR-93-3p/miR-660/FOXO1 axis in papillary thyroid carcinoma. Life Sciences, 244, 117298. https://doi.org/10.1016/j.lfs.2020.117298

Fiandaca, M. S., Kapogiannis, D., Mapstone, M., Boxer, A., Eitan, E., Schwartz, J. B., Abner, E. L., Petersen, R. C., Federoff, H. J., Miller, B. L., & Goetzl, E. J. (2015). Identification of preclinical Alzheimer's disease by a profile of pathogenic proteins in neurally derived blood exosomes: A case-control study. Alzheimer's & Dementia, 11(6), 600-607.e1. https://doi.org/10.1016/j.jalz.2014.06.008

Fiori, L. M., Kos, A., Lin, R., Théroux, J.-F., Lopez, J. P., Kühne, C., Eggert, C., Holzapfel, M., Huettl, R.-E., Mechawar, N., Belzung, C., Ibrahim, E. C., Chen, A., & Turecki, G. (2021). MiR-323a regulates ERBB4 and is involved in depression. Molecular Psychiatry, 26(8), Article 8. https://doi.org/10.1038/s41380-020-00953-7

Fitzner, D., Schnaars, M., Rossum, D. van, Krishnamoorthy, G., Dibaj, P., Bakhti, M., Regen, T., Hanisch, U.-K., & Simons, M. (2011). Selective transfer of exosomes from oligodendrocytes to microglia by macropinocytosis. J Cell Sci, 124(3), 447–458. https://doi.org/10.1242/jcs.074088

Fontana, L., Fiori, M. E., Albini, S., Cifaldi, L., Giovinazzi, S., Forloni, M., Boldrini, R., Donfrancesco, A., Federici, V., Giacomini, P., Peschle, C., & Fruci, D. (2008). Antagomir-17-5p Abolishes the Growth of Therapy-Resistant Neuroblastoma through p21 and BIM. PLOS ONE, 3(5), e2236. https://doi.org/10.1371/journal.pone.0002236

Freir, D. B., Nicoll, A. J., Klyubin, I., Panico, S., Mc Donald, J. M., Risse, E., Asante, E. A., Farrow, M. A., Sessions, R. B., Saibil, H. R., Clarke, A. R., Rowan, M. J., Walsh, D. M., & Collinge, J. (2011). Interaction between prion protein and toxic amyloid β assemblies can be therapeutically targeted at multiple sites. Nature Communications, 2, 336. https://doi.org/10.1038/ncomms1341

Frey, B., & Gaipl, U. S. (2011). The immune functions of phosphatidylserine in membranes of dying cells and microvesicles. Seminars in Immunopathology, 33(5), 497–516. https://doi.org/10.1007/s00281-010-0228-6

Frick, M., Bright, N. A., Riento, K., Bray, A., Merrified, C., & Nichols, B. J. (2007). Coassembly of Flotillins Induces Formation of Membrane Microdomains, Membrane Curvature, and Vesicle Budding. Current Biology, 17(13), 1151–1156. https://doi.org/10.1016/j.cub.2007.05.078

Frigerio, C. S., Lau, P., Salta, E., Tournoy, J., Bossers, K., Vandenberghe, R., Wallin, A., Bjerke, M., Zetterberg, H., Blennow, K., & Strooper, B. D. (2013). Reduced expression of hsa-miR-27a-3p in CSF of patients with Alzheimer disease. Neurology, 81(24), 2103–2106. https://doi.org/10.1212/01.wnl.0000437306.37850.22

Frost, B., & Diamond, M. I. (2010). Prion-like Mechanisms in Neurodegenerative Diseases. Nature Reviews. Neuroscience, 11(3), 155–159. https://doi.org/10.1038/nrn2786

Frost, B., Hemberg, M., Lewis, J., & Feany, M. B. (2014). Tau promotes neurodegeneration through global chromatin relaxation. Nature Neuroscience, 17(3), Article 3. https://doi.org/10.1038/nn.3639

Frühbeis, C., Fröhlich, D., Kuo, W. P., Amphornrat, J., Thilemann, S., Saab, A. S., Kirchhoff, F., Möbius, W., Goebbels, S., Nave, K.-A., Schneider, A., Simons, M., Klugmann, M., Trotter, J., & Krämer-Albers, E.-M. (2013). Neurotransmitter-Triggered Transfer of Exosomes Mediates Oligodendrocyte–Neuron Communication. PLOS Biology, 11(7), e1001604. https://doi.org/10.1371/journal.pbio.1001604

Fussi, N., Höllerhage, M., Chakroun, T., Nykänen, N.-P., Rösler, T. W., Koeglsperger, T., Wurst, W., Behrends, C., & Höglinger, G. U. (2018). Exosomal secretion of α-synuclein as protective mechanism after upstream blockage of macroautophagy. Cell Death & Disease, 9(7), 757. https://doi.org/10.1038/s41419-018-0816-2

Gabrielli, M., Battista, N., Riganti, L., Prada, I., Antonucci, F., Cantone, L., Matteoli, M., Maccarrone, M., & Verderio, C. (2015). Active endocannabinoids are secreted on extracellular membrane vesicles. EMBO Reports, 16(2), 213–220. https://doi.org/10.15252/embr.201439668

Gallart-Palau, X., Guo, X., Serra, A., & Sze, S. K. (2020). Alzheimer's disease progression characterized by alterations in the molecular profiles and biogenesis of brain extracellular vesicles. Alzheimer's Research & Therapy, 12, 54. https://doi.org/10.1186/s13195-020-00623-4

Gámez-Valero, A., Campdelacreu, J., Vilas, D., Ispierto, L., Reñé, R., Álvarez, R., Armengol, M. P., Borràs, F. E., & Beyer, K. (2019). Exploratory study on microRNA profiles from plasma-derived extracellular vesicles in Alzheimer's disease and dementia with Lewy bodies. Translational Neurodegeneration, 8(1), 31. https://doi.org/10.1186/s40035-019-0169-5

Gao, J., Wang, W.-Y., Mao, Y.-W., Gräff, J., Guan, J.-S., Pan, L., Mak, G., Kim, D., Su, S. C., & Tsai, L.-H. (2010). A novel pathway regulates memory and plasticity via SIRT1 and miR-134. Nature, 466(7310), 1105–1109. https://doi.org/10.1038/nature09271

Gao, Y., Zhang, N., Lv, C., Li, N., Li, X., & Li, W. (2020). LncRNA SNHG1 Knockdown Alleviates Amyloid-β-Induced Neuronal Injury by Regulating ZNF217 via Sponging miR-361-3p in Alzheimer's Disease. Journal of Alzheimer's Disease, 77(1), 85–98. https://doi.org/10.3233/JAD-191303

Garcia-Martin, R., Wang, G., Brandão, B. B., Zanotto, T. M., Shah, S., Kumar Patel, S., Schilling, B., & Kahn, C. R. (2022). MicroRNA sequence codes for small extracellular vesicle release and cellular retention. Nature, 601(7893), Article 7893. https://doi.org/10.1038/s41586-021-04234-3

García-Romero, N., Carrión-Navarro, J., Esteban-Rubio, S., Lázaro-Ibáñez, E., Peris-Celda, M., Alonso, M. M., Guzmán-De-Villoria, J., Fernández-Carballal, C., de Mendivil, A. O., García-Duque, S., Escobedo-Lucea, C., Prat-Acín, R., Belda-Iniesta, C., & Ayuso-Sacido, A. (2016). DNA sequences within glioma-derived extracellular vesicles can cross the intact blood-brain barrier and be detected in peripheral blood of patients. Oncotarget, 8(1), 1416–1428. https://doi.org/10.18632/oncotarget.13635

Gayen, M., Bhomia, M., Balakathiresan, N., & Knollmann-Ritschel, B. (2020). Exosomal MicroRNAs Released by Activated Astrocytes as Potential Neuroinflammatory Biomarkers. International Journal of Molecular Sciences, 21(7), Article 7. https://doi.org/10.3390/ijms21072312

Ge, Q., Zhou, Y., Lu, J., Bai, Y., Xie, X., & Lu, Z. (2014). MiRNA in Plasma Exosome is Stable under Different Storage Conditions. Molecules, 19(2), 1568–1575. https://doi.org/10.3390/molecules19021568

Gerasymchuk, M., Cherkasova, V., Kovalchuk, O., & Kovalchuk, I. (2020). The Role of microRNAs in Organismal and Skin Aging. International Journal of Molecular Sciences, 21(15), Article 15. https://doi.org/10.3390/ijms21155281

Ghanbari, M., Ikram, M. A., de Looper, H. W. J., Hofman, A., Erkeland, S. J., Franco, O. H., & Dehghan, A. (2016). Genome-wide identification of microRNA-related variants associated with risk of Alzheimer's disease. Scientific Reports, 6, 28387. https://doi.org/10.1038/srep28387

Ghidoni, R., Paterlini, A., Albertini, V., Glionna, M., Monti, E., Schiaffonati, L., Benussi, L., Levy, E., & Binetti, G. (2011). Cystatin C is released in association with exosomes: A new tool of neuronal communication which is unbalanced in Alzheimer's disease. Neurobiology of Aging, 32(8), 1435–1442. https://doi.org/10.1016/j.neurobiolaging.2009.08.013

Ghosh, A., Davey, M., Chute, I. C., Griffiths, S. G., Lewis, S., Chacko, S., Barnett, D., Crapoulet, N., Fournier, S., Joy, A., Caissie, M. C., Ferguson, A. D., Daigle, M., Meli, M. V., Lewis, S. M., & Ouellette, R. J. (2014). Rapid Isolation of Extracellular Vesicles from Cell Culture and Biological Fluids Using a Synthetic Peptide with Specific Affinity for Heat Shock Proteins. PLOS ONE, 9(10), e110443. https://doi.org/10.1371/journal.pone.0110443

Giusti, I., Di Francesco, M., D'Ascenzo, S., Palmerini, M. G., Macchiarelli, G., Carta, G., & Dolo, V. (2018). Ovarian cancer-derived extracellular vesicles affect normal human fibroblast behavior. Cancer Biology & Therapy, 19(8), 722–734. https://doi.org/10.1080/15384047.2018.1451286

Glazov, E. A., McWilliam, S., Barris, W. C., & Dalrymple, B. P. (2008). Origin, Evolution, and Biological Role of miRNA Cluster in DLK-DIO3 Genomic Region in Placental Mammals. Molecular Biology and Evolution, 25(5), 939–948. https://doi.org/10.1093/molbev/msn045

Glebov, O. O., Bright, N. A., & Nichols, B. J. (2006). Flotillin-1 defines a clathrin-independent endocytic pathway in mammalian cells. Nature Cell Biology, 8(1), Article 1. https://doi.org/10.1038/ncb1342

Glenner, G. G., & Wong, C. W. (1984). Alzheimer's disease: Initial report of the purification and characterization of a novel cerebrovascular amyloid protein. Biochemical and Biophysical Research Communications, 120(3), 885–890. https://doi.org/10.1016/S0006-291X(84)80190-4

Godoy, M. A. de, Saraiva, L. M., Carvalho, L. R. P., Vasconcelos-dos-Santos, A., Beiral, H. J. V., Ramos, A. B., Silva, L. R. de P., Leal, R. B., Monteiro, V. H. S., Braga, C. V., Araujo-Silva, C. A. de, Sinis, L. C., Santos, V. B., Brunswick, T. H. K., Alcantara, C. de L., Lima, A. P. C. A., Silva, N. L. da C. e, Galina, A., Vieyra, A., … Ferreira, S. T. (2017). Mesenchymal stem cells and cell-derived extracellular vesicles protect hippocampal neurons from oxidative stress and synapse damage induced by amyloid-β oligomers. Journal of Biological Chemistry, jbc.M117.807180. https://doi.org/10.1074/jbc.M117.807180

Goedeke, L., & Fernández-Hernando, C. (2014). microRNAs: A connection between cholesterol metabolism and neurodegeneration. Neurobiology of Disease, 72PA, 48–53. https://doi.org/10.1016/j.nbd.2014.05.034

Goetzl, E. J., Abner, E. L., Jicha, G. A., Kapogiannis, D., & Schwartz, J. B. (2018). Declining levels of functionally specialized synaptic proteins in plasma neuronal exosomes with progression of Alzheimer's disease. The FASEB Journal, 32(2), 888–893. https://doi.org/10.1096/fj.201700731R

Goetzl, E. J., Boxer, A., Schwartz, J. B., Abner, E. L., Petersen, R. C., Miller, B. L., & Kapogiannis, D. (2015). Altered lysosomal proteins in neural-derived plasma exosomes in preclinical Alzheimer disease. Neurology, 85(1), 40–47. https://doi.org/10.1212/WNL.0000000000001702

Goetzl, E. J., Mustapic, M., Kapogiannis, D., Eitan, E., Lobach, I. V., Goetzl, L., Schwartz, J. B., & Miller, B. L. (2016). Cargo proteins of plasma astrocyte-derived exosomes in Alzheimer's disease. The FASEB Journal, 30(11), 3853–3859. https://doi.org/10.1096/fj.201600756R

Goetzl, E. J., Nogueras-Ortiz, C., Mustapic, M., Mullins, R. J., Abner, E. L., Schwartz, J. B., & Kapogiannis, D. (2019). Deficient neurotrophic factors of CSPG4-type neural cell exosomes in Alzheimer disease. The FASEB Journal, 33(1), 231–238. https://doi.org/10.1096/fj.201801001

Goetzl, E. J., Schwartz, J. B., Abner, E. L., Jicha, G. A., & Kapogiannis, D. (2018). High complement levels in astrocyte-derived exosomes of Alzheimer disease. Annals of Neurology, 83(3), 544–552. https://doi.org/10.1002/ana.25172

Goldie, B. J., Dun, M. D., Lin, M., Smith, N. D., Verrills, N. M., Dayas, C. V., & Cairns, M. J. (2014). Activity-associated miRNA are packaged in Map1b-enriched exosomes released from depolarized neurons. Nucleic Acids Research, 42(14), 9195–9208. https://doi.org/10.1093/nar/gku594

Gomes, S., Martins, I., Fonseca, A. C. R. G., Oliveira, C. R., Resende, R., & Pereira, C. M. F. (2014). Protective Effect of Leptin and Ghrelin against Toxicity Induced by Amyloid-β Oligomers in a Hypothalamic cell Line. Journal of Neuroendocrinology, 26(3), 176–185. https://doi.org/10.1111/jne.12138

Goncalves, M. B., Malmqvist, T., Clarke, E., Hubens, C. J., Grist, J., Hobbs, C., Trigo, D., Risling, M., Angeria, M., Damberg, P., Carlstedt, T. P., & Corcoran, J. P. T. (2015). Neuronal RARβ Signaling Modulates PTEN Activity Directly in Neurons and via Exosome Transfer in Astrocytes to Prevent Glial Scar Formation and Induce Spinal Cord Regeneration. The Journal of Neuroscience, 35(47), 15731–15745. https://doi.org/10.1523/JNEUROSCI.1339-15.2015

Gould, S. J., & Raposo, G. (2013). As we wait: Coping with an imperfect nomenclature for extracellular vesicles. Journal of Extracellular Vesicles, 2(1), 20389. https://doi.org/10.3402/jev.v2i0.20389

Gravina, S. A., Ho, L., Eckman, C. B., Long, K. E., Otvos, L., Younkin, L. H., Suzuki, N., & Younkin, S. G. (1995). Amyloid β Protein (Aβ) in Alzheimeri's Disease Brain: BIOCHEMICAL AND IMMUNOCYTOCHEMICAL ANALYSIS WITH ANTIBODIES SPECIFIC FOR FORMS ENDING AT Aβ40 OR Aβ42(43) (∗). Journal of Biological Chemistry, 270(13), 7013–7016. https://doi.org/10.1074/jbc.270.13.7013

Greco, V., Hannus, M., & Eaton, S. (2001). Argosomes: A Potential Vehicle for the Spread of Morphogens through Epithelia. Cell, 106(5), 633–645. https://doi.org/10.1016/S0092-8674(01)00484-6

Gruszka, R., & Zakrzewska, M. (2018). The Oncogenic Relevance of miR-17-92 Cluster and Its Paralogous miR-106b-25 and miR-106a-363 Clusters in Brain Tumors. International Journal of Molecular Sciences, 19(3), Article 3. https://doi.org/10.3390/ijms19030879

Guan, Y.-J., Li, J., Yang, X., Du, S., Ding, J., Gao, Y., Zhang, Y., Yang, K., & Chen, Q. (2018). Evidence that miR-146a attenuates aging- and trauma-induced osteoarthritis by inhibiting Notch1, IL-6, and IL-1 mediated catabolism. Aging Cell, 17(3), e12752. https://doi.org/10.1111/acel.12752

Guedes, J. R., Custódia, C. M., Silva, R. J., de Almeida, L. P., Pedroso de Lima, M. C., & Cardoso, A. L. (2014). Early miR-155 upregulation contributes to neuroinflammation in Alzheimer's disease triple transgenic mouse model. Human Molecular Genetics, 23(23), 6286–6301. https://doi.org/10.1093/hmg/ddu348

Guerreiro, E. M., Vestad, B., Steffensen, L. A., Aass, H. C. D., Saeed, M., Øvstebø, R., Costea, D. E., Galtung, H. K., & Søland, T. M. (2018). Efficient extracellular vesicle isolation by combining cell media modifications, ultrafiltration, and size-exclusion chromatography. PLoS ONE, 13(9), e0204276. https://doi.org/10.1371/journal.pone.0204276

Guisle, I., Gratuze, M., Petry, S., Morin, F., Keraudren, R., Whittington, R. A., Hébert, S. S., Mongrain, V., & Planel, E. (2020). Circadian and sleep/wake-dependent variations in tau phosphorylation are driven by temperature. Sleep, 43(4), zsz266. https://doi.org/10.1093/sleep/zsz266

Guo, D., Ye, Y., Qi, J., Tan, X., Zhang, Y., Ma, Y., & Li, Y. (2017). Age and sex differences in microRNAs expression during the process of thymus aging. Acta Biochimica et Biophysica Sinica, 49(5), 409–419. https://doi.org/10.1093/abbs/gmx029

Guo, L., Zhong, M. B., Zhang, L., Zhang, B., & Cai, D. (2022). Sex Differences in Alzheimer's Disease: Insights From the Multiomics Landscape. Biological Psychiatry, 91(1), 61–71. https://doi.org/10.1016/j.biopsych.2021.02.968

Guo, R., Fan, G., Zhang, J., Wu, C., Du, Y., Ye, H., Li, Z., Wang, L., Zhang, Z., Zhang, L., Zhao, Y., & Lu, Z. (2017). A 9-microRNA Signature in Serum Serves as a Noninvasive Biomarker in Early Diagnosis of Alzheimer's Disease. Journal of Alzheimer's Disease, 60(4), 1365–1377. https://doi.org/10.3233/JAD-170343

Guo, S.-C., Tao, S.-C., & Dawn, H. (2018). Microfluidics-based on-a-chip systems for isolating and analysing extracellular vesicles. Journal of Extracellular Vesicles, 7(1), 1508271. https://doi.org/10.1080/20013078.2018.1508271

Guo, X., Han, C., Ma, K., Xia, Y., Wan, F., Yin, S., Kou, L., Sun, Y., Wu, J., Hu, J., Huang, J., Xiong, N., & Wang, T. (2019). Hydralazine Protects Nigrostriatal Dopaminergic Neurons From MPP+ and MPTP Induced Neurotoxicity: Roles of Nrf2-ARE Signaling Pathway. Frontiers in Neurology, 10. https://www.frontiersin.org/articles/10.3389/fneur.2019.00271

Gustafsson, G., Lööv, C., Persson, E., Lázaro, D. F., Takeda, S., Bergström, J., Erlandsson, A., Sehlin, D., Balaj, L., György, B., Hallbeck, M., Outeiro, T. F., Breakefield, X. O., Hyman, B. T., & Ingelsson, M. (2018). Secretion and Uptake of α-Synuclein Via Extracellular Vesicles in Cultured Cells. Cellular and Molecular Neurobiology, 38(8), 1539–1550. https://doi.org/10.1007/s10571-018-0622-5

Gyuris, A., Navarrete-Perea, J., Jo, A., Cristea, S., Zhou, S., Fraser, K., Wei, Z., Krichevsky, A. M., Weissleder, R., Lee, H., Gygi, S. P., & Charest, A. (2019). Physical and Molecular Landscapes of Mouse Glioma Extracellular Vesicles Define Heterogeneity. Cell Reports, 27(13), 3972-3987.e6. https://doi.org/10.1016/j.celrep.2019.05.089

Hadar, A., Milanesi, E., Walczak, M., Puzianowska-Kuźnicka, M., Kuźnicki, J., Squassina, A., Niola, P., Chillotti, C., Attems, J., Gozes, I., & Gurwitz, D. (2018). SIRT1, miR-132 and miR-212 link human longevity to Alzheimer's Disease. Scientific Reports, 8, 8465. https://doi.org/10.1038/s41598-018-26547-6

Hamlett, E. D., Goetzl, E. J., Ledreux, A., Vasilevko, V., Boger, H. A., LaRosa, A., Clark, D., Carroll, S. L., Iragui, M. C., Fortea, J., Mufson, E. J., Sabbagh, M., Mohammed, A. H., Hartley, D., Doran, E., Lott, I. T., & Granholm, A.-C. (2017). Neuronal exosomes reveal Alzheimer's disease biomarkers in Down syndrome. Alzheimer's & Dementia : The Journal of the Alzheimer's Association, 13(5), 541–549. https://doi.org/10.1016/j.jalz.2016.08.012

Haqqani, A. S., Delaney, C. E., Tremblay, T.-L., Sodja, C., Sandhu, J. K., & Stanimirovic, D. B. (2013). Method for isolation and molecular characterization of extracellular microvesicles released from brain endothelial cells. Fluids and Barriers of the CNS, 10(1), 4. https://doi.org/10.1186/2045-8118-10-4

Haraszti, R. A., Didiot, M.-C., Sapp, E., Leszyk, J., Shaffer, S. A., Rockwell, H. E., Gao, F., Narain, N. R., DiFiglia, M., Kiebish, M. A., Aronin, N., & Khvorova, A. (2016). High-resolution proteomic and lipidomic analysis of exosomes and microvesicles from different cell sources. Journal of Extracellular Vesicles, 5(1), 32570. https://doi.org/10.3402/jev.v5.32570

Harati, R., Hammad, S., Tlili, A., Mahfood, M., Mabondzo, A., & Hamoudi, R. (2022a). MiR-27a-3p regulates expression of intercellular junctions at the brain endothelium and controls the endothelial barrier permeability. PLOS ONE, 17(1), e0262152. https://doi.org/10.1371/journal.pone.0262152

Harati, R., Hammad, S., Tlili, A., Mahfood, M., Mabondzo, A., & Hamoudi, R. (2022b). MiR-27a-3p regulates expression of intercellular junctions at the brain endothelium and controls the endothelial barrier permeability. PLOS ONE, 17(1), e0262152. https://doi.org/10.1371/journal.pone.0262152

Hardy, J. A., & Higgins, G. A. (1992). Alzheimer's Disease: The Amyloid Cascade Hypothesis. Science; Washington, 256(5054), 184.

Harischandra, D. S., Ghaisas, S., Rokad, D., Zamanian, M., Jin, H., Anantharam, V., Kimber, M., Kanthasamy, A., & Kanthasamy, A. (2018). Environmental Neurotoxicant Manganese Regulates Exosome-mediated Extracellular miRNAs in Cell Culture Model of Parkinson's Disease: Relevance to α-Synuclein Misfolding in Metal Neurotoxicity. Neurotoxicology, 64, 267–277. https://doi.org/10.1016/j.neuro.2017.04.007

Hartley, D., Blumenthal, T., Carrillo, M., DiPaolo, G., Esralew, L., Gardiner, K., Granholm, A.-C., Iqbal, K., Krams, M., Lemere, C., Lott, I., Mobley, W., Ness, S., Nixon, R., Potter, H., Reeves, R., Sabbagh, M., Silverman, W., Tycko, B., … Wisniewski, T. (2015). Down syndrome and Alzheimer's disease: Common pathways, common goals. Alzheimer's & Dementia, 11(6), 700–709. https://doi.org/10.1016/j.jalz.2014.10.007

Hartmann, P., Zhou, Z., Natarelli, L., Wei, Y., Nazari-Jahantigh, M., Zhu, M., Grommes, J., Steffens, S., Weber, C., & Schober, A. (2016). Endothelial Dicer promotes atherosclerosis and vascular inflammation by miRNA-103-mediated suppression of KLF4. Nature Communications, 7. https://doi.org/10.1038/ncomms10521

Harvey, B. S., Ohlsson, K. S., Mååg, J. L. V., Musgrave, I. F., & Smid, S. D. (2012). Contrasting protective effects of cannabinoids against oxidative stress and amyloid-β evoked neurotoxicity in vitro. NeuroToxicology, 33(1), 138–146. https://doi.org/10.1016/j.neuro.2011.12.015

Hatch, R. J., Wei, Y., Xia, D., & Götz, J. (2017). Hyperphosphorylated tau causes reduced hippocampal CA1 excitability by relocating the axon initial segment. Acta Neuropathologica, 133(5), 717–730. https://doi.org/10.1007/s00401-017-1674-1

He, S., Zhang, G., Dong, H., Ma, M., & Sun, Q. (2016). MiR-203 facilitates tumor growth and metastasis by targeting fibroblast growth factor 2 in breast cancer. OncoTargets and Therapy, 9, 6203–6210. https://doi.org/10.2147/OTT.S108712

He, T., Chen, P., Jin, L., Hu, J., Li, Y., Zhou, L., Yang, S., Mao, X., Gui, Y., Chen, Y., & Lai, Y. (2018). MiR-660-5p is associated with cell migration, invasion, proliferation and apoptosis in renal cell carcinoma. Molecular Medicine Reports, 17(1), 2051–2060. https://doi.org/10.3892/mmr.2017.8052

Hébert, S. S., Horré, K., Nicolaï, L., Bergmans, B., Papadopoulou, A. S., Delacourte, A., & De Strooper, B. (2009). MicroRNA regulation of Alzheimer's Amyloid precursor protein expression. Neurobiology of Disease, 33(3), 422–428. https://doi.org/10.1016/j.nbd.2008.11.009

Hébert, S. S., Horré, K., Nicolaï, L., Papadopoulou, A. S., Mandemakers, W., Silahtaroglu, A. N., Kauppinen, S., Delacourte, A., & Strooper, B. D. (2008). Loss of microRNA cluster miR-29a/b-1 in sporadic Alzheimer's disease correlates with increased BACE1/β-secretase expression. Proceedings of the National Academy of Sciences, 105(17), 6415–6420. https://doi.org/10.1073/pnas.0710263105

Hébert, S. S., Papadopoulou, A. S., Smith, P., Galas, M.-C., Planel, E., Silahtaroglu, A. N., Sergeant, N., Buée, L., & De Strooper, B. (2010). Genetic ablation of Dicer in adult forebrain neurons results in abnormal tau hyperphosphorylation and neurodegeneration. Human Molecular Genetics, 19(20), 3959–3969. https://doi.org/10.1093/hmg/ddq311

Hébert, S. S., Sergeant, N., & Buée, L. (2012). MicroRNAs and the Regulation of Tau Metabolism. International Journal of Alzheimer's Disease, 2012, e406561. https://doi.org/10.1155/2012/406561

Hedlund, M., Nagaeva, O., Kargl, D., Baranov, V., & Mincheva-Nilsson, L. (2011). Thermal- and Oxidative Stress Causes Enhanced Release of NKG2D Ligand-Bearing Immunosuppressive Exosomes in Leukemia/Lymphoma T and B Cells. PLOS ONE, 6(2), e16899. https://doi.org/10.1371/journal.pone.0016899

Heisler, F. F., Pechmann, Y., Wieser, I., Altmeppen, H. C., Veenendaal, L., Muhia, M., Schweizer, M., Glatzel, M., Krasemann, S., & Kneussel, M. (2018). Muskelin Coordinates PrPC Lysosome versus Exosome Targeting and Impacts Prion Disease Progression. Neuron, 99(6), 1155-1169.e9. https://doi.org/10.1016/j.neuron.2018.08.010

Heneka, M. T., Kummer, M. P., Stutz, A., Delekate, A., Schwartz, S., Vieira-Saecker, A., Griep, A., Axt, D., Remus, A., Tzeng, T.-C., Gelpi, E., Halle, A., Korte, M., Latz, E., & Golenbock, D. T. (2013). NLRP3 is activated in Alzheimer's disease and contributes to pathology in APP/PS1 mice. Nature, 493(7434), Article 7434. https://doi.org/10.1038/nature11729

Henstridge, C. M., Hyman, B. T., & Spires-Jones, T. L. (2019). Beyond the neuron–cellular interactions early in Alzheimer disease pathogenesis. Nature Reviews Neuroscience, 20(2), 94. https://doi.org/10.1038/s41583-018-0113-1

Hernandez-Rapp, J., Rainone, S., Goupil, C., Dorval, V., Smith, P. Y., Saint-Pierre, M., Vallée, M., Planel, E., Droit, A., Calon, F., Cicchetti, F., & Hébert, S. S. (2016). MicroRNA-132/212 deficiency enhances Aβ production and senile plaque deposition in Alzheimer's disease triple transgenic mice. Scientific Reports, 6(1), Article 1. https://doi.org/10.1038/srep30953

Hick, M., Herrmann, U., Weyer, S. W., Mallm, J.-P., Tschäpe, J.-A., Borgers, M., Mercken, M., Roth, F. C., Draguhn, A., Slomianka, L., Wolfer, D. P., Korte, M., & Müller, U. C. (2015). Acute function of secreted amyloid precursor protein fragment APPsα in synaptic plasticity. Acta Neuropathologica, 129(1), 21–37. https://doi.org/10.1007/s00401-014-1368-x

Hickman, S., Izzy, S., Sen, P., Morsett, L., & Khoury, J. E. (2018). Microglia in neurodegeneration. Nature Neuroscience, 21(10), 1359. https://doi.org/10.1038/s41593-018-0242-x

Hippius, H., & Neundörfer, G. (2003). The discovery of Alzheimer's disease. Dialogues in Clinical Neuroscience, 5(1), 101–108.

Ho, C.-Y., Bar, E., Giannini, C., Marchionni, L., Karajannis, M. A., Zagzag, D., Gutmann, D. H., Eberhart, C. G., & Rodriguez, F. J. (2013). MicroRNA profiling in pediatric pilocytic astrocytoma reveals biologically relevant targets, including PBX3, NFIB, and METAP2. Neuro-Oncology, 15(1), 69–82. https://doi.org/10.1093/neuonc/nos269

Hollins, S. L., Zavitsanou, K., Walker, F. R., & Cairns, M. J. (2014). Alteration of imprinted Dlk1-Dio3 miRNA cluster expression in the entorhinal cortex induced by maternal immune activation and adolescent cannabinoid exposure. Translational Psychiatry, 4(9), Article 9. https://doi.org/10.1038/tp.2014.99

Holmes, B. B., & Diamond, M. I. (2014). Prion-like Properties of Tau Protein: The Importance of Extracellular Tau as a Therapeutic Target. Journal of Biological Chemistry, 289(29), 19855–19861. https://doi.org/10.1074/jbc.R114.549295

Holmes, B. B., Furman, J. L., Mahan, T. E., Yamasaki, T. R., Mirbaha, H., Eades, W. C., Belaygorod, L., Cairns, N. J., Holtzman, D. M., & Diamond, M. I. (2014). Proteopathic tau seeding predicts tauopathy in vivo.

Proceedings of the National Academy of Sciences, 111(41), E4376–E4385. https://doi.org/10.1073/pnas.1411649111

Höög, J. L., & Lötvall, J. (2015). Diversity of extracellular vesicles in human ejaculates revealed by cryo-electron microscopy. Journal of Extracellular Vesicles, 4(1), 28680. https://doi.org/10.3402/jev.v4.28680

Hooper, C., Sainz-Fuertes, R., Lynham, S., Hye, A., Killick, R., Warley, A., Bolondi, C., Pocock, J., & Lovestone, S. (2012). Wnt3a induces exosome secretion from primary cultured rat microglia. BMC Neuroscience, 13(1), 144. https://doi.org/10.1186/1471-2202-13-144

Hooten, N. N., Fitzpatrick, M., Wood, W. H., De, S., Ejiogu, N., Zhang, Y., Mattison, J. A., Becker, K. G., Zonderman, A. B., & Evans, M. K. (2013). Age-related changes in microRNA levels in serum. Aging (Albany NY), 5(10), 725–740.

Hoover, B. R., Reed, M. N., Su, J., Penrod, R. D., Kotilinek, L. A., Grant, M. K., Pitstick, R., Carlson, G. A., Lanier, L. M., Yuan, L.-L., Ashe, K. H., & Liao, D. (2010). Tau Mislocalization to Dendritic Spines Mediates Synaptic Dysfunction Independently of Neurodegeneration. Neuron, 68(6), 1067–1081. https://doi.org/10.1016/j.neuron.2010.11.030

Horie, K., Barthélemy, N. R., Mallipeddi, N., Li, Y., Franklin, E. E., Perrin, R. J., Bateman, R. J., & Sato, C. (2020). Regional correlation of biochemical measures of amyloid and tau phosphorylation in the brain. Acta Neuropathologica Communications, 8, 149. https://doi.org/10.1186/s40478-020-01019-z

Hoshino, A., Kim, H. S., Bojmar, L., Gyan, K. E., Cioffi, M., Hernandez, J., Zambirinis, C. P., Rodrigues, G., Molina, H., Heissel, S., Mark, M. T., Steiner, L., Benito-Martin, A., Lucotti, S., Di Giannatale, A., Offer, K., Nakajima, M., Williams, C., Nogués, L., … Lyden, D. (2020). Extracellular Vesicle and Particle Biomarkers Define Multiple Human Cancers. Cell, 182(4), 1044-1061.e18. https://doi.org/10.1016/j.cell.2020.07.009

Hu, G., Liao, K., Niu, F., Yang, L., Dallon, B. W., Callen, S., Tian, C., Shu, J., Cui, J., Sun, Z., Lyubchenko, Y. L., Ka, M., Chen, X.-M., & Buch, S. (2018). Astrocyte EV-Induced lincRNA-Cox2 Regulates Microglial Phagocytosis: Implications for Morphine-Mediated Neurodegeneration. Molecular Therapy. Nucleic Acids, 13, 450–463. https://doi.org/10.1016/j.omtn.2018.09.019

Hu, Y.-W., Zhao, J.-Y., Li, S.-F., Huang, J.-L., Qiu, Y.-R., Ma, X., Wu, S.-G., Chen, Z.-P., Hu, Y.-R., Yang, J.-Y., Wang, Y.-C., Gao, J.-J., Sha, Y.-H., Zheng, L., & Wang, Q. (2015). RP5-833A20.1/miR-382-5p/NFIA–Dependent Signal Transduction Pathway Contributes to the Regulation of Cholesterol Homeostasis and Inflammatory Reaction. Arteriosclerosis, Thrombosis, and Vascular Biology, 35(1), 87–101. https://doi.org/10.1161/ATVBAHA.114.304296

Hu, Y.-W., Zheng, L., & Wang, Q. (2010). Regulation of cholesterol homeostasis by liver X receptors. Clinica Chimica Acta, 411(9), 617–625. https://doi.org/10.1016/j.cca.2009.12.027

Huang, S., Ge, X., Yu, J., Han, Z., Yin, Z., Li, Y., Chen, F., Wang, H., Zhang, J., & Lei, P. (2018). Increased miR-124-3p in microglial exosomes following traumatic brain injury inhibits neuronal inflammation and contributes to neurite outgrowth via their transfer into neurons. FASEB Journal: Official Publication of the Federation of American Societies for Experimental Biology, 32(1), 512–528. https://doi.org/10.1096/fj.201700673R

Huang, X., Atwood, C. S., Hartshorn, M. A., Multhaup, G., Goldstein, L. E., Scarpa, R. C., Cuajungco, M. P., Gray, D. N., Lim, J., Moir, R. D., Tanzi, R. E., & Bush, A. I. (1999). The Aβ Peptide of Alzheimer's Disease Directly Produces Hydrogen Peroxide through Metal Ion Reduction. Biochemistry, 38(24), 7609–7616. https://doi.org/10.1021/bi990438f

Huang, X., Yuan, T., Tschannen, M., Sun, Z., Jacob, H., Du, M., Liang, M., Dittmar, R. L., Liu, Y., Liang, M., Kohli, M., Thibodeau, S. N., Boardman, L., & Wang, L. (2013). Characterization of human plasma-derived exosomal RNAs by deep sequencing. BMC Genomics, 14(1), 319. https://doi.org/10.1186/1471-2164-14-319

Huang, Y., Cheng, L., Turchinovich, A., Mahairaki, V., Troncoso, J. C., Pletniková, O., Haughey, N. J., Vella, L. J., Hill, A. F., Zheng, L., & Witwer, K. W. (2020). Influence of species and processing parameters on recovery and content of brain tissue-derived extracellular vesicles. Journal of Extracellular Vesicles, 9(1), 1785746. https://doi.org/10.1080/20013078.2020.1785746

Huang, Y., Driedonks, T. A. P., Cheng, L., Rajapaksha, H., Routenberg, D. A., Nagaraj, R., Redding, J., Arab, T., Powell, B. H., Pletniková, O., Troncoso, J. C., Zheng, L., Hill, A. F., Mahairaki, V., & Witwer, K. W. (2022). Brain Tissue-Derived Extracellular Vesicles in Alzheimer's Disease Display Altered Key Protein Levels Including Cell Type-Specific Markers. Journal of Alzheimer's Disease, 90(3), 1057–1072. https://doi.org/10.3233/JAD-220322

Huang, Y., Driedonks, T. A. P., Cheng, L., Rajapaksha, H., Turchinovich, A., Routenberg, D. A., Nagaraj, R., Redding-Ochoa, J., Arab, T., Powell, B. H., Pletnikova, O., Troncoso, J. C., Zheng, L., Hill, A. F., Mahairaki, V., & Witwer, K. W. (2022). Relationships of APOE Genotypes With Small RNA and Protein Cargo of Brain Tissue Extracellular Vesicles From Patients With Late-Stage AD. Neurology Genetics, 8(6). https://doi.org/10.1212/NXG.0000000000200026

Iranifar, E., Seresht, B. M., Momeni, F., Fadaei, E., Mehr, M. H., Ebrahimi, Z., Rahmati, M., Kharazinejad, E., & Mirzaei, H. (2019). Exosomes and microRNAs: New potential therapeutic candidates in Alzheimer disease therapy. Journal of Cellular Physiology, 234(3), 2296–2305. https://doi.org/10.1002/jcp.27214

Irwin, M. R., & Vitiello, M. V. (2019). Implications of sleep disturbance and inflammation for Alzheimer's disease dementia. The Lancet Neurology, 18(3), 296–306. https://doi.org/10.1016/S1474-4422(18)30450-2

Ito, E., Oka, K., Etcheberrigaray, R., Nelson, T. J., McPhie, D. L., Tofel-Grehl, B., Gibson, G. E., & Alkon, D. L. (1994). Internal Ca2+ mobilization is altered in fibroblasts from patients with Alzheimer disease. Proceedings of the National Academy of Sciences of the United States of America, 91(2), 534–538.

Jack, C. R., Bennett, D. A., Blennow, K., Carrillo, M. C., Feldman, H. H., Frisoni, G. B., Hampel, H., Jagust, W. J., Johnson, K. A., Knopman, D. S., Petersen, R. C., Scheltens, P., Sperling, R. A., & Dubois, B. (2016). A/T/N: An unbiased descriptive classification scheme for Alzheimer disease biomarkers. Neurology, 87(5), 539–547. https://doi.org/10.1212/WNL.0000000000002923

Janelidze, S., Mattsson, N., Palmqvist, S., Smith, R., Beach, T. G., Serrano, G. E., Chai, X., Proctor, N. K., Eichenlaub, U., Zetterberg, H., Blennow, K., Reiman, E. M., Stomrud, E., Dage, J. L., & Hansson, O. (2020). Plasma P-tau181 in Alzheimer's disease: Relationship to other biomarkers, differential diagnosis, neuropathology and longitudinal progression to Alzheimer's dementia. Nature Medicine, 26(3), Article 3. https://doi.org/10.1038/s41591-020-0755-1

Jang, S.-I., Tandon, M., Teos, L., Zheng, C., Warner, B. M., & Alevizos, I. (2019). Dual function of miR-1248 links interferon induction and calcium signaling defects in Sjögren's syndrome. EBioMedicine, 48, 526–538. https://doi.org/10.1016/j.ebiom.2019.09.010

Jaraj, D., Wikkelsø, C., Rabiei, K., Marlow, T., Jensen, C., Östling, S., & Skoog, I. (2017). Mortality and risk of dementia in normal-pressure hydrocephalus: A population study. Alzheimer's & Dementia, 13(8), 850–857. https://doi.org/10.1016/j.jalz.2017.01.013

Jaunmuktane, Z., Mead, S., Ellis, M., Wadsworth, J. D. F., Nicoll, A. J., Kenny, J., Launchbury, F., Linehan, J., Richard-Loendt, A., Walker, A. S., Rudge, P., Collinge, J., & Brandner, S. (2015). Evidence for human transmission of amyloid-β pathology and cerebral amyloid angiopathy. Nature, 525(7568), 247–250. https://doi.org/10.1038/nature15369

Jeyaram, A., & Jay, S. M. (2017). Preservation and Storage Stability of Extracellular Vesicles for Therapeutic Applications. The AAPS Journal, 20(1), 1. https://doi.org/10.1208/s12248-017-0160-y

Ji, J., Qin, Y., Ren, J., Lu, C., Wang, R., Dai, X., Zhou, R., Huang, Z., Xu, M., Chen, M., Wu, W., Song, L., Shen, H., Hu, Z., Miao, D., Xia, Y., & Wang, X. (2015). Mitochondria-related miR-141-3p contributes to mitochondrial

dysfunction in HFD-induced obesity by inhibiting PTEN. Scientific Reports, 5, 16262. https://doi.org/10.1038/srep16262

Ji, Y., Wang, D., Zhang, B., & Lu, H. (2019). MiR-361-3p inhibits β-amyloid accumulation and attenuates cognitive deficits through targeting BACE1 in Alzheimer's disease. Journal of Integrative Neuroscience, 18(3), Article 3. https://doi.org/10.31083/j.jin.2019.03.1136

Jia, L., Zhu, M., Yang, J., Pang, Y., Wang, Q., Li, Y., Li, T., Li, F., Wang, Q., Li, Y., & Wei, Y. (2021). Prediction of P-tau/Aβ42 in the cerebrospinal fluid with blood microRNAs in Alzheimer's disease. BMC Medicine, 19, 264. https://doi.org/10.1186/s12916-021-02142-x

Jiang, M., Xiang, Y., Wang, D., Gao, J., Liu, D., Liu, Y., Liu, S., & Zheng, D. (2012). Dysregulated expression of miR-146a contributes to age-related dysfunction of macrophages. Aging Cell, 11(1), 29–40. https://doi.org/10.1111/j.1474-9726.2011.00757.x

Jones, T. A., Jeyapalan, J. N., Forshew, T., Tatevossian, R. G., Lawson, A. R. J., Patel, S. N., Doctor, G. T., Mumin, M. A., Picker, S. R., Phipps, K. P., Michalski, A., Jacques, T. S., & Sheer, D. (2015). Molecular analysis of pediatric brain tumors identifies microRNAs in pilocytic astrocytomas that target the MAPK and NF-κB pathways. Acta Neuropathologica Communications, 3(1), 86. https://doi.org/10.1186/s40478-015-0266-3

Joshi, A. U., Minhas, P. S., Liddelow, S. A., Haileselassie, B., Andreasson, K. I., Dorn II, G. W., & Mochly-Rosen, D. (2019). Fragmented mitochondria released from microglia trigger A1 astrocytic response and propagate inflammatory neurodegeneration. Nature Neuroscience, 22(10), 1635–1648. https://doi.org/10.1038/s41593-019-0486-0

Joshi, P., Turola, E., Ruiz, A., Bergami, A., Libera, D. D., Benussi, L., Giussani, P., Magnani, G., Comi, G., Legname, G., Ghidoni, R., Furlan, R., Matteoli, M., & Verderio, C. (2014). Microglia convert aggregated amyloid-β into neurotoxic forms through the shedding of microvesicles. Cell Death and Differentiation, 21(4), 582–593. https://doi.org/10.1038/cdd.2013.180

Kamerkar, S., LeBleu, V. S., Sugimoto, H., Yang, S., Ruivo, C. F., Melo, S. A., Lee, J. J., & Kalluri, R. (2017). Exosomes facilitate therapeutic targeting of oncogenic KRAS in pancreatic cancer. Nature, 546(7659), 498–503. https://doi.org/10.1038/nature22341

Kane, M. D., Lipinski, W. J., Callahan, M. J., Bian, F., Durham, R. A., Schwarz, R. D., Roher, A. E., & Walker, L. C. (2000). Evidence for Seeding of β-Amyloid by Intracerebral Infusion of Alzheimer Brain Extracts in β-Amyloid Precursor Protein-Transgenic Mice. Journal of Neuroscience, 20(10), 3606–3611. https://doi.org/10.1523/JNEUROSCI.20-10-03606.2000

Kang, S.-W., Kim, S. J., & Kim, M.-S. (2017). Oxidative stress with tau hyperphosphorylation in memory impaired 1,2-diacetylbenzene-treated mice. Toxicology Letters, 279, 53–59. https://doi.org/10.1016/j.toxlet.2017.07.892

Kapasi, A., DeCarli, C., & Schneider, J. A. (2017). Impact of Multiple Pathologies on the Threshold for Clinically Overt Dementia. Acta Neuropathologica, 134(2), 171–186. https://doi.org/10.1007/s00401-017-1717-7

Kapogiannis, D., Mustapic, M., Shardell, M. D., Berkowitz, S. T., Diehl, T. C., Spangler, R. D., Tran, J., Lazaropoulos, M. P., Chawla, S., Gulyani, S., Eitan, E., An, Y., Huang, C.-W., Oh, E. S., Lyketsos, C. G., Resnick, S. M., Goetzl, E. J., & Ferrucci, L. (2019). Association of Extracellular Vesicle Biomarkers With Alzheimer Disease in the Baltimore Longitudinal Study of Aging. JAMA Neurology, 76(11), 1340–1351. https://doi.org/10.1001/jamaneurol.2019.2462

Karikari, T. K., Pascoal, T. A., Ashton, N. J., Janelidze, S., Benedet, A. L., Rodriguez, J. L., Chamoun, M., Savard, M., Kang, M. S., Therriault, J., Schöll, M., Massarweh, G., Soucy, J.-P., Höglund, K., Brinkmalm, G., Mattsson, N., Palmqvist, S., Gauthier, S., Stomrud, E., … Blennow, K. (2020). Blood phosphorylated tau 181 as a biomarker for Alzheimer's disease: A diagnostic performance and prediction modelling study using data from

four prospective cohorts. The Lancet Neurology, 19(5), 422–433. https://doi.org/10.1016/S1474-4422(20)30071-5

Karimi, N., Cvjetkovic, A., Jang, S. C., Crescitelli, R., Hosseinpour Feizi, M. A., Nieuwland, R., Lötvall, J., & Lässer, C. (2018). Detailed analysis of the plasma extracellular vesicle proteome after separation from lipoproteins. Cellular and Molecular Life Sciences, 75(15), 2873–2886. https://doi.org/10.1007/s00018-018-2773-4

Karran, E., & Strooper, B. D. (2016). The amyloid cascade hypothesis: Are we poised for success or failure? Journal of Neurochemistry, 139(S2), 237–252. https://doi.org/10.1111/jnc.13632

Kawahara, Y., & Mieda-Sato, A. (2012). TDP-43 promotes microRNA biogenesis as a component of the Drosha and Dicer complexes. Proceedings of the National Academy of Sciences, 109(9), 3347–3352. https://doi.org/10.1073/pnas.1112427109

Kehl, T., Kern, F., Backes, C., Fehlmann, T., Stöckel, D., Meese, E., Lenhof, H.-P., & Keller, A. (2020). miRPathDB 2.0: A novel release of the miRNA Pathway Dictionary Database. Nucleic Acids Research, 48(D1), D142–D147. https://doi.org/10.1093/nar/gkz1022

Kent, S. A., Spires-Jones, T. L., & Durrant, C. S. (2020). The physiological roles of tau and Aβ: Implications for Alzheimer's disease pathology and therapeutics. Acta Neuropathologica, 140(4), 417–447. https://doi.org/10.1007/s00401-020-02196-w

Keren-Shaul, H., Spinrad, A., Weiner, A., Matcovitch-Natan, O., Dvir-Szternfeld, R., Ulland, T. K., David, E., Baruch, K., Lara-Astaiso, D., Toth, B., Itzkovitz, S., Colonna, M., Schwartz, M., & Amit, I. (2017). A Unique Microglia Type Associated with Restricting Development of Alzheimer's Disease. Cell, 169(7), 1276-1290.e17. https://doi.org/10.1016/j.cell.2017.05.018

Kiko, T., Nakagawa, K., Tsuduki, T., Furukawa, K., Arai, H., & Miyazawa, T. (2014). MicroRNAs in Plasma and Cerebrospinal Fluid as Potential Markers for Alzheimer's Disease. Journal of Alzheimer's Disease, 39(2), 253–259. https://doi.org/10.3233/JAD-130932

Kim, J., Yoon, H., Horie, T., Burchett, J. M., Restivo, J. L., Rotllan, N., Ramírez, C. M., Verghese, P. B., Ihara, M., Hoe, H.-S., Esau, C., Fernández-Hernando, C., Holtzman, D. M., Cirrito, J. R., Ono, K., & Kim, J. (2015). MicroRNA-33 Regulates ApoE Lipidation and Amyloid-β Metabolism in the Brain. Journal of Neuroscience, 35(44), 14717–14726. https://doi.org/10.1523/JNEUROSCI.2053-15.2015

Kim, J., Yoon, H., Ramírez, C. M., Lee, S.-M., Hoe, H.-S., Fernández-Hernando, C., & Kim, J. (2012). MiR-106b impairs cholesterol efflux and increases Aβ levels by repressing ABCA1 expression. Experimental Neurology, 235(2), 476–483. https://doi.org/10.1016/j.expneurol.2011.11.010

Kim, K. M., Abdelmohsen, K., Mustapic, M., Kapogiannis, D., & Gorospe, M. (2017). RNA in extracellular vesicles. Wiley Interdisciplinary Reviews. RNA, 8(4). https://doi.org/10.1002/wrna.1413

Kivipelto, M., Mangialasche, F., & Ngandu, T. (2018). Lifestyle interventions to prevent cognitive impairment, dementia and Alzheimer disease. Nature Reviews Neurology, 14(11), 653. https://doi.org/10.1038/s41582-018-0070-3

Kivipelto, M., Mangialasche, F., Snyder, H. M., Allegri, R., Andrieu, S., Arai, H., Baker, L., Belleville, S., Brodaty, H., Brucki, S. M., Calandri, I., Caramelli, P., Chen, C., Chertkow, H., Chew, E., Choi, S. H., Chowdhary, N., Crivelli, L., Torre, R. D. L., … Carrillo, M. C. (2020). World-Wide FINGERS Network: A global approach to risk reduction and prevention of dementia. Alzheimer's & Dementia, 16(7), 1078–1094. https://doi.org/10.1002/alz.12123

Klyucherev, T. O., Olszewski, P., Shalimova, A. A., Chubarev, V. N., Tarasov, V. V., Attwood, M. M., Syvänen, S., & Schiöth, H. B. (2022). Advances in the development of new biomarkers for Alzheimer's disease. Translational Neurodegeneration, 11(1), 25. https://doi.org/10.1186/s40035-022-00296-z

Ko, J., Hemphill, M., Yang, Z., Beard, K., Sewell, E., Shallcross, J., Schweizer, M., Sandsmark, D. K., Diaz-Arrastia, R., Kim, J., Meaney, D., & Issadore, D. (2020). Multi-Dimensional Mapping of Brain-Derived Extracellular

Vesicle MicroRNA Biomarker for Traumatic Brain Injury Diagnostics. Journal of Neurotrauma, 37(22), 2424–2434. https://doi.org/10.1089/neu.2018.6220

Kodama, L., Guzman, E., Etchegaray, J. I., Li, Y., Sayed, F. A., Zhou, L., Zhou, Y., Zhan, L., Le, D., Udeochu, J. C., Clelland, C. D., Cheng, Z., Yu, G., Li, Q., Kosik, K. S., & Gan, L. (2020). Microglial microRNAs mediate sex-specific responses to tau pathology. Nature Neuroscience, 23(2), Article 2. https://doi.org/10.1038/s41593-019-0560-7

Koffie, R. M., Meyer-Luehmann, M., Hashimoto, T., Adams, K. W., Mielke, M. L., Garcia-Alloza, M., Micheva, K. D., Smith, S. J., Kim, M. L., Lee, V. M., Hyman, B. T., & Spires-Jones, T. L. (2009). Oligomeric amyloid β associates with postsynaptic densities and correlates with excitatory synapse loss near senile plaques. Proceedings of the National Academy of Sciences, 106(10), 4012–4017. https://doi.org/10.1073/pnas.0811698106

Kornilov, R., Puhka, M., Mannerström, B., Hiidenmaa, H., Peltoniemi, H., Siljander, P., Seppänen-Kaijansinkko, R., & Kaur, S. (2018). Efficient ultrafiltration-based protocol to deplete extracellular vesicles from fetal bovine serum. Journal of Extracellular Vesicles, 7(1), 1422674. https://doi.org/10.1080/20013078.2017.1422674

Kowal, J., Arras, G., Colombo, M., Jouve, M., Morath, J. P., Primdal-Bengtson, B., Dingli, F., Loew, D., Tkach, M., & Théry, C. (2016). Proteomic comparison defines novel markers to characterize heterogeneous populations of extracellular vesicle subtypes. Proceedings of the National Academy of Sciences, 113(8), E968–E977. https://doi.org/10.1073/pnas.1521230113

Kucharzewska, P., Christianson, H. C., Welch, J. E., Svensson, K. J., Fredlund, E., Ringnér, M., Mörgelin, M., Bourseau-Guilmain, E., Bengzon, J., & Belting, M. (2013). Exosomes reflect the hypoxic status of glioma cells and mediate hypoxia-dependent activation of vascular cells during tumor development. Proceedings of the National Academy of Sciences of the United States of America, 110(18), 7312–7317. https://doi.org/10.1073/pnas.1220998110

Kumar, A., Nayak, S., Pathak, P., Purkait, S., Malgulawar, P. B., Sharma, M. C., Suri, V., Mukhopadhyay, A., Suri, A., & Sarkar, C. (2018). Identification of miR-379/miR-656 (C14MC) cluster downregulation and associated epigenetic and transcription regulatory mechanism in oligodendrogliomas. Journal of Neuro-Oncology, 139(1), 23–31. https://doi.org/10.1007/s11060-018-2840-6

Kumar, P., Dezso, Z., MacKenzie, C., Oestreicher, J., Agoulnik, S., Byrne, M., Bernier, F., Yanagimachi, M., Aoshima, K., & Oda, Y. (2013). Circulating miRNA Biomarkers for Alzheimer's Disease. PLOS ONE, 8(7), e69807. https://doi.org/10.1371/journal.pone.0069807

Kunkle, B. W., Grenier-Boley, B., Sims, R., Bis, J. C., Damotte, V., Naj, A. C., Boland, A., Vronskaya, M., van der Lee, S. J., Amlie-Wolf, A., Bellenguez, C., Frizatti, A., Chouraki, V., Martin, E. R., Sleegers, K., Badarinarayan, N., Jakobsdottir, J., Hamilton-Nelson, K. L., Moreno-Grau, S., … Pericak-Vance, M. A. (2019). Genetic meta-analysis of diagnosed Alzheimer's disease identifies new risk loci and implicates Aβ, tau, immunity and lipid processing. Nature Genetics, 51(3), Article 3. https://doi.org/10.1038/s41588-019-0358-2

Kuo, Y.-M., Kokjohn, T. A., Watson, M. D., Woods, A. S., Cotter, R. J., Sue, L. I., Kalback, W. M., Emmerling, M. R., Beach, T. G., & Roher, A. E. (2000). Elevated Aβ42 in Skeletal Muscle of Alzheimer Disease Patients Suggests Peripheral Alterations of AβPP Metabolism. The American Journal of Pathology, 156(3), 797–805.

Kurkinen, K. M. A., Marttinen, M., Turner, L., Natunen, T., Mäkinen, P., Haapalinna, F., Sarajärvi, T., Gabbouj, S., Kurki, M., Paananen, J., Koivisto, A. M., Rauramaa, T., Leinonen, V., Tanila, H., Soininen, H., Lucas, F. R., Haapasalo, A., & Hiltunen, M. (2016). SEPT8 modulates β-amyloidogenic processing of APP by affecting the sorting and accumulation of BACE1. J Cell Sci, 129(11), 2224–2238. https://doi.org/10.1242/jcs.185215

Lace, G., Savva, G. M., Forster, G., de Silva, R., Brayne, C., Matthews, F. E., Barclay, J. J., Dakin, L., Ince, P. G., Wharton, S. B., & on behalf of MRC-CFAS. (2009). Hippocampal tau pathology is related to neuroanatomical connections: An ageing population-based study. Brain, 132(5), 1324–1334. https://doi.org/10.1093/brain/awp059

Lace-Costigan, G., Wharton, S. B., & Ince, P. (2007). A brief history of τ: The evolving view of the microtubule-associated protein τ in neurodegenerative diseases (Vol. 26). https://doi.org/10.5414/NPP26043

Lachenal, G., Pernet-Gallay, K., Chivet, M., Hemming, F. J., Belly, A., Bodon, G., Blot, B., Haase, G., Goldberg, Y., & Sadoul, R. (2011). Release of exosomes from differentiated neurons and its regulation by synaptic glutamatergic activity. Molecular and Cellular Neuroscience, 46(2), 409–418. https://doi.org/10.1016/j.mcn.2010.11.004

Lau, P., Bossers, K., Janky, R., Salta, E., Frigerio, C. S., Barbash, S., Rothman, R., Sierksma, A. S. R., Thathiah, A., Greenberg, D., Papadopoulou, A. S., Achsel, T., Ayoubi, T., Soreq, H., Verhaagen, J., Swaab, D. F., Aerts, S., & De Strooper, B. (2013). Alteration of the microRNA network during the progression of Alzheimer's disease. EMBO Molecular Medicine, 5(10), 1613–1634. https://doi.org/10.1002/emmm.201201974

Laurén, J., Gimbel, D. A., Nygaard, H. B., Gilbert, J. W., & Strittmatter, S. M. (2009). Cellular Prion Protein Mediates Impairment of Synaptic Plasticity by Amyloid-β Oligomers. Nature, 457(7233), 1128–1132. https://doi.org/10.1038/nature07761

Le, M. T. N., Teh, C., Shyh-Chang, N., Xie, H., Zhou, B., Korzh, V., Lodish, H. F., & Lim, B. (2009). MicroRNA-125b is a novel negative regulator of p53. Genes & Development, 23(7), 862–876. https://doi.org/10.1101/gad.1767609

Lech, A., Wiera, G., & Mozrzymas, J. (2019). Matrix metalloproteinase-3 in brain physiology and neurodegeneration. Advances in Clinical and Experimental Medicine, 28(12), 1717–1722. https://doi.org/10.17219/acem/110319

Lee, H., Li, C., Zhang, Y., Zhang, D., Otterbein, L. E., & Jin, Y. (2019). Caveolin-1 selectively regulates microRNA sorting into microvesicles after noxious stimuli. Journal of Experimental Medicine, 216(9), 2202–2220. https://doi.org/10.1084/jem.20182313

Lee, J.-H., Choi, J.-H., Chueng, S.-T. D., Pongkulapa, T., Yang, L., Cho, H.-Y., Choi, J.-W., & Lee, K.-B. (2019). Nondestructive Characterization of Stem Cell Neurogenesis by a Magneto-Plasmonic Nanomaterial-Based Exosomal miRNA Detection. ACS Nano, 13(8), 8793–8803. https://doi.org/10.1021/acsnano.9b01875

Lee, J.-H., Ostalecki, C., Oberstein, T., Schierer, S., Zinser, E., Eberhardt, M., Blume, K., Plosnita, B., Stich, L., Bruns, H., Coras, R., Vera-Gonzales, J., Maler, M., & Baur, A. S. (2022). Alzheimer's disease protease-containing plasma extracellular vesicles transfer to the hippocampus via the choroid plexus. EBioMedicine, 77, 103903. https://doi.org/10.1016/j.ebiom.2022.103903

Lehrich, B. M., Liang, Y., Khosravi, P., Federoff, H. J., & Fiandaca, M. S. (2018). Fetal Bovine Serum-Derived Extracellular Vesicles Persist within Vesicle-Depleted Culture Media. International Journal of Molecular Sciences, 19(11), Article 11. https://doi.org/10.3390/ijms19113538

Lei, B., Liu, J., Yao, Z., Xiao, Y., Zhang, X., Zhang, Y., & Xu, J. (2021). NF-κB-Induced Upregulation of miR-146a-5p Promoted Hippocampal Neuronal Oxidative Stress and Pyroptosis via TIGAR in a Model of Alzheimer's Disease. Frontiers in Cellular Neuroscience, 15. https://www.frontiersin.org/articles/10.3389/fncel.2021.653881

Leidal, A. M., Huang, H. H., Marsh, T., Solvik, T., Zhang, D., Ye, J., Kai, F., Goldsmith, J., Liu, J. Y., Huang, Y.-H., Monkkonen, T., Vlahakis, A., Huang, E. J., Goodarzi, H., Yu, L., Wiita, A. P., & Debnath, J. (2020). The LC3-Conjugation Machinery Specifies the Loading of RNA-Binding Proteins into Extracellular Vesicles. Nature Cell Biology, 22(2), 187. https://doi.org/10.1038/s41556-019-0450-y

Leroux, E., Perbet, R., Caillierez, R., Richetin, K., Lieger, S., Espourteille, J., Bouillet, T., Bégard, S., Danis, C., Loyens, A., Toni, N., Déglon, N., Deramecourt, V., Schraen-Maschke, S., Buée, L., & Colin, M. (2022). Extracellular vesicles: Major actors of heterogeneity in tau spreading among human tauopathies. Molecular Therapy, 30(2), 782–797. https://doi.org/10.1016/j.ymthe.2021.09.020

Lewis, B. P., Burge, C. B., & Bartel, D. P. (2005). Conserved Seed Pairing, Often Flanked by Adenosines, Indicates that Thousands of Human Genes are MicroRNA Targets. Cell, 120(1), 15–20. https://doi.org/10.1016/j.cell.2004.12.035

Li, F., Xie, X.-Y., Sui, X.-F., Wang, P., Chen, Z., & Zhang, J.-B. (2020). Profile of Pathogenic Proteins and MicroRNAs in Plasma-derived Extracellular Vesicles in Alzheimer's Disease: A Pilot Study. Neuroscience, 432, 240–246. https://doi.org/10.1016/j.neuroscience.2020.02.044

Li, H., Lu, C., Yao, W., Xu, L., Zhou, J., & Zheng, B. (2020). Dexmedetomidine inhibits inflammatory response and autophagy through the circLrp1b/miR-27a-3p/Dram2 pathway in a rat model of traumatic brain injury. Aging (Albany NY), 12(21), 21687–21705. https://doi.org/10.18632/aging.103975

Li, J. J., Wang, B., Kodali, M. C., Chen, C., Kim, E., Patters, B. J., Lan, L., Kumar, S., Wang, X., Yue, J., & Liao, F.-F. (2018). In vivo evidence for the contribution of peripheral circulating inflammatory exosomes to neuroinflammation. Journal of Neuroinflammation, 15, 8. https://doi.org/10.1186/s12974-017-1038-8

Li, J.-Y., Englund, E., Holton, J. L., Soulet, D., Hagell, P., Lees, A. J., Lashley, T., Quinn, N. P., Rehncrona, S., Björklund, A., Widner, H., Revesz, T., Lindvall, O., & Brundin, P. (2008). Lewy bodies in grafted neurons in subjects with Parkinson's disease suggest host-to-graft disease propagation. Nature Medicine, 14(5), Article 5. https://doi.org/10.1038/nm1746

Li, K., Ching, D., Luk, F. S., & Raffai, R. L. (2015). Apolipoprotein E Enhances MicroRNA-146a in Monocytes and Macrophages to Suppress Nuclear Factor-κB–Driven Inflammation and Atherosclerosis. Circulation Research, 117(1), e1–e11. https://doi.org/10.1161/CIRCRESAHA.117.305844

Li, M., Xiao, A., Floyd, D., Olmez, I., Lee, J., Godlewski, J., Bronisz, A., Bhat, K. P. L., Sulman, E. P., Nakano, I., & Purow, B. (2017). CDK4/6 inhibition is more active against the glioblastoma proneural subtype. Oncotarget, 8(33), 55319–55331. https://doi.org/10.18632/oncotarget.19429

Li, P., Xu, Y., Wang, B., Huang, J., & Li, Q. (2020). MiR-34a-5p and miR-125b-5p attenuate Aβ-induced neurotoxicity through targeting BACE1. Journal of the Neurological Sciences, 413, 116793. https://doi.org/10.1016/j.jns.2020.116793

Li, Q. S., & Cai, D. (2021). Integrated miRNA-Seq and mRNA-Seq Study to Identify miRNAs Associated With Alzheimer's Disease Using Post-mortem Brain Tissue Samples. Frontiers in Neuroscience, 15. https://www.frontiersin.org/articles/10.3389/fnins.2021.620899

Li, Q., Wang, Y., Peng, W., Jia, Y., Tang, J., Li, W., Zhang, J. H., & Yang, J. (2019). MicroRNA-101a Regulates Autophagy Phenomenon via the MAPK Pathway to Modulate Alzheimer's-Associated Pathogenesis. Cell Transplantation, 28(8), 1076–1084. https://doi.org/10.1177/0963689719857085

Li, S., Stöckl, S., Lukas, C., Herrmann, M., Brochhausen, C., König, M. A., Johnstone, B., & Grässel, S. (2021). Curcumin-primed human BMSC-derived extracellular vesicles reverse IL-1β-induced catabolic responses of OA chondrocytes by upregulating miR-126-3p. Stem Cell Research & Therapy, 12, 252. https://doi.org/10.1186/s13287-021-02317-6

Li, S., Wu, L., Ma, M., Yang, L., & Qin, C. (2022). MicroRNA-668-3p regulates oxidative stress and cell damage induced by Aβ1-42 by targeting the OXR1/p53-p21 axis. Annals of Translational Medicine, 10(17), 928. https://doi.org/10.21037/atm-22-3598

Li, X., Zhang, J., Li, D., He, C., He, K., Xue, T., Wan, L., Zhang, C., & Liu, Q. (2021). Astrocytic ApoE reprograms neuronal cholesterol metabolism and histone-acetylation-mediated memory. Neuron, 109(6), 957-970.e8. https://doi.org/10.1016/j.neuron.2021.01.005

Li, Y. Y., Cui, J. G., Hill, J. M., Bhattacharjee, S., Zhao, Y., & Lukiw, W. J. (2011). Increased expression of miRNA-146a in Alzheimer's disease transgenic mouse models. Neuroscience Letters, 487(1), 94–98. https://doi.org/10.1016/j.neulet.2010.09.079

Liao, Z., Jaular, L. M., Soueidi, E., Jouve, M., Muth, D. C., Schøyen, T. H., Seale, T., Haughey, N. J., Ostrowski, M., Théry, C., & Witwer, K. W. (2019). Acetylcholinesterase is not a generic marker of extracellular vesicles. Journal of Extracellular Vesicles, 8(1), 1628592. https://doi.org/10.1080/20013078.2019.1628592

Lim, Y.-J., & Lee, S.-J. (2017). Are exosomes the vehicle for protein aggregate propagation in neurodegenerative diseases? Acta Neuropathologica Communications, 5. https://doi.org/10.1186/s40478-017-0467-z

Liu, C., Li, Y., Nwosu, A., Ang, T. F. A., Liu, Y., Devine, S., Au, R., & Doraiswamy, P. M. (2022). Sex-specific biomarkers in Alzheimer's disease progression: Framingham Heart Study. Alzheimer's & Dementia: Diagnosis, Assessment & Disease Monitoring, 14(1), e12369. https://doi.org/10.1002/dad2.12369

Liu, C.-C., Kanekiyo, T., Xu, H., & Bu, G. (2013). Apolipoprotein E and Alzheimer disease: Risk, mechanisms, and therapy. Nature Reviews. Neurology, 9(2), 106–118. https://doi.org/10.1038/nrneurol.2012.263

Liu, C.-G., Song, J., Zhang, Y.-Q., & Wang, P.-C. (2014). MicroRNA-193b is a regulator of amyloid precursor protein in the blood and cerebrospinal fluid derived exosomal microRNA-193b is a biomarker of Alzheimer's disease. Molecular Medicine Reports, 10(5), 2395–2400. https://doi.org/10.3892/mmr.2014.2484

Liu, D., Zhao, D., Zhao, Y., Wang, Y., Zhao, Y., & Wen, C. (2019). Inhibition of microRNA-155 Alleviates Cognitive Impairment in Alzheimer's Disease and Involvement of Neuroinflammation. Current Alzheimer Research, 16(6), 473–482. https://doi.org/10.2174/1567205016666190503145207

Liu, Q., Smith, M. A., Avilá, J., DeBernardis, J., Kansal, M., Takeda, A., Zhu, X., Nunomura, A., Honda, K., Moreira, P. I., Oliveira, C. R., Santos, M. S., Shimohama, S., Aliev, G., de la Torre, J., Ghanbari, H. A., Siedlak, S. L., Harris, P. L. R., Sayre, L. M., & Perry, G. (2005). Alzheimer-specific epitopes of tau represent lipid peroxidation-induced conformations. Free Radical Biology and Medicine, 38(6), 746–754. https://doi.org/10.1016/j.freeradbiomed.2004.11.005

Liu, S., Liu, Y., Hao, W., Wolf, L., Kiliaan, A. J., Penke, B., Rübe, C. E., Walter, J., Heneka, M. T., Hartmann, T., Menger, M. D., & Fassbender, K. (2012). TLR2 Is a Primary Receptor for Alzheimer's Amyloid β Peptide To Trigger Neuroinflammatory Activation. The Journal of Immunology, 188(3), 1098–1107. https://doi.org/10.4049/jimmunol.1101121

Liu, W., Cai, H., Lin, M., Zhu, L., Gao, L., Zhong, R., Bi, S., Xue, Y., & Shang, X. (2016). MicroRNA-107 prevents amyloid-beta induced blood-brain barrier disruption and endothelial cell dysfunction by targeting Endophilin-1. Experimental Cell Research, 343(2), 248–257. https://doi.org/10.1016/j.yexcr.2016.03.026

Liu, X., Kwon, H., Li, Z., & Fu, Y. (2017). Is CD47 an innate immune checkpoint for tumor evasion? Journal of Hematology & Oncology, 10(1), 12. https://doi.org/10.1186/s13045-016-0381-z

Liu, X. S., Chopp, M., Wang, X. L., Zhang, L., Hozeska-Solgot, A., Tang, T., Kassis, H., Zhang, R. L., Chen, C., Xu, J., & Zhang, Z. G. (2013). MicroRNA-17-92 Cluster Mediates the Proliferation and Survival of Neural Progenitor Cells after Stroke. The Journal of Biological Chemistry, 288(18), 12478–12488. https://doi.org/10.1074/jbc.M112.449025

Livak, K. J., & Schmittgen, T. D. (2001). Analysis of Relative Gene Expression Data Using Real-Time Quantitative PCR and the 2−ΔΔCT Method. Methods, 25(4), 402–408. https://doi.org/10.1006/meth.2001.1262

Livingston, G., Huntley, J., Sommerlad, A., Ames, D., Ballard, C., Banerjee, S., Brayne, C., Burns, A., Cohen-Mansfield, J., Cooper, C., Costafreda, S. G., Dias, A., Fox, N., Gitlin, L. N., Howard, R., Kales, H. C., Kivimäki, M., Larson, E. B., Ogunniyi, A., … Mukadam, N. (2020). Dementia prevention, intervention, and care: 2020 report of the Lancet Commission. The Lancet, 396(10248), 413–446. https://doi.org/10.1016/S0140-6736(20)30367-6

Long, J. M., Maloney, B., Rogers, J. T., & Lahiri, D. K. (2018). Novel upregulation of amyloid-β precursor protein (APP) by microRNA-346 via targeting of APP mRNA 5'-untranslated region: Implications in Alzheimer's disease. Molecular Psychiatry, 1. https://doi.org/10.1038/s41380-018-0266-3

Lopes, F. M., Schröder, R., Júnior, M. L. C. da F., Zanotto-Filho, A., Müller, C. B., Pires, A. S., Meurer, R. T., Colpo, G. D., Gelain, D. P., Kapczinski, F., Moreira, J. C. F., Fernandes, M. da C., & Klamt, F. (2010). Comparison between proliferative and neuron-like SH-SY5Y cells as an in vitro model for Parkinson disease studies. Brain Research, 1337, 85–94. https://doi.org/10.1016/j.brainres.2010.03.102

Lopez-Verrilli, M. A., Picou, F., & Court, F. A. (2013). Schwann cell-derived exosomes enhance axonal regeneration in the peripheral nervous system. Glia, 61(11), 1795–1806. https://doi.org/10.1002/glia.22558

Love, M. I., Huber, W., & Anders, S. (2014). Moderated estimation of fold change and dispersion for RNA-seq data with DESeq2. Genome Biology, 15(12), 550. https://doi.org/10.1186/s13059-014-0550-8

Lugli, G., Cohen, A. M., Bennett, D. A., Shah, R. C., Fields, C. J., Hernandez, A. G., & Smalheiser, N. R. (2015a). Plasma Exosomal miRNAs in Persons with and without Alzheimer Disease: Altered Expression and Prospects for Biomarkers. PLOS ONE, 10(10), e0139233. https://doi.org/10.1371/journal.pone.0139233

Lugli, G., Cohen, A. M., Bennett, D. A., Shah, R. C., Fields, C. J., Hernandez, A. G., & Smalheiser, N. R. (2015b). Plasma Exosomal miRNAs in Persons with and without Alzheimer Disease: Altered Expression and Prospects for Biomarkers. PLOS ONE, 10(10), e0139233. https://doi.org/10.1371/journal.pone.0139233

Ma, Y., Wang, K., Pan, J., Fan, Z., Tian, C., Deng, X., Ma, K., Xia, X., Huang, Y., & Zheng, J. C. (2019). Induced neural progenitor cells abundantly secrete extracellular vesicles and promote the proliferation of neural progenitors via extracellular signal–regulated kinase pathways. Neurobiology of Disease, 124, 322–334. https://doi.org/10.1016/j.nbd.2018.12.003

Maacha, S., Bhat, A. A., Jimenez, L., Raza, A., Haris, M., Uddin, S., & Grivel, J.-C. (2019). Extracellular vesicles-mediated intercellular communication: Roles in the tumor microenvironment and anti-cancer drug resistance. Molecular Cancer, 18(1), 55. https://doi.org/10.1186/s12943-019-0965-7

Maas, S. L. N., Breakefield, X. O., & Weaver, A. M. (2017). Extracellular Vesicles: Unique Intercellular Delivery Vehicles. Trends in Cell Biology, 27(3), 172–188. https://doi.org/10.1016/j.tcb.2016.11.003

Maffioletti, E., Milanesi, E., Ansari, A., Zanetti, O., Galluzzi, S., Geroldi, C., Gennarelli, M., & Bocchio-Chiavetto, L. (2020). MiR-146a Plasma Levels Are Not Altered in Alzheimer's Disease but Correlate With Age and Illness Severity. Frontiers in Aging Neuroscience, 11. https://www.frontiersin.org/articles/10.3389/fnagi.2019.00366

Mallach, A., Gobom, J., Arber, C., Piers, T. M., Hardy, J., Wray, S., Zetterberg, H., & Pocock, J. (2021). Differential Stimulation of Pluripotent Stem Cell-Derived Human Microglia Leads to Exosomal Proteomic Changes Affecting Neurons. Cells, 10(11), Article 11. https://doi.org/10.3390/cells10112866

Mallach, A., Gobom, J., Zetterberg, H., Hardy, J., Piers, T. M., Wray, S., & Pocock, J. M. (2021). The influence of the R47H triggering receptor expressed on myeloid cells 2 variant on microglial exosome profiles. Brain Communications, 3(2), fcab009. https://doi.org/10.1093/braincomms/fcab009

Maphis, N., Xu, G., Kokiko-Cochran, O. N., Jiang, S., Cardona, A., Ransohoff, R. M., Lamb, B. T., & Bhaskar, K. (2015). Reactive microglia drive tau pathology and contribute to the spreading of pathological tau in the brain. Brain, 138(6), 1738–1755. https://doi.org/10.1093/brain/awv081

Markesbery, W. R. (1997). Oxidative Stress Hypothesis in Alzheimer's Disease. Free Radical Biology and Medicine, 23(1), 134–147. https://doi.org/10.1016/S0891-5849(96)00629-6

Martini, F., Rosa, S. G., Klann, I. P., Fulco, B. C. W., Carvalho, F. B., Rahmeier, F. L., Fernandes, M. C., & Nogueira, C. W. (2019). A multifunctional compound ebselen reverses memory impairment, apoptosis and

oxidative stress in a mouse model of sporadic Alzheimer's disease. Journal of Psychiatric Research, 109, 107–117. https://doi.org/10.1016/j.jpsychires.2018.11.021

Martín-Maestro, P., Gargini, R., A. Sproul, A., García, E., Antón, L. C., Noggle, S., Arancio, O., Avila, J., & García-Escudero, V. (2017). Mitophagy Failure in Fibroblasts and iPSC-Derived Neurons of Alzheimer's Disease-Associated Presenilin 1 Mutation. Frontiers in Molecular Neuroscience, 10, 291. https://doi.org/10.3389/fnmol.2017.00291

Martins, M., Rosa, A., Guedes, L. C., Fonseca, B. V., Gotovac, K., Violante, S., Mestre, T., Coelho, M., Rosa, M. M., Martin, E. R., Vance, J. M., Outeiro, T. F., Wang, L., Borovecki, F., Ferreira, J. J., & Oliveira, S. A. (2011). Convergence of miRNA Expression Profiling, α-Synuclein Interacton and GWAS in Parkinson's Disease. PLOS ONE, 6(10), e25443. https://doi.org/10.1371/journal.pone.0025443

Martins, R. N., Villemagne, V., Sohrabi, H. R., Chatterjee, P., Shah, T. M., Verdile, G., Fraser, P., Taddei, K., Gupta, V. B., Rainey-Smith, S. R., Hone, E., Pedrini, S., Lim, W. L., Martins, I., Frost, S., Gupta, S., O'Bryant, S., Rembach, A., Ames, D., … Masters, C. L. (2018). Alzheimer's Disease: A Journey from Amyloid Peptides and Oxidative Stress, to Biomarker Technologies and Disease Prevention Strategies—Gains from AIBL and DIAN Cohort Studies. Journal of Alzheimer's Disease, 62(3), 965–992. https://doi.org/10.3233/JAD-171145

Marzesco, A.-M., Janich, P., Wilsch-Bräuninger, M., Dubreuil, V., Langenfeld, K., Corbeil, D., & Huttner, W. B. (2005). Release of extracellular membrane particles carrying the stem cell marker prominin-1 (CD133) from neural progenitors and other epithelial cells. Journal of Cell Science, 118(13), 2849–2858. https://doi.org/10.1242/jcs.02439

Masters, C. L., Bateman, R., Blennow, K., Rowe, C. C., Sperling, R. A., & Cummings, J. L. (2015). Alzheimer's disease. Nature Reviews Disease Primers, 1, 15056. https://doi.org/10.1038/nrdp.2015.56

Mateescu, B., Kowal, E. J. K., Balkom, B. W. M. van, Bartel, S., Bhattacharyya, S. N., Buzás, E. I., Buck, A. H., Candia, P. de, Chow, F. W. N., Das, S., Driedonks, T. A. P., Fernández-Messina, L., Haderk, F., Hill, A. F., Jones, J. C., Keuren-Jensen, K. R. V., Lai, C. P., Lässer, C., Liegro, I. di, … Hoen, E. N. M. N.-'t. (2017). Obstacles and opportunities in the functional analysis of extracellular vesicle RNA – an ISEV position paper. Journal of Extracellular Vesicles, 6(1), 1286095. https://doi.org/10.1080/20013078.2017.1286095

Matsumoto, J., Stewart, T., Sheng, L., Li, N., Bullock, K., Song, N., Shi, M., Banks, W. A., & Zhang, J. (2017). Transmission of α-synuclein-containing erythrocyte-derived extracellular vesicles across the blood-brain barrier via adsorptive mediated transcytosis: Another mechanism for initiation and progression of Parkinson's disease? Acta Neuropathologica Communications, 5. https://doi.org/10.1186/s40478-017-0470-4

Mattsson-Carlgren, N., Janelidze, S., Palmqvist, S., Cullen, N., Svenningsson, A. L., Strandberg, O., Mengel, D., Walsh, D. M., Stomrud, E., Dage, J. L., & Hansson, O. (2020). Longitudinal plasma p-tau217 is increased in early stages of Alzheimer's disease. Brain, 143(11), 3234–3241. https://doi.org/10.1093/brain/awaa286

Mays, C. E., & Soto, C. (2016). The stress of prion disease. Brain Research, 1648, 553–560. https://doi.org/10.1016/j.brainres.2016.04.009

McKeever, P. M., Schneider, R., Taghdiri, F., Weichert, A., Multani, N., Brown, R. A., Boxer, A. L., Karydas, A., Miller, B., Robertson, J., & Tartaglia, M. C. (2018). MicroRNA Expression Levels Are Altered in the Cerebrospinal Fluid of Patients with Young-Onset Alzheimer's Disease. Molecular Neurobiology, 55(12), 8826–8841. https://doi.org/10.1007/s12035-018-1032-x

McKhann, G. M., Knopman, D. S., Chertkow, H., Hyman, B. T., Jack, C. R., Kawas, C. H., Klunk, W. E., Koroshetz, W. J., Manly, J. J., Mayeux, R., Mohs, R. C., Morris, J. C., Rossor, M. N., Scheltens, P., Carrillo, M. C., Thies, B., Weintraub, S., & Phelps, C. H. (2011). The diagnosis of dementia due to Alzheimer's disease: Recommendations from the National Institute on Aging-Alzheimer's Association workgroups on diagnostic guidelines for Alzheimer's disease. Alzheimer's & Dementia, 7(3), 263–269. https://doi.org/10.1016/j.jalz.2011.03.005

Mendes-Silva, A. P., Pereira, K. S., Tolentino-Araujo, G. T., Nicolau, E. de S., Silva-Ferreira, C. M., Teixeira, A. L., & Diniz, B. S. (2016). Shared Biologic Pathways Between Alzheimer Disease and Major Depression: A Systematic Review of MicroRNA Expression Studies. The American Journal of Geriatric Psychiatry, 24(10), 903–912. https://doi.org/10.1016/j.jagp.2016.07.017

Menkes-Caspi, N., Yamin, H. G., Kellner, V., Spires-Jones, T. L., Cohen, D., & Stern, E. A. (2015). Pathological Tau Disrupts Ongoing Network Activity. Neuron, 85(5), 959–966. https://doi.org/10.1016/j.neuron.2015.01.025

Meyer-Luehmann, M., Spires-Jones, T. L., Prada, C., Garcia-Alloza, M., de Calignon, A., Rozkalne, A., Koenigsknecht-Talboo, J., Holtzman, D. M., Bacskai, B. J., & Hyman, B. T. (2008). Rapid appearance and local toxicity of amyloid-β plaques in a mouse model of Alzheimer's disease. Nature, 451(7179), 720–724. https://doi.org/10.1038/nature06616

Mi, W., Pawlik, M., Sastre, M., Jung, S. S., Radvinsky, D. S., Klein, A. M., Sommer, J., Schmidt, S. D., Nixon, R. A., Mathews, P. M., & Levy, E. (2007). Cystatin C inhibits amyloid-β deposition in Alzheimer's disease mouse models. Nature Genetics, 39(12), 1440–1442. https://doi.org/10.1038/ng.2007.29

Michaluk, P., & Kaczmarek, L. (2007). Matrix metalloproteinase-9 in glutamate-dependent adult brain function and dysfunction. Cell Death & Differentiation, 14(7), Article 7. https://doi.org/10.1038/sj.cdd.4402141

microRNA-132: A key noncoding RNA operating in the cellular phase of Alzheimer's disease. (n.d.). https://doi.org/10.1096/fj.201601308

Milà-Alomà, M., Ashton, N. J., Shekari, M., Salvadó, G., Ortiz-Romero, P., Montoliu-Gaya, L., Benedet, A. L., Karikari, T. K., Lantero-Rodriguez, J., Vanmechelen, E., Day, T. A., González-Escalante, A., Sánchez-Benavides, G., Minguillon, C., Fauria, K., Molinuevo, J. L., Dage, J. L., Zetterberg, H., Gispert, J. D., … Blennow, K. (2022). Plasma p-tau231 and p-tau217 as state markers of amyloid-β pathology in preclinical Alzheimer's disease. Nature Medicine, 28(9), Article 9. https://doi.org/10.1038/s41591-022-01925-w

Miller, M. W., & Sadeh, N. (2014). Traumatic stress, oxidative stress and post-traumatic stress disorder: Neurodegeneration and the accelerated-aging hypothesis. Molecular Psychiatry, 19(11), Article 11. https://doi.org/10.1038/mp.2014.111

Min, L., Zhu, S., Chen, L., Liu, X., Wei, R., Zhao, L., Yang, Y., Zhang, Z., Kong, G., Li, P., & Zhang, S. (2019). Evaluation of circulating small extracellular vesicles derived miRNAs as biomarkers of early colon cancer: A comparison with plasma total miRNAs. Journal of Extracellular Vesicles, 8(1), 1643670. https://doi.org/10.1080/20013078.2019.1643670

Mintun, M. A., Lo, A. C., Duggan Evans, C., Wessels, A. M., Ardayfio, P. A., Andersen, S. W., Shcherbinin, S., Sparks, J., Sims, J. R., Brys, M., Apostolova, L. G., Salloway, S. P., & Skovronsky, D. M. (2021). Donanemab in Early Alzheimer's Disease. New England Journal of Medicine, 384(18), 1691–1704. https://doi.org/10.1056/NEJMoa2100708

Miranda, A. M., Lasiecka, Z. M., Xu, Y., Neufeld, J., Shahriar, S., Simoes, S., Chan, R. B., Oliveira, T. G., Small, S. A., & Di Paolo, G. (2018). Neuronal lysosomal dysfunction releases exosomes harboring APP C-terminal fragments and unique lipid signatures. Nature Communications, 9. https://doi.org/10.1038/s41467-017-02533-w

Misrani, A., Tabassum, S., & Yang, L. (2021). Mitochondrial Dysfunction and Oxidative Stress in Alzheimer's Disease. Frontiers in Aging Neuroscience, 13. https://www.frontiersin.org/articles/10.3389/fnagi.2021.617588

Miyazaki, K., Hasegawa, M., Funahashi, K., & Umeda, M. (1993). A metalloproteinase inhibitor domain in Alzheimer amyloid protein precursor. Nature, 362(6423), Article 6423. https://doi.org/10.1038/362839a0

Mor, E., Kano, S.-I., Colantuoni, C., Sawa, A., Navon, R., & Shomron, N. (2013). MicroRNA-382 expression is elevated in the olfactory neuroepithelium of schizophrenia patients. Neurobiology of Disease, 55, 1–10. https://doi.org/10.1016/j.nbd.2013.03.011

Morad, G., Carman, C. V., Hagedorn, E. J., Perlin, J. R., Zon, L. I., Mustafaoglu, N., Park, T.-E., Ingber, D. E., Daisy, C. C., & Moses, M. A. (2019). Tumor-Derived Extracellular Vesicles Breach the Intact Blood–Brain Barrier via Transcytosis. ACS Nano, 13(12), 13853–13865. https://doi.org/10.1021/acsnano.9b04397

Moreno-Jiménez, E. P., Flor-García, M., Terreros-Roncal, J., Rábano, A., Cafini, F., Pallas-Bazarra, N., Ávila, J., & Llorens-Martín, M. (2019). Adult hippocampal neurogenesis is abundant in neurologically healthy subjects and drops sharply in patients with Alzheimer's disease. Nature Medicine, 25(4), Article 4. https://doi.org/10.1038/s41591-019-0375-9

Müller, M., Jäkel, L., Bruinsma, I. B., Claassen, J. A., Kuiperij, H. B., & Verbeek, M. M. (2016). MicroRNA-29a Is a Candidate Biomarker for Alzheimer's Disease in Cell-Free Cerebrospinal Fluid. Molecular Neurobiology, 53(5), 2894–2899. https://doi.org/10.1007/s12035-015-9156-8

Muraoka, S., DeLeo, A. M., Sethi, M. K., Yukawa-Takamatsu, K., Yang, Z., Ko, J., Hogan, J. D., Ruan, Z., You, Y., Wang, Y., Medalla, M., Ikezu, S., Chen, M., Xia, W., Gorantla, S., Gendelman, H. E., Issadore, D., Zaia, J., & Ikezu, T. (2020). Proteomic and biological profiling of extracellular vesicles from Alzheimer's disease human brain tissues. Alzheimer's & Dementia, 16(6), 896–907. https://doi.org/10.1002/alz.12089

Nayak, S., Aich, M., Kumar, A., Sengupta, S., Bajad, P., Dhapola, P., Paul, D., Narta, K., Purkrait, S., Mehani, B., Suri, A., Chakraborty, D., Mukhopadhyay, A., & Sarkar, C. (2018). Novel internal regulators and candidate miRNAs within miR-379/miR-656 miRNA cluster can alter cellular phenotype of human glioblastoma. Scientific Reports, 8(1), Article 1. https://doi.org/10.1038/s41598-018-26000-8

Nebel, R. A., Aggarwal, N. T., Barnes, L. L., Gallagher, A., Goldstein, J. M., Kantarci, K., Mallampalli, M. P., Mormino, E. C., Scott, L., Yu, W. H., Maki, P. M., & Mielke, M. M. (2018). Understanding the impact of sex and gender in Alzheimer's disease: A call to action. Alzheimer's & Dementia, 14(9), 1171–1183. https://doi.org/10.1016/j.jalz.2018.04.008

Nestor, S. M., Rupsingh, R., Borrie, M., Smith, M., Accomazzi, V., Wells, J. L., Fogarty, J., Bartha, R., & the Alzheimer's Disease Neuroimaging Initiative. (2008). Ventricular enlargement as a possible measure of Alzheimer's disease progression validated using the Alzheimer's disease neuroimaging initiative database. Brain, 131(9), 2443–2454. https://doi.org/10.1093/brain/awn146

Neve, R. L., Harris, P., Kosik, K. S., Kurnit, D. M., & Donlon, T. A. (1986). Identification of cDNA clones for the human microtubule-associated protein tau and chromosomal localization of the genes for tau and microtubule-associated protein 2. Molecular Brain Research, 1(3), 271–280. https://doi.org/10.1016/0169-328X(86)90033-1

Ng, F., Wijaya, L., & Tang, B. L. (2015). SIRT1 in the brain—Connections with aging-associated disorders and lifespan. Frontiers in Cellular Neuroscience, 9, 64. https://doi.org/10.3389/fncel.2015.00064

Nguyen, L. S., Fregeac, J., Bole-Feysot, C., Cagnard, N., Iyer, A., Anink, J., Aronica, E., Alibeu, O., Nitschke, P., & Colleaux, L. (2018). Role of miR-146a in neural stem cell differentiation and neural lineage determination: Relevance for neurodevelopmental disorders. Molecular Autism, 9(1), 38. https://doi.org/10.1186/s13229-018-0219-3

Nguyen, L. S., Lepleux, M., Makhlouf, M., Martin, C., Fregeac, J., Siquier-Pernet, K., Philippe, A., Feron, F., Gepner, B., Rougeulle, C., Humeau, Y., & Colleaux, L. (2016). Profiling olfactory stem cells from living patients identifies miRNAs relevant for autism pathophysiology. Molecular Autism, 7(1), 1. https://doi.org/10.1186/s13229-015-0064-6

Nicolas, G., Wallon, D., Goupil, C., Richard, A.-C., Pottier, C., Dorval, V., Sarov-Rivière, M., Riant, F., Hervé, D., Amouyel, P., Guerchet, M., Ndamba-Bandzouzi, B., Mbelesso, P., Dartigues, J.-F., Lambert, J.-C., Preux, P.-M.,

Frebourg, T., Campion, D., Hannequin, D., … Rovelet-Lecrux, A. (2016). Mutation in the 3'untranslated region of APP as a genetic determinant of cerebral amyloid angiopathy. European Journal of Human Genetics, 24(1), Article 1. https://doi.org/10.1038/ejhg.2015.61

Nikoletopoulou, V., & Tavernarakis, N. (2018). Regulation and Roles of Autophagy at Synapses. Trends in Cell Biology, 28(8), 646–661. https://doi.org/10.1016/j.tcb.2018.03.006

Nortley, R., Korte, N., Izquierdo, P., Hirunpattarasilp, C., Mishra, A., Jaunmuktane, Z., Kyrargyri, V., Pfeiffer, T., Khennouf, L., Madry, C., Gong, H., Richard-Loendt, A., Huang, W., Saito, T., Saido, T. C., Brandner, S., Sethi, H., & Attwell, D. (2019). Amyloid β oligomers constrict human capillaries in Alzheimer's disease via signaling to pericytes. Science, 365(6450), eaav9518. https://doi.org/10.1126/science.aav9518

Norton, S., Matthews, F. E., Barnes, D. E., Yaffe, K., & Brayne, C. (2014). Potential for primary prevention of Alzheimer's disease: An analysis of population-based data. The Lancet Neurology, 13(8), 788–794. https://doi.org/10.1016/S1474-4422(14)70136-X

Nuriel, T., Peng, K. Y., Ashok, A., Dillman, A. A., Figueroa, H. Y., Apuzzo, J., Ambat, J., Levy, E., Cookson, M. R., Mathews, P. M., & Duff, K. E. (2017). The Endosomal–Lysosomal Pathway Is Dysregulated by APOE4 Expression in Vivo. Frontiers in Neuroscience, 11. https://doi.org/10.3389/fnins.2017.00702

Nwokwu, C. D., Xiao, A. Y., Harrison, L., & Nestorova, G. G. (2022). Identification of microRNA-mRNA regulatory network associated with oxidative DNA damage in human astrocytes. ASN Neuro, 14, 17590914221101704. https://doi.org/10.1177/17590914221101704

O'Connor, A., Karikari, T. K., Poole, T., Ashton, N. J., Lantero Rodriguez, J., Khatun, A., Swift, I., Heslegrave, A. J., Abel, E., Chung, E., Weston, P. S. J., Pavisic, I. M., Ryan, N. S., Barker, S., Rossor, M. N., Polke, J. M., Frost, C., Mead, S., Blennow, K., … Fox, N. C. (2021). Plasma phospho-tau181 in presymptomatic and symptomatic familial Alzheimer's disease: A longitudinal cohort study. Molecular Psychiatry, 26(10), Article 10. https://doi.org/10.1038/s41380-020-0838-x

O'Donnell, K. A., Wentzel, E. A., Zeller, K. I., Dang, C. V., & Mendell, J. T. (2005). C-Myc-regulated microRNAs modulate E2F1 expression. Nature, 435(7043), Article 7043. https://doi.org/10.1038/nature03677

Onodera, Y., Teramura, T., Takehara, T., Obora, K., Mori, T., & Fukuda, K. (2017). MiR-155 induces ROS generation through downregulation of antioxidation-related genes in mesenchymal stem cells. Aging Cell, 16(6), 1369–1380. https://doi.org/10.1111/acel.12680

O'Nuallain, B., Freir, D. B., Nicoll, A. J., Risse, E., Ferguson, N., Herron, C. E., Collinge, J., & Walsh, D. M. (2010). Amyloid β-Protein Dimers Rapidly Form Stable Synaptotoxic Protofibrils. Journal of Neuroscience, 30(43), 14411–14419. https://doi.org/10.1523/JNEUROSCI.3537-10.2010

Palmer, T. D., Schwartz, P. H., Taupin, P., Kaspar, B., Stein, S. A., & Gage, F. H. (2001). Cell culture: Progenitor cells from human brain after death. Nature, 411(6833), 42–43. https://doi.org/10.1038/35075141

Pan, Q., Guo, K., Xue, M., & Tu, Q. (2021). Estradiol exerts a neuroprotective effect on SH-SY5Y cells through the miR-106b-5p/TXNIP axis. Journal of Biochemical and Molecular Toxicology, 35(9), e22861. https://doi.org/10.1002/jbt.22861

Panganiban, R. P. L., Pinkerton, M. H., Maru, S. Y., Jefferson, S. J., Roff, A. N., & Ishmael, F. T. (2012). Differential microRNA epression in asthma and the role of miR-1248 in regulation of IL-5. American Journal of Clinical and Experimental Immunology, 1(2), 154–165.

Paolicelli, R. C., Bergamini, G., & Rajendran, L. (2018). Cell-to-cell Communication by Extracellular Vesicles: Focus on Microglia. Neuroscience. https://doi.org/10.1016/j.neuroscience.2018.04.003

Paolicelli, R. C., Bolasco, G., Pagani, F., Maggi, L., Scianni, M., Panzanelli, P., Giustetto, M., Ferreira, T. A., Guiducci, E., Dumas, L., Ragozzino, D., & Gross, C. T. (2011). Synaptic Pruning by Microglia Is Necessary for Normal Brain Development. Science, 333(6048), 1456–1458. https://doi.org/10.1126/science.1202529

Park, K. K., Liu, K., Hu, Y., Kanter, J. L., & He, Z. (2010). PTEN/mTOR and axon regeneration. Experimental Neurology, 223(1), 45–50. https://doi.org/10.1016/j.expneurol.2009.12.032

Parkhurst, C. N., Yang, G., Ninan, I., Savas, J. N., Yates, J. R., Lafaille, J. J., Hempstead, B. L., Littman, D. R., & Gan, W.-B. (2013). Microglia Promote Learning-Dependent Synapse Formation through Brain-Derived Neurotrophic Factor. Cell, 155(7), 1596–1609. https://doi.org/10.1016/j.cell.2013.11.030

Paschon, V., Takada, S. H., Ikebara, J. M., Sousa, E., Raeisossadati, R., Ulrich, H., & Kihara, A. H. (2016). Interplay Between Exosomes, microRNAs and Toll-Like Receptors in Brain Disorders. Molecular Neurobiology, 53(3), 2016–2028. https://doi.org/10.1007/s12035-015-9142-1

Pascoal, T. A., Mathotaarachchi, S., Mohades, S., Benedet, A. L., Chung, C.-O., Shin, M., Wang, S., Beaudry, T., Kang, M. S., Soucy, J.-P., Labbe, A., Gauthier, S., & Rosa-Neto, P. (2017). Amyloid-β and hyperphosphorylated tau synergy drives metabolic decline in preclinical Alzheimer's disease. Molecular Psychiatry, 22(2), Article 2. https://doi.org/10.1038/mp.2016.37

Pascua-Maestro, R., González, E., Lillo, C., Ganfornina, M. D., Falcón-Pérez, J. M., & Sanchez, D. (2019). Extracellular Vesicles Secreted by Astroglial Cells Transport Apolipoprotein D to Neurons and Mediate Neuronal Survival Upon Oxidative Stress. Frontiers in Cellular Neuroscience, 12. https://www.frontiersin.org/articles/10.3389/fncel.2018.00526

Patel, N., Hoang, D., Miller, N., Ansaloni, S., Huang, Q., Rogers, J. T., Lee, J. C., & Saunders, A. J. (2008). MicroRNAs can regulate human APP levels. Molecular Neurodegeneration, 3(1), 10. https://doi.org/10.1186/1750-1326-3-10

Patil, A. H., Baran, A., Brehm, Z. P., McCall, M. N., & Halushka, M. K. (2022). A curated human cellular microRNAome based on 196 primary cell types. GigaScience, 11, giac083. https://doi.org/10.1093/gigascience/giac083

Peinado, H., Alečković, M., Lavotshkin, S., Matei, I., Costa-Silva, B., Moreno-Bueno, G., Hergueta-Redondo, M., Williams, C., García-Santos, G., Nitadori-Hoshino, A., Hoffman, C., Badal, K., Garcia, B. A., Callahan, M. K., Yuan, J., Martins, V. R., Skog, J., Kaplan, R. N., Brady, M. S., … Lyden, D. (2012). Melanoma exosomes educate bone marrow progenitor cells toward a pro-metastatic phenotype through MET. Nature Medicine, 18(6), 883–891. https://doi.org/10.1038/nm.2753

Pencheva, N., Tran, H., Buss, C., Huh, D., Drobnjak, M., Busam, K., & Tavazoie, S. F. (2012). Convergent Multi-miRNA Targeting of ApoE Drives LRP1/LRP8-Dependent Melanoma Metastasis and Angiogenesis. Cell, 151(5), 1068–1082. https://doi.org/10.1016/j.cell.2012.10.028

Peng, B., Li, C., He, L., Tian, M., & Li, X. (2020). MiR-660-5p promotes breast cancer progression through down-regulating TET2 and activating PI3K/AKT/mTOR signaling. Brazilian Journal of Medical and Biological Research, 53. https://doi.org/10.1590/1414-431X20209740

Peng, K. Y., Pérez-González, R., Alldred, M. J., Goulbourne, C. N., Morales-Corraliza, J., Saito, M., Saito, M., Ginsberg, S. D., Mathews, P. M., & Levy, E. (2019). Apolipoprotein E4 genotype compromises brain exosome production. Brain, 142(1), 163–175. https://doi.org/10.1093/brain/awy289

Pérez, M. J., Ponce, D. P., Osorio-Fuentealba, C., Behrens, M. I., & Quintanilla, R. A. (2017). Mitochondrial Bioenergetics Is Altered in Fibroblasts from Patients with Sporadic Alzheimer's Disease. Frontiers in Neuroscience, 11. https://doi.org/10.3389/fnins.2017.00553

Petyuk, V. A., Chang, R., Ramirez-Restrepo, M., Beckmann, N. D., Henrion, M. Y. R., Piehowski, P. D., Zhu, K., Wang, S., Clarke, J., Huentelman, M. J., Xie, F., Andreev, V., Engel, A., Guettoche, T., Navarro, L., De Jager, P., Schneider, J. A., Morris, C. M., McKeith, I. G., … Myers, A. J. (2018). The human brainome: Network analysis identifies HSPA2 as a novel Alzheimer’s disease target. Brain, 141(9), 2721–2739. https://doi.org/10.1093/brain/awy215

Pichardo-Casas, I., Goff, L. A., Swerdel, M. R., Athie, A., Davila, J., Ramos-Brossier, M., Lapid-Volosin, M., Friedman, W. J., Hart, R. P., & Vaca, L. (2012). Expression profiling of synaptic microRNAs from the adult rat brain identifies regional differences and seizure-induced dynamic modulation. Brain Research, 1436, 20–33. https://doi.org/10.1016/j.brainres.2011.12.001

Pichler, S., Gu, W., Hartl, D., Gasparoni, G., Leidinger, P., Keller, A., Meese, E., Mayhaus, M., Hampel, H., & Riemenschneider, M. (2017). The miRNome of Alzheimer's disease: Consistent downregulation of the miR-132/212 cluster. Neurobiology of Aging, 50, 167.e1-167.e10. https://doi.org/10.1016/j.neurobiolaging.2016.09.019

Pickett, E. K., Henstridge, C. M., Allison, E., Pitstick, R., Pooler, A., Wegmann, S., Carlson, G., Hyman, B. T., & Spires-Jones, T. L. (2017). Spread of tau down neural circuits precedes synapse and neuronal loss in the rTgTauEC mouse model of early Alzheimer's disease. Synapse, 71(6), e21965. https://doi.org/10.1002/syn.21965

Pinto, S., Cunha, C., Barbosa, M., Vaz, A. R., & Brites, D. (2017). Exosomes from NSC-34 Cells Transfected with hSOD1-G93A Are Enriched in miR-124 and Drive Alterations in Microglia Phenotype. Frontiers in Neuroscience, 11. https://doi.org/10.3389/fnins.2017.00273

Pluta, R., Ułamek-Kozioł, M., Januszewski, S., & Czuczwar, S. J. (2018). Exosomes as possible spread factor and potential biomarkers in Alzheimer's disease: Current concepts. Biomarkers in Medicine, 12(9), 1025–1033. https://doi.org/10.2217/bmm-2018-0034

Podcasy, J. L., & Epperson, C. N. (2016). Considering sex and gender in Alzheimer disease and other dementias. Dialogues in Clinical Neuroscience, 18(4), 437–446. https://doi.org/10.31887/DCNS.2016.18.4/cepperson

Polanco, J. C., Hand, G. R., Briner, A., Li, C., & Götz, J. (2021). Exosomes induce endolysosomal permeabilization as a gateway by which exosomal tau seeds escape into the cytosol. Acta Neuropathologica, 141(2), 235–256. https://doi.org/10.1007/s00401-020-02254-3

Polanco, J. C., Li, C., Durisic, N., Sullivan, R., & Götz, J. (2018). Exosomes taken up by neurons hijack the endosomal pathway to spread to interconnected neurons. Acta Neuropathologica Communications, 6. https://doi.org/10.1186/s40478-018-0514-4

Polanco, J. C., Scicluna, B. J., Hill, A. F., & Götz, J. (2016). Extracellular Vesicles Isolated from the Brains of rTg4510 Mice Seed Tau Protein Aggregation in a Threshold-dependent Manner. Journal of Biological Chemistry, 291(24), 12445–12466. https://doi.org/10.1074/jbc.M115.709485

Polymenidou, M., & Cleveland, D. W. (2011). The Seeds of Neurodegeneration: Prion-like Spreading in ALS. Cell, 147(3), 498–508. https://doi.org/10.1016/j.cell.2011.10.011

Polymenidou, M., & Cleveland, D. W. (2012). Prion-like spread of protein aggregates in neurodegeneration. Journal of Experimental Medicine, 209(5), 889–893. https://doi.org/10.1084/jem.20120741

Pooler, A. M., Phillips, E. C., Lau, D. H. W., Noble, W., & Hanger, D. P. (2013). Physiological release of endogenous tau is stimulated by neuronal activity. EMBO Reports, 14(4), 389–394. https://doi.org/10.1038/embor.2013.15

Prabhakar, P., Chandra, S. R., & Christopher, R. (2017). Circulating microRNAs as potential biomarkers for the identification of vascular dementia due to cerebral small vessel disease. Age and Ageing, 46(5), 861–864. https://doi.org/10.1093/ageing/afx090

Prada, I., Furlan, R., Matteoli, M., & Verderio, C. (2013). Classical and unconventional pathways of vesicular release in microglia. Glia, 61(7), 1003–1017. https://doi.org/10.1002/glia.22497

Prada, I., Gabrielli, M., Turola, E., Iorio, A., D'Arrigo, G., Parolisi, R., De Luca, M., Pacifici, M., Bastoni, M., Lombardi, M., Legname, G., Cojoc, D., Buffo, A., Furlan, R., Peruzzi, F., & Verderio, C. (2018). Glia-to-neuron

transfer of miRNAs via extracellular vesicles: A new mechanism underlying inflammation-induced synaptic alterations. Acta Neuropathologica, 135(4), 529–550. https://doi.org/10.1007/s00401-017-1803-x

Preische, O., Schultz, S. A., Apel, A., Kuhle, J., Kaeser, S. A., Barro, C., Gräber, S., Kuder-Buletta, E., LaFougere, C., Laske, C., Vöglein, J., Levin, J., Masters, C. L., Martins, R., Schofield, P. R., Rossor, M. N., Graff-Radford, N. R., Salloway, S., Ghetti, B., … Jucker, M. (2019). Serum neurofilament dynamics predicts neurodegeneration and clinical progression in presymptomatic Alzheimer's disease. Nature Medicine, 25(2), Article 2. https://doi.org/10.1038/s41591-018-0304-3

Prince, M. J., Wu, F., Guo, Y., Robledo, L. M. G., O'Donnell, M., Sullivan, R., & Yusuf, S. (2015). The burden of disease in older people and implications for health policy and practice. The Lancet, 385(9967), 549–562. https://doi.org/10.1016/S0140-6736(14)61347-7

Prokop, S., Miller, K. R., Labra, S. R., Pitkin, R. M., Hoxha, K., Narasimhan, S., Changolkar, L., Rosenbloom, A., Lee, V. M.-Y., & Trojanowski, J. Q. (2019). Impact of TREM2 risk variants on brain region-specific immune activation and plaque microenvironment in Alzheimer's disease patient brain samples. Acta Neuropathologica, 138(4), 613–630. https://doi.org/10.1007/s00401-019-02048-2

Prusiner, S. B. (1982). Novel proteinaceous infectious particles cause scrapie. Science, 216(4542), 136–144. https://doi.org/10.1126/science.6801762

Pruunsild, P., Kazantseva1, A., Aid, T., Palm, K., & Timmusk, T. (2007). Dissecting the human BDNF locus: Bidirectional transcription, complex splicing, and multiple promoters. Genomics, 90(3), 397–406. https://doi.org/10.1016/j.ygeno.2007.05.004

Puig, K. L., Floden, A. M., Adhikari, R., Golovko, M. Y., & Combs, C. K. (2012). Amyloid Precursor Protein and Proinflammatory Changes Are Regulated in Brain and Adipose Tissue in a Murine Model of High Fat Diet-Induced Obesity. PLoS ONE, 7(1), e30378. https://doi.org/10.1371/journal.pone.0030378

Purro, S. A., Farrow, M. A., Linehan, J., Nazari, T., Thomas, D. X., Chen, Z., Mengel, D., Saito, T., Saido, T., Rudge, P., Brandner, S., Walsh, D. M., & Collinge, J. (2018). Transmission of amyloid-β protein pathology from cadaveric pituitary growth hormone. Nature, 564(7736), 415. https://doi.org/10.1038/s41586-018-0790-y

Putteeraj, M., Fairuz, Y. M., & Teoh, S. L. (2017). MicroRNA Dysregulation in Alzheimer's Disease. CNS & Neurological Disorders - Drug Targets- CNS & Neurological Disorders), 16(9), 1000–1009. https://doi.org/10.2174/1871527316666170807142311

Qian, Y., Song, J., Ouyang, Y., Han, Q., Chen, W., Zhao, X., Xie, Y., Chen, Y., Yuan, W., & Fan, C. (2017). Advances in Roles of miR-132 in the Nervous System. Frontiers in Pharmacology, 8. https://www.frontiersin.org/articles/10.3389/fphar.2017.00770

Qin, W., Li, J., Zhu, R., Gao, S., Fan, J., Xia, M., Zhao, R. C., & Zhang, J. (2019). Melatonin protects blood-brain barrier integrity and permeability by inhibiting matrix metalloproteinase-9 via the NOTCH3/NF-κB pathway. Aging (Albany NY), 11(23), 11391–11415. https://doi.org/10.18632/aging.102537

Rajendran, L., Honsho, M., Zahn, T. R., Keller, P., Geiger, K. D., Verkade, P., & Simons, K. (2006). Alzheimer's disease β-amyloid peptides are released in association with exosomes. Proceedings of the National Academy of Sciences, 103(30), 11172–11177. https://doi.org/10.1073/pnas.0603838103

Rajendran, L., Knobloch, M., Geiger, K. D., Dienel, S., Nitsch, R., Simons, K., & Konietzko, U. (2007). Increased Aβ Production Leads to Intracellular Accumulation of Aβ in Flotillin-1-Positive Endosomes. Neurodegenerative Diseases, 4(2–3), 164–170. https://doi.org/10.1159/000101841

Ramamoorthy, M., Sykora, P., Scheibye-Knudsen, M., Dunn, C., Kasmer, C., Zhang, Y., Becker, K. G., Croteau, D. L., & Bohr, V. A. (2012). Sporadic Alzheimer's disease fibroblasts display an oxidative stress phenotype. Free Radical Biology & Medicine, 53(6), 1371–1380. https://doi.org/10.1016/j.freeradbiomed.2012.07.018

Rani, A., O'Shea, A., Ianov, L., Cohen, R. A., Woods, A. J., & Foster, T. C. (2017). MiRNA in Circulating Microvesicles as Biomarkers for Age-Related Cognitive Decline. Frontiers in Aging Neuroscience, 9, 323. https://doi.org/10.3389/fnagi.2017.00323

Raposo, G., Nijman, H. W., Stoorvogel, W., Liejendekker, R., Harding, C. V., Melief, C. J., & Geuze, H. J. (1996). B lymphocytes secrete antigen-presenting vesicles. Journal of Experimental Medicine, 183(3), 1161–1172. https://doi.org/10.1084/jem.183.3.1161

Ratajczak, J., Miekus, K., Kucia, M., Zhang, J., Reca, R., Dvorak, P., & Ratajczak, M. Z. (2006). Embryonic stem cell-derived microvesicles reprogram hematopoietic progenitors: Evidence for horizontal transfer of mRNA and protein delivery. Leukemia, 20(5), 847–856. https://doi.org/10.1038/sj.leu.2404132

Rauch, J. N., Luna, G., Guzman, E., Audouard, M., Challis, C., Sibih, Y. E., Leshuk, C., Hernandez, I., Wegmann, S., Hyman, B. T., Gradinaru, V., Kampmann, M., & Kosik, K. S. (2020). LRP1 is a master regulator of tau uptake and spread. Nature, 580(7803), Article 7803. https://doi.org/10.1038/s41586-020-2156-5

Redelmeier, D. A., Manzoor, F., & Thiruchelvam, D. (2019). Association Between Statin Use and Risk of Dementia After a Concussion. JAMA Neurology, 76(8), 887–896. https://doi.org/10.1001/jamaneurol.2019.1148

Reiman, E. M., Arboleda-Velasquez, J. F., Quiroz, Y. T., Huentelman, M. J., Beach, T. G., Caselli, R. J., Chen, Y., Su, Y., Myers, A. J., Hardy, J., Paul Vonsattel, J., Younkin, S. G., Bennett, D. A., De Jager, P. L., Larson, E. B., Crane, P. K., Keene, C. D., Kamboh, M. I., Kofler, J. K., … Alzheimer's Disease Genetics Consortium. (2020). Exceptionally low likelihood of Alzheimer's dementia in APOE2 homozygotes from a 5,000-person neuropathological study. Nature Communications, 11(1), 667. https://doi.org/10.1038/s41467-019-14279-8

Reiss, A. B., Montufar, N., DeLeon, J., Pinkhasov, A., Gomolin, I. H., Glass, A. D., Arain, H. A., & Stecker, M. M. (2021). Alzheimer Disease Clinical Trials Targeting Amyloid: Lessons Learned From Success in Mice and Failure in Humans. The Neurologist, 26(2), 52–61. https://doi.org/10.1097/NRL.0000000000000320

Riancho, J., Castanedo-Vázquez, D., Gil-Bea, F., Tapia, O., Arozamena, J., Durán-Vían, C., Sedano, M. J., Berciano, M. T., Lopez de Munain, A., & Lafarga, M. (2020). ALS-derived fibroblasts exhibit reduced proliferation rate, cytoplasmic TDP-43 aggregation and a higher susceptibility to DNA damage. Journal of Neurology, 267(5), 1291–1299. https://doi.org/10.1007/s00415-020-09704-8

Riancho, J., Santurtun, A., & Sánchez-Juan, P. (2019). Characterization of Alzheimer's Disease Micro-RNA Profile in Exosome-Enriched CSF Samples. In E. Santamaría & J. Fernández-Irigoyen (Eds.), Cerebrospinal Fluid (CSF) Proteomics: Methods and Protocols (pp. 343–352). Springer. https://doi.org/10.1007/978-1-4939-9706-0_22

Riancho, J., Vázquez-Higuera, J. L., Pozueta, A., Lage, C., Kazimierczak, M., Bravo, M., Calero, M., Gonalezález, A., Rodríguez, E., Lleó, A., & Sánchez-Juan, P. (2017). MicroRNA Profile in Patients with Alzheimer's Disease: Analysis of miR-9-5p and miR-598 in Raw and Exosome Enriched Cerebrospinal Fluid Samples. Journal of Alzheimer's Disease, 57(2), 483–491. https://doi.org/10.3233/JAD-161179

Rice, H. C., de Malmazet, D., Schreurs, A., Frere, S., Van Molle, I., Volkov, A. N., Creemers, E., Vertkin, I., Nys, J., Ranaivoson, F. M., Comoletti, D., Savas, J. N., Remaut, H., Balschun, D., Wierda, K. D., Slutsky, I., Farrow, K., De Strooper, B., & de Wit, J. (2019). Secreted amyloid-β precursor protein functions as a GABABR1a ligand to modulate synaptic transmission. Science, 363(6423), eaao4827. https://doi.org/10.1126/science.aao4827

Richard, E., Charante, E. P. M. van, Hoevenaar-Blom, M. P., Coley, N., Barbera, M., Groep, A. van der, Meiller, Y., Mangialasche, F., Beishuizen, C. B., Jongstra, S., Middelaar, T. van, Wanrooij, L. L. V., Ngandu, T., Guillemont, J., Andrieu, S., Brayne, C., Kivipelto, M., Soininen, H., & Gool, W. A. V. (2019). Healthy ageing through internet counselling in the elderly (HATICE): A multinational, randomised controlled trial. The Lancet Digital Health, 1(8), e424–e434. https://doi.org/10.1016/S2589-7500(19)30153-0

Rizvi, F., Mathur, A., Krishna, S., Siddiqi, M. I., & Kakkar, P. (2015). Suppression in PHLPP2 induction by morin promotes Nrf2-regulated cellular defenses against oxidative injury to primary rat hepatocytes. Redox Biology, 6, 587–598. https://doi.org/10.1016/j.redox.2015.10.002

Roberts, R. O., Aakre, J. A., Kremers, W. K., Vassilaki, M., Knopman, D. S., Mielke, M. M., Alhurani, R., Geda, Y. E., Machulda, M. M., Coloma, P., Schauble, B., Lowe, V. J., Jack, C. R., Jr, & Petersen, R. C. (2018). Prevalence and Outcomes of Amyloid Positivity Among Persons Without Dementia in a Longitudinal, Population-Based Setting. JAMA Neurology, 75(8), 970–979. https://doi.org/10.1001/jamaneurol.2018.0629

Rogaev, E. I., Sherrington, R., Rogaeva, E. A., Levesque, G., Ikeda, M., Liang, Y., Chi, H., Lin, C., Holman, K., Tsuda, T., Mar, L., Sorbi, S., Nacmias, B., Piacentini, S., Amaducci, L., Chumakov, I., Cohen, D., Lannfelt, L., Fraser, P. E., … George-Hyslop, P. H. S. (1995). Familial Alzheimer's disease in kindreds with missense mutations in a gene on chromosome 1 related to the Alzheimer's disease type 3 gene. Nature, 376(6543), Article 6543. https://doi.org/10.1038/376775a0

Rohrer, J. D., Lashley, T., Schott, J. M., Warren, J. E., Mead, S., Isaacs, A. M., Beck, J., Hardy, J., de Silva, R., Warrington, E., Troakes, C., Al-Sarraj, S., King, A., Borroni, B., Clarkson, M. J., Ourselin, S., Holton, J. L., Fox, N. C., Revesz, T., … Warren, J. D. (2011). Clinical and neuroanatomical signatures of tissue pathology in frontotemporal lobar degeneration. Brain, 134(9), 2565–2581. https://doi.org/10.1093/brain/awr198

Rosales-Corral, S. A., Lopez-Armas, G., Cruz-Ramos, J., Melnikov, V. G., Tan, D.-X., Manchester, L. C., Munoz, R., & Reiter, R. J. (2012). Alterations in Lipid Levels of Mitochondrial Membranes Induced by Amyloid-β: A Protective Role of Melatonin. International Journal of Alzheimer's Disease, 2012, 459806. https://doi.org/10.1155/2012/459806

Rosenberg, A., Ngandu, T., Rusanen, M., Antikainen, R., Bäckman, L., Havulinna, S., Hänninen, T., Laatikainen, T., Lehtisalo, J., Levälahti, E., Lindström, J., Paajanen, T., Peltonen, M., Soininen, H., Stigsdotter-Neely, A., Strandberg, T., Tuomilehto, J., Solomon, A., & Kivipelto, M. (2018). Multidomain lifestyle intervention benefits a large elderly population at risk for cognitive decline and dementia regardless of baseline characteristics: The FINGER trial. Alzheimer's & Dementia, 14(3), 263–270. https://doi.org/10.1016/j.jalz.2017.09.006

Rostamian Delavar, M., Baghi, M., Safaeinejad, Z., Kiani-Esfahani, A., Ghaedi, K., & Nasr-Esfahani, M. H. (2018). Differential expression of miR-34a, miR-141, and miR-9 in MPP+-treated differentiated PC12 cells as a model of Parkinson's disease. Gene, 662, 54–65. https://doi.org/10.1016/j.gene.2018.04.010

Rovelet-Lecrux, A., Hannequin, D., Raux, G., Meur, N. L., Laquerrière, A., Vital, A., Dumanchin, C., Feuillette, S., Brice, A., Vercelletto, M., Dubas, F., Frebourg, T., & Campion, D. (2006). APP locus duplication causes autosomal dominant early-onset Alzheimer disease with cerebral amyloid angiopathy. Nature Genetics, 38(1), Article 1. https://doi.org/10.1038/ng1718

Ruan, Z., Pathak, D., Venkatesan Kalavai, S., Yoshii-Kitahara, A., Muraoka, S., Bhatt, N., Takamatsu-Yukawa, K., Hu, J., Wang, Y., Hersh, S., Ericsson, M., Gorantla, S., Gendelman, H. E., Kayed, R., Ikezu, S., Luebke, J. I., & Ikezu, T. (2020). Alzheimer's disease brain-derived extracellular vesicles spread tau pathology in interneurons. Brain, 144(1), 288–309. https://doi.org/10.1093/brain/awaa376

Rusca, N., & Monticelli, S. (2011). MiR-146a in Immunity and Disease. Molecular Biology International, 2011, 1–7. https://doi.org/10.4061/2011/437301

Ryman, D., Morris, J., Bateman, R., & Network (DIAN), the D. I. A. (2014). O3-06-01: Predicting Symptom Onset in Autosomal Dominant Alzheimer's Disease: A Systematic Review and Meta-Analysis. Alzheimer's & Dementia, 10(4S_Part_3), P218–P219. https://doi.org/10.1016/j.jalz.2014.04.299

Saba, R., Gushue, S., Huzarewich, R. L. C. H., Manguiat, K., Medina, S., Robertson, C., & Booth, S. A. (2012). MicroRNA 146a (miR-146a) Is Over-Expressed during Prion Disease and Modulates the Innate Immune Response and the Microglial Activation State. PLOS ONE, 7(2), e30832. https://doi.org/10.1371/journal.pone.0030832

Sabaie, H., Talebi, M., Gharesouarn, J., Asadi, M. R., Jalaiei, A., Arsang-Jang, S., Hussen, B. M., Taheri, M., Jalili Khoshnoud, R., & Rezazadeh, M. (2022). Identification and Analysis of BCAS4/hsa-miR-185-5p/SHISA7 Competing Endogenous RNA Axis in Late-Onset Alzheimer's Disease Using Bioinformatic and Experimental Approaches. Frontiers in Aging Neuroscience, 14, 812169. https://doi.org/10.3389/fnagi.2022.812169

Salati, S., Salvestrini, V., Carretta, C., Genovese, E., Rontauroli, S., Zini, R., Rossi, C., Ruberti, S., Bianchi, E., Barbieri, G., Curti, A., Castagnetti, F., Gugliotta, G., Rosti, G., Bergamaschi, M., Tafuri, A., Tagliafico, E., Lemoli, R., & Manfredini, R. (2017). Deregulated expression of miR-29a-3p, miR-494-3p and miR-660-5p affects sensitivity to tyrosine kinase inhibitors in CML leukemic stem cells. Oncotarget, 8(30), 49451–49469. https://doi.org/10.18632/oncotarget.17706

Salloway, S., Farlow, M., McDade, E., Clifford, D. B., Wang, G., Llibre-Guerra, J. J., Hitchcock, J. M., Mills, S. L., Santacruz, A. M., Aschenbrenner, A. J., Hassenstab, J., Benzinger, T. L. S., Gordon, B. A., Fagan, A. M., Coalier, K. A., Cruchaga, C., Goate, A. A., Perrin, R. J., Xiong, C., … Bateman, R. J. (2021). A trial of gantenerumab or solanezumab in dominantly inherited Alzheimer's disease. Nature Medicine, 27(7), Article 7. https://doi.org/10.1038/s41591-021-01369-8

Salta, E., Sierksma, A., Vanden Eynden, E., & De Strooper, B. (2016). MiR-132 loss de-represses ITPKB and aggravates amyloid and TAU pathology in Alzheimer's brain. EMBO Molecular Medicine, 8(9), 1005–1018. https://doi.org/10.15252/emmm.201606520

Saman, S., Kim, W., Raya, M., Visnick, Y., Miro, S., Saman, S., Jackson, B., McKee, A. C., Alvarez, V. E., Lee, N. C. Y., & Hall, G. F. (2012). Exosome-associated Tau Is Secreted in Tauopathy Models and Is Selectively Phosphorylated in Cerebrospinal Fluid in Early Alzheimer Disease. Journal of Biological Chemistry, 287(6), 3842–3849. https://doi.org/10.1074/jbc.M111.277061

Saman, S., Lee, N. C. Y., Inoyo, I., Jin, J., Li, Z., Doyle, T., McKee, A. C., & Hall, G. F. (2014). Proteins Recruited to Exosomes by Tau Overexpression Implicate Novel Cellular Mechanisms Linking Tau Secretion with Alzheimer's Disease. Journal of Alzheimer's Disease, 40(s1), S47–S70. https://doi.org/10.3233/JAD-132135

Santa-Maria, I., Alaniz, M. E., Renwick, N., Cela, C., Fulga, T. A., Vactor, D. V., Tuschl, T., Clark, L. N., Shelanski, M. L., McCabe, B. D., & Crary, J. F. (2015). Dysregulation of microRNA-219 promotes neurodegeneration through post-transcriptional regulation of tau. The Journal of Clinical Investigation, 125(2), 681–686. https://doi.org/10.1172/JCI78421

Sardar Sinha, M., Ansell-Schultz, A., Civitelli, L., Hildesjö, C., Larsson, M., Lannfelt, L., Ingelsson, M., & Hallbeck, M. (2018). Alzheimer's disease pathology propagation by exosomes containing toxic amyloid-beta oligomers. Acta Neuropathologica, 136(1), 41–56. https://doi.org/10.1007/s00401-018-1868-1

Sarkar, S., Jun, S., Rellick, S., Quintana, D. D., Cavendish, J. Z., & Simpkins, J. W. (2016). Expression of MicroRNA-34a in Alzheimer's Disease Brain Targets Genes Linked to Synaptic Plasticity, Energy Metabolism, and Resting State Network Activity. Brain Research, 1646, 139–151. https://doi.org/10.1016/j.brainres.2016.05.026

Satoh, J., Kino, Y., & Niida, S. (2015). MicroRNA-Seq Data Analysis Pipeline to Identify Blood Biomarkers for Alzheimer's Disease from Public Data. Biomarker Insights, 10, BMI.S25132. https://doi.org/10.4137/BMI.S25132

Saugstad, J. A., Lusardi, T. A., Van Keuren-Jensen, K. R., Phillips, J. I., Lind, B., Harrington, C. A., McFarland, T. J., Courtright, A. L., Reiman, R. A., Yeri, A. S., Kalani, M. Y. S., Adelson, P. D., Arango, J., Nolan, J. P., Duggan, E., Messer, K., Akers, J. C., Galasko, D. R., Quinn, J. F., … Hochberg, F. H. (2017). Analysis of extracellular RNA in cerebrospinal fluid. Journal of Extracellular Vesicles, 6(1), 1317577. https://doi.org/10.1080/20013078.2017.1317577

Scheff, S. W., Ansari, M. A., & Mufson, E. J. (2016). Oxidative stress and hippocampal synaptic protein levels in elderly cognitively intact individuals with Alzheimer's disease pathology. Neurobiology of Aging, 42, 1–12. https://doi.org/10.1016/j.neurobiolaging.2016.02.030

Scheltens, P., De Strooper, B., Kivipelto, M., Holstege, H., Chételat, G., Teunissen, C. E., Cummings, J., & van der Flier, W. M. (2021). Alzheimer's disease. The Lancet, 397(10284), 1577–1590. https://doi.org/10.1016/S0140-6736(20)32205-4

Scheuner, D., Eckman, C., Jensen, M., Song, X., Citron, M., Suzuki, N., Bird, T. D., Hardy, J., Hutton, M., Kukull, W., Larson, E., Levy-Lahad, L., Viitanen, M., Peskind, E., Poorkaj, P., Schellenberg, G., Tanzi, R., Wasco, W., Lannfelt, L., … Younkin, S. (1996). Secreted amyloid β–protein similar to that in the senile plaques of Alzheimer's disease is increased in vivo by the presenilin 1 and 2 and APP mutations linked to familial Alzheimer's disease. Nature Medicine, 2(8), Article 8. https://doi.org/10.1038/nm0896-864

Schipper, H. M., Maes, O. C., Chertkow, H. M., & Wang, E. (2007). MicroRNA Expression in Alzheimer Blood Mononuclear Cells. Gene Regulation and Systems Biology, 1, GRSB.S361. https://doi.org/10.4137/GRSB.S361

Schonrock, N., Ke, Y. D., Humphreys, D., Staufenbiel, M., Ittner, L. M., Preiss, T., & Götz, J. (2010). Neuronal MicroRNA Deregulation in Response to Alzheimer's Disease Amyloid-β. PLOS ONE, 5(6), e11070. https://doi.org/10.1371/journal.pone.0011070

Schulte, J. H., Horn, S., Otto, T., Samans, B., Heukamp, L. C., Eilers, U.-C., Krause, M., Astrahantseff, K., Klein-Hitpass, L., Buettner, R., Schramm, A., Christiansen, H., Eilers, M., Eggert, A., & Berwanger, B. (2008). MYCN regulates oncogenic MicroRNAs in neuroblastoma. International Journal of Cancer, 122(3), 699–704. https://doi.org/10.1002/ijc.23153

Selkoe, D. J., & Hardy, J. (2016). The amyloid hypothesis of Alzheimer's disease at 25 years. EMBO Molecular Medicine, 8(6), 595–608. https://doi.org/10.15252/emmm.201606210

Sempere, L. F., Freemantle, S., Pitha-Rowe, I., Moss, E., Dmitrovsky, E., & Ambros, V. (2004). Expression profiling of mammalian microRNAs uncovers a subset of brain-expressed microRNAs with possible roles in murine and human neuronal differentiation. Genome Biology, 5(3), R13.

Shankar, G. M., Li, S., Mehta, T. H., Garcia-Munoz, A., Shepardson, N. E., Smith, I., Brett, F. M., Farrell, M. A., Rowan, M. J., Lemere, C. A., Regan, C. M., Walsh, D. M., Sabatini, B. L., & Selkoe, D. J. (2008). Amyloid β-Protein Dimers Isolated Directly from Alzheimer Brains Impair Synaptic Plasticity and Memory. Nature Medicine, 14(8), 837–842. https://doi.org/10.1038/nm1782

Sharaf-Eldin, W. E., Kishk, N. A., Gad, Y. Z., Hassan, H., Ali, M. A. M., Zaki, M. S., Mohamed, M. R., & Essawi, M. L. (2017). Extracellular miR-145, miR-223 and miR-326 expression signature allow for differential diagnosis of immune-mediated neuroinflammatory diseases. Journal of the Neurological Sciences, 383, 188–198. https://doi.org/10.1016/j.jns.2017.11.014

Sharma, P., Ludwig, S., Muller, L., Hong, C. S., Kirkwood, J. M., Ferrone, S., & Whiteside, T. L. (2018). Immunoaffinity-based isolation of melanoma cell-derived exosomes from plasma of patients with melanoma. Journal of Extracellular Vesicles, 7(1), 1435138. https://doi.org/10.1080/20013078.2018.1435138

Sharma, P., Mesci, P., Carromeu, C., McClatchy, D. R., Schiapparelli, L., Yates, J. R., Muotri, A. R., & Cline, H. T. (2019). Exosomes regulate neurogenesis and circuit assembly. Proceedings of the National Academy of Sciences, 116(32), 16086–16094. https://doi.org/10.1073/pnas.1902513116

Sheinerman, K. S., Tsivinsky, V. G., Crawford, F., Mullan, M. J., Abdullah, L., & Umansky, S. R. (2012). Plasma microRNA biomarkers for detection of mild cognitive impairment. Aging, 4(9), 590–605. https://doi.org/10.18632/aging.100486

Shelke, G. V., Lässer, C., Gho, Y. S., & Lötvall, J. (2014). Importance of exosome depletion protocols to eliminate functional and RNA-containing extracellular vesicles from fetal bovine serum. Journal of Extracellular Vesicles, 3(1), 24783. https://doi.org/10.3402/jev.v3.24783

Shen, J., & Kelleher, R. J. (2007). The presenilin hypothesis of Alzheimer's disease: Evidence for a loss-of-function pathogenic mechanism. Proceedings of the National Academy of Sciences, 104(2), 403–409. https://doi.org/10.1073/pnas.0608332104

Shen, X., Chen, J., Li, J., Kofler, J., & Herrup, K. (2016). Neurons in Vulnerable Regions of the Alzheimer's Disease Brain Display Reduced ATM Signaling. ENeuro, 3(1), ENEURO.0124-15.2016. https://doi.org/10.1523/ENEURO.0124-15.2016

Shen, Y., Shen, Z., Guo, L., Zhang, Q., Wang, Z., Miao, L., Wang, M., Wu, J., Guo, W., & Zhu, Y. (2018). MiR-125b-5p is involved in oxygen and glucose deprivation injury in PC-12 cells via CBS/H2S pathway. Nitric Oxide, 78, 11–21. https://doi.org/10.1016/j.niox.2018.05.004

Shi, M., Liu, C., Cook, T. J., Bullock, K. M., Zhao, Y., Ginghina, C., Li, Y., Aro, P., Dator, R., He, C., Hipp, M. J., Zabetian, C. P., Peskind, E. R., Hu, S.-C., Quinn, J. F., Galasko, D. R., Banks, W. A., & Zhang, J. (2014). Plasma exosomal α-synuclein is likely CNS-derived and increased in Parkinson's disease. Acta Neuropathologica, 128(5), 639–650. https://doi.org/10.1007/s00401-014-1314-y

Shin, K.-H., Pucar, A., Kim, R. H., Bae, S. D., Chen, W., Kang, M. K., & Park, N.-H. (2011). Identification of senescence-inducing microRNAs in normal human keratinocytes. International Journal of Oncology, 39(5), 1205–1211. https://doi.org/10.3892/ijo.2011.1111

Shipley, M. M., Mangold, C. A., & Szpara, M. L. (2016). Differentiation of the SH-SY5Y Human Neuroblastoma Cell Line. Journal of Visualized Experiments : JoVE, 108. https://doi.org/10.3791/53193

Shurtleff, M. J., Yao, J., Qin, Y., Nottingham, R. M., Temoche-Diaz, M. M., Schekman, R., & Lambowitz, A. M. (2017). Broad role for YBX1 in defining the small noncoding RNA composition of exosomes. Proceedings of the National Academy of Sciences, 114(43), E8987–E8995. https://doi.org/10.1073/pnas.1712108114

Sierksma, A., Lu, A., Salta, E., Eynden, E. V., Callaerts-Vegh, Z., D'Hooge, R., Blum, D., Buée, L., Fiers, M., & Strooper, B. D. (2018). Deregulation of neuronal miRNAs induced by amyloid-β or TAU pathology. Molecular Neurodegeneration, 13. https://doi.org/10.1186/s13024-018-0285-1

Skog, J., Würdinger, T., van Rijn, S., Meijer, D. H., Gainche, L., Jr, W. T. C., Carter, B. S., Krichevsky, A. M., & Breakefield, X. O. (2008). Glioblastoma microvesicles transport RNA and proteins that promote tumour growth and provide diagnostic biomarkers. Nature Cell Biology, 10(12), 1470–1476. https://doi.org/10.1038/ncb1800

Smits, M., Wurdinger, T., van het Hof, B., Drexhage, J. A. R., Geerts, D., Wesseling, P., Noske, D. P., Vandertop, W. P., de Vries, H. E., & Reijerkerk, A. (2012). Myc-associated zinc finger protein (MAZ) is regulated by miR-125b and mediates VEGF-induced angiogenesis in glioblastoma. The FASEB Journal, 26(6), 2639–2647. https://doi.org/10.1096/fj.11-202820

Snyder, E. M., Nong, Y., Almeida, C. G., Paul, S., Moran, T., Choi, E. Y., Nairn, A. C., Salter, M. W., Lombroso, P. J., Gouras, G. K., & Greengard, P. (2005). Regulation of NMDA receptor trafficking by amyloid-beta. Nature Neuroscience, 8(8), 1051–1058. https://doi.org/10.1038/nn1503

Sohn, P. D., Huang, C. T.-L., Yan, R., Fan, L., Tracy, T. E., Camargo, C. M., Montgomery, K. M., Arhar, T., Mok, S.-A., Freilich, R., Baik, J., He, M., Gong, S., Roberson, E. D., Karch, C. M., Gestwicki, J. E., Xu, K., Kosik, K. S., & Gan, L. (2019). Pathogenic Tau Impairs Axon Initial Segment Plasticity and Excitability Homeostasis. Neuron, 104(3), 458-470.e5. https://doi.org/10.1016/j.neuron.2019.08.008

Song, D., Diao, J., Yang, Y., & Chen, Y. (2017). MicroRNA-382 inhibits cell proliferation and invasion of retinoblastoma by targeting BDNF-mediated PI3K/AKT signalling pathway. Molecular Medicine Reports, 16(5), 6428–6436. https://doi.org/10.3892/mmr.2017.7396

Song, J., & Lee, J. E. (2015). MiR-155 is involved in Alzheimer's disease by regulating T lymphocyte function. Frontiers in Aging Neuroscience, 7, 61. https://doi.org/10.3389/fnagi.2015.00061

Srinivasan, S., Yeri, A., Cheah, P. S., Chung, A., Danielson, K., Hoff, P. D., Filant, J., Laurent, C. D., Laurent, L. D., Magee, R., Moeller, C., Murthy, V. L., Nejad, P., Paul, A., Rigoutsos, I., Rodosthenous, R., Shah, R. V., Simonson, B., To, C., … Laurent, L. C. (2019). Small RNA Sequencing across Diverse Biofluids Identifies Optimal Methods for exRNA Isolation. Cell, 177(2), 446-462.e16. https://doi.org/10.1016/j.cell.2019.03.024

Stancu, I.-C., Cremers, N., Vanrusselt, H., Couturier, J., Vanoosthuyse, A., Kessels, S., Lodder, C., Brône, B., Huaux, F., Octave, J.-N., Terwel, D., & Dewachter, I. (2019). Aggregated Tau activates NLRP3–ASC inflammasome exacerbating exogenously seeded and non-exogenously seeded Tau pathology in vivo. Acta Neuropathologica, 137(4), 599–617. https://doi.org/10.1007/s00401-018-01957-y

Stephen, R., Liu, Y., Ngandu, T., Antikainen, R., Hulkkonen, J., Koikkalainen, J., Kemppainen, N., Lötjönen, J., Levälahti, E., Parkkola, R., Pippola, P., Rinne, J., Strandberg, T., Tuomilehto, J., Vanninen, R., Kivipelto, M., Soininen, H., Solomon, A., & for the FINGER study group. (2019). Brain volumes and cortical thickness on MRI in the Finnish Geriatric Intervention Study to Prevent Cognitive Impairment and Disability (FINGER). Alzheimer's Research & Therapy, 11(1), 53. https://doi.org/10.1186/s13195-019-0506-z

Stoeck, K., Sanchez-Juan, P., Gawinecka, J., Green, A., Ladogana, A., Pocchiari, M., Sanchez-Valle, R., Mitrova, E., Sklaviadis, T., Kulczycki, J., Slivarichova, D., Saiz, A., Calero, M., Knight, R., Aguzzi, A., Laplanche, J.-L., Peoc'h, K., Schelzke, G., Karch, A., … Zerr, I. (2012). Cerebrospinal fluid biomarker supported diagnosis of Creutzfeldt–Jakob disease and rapid dementias: A longitudinal multicentre study over 10 years. Brain, 135(10), 3051–3061. https://doi.org/10.1093/brain/aws238

Stranska, R., Gysbrechts, L., Wouters, J., Vermeersch, P., Bloch, K., Dierickx, D., Andrei, G., & Snoeck, R. (2018). Comparison of membrane affinity-based method with size-exclusion chromatography for isolation of exosome-like vesicles from human plasma. Journal of Translational Medicine, 16(1), 1. https://doi.org/10.1186/s12967-017-1374-6

Strong, M. J., Abrahams, S., Goldstein, L. H., Woolley, S., Mclaughlin, P., Snowden, J., Mioshi, E., Roberts-South, A., Benatar, M., HortobáGyi, T., Rosenfeld, J., Silani, V., Ince, P. G., & Turner, M. R. (2017). Amyotrophic lateral sclerosis - frontotemporal spectrum disorder (ALS-FTSD): Revised diagnostic criteria. Amyotrophic Lateral Sclerosis & Frontotemporal Degeneration, 18(3–4), 153–174. https://doi.org/10.1080/21678421.2016.1267768

Strooper, B. D., Iwatsubo, T., & Wolfe, M. S. (2012). Presenilins and γ-Secretase: Structure, Function, and Role in Alzheimer Disease. Cold Spring Harbor Perspectives in Medicine, 2(1), a006304. https://doi.org/10.1101/cshperspect.a006304

Stuendl, A., Kunadt, M., Kruse, N., Bartels, C., Moebius, W., Danzer, K. M., Mollenhauer, B., & Schneider, A. (2016). Induction of α-synuclein aggregate formation by CSF exosomes from patients with Parkinson's disease and dementia with Lewy bodies. Brain, 139(2), 481–494. https://doi.org/10.1093/brain/awv346

Su, L., Chen, S., Zheng, C., Wei, H., & Song, X. (2019). Meta-Analysis of Gene Expression and Identification of Biological Regulatory Mechanisms in Alzheimer's Disease. Frontiers in Neuroscience, 13. https://www.frontiersin.org/articles/10.3389/fnins.2019.00633

Subramaniam, R., Roediger, F., Jordan, B., Mattson, M. P., Keller, J. N., Waeg, G., & Butterfield, D. A. (1997). The Lipid Peroxidation Product, 4-Hydroxy-2-trans-Nonenal, Alters the Conformation of Cortical Synaptosomal Membrane Proteins. Journal of Neurochemistry, 69(3), 1161–1169. https://doi.org/10.1046/j.1471-4159.1997.69031161.x

Sun, L., Liu, A., Zhang, J., Ji, W., Li, Y., Yang, X., Wu, Z., & Guo, J. (2018). MiR-23b improves cognitive impairments in traumatic brain injury by targeting ATG12-mediated neuronal autophagy. Behavioural Brain Research, 340, 126–136. https://doi.org/10.1016/j.bbr.2016.09.020

Sun, L., Zhou, R., Yang, G., & Shi, Y. (2017). Analysis of 138 pathogenic mutations in presenilin-1 on the in vitro production of Aβ42 and Aβ40 peptides by γ-secretase. Proceedings of the National Academy of Sciences, 114(4), E476–E485. https://doi.org/10.1073/pnas.1618657114

Sun, W., Samimi, H., Gamez, M., Zare, H., & Frost, B. (2018). Pathogenic tau-induced piRNA depletion promotes neuronal death through transposable element dysregulation in neurodegenerative tauopathies. Nature Neuroscience, 21(8), 1038–1048. https://doi.org/10.1038/s41593-018-0194-1

Sun, X., Wu, Y., Gu, M., & Zhang, Y. (2014). MiR-342-5p Decreases Ankyrin G Levels in Alzheimer's Disease Transgenic Mouse Models. Cell Reports, 6(2), 264–270. https://doi.org/10.1016/j.celrep.2013.12.028

Sundermann, E. E., Maki, P., Biegon, A., Lipton, R. B., Mielke, M. M., Machulda, M., Bondi, M. W., & Initiative, for the A. D. N. (2019). Sex-specific norms for verbal memory tests may improve diagnostic accuracy of amnestic MCI. Neurology, 93(20), e1881–e1889. https://doi.org/10.1212/WNL.0000000000008467

Sundermann, E. E., Tran, M., Maki, P. M., & Bondi, M. W. (2018). Sex differences in the association between apolipoprotein E ε4 allele and Alzheimer's disease markers. Alzheimer's & Dementia: Diagnosis, Assessment & Disease Monitoring, 10, 438–447. https://doi.org/10.1016/j.dadm.2018.06.004

Sündermann, F., Fernandez, M.-P., & Morgan, R. O. (2016). An evolutionary roadmap to the microtubule-associated protein MAP Tau. BMC Genomics, 17(1), 264. https://doi.org/10.1186/s12864-016-2590-9

Sweeney, M. D., Sagare, A. P., & Zlokovic, B. V. (2018). Blood–brain barrier breakdown in Alzheimer disease and other neurodegenerative disorders. Nature Reviews Neurology, 14(3), 133–150. https://doi.org/10.1038/nrneurol.2017.188

Szepesi, Z., Manouchehrian, O., Bachiller, S., & Deierborg, T. (2018). Bidirectional Microglia–Neuron Communication in Health and Disease. Frontiers in Cellular Neuroscience, 12. https://doi.org/10.3389/fncel.2018.00323

Tai, H.-C., Serrano-Pozo, A., Hashimoto, T., Frosch, M. P., Spires-Jones, T. L., & Hyman, B. T. (2012). The Synaptic Accumulation of Hyperphosphorylated Tau Oligomers in Alzheimer Disease Is Associated With Dysfunction of the Ubiquitin-Proteasome System. The American Journal of Pathology, 181(4), 1426–1435. https://doi.org/10.1016/j.ajpath.2012.06.033

Takasugi, M. (2018). Emerging roles of extracellular vesicles in cellular senescence and aging. Aging Cell, 17(2), e12734. https://doi.org/10.1111/acel.12734

Takeda, Y. S., & Xu, Q. (2015). Neuronal Differentiation of Human Mesenchymal Stem Cells Using Exosomes Derived from Differentiating Neuronal Cells. PLoS ONE, 10(8). https://doi.org/10.1371/journal.pone.0135111

Takenouchi, T., Tsukimoto, M., Iwamaru, Y., Sugama, S., Sekiyama, K., Sato, M., Kojima, S., Hashimoto, M., & Kitani, H. (2015). Extracellular ATP induces unconventional release of glyceraldehyde-3-phosphate dehydrogenase from microglial cells. Immunology Letters, 167(2), 116–124. https://doi.org/10.1016/j.imlet.2015.08.002

Takov, K., Yellon, D. M., & Davidson, S. M. (2017). Confounding factors in vesicle uptake studies using fluorescent lipophilic membrane dyes. Journal of Extracellular Vesicles, 6(1), 1388731. https://doi.org/10.1080/20013078.2017.1388731

Tam, S., Tsao, M.-S., & McPherson, J. D. (2015). Optimization of miRNA-seq data preprocessing. Briefings in Bioinformatics, 16(6), 950–963. https://doi.org/10.1093/bib/bbv019

Tan, L., Yu, J.-T., Liu, Q.-Y., Tan, M.-S., Zhang, W., Hu, N., Wang, Y.-L., Sun, L., Jiang, T., & Tan, L. (2014). Circulating miR-125b as a biomarker of Alzheimer's disease. Journal of the Neurological Sciences, 336(1), 52–56. https://doi.org/10.1016/j.jns.2013.10.002

Tang, J., Yan, B., Tang, Y., Zhou, X., Ji, Z., & Xu, F. (2022). Baicalein ameliorates oxidative stress and brain injury after intracerebral hemorrhage by activating the Nrf2/ARE pathway via miR-106a-5p/PHLPP2 axis. International Journal of Neuroscience, 0(0), 1–14. https://doi.org/10.1080/00207454.2022.2080676

Taupin, P., Ray, J., Fischer, W. H., Suhr, S. T., Hakansson, K., Grubb, A., & Gage, F. H. (2000). FGF-2-Responsive Neural Stem Cell Proliferation Requires CCg, a Novel Autocrine/Paracrine Cofactor. Neuron, 28(2), 385–397. https://doi.org/10.1016/S0896-6273(00)00119-7

Terrill-Usery, S. E., Mohan, M. J., & Nichols, M. R. (2014). Amyloid-β(1-42) protofibrils stimulate a quantum of secreted IL-1β despite significant intracellular IL-1β accumulation in microglia. Biochimica et Biophysica Acta (BBA) - Molecular Basis of Disease, 1842(11), 2276–2285. https://doi.org/10.1016/j.bbadis.2014.08.001

Teunissen, C. E., Verberk, I. M. W., Thijssen, E. H., Vermunt, L., Hansson, O., Zetterberg, H., van der Flier, W. M., Mielke, M. M., & del Campo, M. (2022). Blood-based biomarkers for Alzheimer's disease: Towards clinical implementation. The Lancet Neurology, 21(1), 66–77. https://doi.org/10.1016/S1474-4422(21)00361-6

Thal, D. R., Rüb, U., Orantes, M., & Braak, H. (2002). Phases of Aβ-deposition in the human brain and its relevance for the development of AD. Neurology, 58(12), 1791–1800. https://doi.org/10.1212/WNL.58.12.1791

Tharp, W. G., & Sarkar, I. N. (2013). Origins of amyloid-β. BMC Genomics, 14(1), 290. https://doi.org/10.1186/1471-2164-14-290

The Galaxy Community. (2022). The Galaxy platform for accessible, reproducible and collaborative biomedical analyses: 2022 update. Nucleic Acids Research, 50(W1), W345–W351. https://doi.org/10.1093/nar/gkac247

Théry, C., Witwer, K. W., Aikawa, E., Alcaraz, M. J., Anderson, J. D., Andriantsitohaina, R., Antoniou, A., Arab, T., Archer, F., Atkin-Smith, G. K., Ayre, D. C., Bach, J.-M., Bachurski, D., Baharvand, H., Balaj, L., Baldacchino, S., Bauer, N. N., Baxter, A. A., Bebawy, M., … Zuba-Surma, E. K. (2018). Minimal information for studies of extracellular vesicles 2018 (MISEV2018): A position statement of the International Society for Extracellular Vesicles and update of the MISEV2014 guidelines. Journal of Extracellular Vesicles, 7(1), 1535750. https://doi.org/10.1080/20013078.2018.1535750

Thind, A., & Wilson, C. (2016). Exosomal miRNAs as cancer biomarkers and therapeutic targets. Journal of Extracellular Vesicles, 5(1), 31292. https://doi.org/10.3402/jev.v5.31292

Thompson, S., Pearson, A. N., Ashley, M. D., Jessick, V., Murphy, B. M., Gafken, P., Henshall, D. C., Morris, K. T., Simon, R. P., & Meller, R. (2011). Identification of a Novel Bcl-2-interacting Mediator of Cell Death (Bim) E3 Ligase, Tripartite Motif-containing Protein 2 (TRIM2), and Its Role in Rapid Ischemic Tolerance-induced Neuroprotection *. Journal of Biological Chemistry, 286(22), 19331–19339. https://doi.org/10.1074/jbc.M110.197707

Tian, F., Zhang, S., Liu, C., Han, Z., Liu, Y., Deng, J., Li, Y., Wu, X., Cai, L., Qin, L., Chen, Q., Yuan, Y., Liu, Y., Cong, Y., Ding, B., Jiang, Z., & Sun, J. (2021). Protein analysis of extracellular vesicles to monitor and predict therapeutic response in metastatic breast cancer. Nature Communications, 12(1), Article 1. https://doi.org/10.1038/s41467-021-22913-7

Tili, E., Michaille, J.-J., Cimino, A., Costinean, S., Dumitru, C. D., Adair, B., Fabbri, M., Alder, H., Liu, C. G., Calin, G. A., & Croce, C. M. (2007). Modulation of miR-155 and miR-125b Levels following Lipopolysaccharide/TNF-α Stimulation and Their Possible Roles in Regulating the Response to Endotoxin Shock1. The Journal of Immunology, 179(8), 5082–5089. https://doi.org/10.4049/jimmunol.179.8.5082

Tofaris, G. K. (n.d.). A Critical Assessment of Exosomes in the Pathogenesis and Stratification of Parkinson's Disease. Journal of Parkinson's Disease, 7(4), 569–576. https://doi.org/10.3233/JPD-171176

Tominaga, N., Kosaka, N., Ono, M., Katsuda, T., Yoshioka, Y., Tamura, K., Lötvall, J., Nakagama, H., & Ochiya, T. (2015). Brain metastatic cancer cells release microRNA-181c-containing extracellular vesicles capable of destructing blood–brain barrier. Nature Communications, 6. https://doi.org/10.1038/ncomms7716

Tosar, J. P., Witwer, K., & Cayota, A. (2021). Revisiting extracellular RNA release, processing, and function. Trends in Biochemical Sciences, 46(6), 438–445. https://doi.org/10.1016/j.tibs.2020.12.008

Tracy, T. E., Sohn, P. D., Minami, S. S., Wang, C., Min, S.-W., Li, Y., Zhou, Y., Le, D., Lo, I., Ponnusamy, R., Cong, X., Schilling, B., Ellerby, L. M., Huganir, R. L., & Gan, L. (2016). Acetylated Tau Obstructs KIBRA-Mediated

Signaling in Synaptic Plasticity and Promotes Tauopathy-Related Memory Loss. Neuron, 90(2), 245–260. https://doi.org/10.1016/j.neuron.2016.03.005

Trotta, T., Antonietta Panaro, M., Cianciulli, A., Mori, G., Di Benedetto, A., & Porro, C. (2018). Microglia-derived extracellular vesicles in Alzheimer's Disease: A double-edged sword. Biochemical Pharmacology, 148, 184–192. https://doi.org/10.1016/j.bcp.2017.12.020

Trushina, E. (2019). Alzheimer's disease mechanisms in peripheral cells: Promises and challenges. Alzheimer's & Dementia : Translational Research & Clinical Interventions, 5, 652–660. https://doi.org/10.1016/j.trci.2019.06.008

Trushina, E., Dutta, T., Persson, X.-M. T., Mielke, M. M., & Petersen, R. C. (2013). Identification of Altered Metabolic Pathways in Plasma and CSF in Mild Cognitive Impairment and Alzheimer's Disease Using Metabolomics. PLoS ONE, 8(5), e63644. https://doi.org/10.1371/journal.pone.0063644

Trushina, E., Nemutlu, E., Zhang, S., Christensen, T., Camp, J., Mesa, J., Siddiqui, A., Tamura, Y., Sesaki, H., Wengenack, T. M., Dzeja, P. P., & Poduslo, J. F. (2012). Defects in Mitochondrial Dynamics and Metabolomic Signatures of Evolving Energetic Stress in Mouse Models of Familial Alzheimer's Disease. PLoS ONE, 7(2). https://doi.org/10.1371/journal.pone.0032737

Tuna, G., Yener, G. G., Oktay, G., İşlekel, G. H., & Kİrkalİ, F. G. (2018). Evaluation of Matrix Metalloproteinase-2 (MMP-2) and -9 (MMP-9) and Their Tissue Inhibitors (TIMP-1 and TIMP-2) in Plasma from Patients with Neurodegenerative Dementia. Journal of Alzheimer's Disease, 66(3), 1265–1273. https://doi.org/10.3233/JAD-180752

Turchinovich, A., Samatov, T. R., Tonevitsky, A. G., & Burwinkel, B. (2013). Circulating miRNAs: Cell–cell communication function? Frontiers in Genetics, 4. https://doi.org/10.3389/fgene.2013.00119

Turchinovich, A., Tonevitsky, A. G., & Burwinkel, B. (2016). Extracellular miRNA: A Collision of Two Paradigms. Trends in Biochemical Sciences, 41(10), 883–892. https://doi.org/10.1016/j.tibs.2016.08.004

Turchinovich, A., Weiz, L., Langheinz, A., & Burwinkel, B. (2011). Characterization of extracellular circulating microRNA. Nucleic Acids Research, 39(16), 7223–7233. https://doi.org/10.1093/nar/gkr254

Valadi, H., Ekström, K., Bossios, A., Sjöstrand, M., Lee, J. J., & Lötvall, J. O. (2007). Exosome-mediated transfer of mRNAs and microRNAs is a novel mechanism of genetic exchange between cells. Nature Cell Biology, 9(6), 654–659. https://doi.org/10.1038/ncb1596

Valla, J., Yaari, R., Wolf, A. B., Kusne, Y., Beach, T. G., Roher, A. E., Corneveaux, J. J., Huentelman, M. J., Caselli, R. J., & Reiman, E. M. (2010). Reduced Posterior Cingulate Mitochondrial Activity in Expired Young Adult Carriers of the APOE ε4 Allele, the Major Late-Onset Alzheimer's Susceptibility Gene. Journal of Alzheimer's Disease : JAD, 22(1), 307–313. https://doi.org/10.3233/JAD-2010-100129

van der Kant, R., Goldstein, L. S. B., & Ossenkoppele, R. (2020). Amyloid-β-independent regulators of tau pathology in Alzheimer disease. Nature Reviews Neuroscience, 21(1), Article 1. https://doi.org/10.1038/s41583-019-0240-3

van der Pol, E., Coumans, F. a. W., Grootemaat, A. E., Gardiner, C., Sargent, I. L., Harrison, P., Sturk, A., van Leeuwen, T. G., & Nieuwland, R. (2014). Particle size distribution of exosomes and microvesicles determined by transmission electron microscopy, flow cytometry, nanoparticle tracking analysis, and resistive pulse sensing. Journal of Thrombosis and Haemostasis: JTH, 12(7), 1182–1192. https://doi.org/10.1111/jth.12602

van der Vos, K. E., Abels, E. R., Zhang, X., Lai, C., Carrizosa, E., Oakley, D., Prabhakar, S., Mardini, O., Crommentuijn, M. H. W., Skog, J., Krichevsky, A. M., Stemmer-Rachamimov, A., Mempel, T. R., El Khoury, J., Hickman, S. E., & Breakefield, X. O. (2016). Directly visualized glioblastoma-derived extracellular vesicles transfer RNA to microglia/macrophages in the brain. Neuro-Oncology, 18(1), 58–69. https://doi.org/10.1093/neuonc/nov244

van Dyck, C. H., Swanson, C. J., Aisen, P., Bateman, R. J., Chen, C., Gee, M., Kanekiyo, M., Li, D., Reyderman, L., Cohen, S., Froelich, L., Katayama, S., Sabbagh, M., Vellas, B., Watson, D., Dhadda, S., Irizarry, M., Kramer, L. D., & Iwatsubo, T. (2022). Lecanemab in Early Alzheimer's Disease. New England Journal of Medicine, 0(0), null. https://doi.org/10.1056/NEJMoa2212948

Vandendriessche, C., Balusu, S., Van Cauwenberghe, C., Brkic, M., Pauwels, M., Plehiers, N., Bruggeman, A., Dujardin, P., Van Imschoot, G., Van Wonterghem, E., Hendrix, A., Baeke, F., De Rycke, R., Gevaert, K., & Vandenbroucke, R. E. (2021). Importance of extracellular vesicle secretion at the blood–cerebrospinal fluid interface in the pathogenesis of Alzheimer's disease. Acta Neuropathologica Communications, 9, 143. https://doi.org/10.1186/s40478-021-01245-z

Vandendriessche, C., Kapogiannis, D., & Vandenbroucke, R. E. (2022). Biomarker and therapeutic potential of peripheral extracellular vesicles in Alzheimer's disease. Advanced Drug Delivery Reviews, 190, 114486. https://doi.org/10.1016/j.addr.2022.114486

Vasa-Nicotera, M., Chen, H., Tucci, P., Yang, A. L., Saintigny, G., Menghini, R., Mahè, C., Agostini, M., Knight, R. A., Melino, G., & Federici, M. (2011). MiR-146a is modulated in human endothelial cell with aging. Atherosclerosis, 217(2), 326–330. https://doi.org/10.1016/j.atherosclerosis.2011.03.034

Veitch, D. P., Weiner, M. W., Aisen, P. S., Beckett, L. A., Cairns, N. J., Green, R. C., Harvey, D., Jack, C. R., Jagust, W., Morris, J. C., Petersen, R. C., Saykin, A. J., Shaw, L. M., Toga, A. W., & Trojanowski, J. Q. (2019). Understanding disease progression and improving Alzheimer's disease clinical trials: Recent highlights from the Alzheimer's Disease Neuroimaging Initiative. Alzheimer's & Dementia, 15(1), 106–152. https://doi.org/10.1016/j.jalz.2018.08.005

Vella, L. J., Scicluna, B. J., Cheng, L., Bawden, E. G., Masters, C. L., Ang, C.-S., Willamson, N., McLean, C., Barnham, K. J., & Hill, A. F. (2017). A rigorous method to enrich for exosomes from brain tissue. Journal of Extracellular Vesicles, 6(1), 1348885. https://doi.org/10.1080/20013078.2017.1348885

Vella, L. J., Sharples, R. A., Nisbet, R. M., Cappai, R., & Hill, A. F. (2008). The role of exosomes in the processing of proteins associated with neurodegenerative diseases. European Biophysics Journal, 37(3), 323–332. https://doi.org/10.1007/s00249-007-0246-z

Venegas, C., Kumar, S., Franklin, B. S., Dierkes, T., Brinkschulte, R., Tejera, D., Vieira-Saecker, A., Schwartz, S., Santarelli, F., Kummer, M. P., Griep, A., Gelpi, E., Beilharz, M., Riedel, D., Golenbock, D. T., Geyer, M., Walter, J., Latz, E., & Heneka, M. T. (2017). Microglia-derived ASC specks cross-seed amyloid-β in Alzheimer's disease. Nature, 552(7685), Article 7685. https://doi.org/10.1038/nature25158

Vergara, C., Houben, S., Suain, V., Yilmaz, Z., De Decker, R., Vanden Dries, V., Boom, A., Mansour, S., Leroy, K., Ando, K., & Brion, J.-P. (2019). Amyloid-β pathology enhances pathological fibrillary tau seeding induced by Alzheimer PHF in vivo. Acta Neuropathologica, 137(3), 397–412. https://doi.org/10.1007/s00401-018-1953-5

Verma, R., Ritzel, R. M., Harris, N. M., Lee, J., Kim, T., Pandi, G., Vemuganti, R., & McCullough, L. D. (2018). Inhibition of miR-141-3p Ameliorates the Negative Effects of Poststroke Social Isolation in Aged Mice. Stroke, 49(7), 1701–1707. https://doi.org/10.1161/STROKEAHA.118.020627

Vieira, M. N. N., Lima-Filho, R. A. S., & De Felice, F. G. (2018). Connecting Alzheimer's disease to diabetes: Underlying mechanisms and potential therapeutic targets. Neuropharmacology, 136, 160–171. https://doi.org/10.1016/j.neuropharm.2017.11.014

Vilardo, E., Barbato, C., Ciotti, M., Cogoni, C., & Ruberti, F. (2010). MicroRNA-101 Regulates Amyloid Precursor Protein Expression in Hippocampal Neurons. Journal of Biological Chemistry, 285(24), 18344–18351. https://doi.org/10.1074/jbc.M110.112664

Villarroya-Beltri, C., Gutiérrez-Vázquez, C., Sánchez-Cabo, F., Pérez-Hernández, D., Vázquez, J., Martin-Cofreces, N., Martinez-Herrera, D. J., Pascual-Montano, A., Mittelbrunn, M., & Sánchez-Madrid, F. (2013).

Sumoylated hnRNPA2B1 controls the sorting of miRNAs into exosomes through binding to specific motifs. Nature Communications, 4(1), Article 1. https://doi.org/10.1038/ncomms3980

Vizoso, F. J., Eiro, N., Cid, S., Schneider, J., & Perez-Fernandez, R. (2017). Mesenchymal Stem Cell Secretome: Toward Cell-Free Therapeutic Strategies in Regenerative Medicine. International Journal of Molecular Sciences, 18(9). https://doi.org/10.3390/ijms18091852

Wahrle, S. E., Jiang, H., Parsadanian, M., Kim, J., Li, A., Knoten, A., Jain, S., Hirsch-Reinshagen, V., Wellington, C. L., Bales, K. R., Paul, S. M., & Holtzman, D. M. (2008). Overexpression of ABCA1 reduces amyloid deposition in the PDAPP mouse model of Alzheimer disease. The Journal of Clinical Investigation, 118(2), 671–682. https://doi.org/10.1172/JCI33622

Waki, H., Nakamura, M., Yamauchi, T., Wakabayashi, K., Yu, J., Hirose-Yotsuya, L., Take, K., Sun, W., Iwabu, M., Okada-Iwabu, M., Fujita, T., Aoyama, T., Tsutsumi, S., Ueki, K., Kodama, T., Sakai, J., Aburatani, H., & Kadowaki, T. (2011). Global Mapping of Cell Type–Specific Open Chromatin by FAIRE-seq Reveals the Regulatory Role of the NFI Family in Adipocyte Differentiation. PLOS Genetics, 7(10), e1002311. https://doi.org/10.1371/journal.pgen.1002311

Walgrave, H., Balusu, S., Snoeck, S., Vanden Eynden, E., Craessaerts, K., Thrupp, N., Wolfs, L., Horré, K., Fourne, Y., Ronisz, A., Silajdžić, E., Penning, A., Tosoni, G., Callaerts-Vegh, Z., D'Hooge, R., Thal, D. R., Zetterberg, H., Thuret, S., Fiers, M., … Salta, E. (2021). Restoring miR-132 expression rescues adult hippocampal neurogenesis and memory deficits in Alzheimer's disease. Cell Stem Cell, 28(10), 1805-1821.e8. https://doi.org/10.1016/j.stem.2021.05.001

Walsh, D. M., & Selkoe, D. J. (2016). A critical appraisal of the pathogenic protein spread hypothesis of neurodegeneration. Nature Reviews Neuroscience, 17(4), 251–260. https://doi.org/10.1038/nrn.2016.13

Walsh, S., Merrick, R., Milne, R., & Brayne, C. (2021). Aducanumab for Alzheimer's disease? BMJ, 374, n1682. https://doi.org/10.1136/bmj.n1682

Wanet, A., Tacheny, A., Arnould, T., & Renard, P. (2012). miR-212/132 expression and functions: Within and beyond the neuronal compartment. Nucleic Acids Research, 40(11), 4742–4753. https://doi.org/10.1093/nar/gks151

Wang, G., Huang, Y., Wang, L.-L., Zhang, Y.-F., Xu, J., Zhou, Y., Lourenco, G. F., Zhang, B., Wang, Y., Ren, R.-J., Halliday, G. M., & Chen, S.-D. (2016). MicroRNA-146a suppresses ROCK1 allowing hyperphosphorylation of tau in Alzheimer's disease. Scientific Reports, 6(1), Article 1. https://doi.org/10.1038/srep26697

Wang, H., Li, Y., Ryder, J. W., Hole, J. T., Ebert, P. J., Airey, D. C., Qian, H.-R., Logsdon, B., Fisher, A., Ahmed, Z., Murray, T. K., Cavallini, A., Bose, S., Eastwood, B. J., Collier, D. A., Dage, J. L., Miller, B. B., Merchant, K. M., O'Neill, M. J., & Demattos, R. B. (2018). Genome-wide RNAseq study of the molecular mechanisms underlying microglia activation in response to pathological tau perturbation in the rTg4510 tau transgenic animal model. Molecular Neurodegeneration, 13, 65. https://doi.org/10.1186/s13024-018-0296-y

Wang, J., Gu, B. J., Masters, C. L., & Wang, Y.-J. (2017). A systemic view of Alzheimer disease—Insights from amyloid-β metabolism beyond the brain. Nature Reviews Neurology, 13(10), Article 10. https://doi.org/10.1038/nrneurol.2017.111

Wang, J. K. T., Langfelder, P., Horvath, S., & Palazzolo, M. J. (2017). Exosomes and Homeostatic Synaptic Plasticity Are Linked to Each other and to Huntington's, Parkinson's, and Other Neurodegenerative Diseases by Database-Enabled Analyses of Comprehensively Curated Datasets. Frontiers in Neuroscience, 11. https://doi.org/10.3389/fnins.2017.00149

Wang, L., Tong, D., Guo, Q., Wang, X., Wu, F., Li, Q., Yang, J., Zhao, L., Qin, Y., Liu, Y., & Huang, C. (2018). HOXD3 targeted by miR-203a suppresses cell metastasis and angiogenesis through VEGFR in human hepatocellular carcinoma cells. Scientific Reports, 8(1), Article 1. https://doi.org/10.1038/s41598-018-20859-3

Wang, P., Liang, J., Li, Y., Li, J., Yang, X., Zhang, X., Han, S., Li, S., & Li, J. (2014). Down-Regulation of miRNA-30a Alleviates Cerebral Ischemic Injury Through Enhancing Beclin 1-Mediated Autophagy. Neurochemical Research, 39(7), 1279–1291. https://doi.org/10.1007/s11064-014-1310-6

Wang, W.-X., Huang, Q., Hu, Y., Stromberg, A. J., & Nelson, P. T. (2011). Patterns of microRNA expression in normal and early Alzheimer's disease human temporal cortex: White matter versus gray matter. Acta Neuropathologica, 121(2), 193–205. https://doi.org/10.1007/s00401-010-0756-0

Wang, W.-X., Prajapati, P., Vekaria, H. J., Spry, M., Cloud, A. L., Sullivan, P. G., & Springer, J. E. (2020). Temporal changes in inflammatory mitochondria-enriched microRNAs following traumatic brain injury and effects of miR-146a nanoparticle delivery. Neural Regeneration Research, 16(3), 514–522. https://doi.org/10.4103/1673-5374.293149

Wang, W.-X., Visavadiya, N. P., Pandya, J. D., Nelson, P. T., Sullivan, P. G., & Springer, J. E. (2015). Mitochondria-associated microRNAs in rat hippocampus following traumatic brain injury. Experimental Neurology, 265, 84–93. https://doi.org/10.1016/j.expneurol.2014.12.018

Wang, X., Su, B., Fujioka, H., & Zhu, X. (2008). Dynamin-Like Protein 1 Reduction Underlies Mitochondrial Morphology and Distribution Abnormalities in Fibroblasts from Sporadic Alzheimer's Disease Patients. The American Journal of Pathology, 173(2), 470–482. https://doi.org/10.2353/ajpath.2008.071208

Wang, X., Tan, L., Lu, Y., Peng, J., Zhu, Y., Zhang, Y., & Sun, Z. (2015). MicroRNA-138 promotes tau phosphorylation by targeting retinoic acid receptor alpha. FEBS Letters, 589(6), 726–729. https://doi.org/10.1016/j.febslet.2015.02.001

Wang, X., Wang, W., Li, L., Perry, G., Lee, H., & Zhu, X. (2014). Oxidative stress and mitochondrial dysfunction in Alzheimer's disease. Biochimica et Biophysica Acta (BBA) - Molecular Basis of Disease, 1842(8), 1240–1247. https://doi.org/10.1016/j.bbadis.2013.10.015

Wang, X., Zhou, Y., Gao, Q., Ping, D., Wang, Y., Wu, W., Lin, X., Fang, Y., Zhang, J., & Shao, A. (2020). The Role of Exosomal microRNAs and Oxidative Stress in Neurodegenerative Diseases. Oxidative Medicine and Cellular Longevity, 2020, e3232869. https://doi.org/10.1155/2020/3232869

Wang, Y., Balaji, V., Kaniyappan, S., Krüger, L., Irsen, S., Tepper, K., Chandupatla, R., Maetzler, W., Schneider, A., Mandelkow, E., & Mandelkow, E.-M. (2017). The release and trans-synaptic transmission of Tau via exosomes. Molecular Neurodegeneration, 12(1), 5. https://doi.org/10.1186/s13024-016-0143-y

Wang, Y., Luo, J., Wang, X., Yang, B., & Cui, L. (2017). MicroRNA-199a-5p Induced Autophagy and Inhibits the Pathogenesis of Ankylosing Spondylitis by Modulating the mTOR Signaling via Directly Targeting Ras Homolog Enriched in Brain (Rheb). Cellular Physiology and Biochemistry, 42(6), 2481–2491. https://doi.org/10.1159/000480211

Wang, Y., Veremeyko, T., Wong, A. H.-K., El Fatimy, R., Wei, Z., Cai, W., & Krichevsky, A. M. (2017). Downregulation of miR-132/212 impairs S-nitrosylation balance and induces tau phosphorylation in Alzheimer's disease. Neurobiology of Aging, 51, 156–166. https://doi.org/10.1016/j.neurobiolaging.2016.12.015

Wang, Z., Wang, B., Shi, Y., Xu, C., Xiao, H. L., Ma, L. N., Xu, S. L., Yang, L., Wang, Q. L., Dang, W. Q., Cui, W., Yu, S. C., Ping, Y. F., Cui, Y. H., Kung, H. F., Qian, C., Zhang, X., & Bian, X. W. (2015). Oncogenic miR-20a and miR-106a enhance the invasiveness of human glioma stem cells by directly targeting TIMP-2. Oncogene, 34(11), Article 11. https://doi.org/10.1038/onc.2014.75

Ward, A., Crean, S., Mercaldi, C. J., Collins, J. M., Boyd, D., Cook, M. N., & Arrighi, H. M. (2012). Prevalence of apolipoprotein E4 genotype and homozygotes (APOE e4/4) among patients diagnosed with Alzheimer's disease: A systematic review and meta-analysis. Neuroepidemiology, 38(1), 1–17. https://doi.org/10.1159/000334607

Wei, H., Xu, Y., Xu, W., Zhou, Q., Chen, Q., Yang, M., Feng, F., Liu, Y., Zhu, X., Yu, M., & Li, Y. (2018). Serum Exosomal miR-223 Serves as a Potential Diagnostic and Prognostic Biomarker for Dementia. Neuroscience, 379, 167–176. https://doi.org/10.1016/j.neuroscience.2018.03.016

Welsh, J. A., van der Pol, E., Bettin, B. A., Carter, D. R. F., Hendrix, A., Lenassi, M., Langlois, M.-A., Llorente, A., van de Nes, A. S., Nieuwland, R., Tang, V., Wang, L., Witwer, K. W., & Jones, J. C. (n.d.). Towards defining reference materials for measuring extracellular vesicle refractive index, epitope abundance, size and concentration. Journal of Extracellular Vesicles, 9(1), 1816641. https://doi.org/10.1080/20013078.2020.1816641

Wen, Z., Zhang, J., Tang, P., Tu, N., Wang, K., & Wu, G. (2018). Overexpression of miR-185 inhibits autophagy and apoptosis of dopaminergic neurons by regulating the AMPK/mTOR signaling pathway in Parkinson's disease. Molecular Medicine Reports, 17(1), 131–137. https://doi.org/10.3892/mmr.2017.7897

Wesseling, H., Mair, W., Kumar, M., Schlaffner, C. N., Tang, S., Beerepoot, P., Fatou, B., Guise, A. J., Cheng, L., Takeda, S., Muntel, J., Rotunno, M. S., Dujardin, S., Davies, P., Kosik, K. S., Miller, B. L., Berretta, S., Hedreen, J. C., Grinberg, L. T., … Steen, J. A. (2020). Tau PTM Profiles Identify Patient Heterogeneity and Stages of Alzheimer's Disease. Cell, 183(6), 1699-1713.e13. https://doi.org/10.1016/j.cell.2020.10.029

Wibrand, K., Pai, B., Siripornmongcolchai, T., Bittins, M., Berentsen, B., Ofte, M. L., Weigel, A., Skaftnesmo, K. O., & Bramham, C. R. (2012). MicroRNA Regulation of the Synaptic Plasticity-Related Gene Arc. PLoS ONE, 7(7). https://doi.org/10.1371/journal.pone.0041688

Wiera, G., Wozniak, G., Bajor, M., Kaczmarek, L., & Mozrzymas, J. W. (2013). Maintenance of long-term potentiation in hippocampal mossy fiber—CA3 pathway requires fine-tuned MMP-9 proteolytic activity. Hippocampus, 23(6), 529–543. https://doi.org/10.1002/hipo.22112

Winblad, B., Amouyel, P., Andrieu, S., Ballard, C., Brayne, C., Brodaty, H., Cedazo-Minguez, A., Dubois, B., Edvardsson, D., Feldman, H., Fratiglioni, L., Frisoni, G. B., Gauthier, S., Georges, J., Graff, C., Iqbal, K., Jessen, F., Johansson, G., Jönsson, L., … Zetterberg, H. (2016). Defeating Alzheimer's disease and other dementias: A priority for European science and society. The Lancet Neurology, 15(5), 455–532. https://doi.org/10.1016/S1474-4422(16)00062-4

Winston, C. N., Goetzl, E. J., Baker, L. D., Vitiello, M. V., & Rissman, R. A. (2018). Growth Hormone-Releasing Hormone Modulation of Neuronal Exosome Biomarkers in Mild Cognitive Impairment. Journal of Alzheimer's Disease, 66(3), 971–981. https://doi.org/10.3233/JAD-180302

Winston, C. N., Romero, H. K., Ellisman, M., Nauss, S., Julovich, D. A., Conger, T., Hall, J. R., Campana, W., O'Bryant, S. E., Nievergelt, C. M., Baker, D. G., Risbrough, V. B., & Rissman, R. A. (2019). Assessing Neuronal and Astrocyte Derived Exosomes From Individuals With Mild Traumatic Brain Injury for Markers of Neurodegeneration and Cytotoxic Activity. Frontiers in Neuroscience, 13. https://www.frontiersin.org/articles/10.3389/fnins.2019.01005

Winter, J. (2015). MicroRNAs of the miR379–410 cluster: New players in embryonic neurogenesis and regulators of neuronal function. Neurogenesis, 2(1), e1004970. https://doi.org/10.1080/23262133.2015.1004970

Wittenberg, R., Hu, B., Barraza-Araiza, L., & Rehill, A. (n.d.). Care Policy and Evaluation Centre, London School of Economics and Political Science.

Witwer, K. W., Buzás, E. I., Bemis, L. T., Bora, A., Lässer, C., Lötvall, J., Nolte-'t Hoen, E. N., Piper, M. G., Sivaraman, S., Skog, J., Théry, C., Wauben, M. H., & Hochberg, F. (2013). Standardization of sample collection, isolation and analysis methods in extracellular vesicle research. Journal of Extracellular Vesicles, 2, 10.3402/jev.v2i0.20360. https://doi.org/10.3402/jev.v2i0.20360

Wood, J. G., Jones, B. C., Jiang, N., Chang, C., Hosier, S., Wickremesinghe, P., Garcia, M., Hartnett, D. A., Burhenn, L., Neretti, N., & Helfand, S. L. (2016). Chromatin-modifying genetic interventions suppress age-

associated transposable element activation and extend life span in Drosophila. Proceedings of the National Academy of Sciences of the United States of America, 113(40), 11277–11282. https://doi.org/10.1073/pnas.1604621113

Wood, J. G., Mirra, S. S., Pollock, N. J., & Binder, L. I. (1986). Neurofibrillary tangles of Alzheimer disease share antigenic determinants with the axonal microtubule-associated protein tau (tau). Proceedings of the National Academy of Sciences, 83(11), 4040–4043. https://doi.org/10.1073/pnas.83.11.4040

Wu, D., Cerutti, C., Lopez-Ramirez, M. A., Pryce, G., King-Robson, J., Simpson, J. E., van der Pol, S. M., Hirst, M. C., de Vries, H. E., Sharrack, B., Baker, D., Male, D. K., Michael, G. J., & Romero, I. A. (2015). Brain Endothelial miR-146a Negatively Modulates T-Cell Adhesion through Repressing Multiple Targets to Inhibit NF-κB Activation. Journal of Cerebral Blood Flow & Metabolism, 35(3), 412–423. https://doi.org/10.1038/jcbfm.2014.207

Wu, Y.-T., Beiser, A. S., Breteler, M. M. B., Fratiglioni, L., Helmer, C., Hendrie, H. C., Honda, H., Ikram, M. A., Langa, K. M., Lobo, A., Matthews, F. E., Ohara, T., Pérès, K., Qiu, C., Seshadri, S., Sjölund, B.-M., Skoog, I., & Brayne, C. (2017). The changing prevalence and incidence of dementia over time—Current evidence. Nature Reviews Neurology, 13(6), 327–339. https://doi.org/10.1038/nrneurol.2017.63

Wulff-Fuentes, E., Berendt, R. R., Massman, L., Danner, L., Malard, F., Vora, J., Kahsay, R., & Olivier-Van Stichelen, S. (2021). The human O-GlcNAcome database and meta-analysis. Scientific Data, 8, 25. https://doi.org/10.1038/s41597-021-00810-4

Xi, T., Jin, F., Zhu, Y., Wang, J., Tang, L., Wang, Y., Liebeskind, D. S., Scalzo, F., & He, Z. (2018). MiR-27a-3p protects against blood–brain barrier disruption and brain injury after intracerebral hemorrhage by targeting endothelial aquaporin-11. Journal of Biological Chemistry, 293(52), 20041–20050. https://doi.org/10.1074/jbc.RA118.001858

Xia, D., Watanabe, H., Wu, B., Lee, S. H., Li, Y., Tsvetkov, E., Bolshakov, V. Y., Shen, J., & Kelleher, R. J. (2015). Presenilin-1 Knockin Mice Reveal Loss-of-Function Mechanism for Familial Alzheimer's Disease. Neuron, 85(5), 967–981. https://doi.org/10.1016/j.neuron.2015.02.010

Xia, X., Wang, Y., & Zheng, J. C. (2022). The microRNA-17 ~ 92 Family as a Key Regulator of Neurogenesis and Potential Regenerative Therapeutics of Neurological Disorders. Stem Cell Reviews and Reports, 18(2), 401–411. https://doi.org/10.1007/s12015-020-10050-5

Xiao, S., Zhang, D., Liu, Z., Jin, W., Huang, G., Wei, Z., Wang, D., & Deng, C. (2020). Diabetes-induced glucolipotoxicity impairs wound healing ability of adipose-derived stem cells-through the miR-1248/CITED2/HIF-1α pathway. Aging (Albany NY), 12(8), 6947–6965. https://doi.org/10.18632/aging.103053

Xie, Y., Chu, A., Feng, Y., Chen, L., Shao, Y., Luo, Q., Deng, X., Wu, M., Shi, X., & Chen, Y. (2018). MicroRNA-146a: A Comprehensive Indicator of Inflammation and Oxidative Stress Status Induced in the Brain of Chronic T2DM Rats. Frontiers in Pharmacology, 9. https://www.frontiersin.org/articles/10.3389/fphar.2018.00478

Xin, H., Katakowski, M., Wang, F., Qian, J.-Y., Shuang Liu, X., Ali, M. M., Buller, B., Zhang, Z. G., & Chopp, M. (2017). MiR-17-92 cluster in exosomes enhance neuroplasticity and functional recovery after stroke in rats. Stroke, 48(3), 747–753. https://doi.org/10.1161/STROKEAHA.116.015204

Xu, B., Zhang, Y., Du, X.-F., Li, J., Zi, H.-X., Bu, J.-W., Yan, Y., Han, H., & Du, J.-L. (2017). Neurons secrete miR-132-containing exosomes to regulate brain vascular integrity. Cell Research, 27(7), 882–897. https://doi.org/10.1038/cr.2017.62

Xu, J., Camfield, R., & Gorski, S. M. (2018). The interplay between exosomes and autophagy – partners in crime. J Cell Sci, 131(15), jcs215210. https://doi.org/10.1242/jcs.215210

Xu, J., Wang, Y., Tan, X., & Jing, H. (2012). MicroRNAs in autophagy and their emerging roles in crosstalk with apoptosis. Autophagy, 8(6), 873–882. https://doi.org/10.4161/auto.19629

Xu, J.-Z., Shao, C.-C., Wang, X.-J., Zhao, X., Chen, J.-Q., Ouyang, Y.-X., Feng, J., Zhang, F., Huang, W.-H., Ying, Q., Chen, C.-F., Wei, X.-L., Dong, H.-Y., Zhang, G.-J., & Chen, M. (2019). CircTADA2As suppress breast cancer progression and metastasis via targeting miR-203a-3p/SOCS3 axis. Cell Death & Disease, 10(3), Article 3. https://doi.org/10.1038/s41419-019-1382-y

Xu, X., Gao, W., Cheng, S., Yin, D., Li, F., Wu, Y., Sun, D., Zhou, S., Wang, D., Zhang, Y., Jiang, R., & Zhang, J. (2017). Anti-inflammatory and immunomodulatory mechanisms of atorvastatin in a murine model of traumatic brain injury. Journal of Neuroinflammation, 14(1), 167. https://doi.org/10.1186/s12974-017-0934-2

Xue, M., Peng, N., Zhu, X., & Zhang, H. (2021). Hsa_circ_0006872 promotes cigarette smoke-induced apoptosis, inflammation and oxidative stress in HPMECs and BEAS-2B cells through the miR-145-5p/NF-κB axis. Biochemical and Biophysical Research Communications, 534, 553–560. https://doi.org/10.1016/j.bbrc.2020.11.044

Yamada, K. (2017). Extracellular Tau and Its Potential Role in the Propagation of Tau Pathology. Frontiers in Neuroscience, 11. https://doi.org/10.3389/fnins.2017.00667

Yamada, N., Kuranaga, Y., Kumazaki, M., Shinohara, H., Taniguchi, K., & Akao, Y. (2016). Colorectal cancer cell-derived extracellular vesicles induce phenotypic alteration of T cells into tumor-growth supporting cells with transforming growth factor-β1-mediated suppression. Oncotarget, 7(19), 27033–27043. https://doi.org/10.18632/oncotarget.7041

Yamoah, A., Tripathi, P., Sechi, A., Köhler, C., Guo, H., Chandrasekar, A., Nolte, K. W., Wruck, C. J., Katona, I., Anink, J., Troost, D., Aronica, E., Steinbusch, H., Weis, J., & Goswami, A. (2020). Aggregates of RNA Binding Proteins and ER Chaperones Linked to Exosomes in Granulovacuolar Degeneration of the Alzheimer's Disease Brain. Journal of Alzheimer's Disease, 75(1), 139–156. https://doi.org/10.3233/JAD-190722

Yang, C. H., Wang, Y., Sims, M., Cai, C., He, P., Häcker, H., Yue, J., Cheng, J., Boop, F. A., & Pfeffer, L. M. (2017). MicroRNA203a suppresses glioma tumorigenesis through an ATM-dependent interferon response pathway. Oncotarget, 8(68), 112980–112991. https://doi.org/10.18632/oncotarget.22945

Yao, P. J., Eren, E., Goetzl, E. J., & Kapogiannis, D. (2021). Mitochondrial Electron Transport Chain Protein Abnormalities Detected in Plasma Extracellular Vesicles in Alzheimer's Disease. Biomedicines, 9(11), Article 11. https://doi.org/10.3390/biomedicines9111587

Yılmaz, Ş. G., Erdal, M. E., Özge, A. A., & Sungur, M. A. (2016). Can Peripheral MicroRNA Expression Data Serve as Epigenomic (Upstream) Biomarkers of Alzheimer's Disease? OMICS: A Journal of Integrative Biology, 20(8), 456–461. https://doi.org/10.1089/omi.2016.0099

Yoshihara, E., Masaki, S., Matsuo, Y., Chen, Z., Tian, H., & Yodoi, J. (2014). Thioredoxin/Txnip: Redoxisome, as a Redox Switch for the Pathogenesis of Diseases. Frontiers in Immunology, 4. https://www.frontiersin.org/articles/10.3389/fimmu.2013.00514

Youssef, P., Chami, B., Lim, J., Middleton, T., Sutherland, G. T., & Witting, P. K. (2018). Evidence supporting oxidative stress in a moderately affected area of the brain in Alzheimer's disease. Scientific Reports, 8(1), Article 1. https://doi.org/10.1038/s41598-018-29770-3

Yu, Y., Run, X., Liang, Z., Li, Y., Liu, F., Liu, Y., Iqbal, K., Grundke-Iqbal, I., & Gong, C.-X. (2009). Developmental regulation of tau phosphorylation, tau kinases, and tau phosphatases. Journal of Neurochemistry, 108(6), 1480–1494. https://doi.org/10.1111/j.1471-4159.2009.05882.x

Yuen, S. C., Liang, X., Zhu, H., Jia, Y., & Leung, S. (2021). Prediction of differentially expressed microRNAs in blood as potential biomarkers for Alzheimer's disease by meta-analysis and adaptive boosting ensemble learning. Alzheimer's Research & Therapy, 13(1), 126. https://doi.org/10.1186/s13195-021-00862-z

Yuyama, K., Sun, H., Mitsutake, S., & Igarashi, Y. (2012). Sphingolipid-modulated Exosome Secretion Promotes Clearance of Amyloid-β by Microglia. Journal of Biological Chemistry, 287(14), 10977–10989. https://doi.org/10.1074/jbc.M111.324616

Yuyama, K., Sun, H., Sakai, S., Mitsutake, S., Okada, M., Tahara, H., Furukawa, J., Fujitani, N., Shinohara, Y., & Igarashi, Y. (2014). Decreased Amyloid-β Pathologies by Intracerebral Loading of Glycosphingolipid-enriched Exosomes in Alzheimer Model Mice. Journal of Biological Chemistry, 289(35), 24488–24498. https://doi.org/10.1074/jbc.M114.577213

Yuyama, K., Sun, H., Usuki, S., Sakai, S., Hanamatsu, H., Mioka, T., Kimura, N., Okada, M., Tahara, H., Furukawa, J., Fujitani, N., Shinohara, Y., & Igarashi, Y. (2015). A potential function for neuronal exosomes: Sequestering intracerebral amyloid-β peptide. FEBS Letters, 589(1), 84–88. https://doi.org/10.1016/j.febslet.2014.11.027

Zandberga, E., Kozirovskis, V., Ābols, A., Andrējeva, D., Purkalne, G., & Linē, A. (2013). Cell-free microRNAs as diagnostic, prognostic, and predictive biomarkers for lung cancer. Genes, Chromosomes and Cancer, 52(4), 356–369. https://doi.org/10.1002/gcc.22032

Zannis, V. I., Breslow, J. L., Utermann, G., Mahley, R. W., Weisgraber, K. H., Havel, R. J., Goldstein, J. L., Brown, M. S., Schonfeld, G., Hazzard, W. R., & Blum, C. (1982). Proposed nomenclature of apoE isoproteins, apoE genotypes, and phenotypes. Journal of Lipid Research, 23(6), 911–914. https://doi.org/10.1016/S0022-2275(20)38094-9

Zhan, Y., Paolicelli, R. C., Sforazzini, F., Weinhard, L., Bolasco, G., Pagani, F., Vyssotski, A. L., Bifone, A., Gozzi, A., Ragozzino, D., & Gross, C. T. (2014). Deficient neuron-microglia signaling results in impaired functional brain connectivity and social behavior. Nature Neuroscience, 17(3), 400–406. https://doi.org/10.1038/nn.3641

Zhang, B., Wang, A., Xia, C., Lin, Q., & Chen, C. (2015). A single nucleotide polymorphism in primary-microRNA-146a reduces the expression of mature microRNA-146a in patients with Alzheimer's disease and is associated with the pathogenesis of Alzheimer's disease. Molecular Medicine Reports, 12(3), 4037–4042. https://doi.org/10.3892/mmr.2015.3968

Zhang, H., Liang, J., & Chen, N. (2022). The Potential Role of miRNA-Regulated Autophagy in Alzheimer's Disease. International Journal of Molecular Sciences, 23(14), Article 14. https://doi.org/10.3390/ijms23147789

Zhang, L., Fang, Y., Cheng, X., Lian, Y.-J., & Xu, H.-L. (2019). Silencing of Long Noncoding RNA SOX21-AS1 Relieves Neuronal Oxidative Stress Injury in Mice with Alzheimer's Disease by Upregulating FZD3/5 via the Wnt Signaling Pathway. Molecular Neurobiology, 56(5), 3522–3537. https://doi.org/10.1007/s12035-018-1299-y

Zhang, L., Yu, H., Sun, Y., Lin, X., Chen, B., Tan, C., Cao, G., & Wang, Z. (2007). Protective effects of salidroside on hydrogen peroxide-induced apoptosis in SH-SY5Y human neuroblastoma cells. European Journal of Pharmacology, 564(1), 18–25. https://doi.org/10.1016/j.ejphar.2007.01.089

Zhang, R., Zhang, Q., Niu, J., Lu, K., Xie, B., Cui, D., & Xu, S. (2014). Screening of microRNAs associated with Alzheimer's disease using oxidative stress cell model and different strains of senescence accelerated mice. Journal of the Neurological Sciences, 338(1), 57–64. https://doi.org/10.1016/j.jns.2013.12.017

Zhang Rui Lan, Pan Wanlong, Zhang Xiaoming, Liu Xianshuang, Landschoot-Ward Julie, Li Chao, Fan Baoyan, Wang Xinli, Chopp Michael, & Zhang Zheng Gang. (2017). Abstract WMP48: Cerebral Endothelial Derived Exosomes Abolish Cognitive Impairment Induced by Ablation of Dicer in Adult Neural Progenitor Cells. Stroke, 48(suppl_1), AWMP48–AWMP48. https://doi.org/10.1161/str.48.suppl_1.wmp48

Zhang, T., Shen, Y., Guo, Y., & Yao, J. (2021). Identification of key transcriptome biomarkers based on a vital gene module associated with pathological changes in Alzheimer's disease. Aging (Albany NY), 13(11), 14940–14967. https://doi.org/10.18632/aging.203017

Zhang, X., Abels, E. R., Redzic, J. S., Margulis, J., Finkbeiner, S., & Breakefield, X. O. (2016). Potential Transfer of Polyglutamine and CAG-Repeat RNA in Extracellular Vesicles in Huntington's Disease: Background and Evaluation in Cell Culture. Cellular and Molecular Neurobiology, 36(3), 459–470. https://doi.org/10.1007/s10571-016-0350-7

Zhang, Y., Chopp, M., Liu, X. S., Katakowski, M., Wang, X., Tian, X., Wu, D., & Zhang, Z. G. (2017). Exosomes Derived from Mesenchymal Stromal Cells Promote Axonal Growth of Cortical Neurons. Molecular Neurobiology, 54(4), 2659–2673. https://doi.org/10.1007/s12035-016-9851-0

Zhang, Y., Kim, M. S., Jia, B., Yan, J., Zuniga-Hertz, J. P., Han, C., & Cai, D. (2017). Hypothalamic stem cells control aging speed partly through exosomal miRNAs. Nature, 548(7665), 52–57. https://doi.org/10.1038/nature23282

Zhang, Y., Li, Q., Liu, C., Gao, S., Ping, H., Wang, J., & Wang, P. (2016). MiR-214-3p attenuates cognition defects via the inhibition of autophagy in SAMP8 mouse model of sporadic Alzheimer's disease. NeuroToxicology, 56, 139–149. https://doi.org/10.1016/j.neuro.2016.07.004

Zhang, Y., Ueno, Y., Liu, X. S., Buller, B., Wang, X., Chopp, M., & Zhang, Z. G. (2013). The microRNA-17-92 cluster enhances axonal outgrowth in embryonic cortical neurons. The Journal of Neuroscience : The Official Journal of the Society for Neuroscience, 33(16), 6885–6894. https://doi.org/10.1523/JNEUROSCI.5180-12.2013

Zhang, Y., & Zhang, Y. (2020). LncRNA ZFAS1 Improves Neuronal Injury and Inhibits Inflammation, Oxidative Stress, and Apoptosis by Sponging miR-582 and Upregulating NOS3 Expression in Cerebral Ischemia/Reperfusion Injury. Inflammation, 43(4), 1337–1350. https://doi.org/10.1007/s10753-020-01212-1

Zhang, Z. G., Buller, B., & Chopp, M. (2019). Exosomes—Beyond stem cells for restorative therapy in stroke and neurological injury. Nature Reviews Neurology, 1. https://doi.org/10.1038/s41582-018-0126-4

Zhang, Z., Xu, Y., Chi, S., & Cui, L. (2020). MicroRNA-582-5p Reduces Propofol-induced Apoptosis in Developing Neurons by Targeting ROCK1. Current Neurovascular Research, 17(2), 140–146. https://doi.org/10.2174/1567202617666200207124817

Zhao, L., Zhang, L., Zhu, W., Chen, H., Ding, Y., & Cui, G. (2021). Inhibition of microRNA-203 protects against traumatic brain injury induced neural damages via suppressing neuronal apoptosis and dementia-related molecues. Physiology & Behavior, 228, 113190. https://doi.org/10.1016/j.physbeh.2020.113190

Zhao, N., Zhang, X., Li, B., Wang, J., Zhang, C., & Xu, B. (2023). Treadmill Exercise Improves PINK1/Parkin-Mediated Mitophagy Activity Against Alzheimer's Disease Pathologies by Upregulated SIRT1-FOXO1/3 Axis in APP/PS1 Mice. Molecular Neurobiology, 60(1), 277–291. https://doi.org/10.1007/s12035-022-03035-7

Zhao, Y., Wu, X., Li, X., Jiang, L.-L., Gui, X., Liu, Y., Sun, Y., Zhu, B., Piña-Crespo, J. C., Zhang, M., Zhang, N., Chen, X., Bu, G., An, Z., Huang, T. Y., & Xu, H. (2018). TREM2 is a receptor for β-amyloid which mediates microglial function. Neuron, 97(5), 1023-1031.e7. https://doi.org/10.1016/j.neuron.2018.01.031

Zhou, L., McInnes, J., Wierda, K., Holt, M., Herrmann, A. G., Jackson, R. J., Wang, Y.-C., Swerts, J., Beyens, J., Miskiewicz, K., Vilain, S., Dewachter, I., Moechars, D., De Strooper, B., Spires-Jones, T. L., De Wit, J., & Verstreken, P. (2017). Tau association with synaptic vesicles causes presynaptic dysfunction. Nature Communications, 8(1), Article 1. https://doi.org/10.1038/ncomms15295

Zhou, M., Wang, M., Wang, X., Liu, K., Wan, Y., Li, M., Liu, L., & Zhang, C. (2018). Abnormal Expression of MicroRNAs Induced by Chronic Unpredictable Mild Stress in Rat Hippocampal Tissues. Molecular Neurobiology, 55(2), 917–935. https://doi.org/10.1007/s12035-016-0365-6

Zimbone, S., Monaco, I., Gianì, F., Pandini, G., Copani, A. G., Giuffrida, M. L., & Rizzarelli, E. (2018). Amyloid Beta monomers regulate cyclic adenosine monophosphate response element binding protein functions by activating type-1 insulin-like growth factor receptors in neuronal cells. Aging Cell, 17(1), e12684. https://doi.org/10.1111/acel.12684

Zott, B., Simon, M. M., Hong, W., Unger, F., Chen-Engerer, H.-J., Frosch, M. P., Sakmann, B., Walsh, D. M., & Konnerth, A. (2019). A vicious cycle of β amyloid–dependent neuronal hyperactivation. Science, 365(6453), 559–565. https://doi.org/10.1126/science.aay0198

Zuo, L., Prather, E. R., Stetskiv, M., Garrison, D. E., Meade, J. R., Peace, T. I., & Zhou, T. (2019). Inflammaging and Oxidative Stress in Human Diseases: From Molecular Mechanisms to Novel Treatments. International Journal of Molecular Sciences, 20(18), Article 18. https://doi.org/10.3390/ijms20184472

Zyprych-Walczak, J., Szabelska, A., Handschuh, L., Górczak, K., Klamecka, K., Figlerowicz, M., & Siatkowski, I. (2015). The Impact of Normalization Methods on RNA-Seq Data Analysis. BioMed Research International, 2015, 621690. https://doi.org/10.1155/2015/621690